DOCTOR OF ECONOMICS AND BUSINESS MANAGEMENT

Interbank Networks and Financial Stability

Scholtes, Nicolas

Award date:
2018

Awarding institution:
University of Namur

Université catholique de Louvain

Faculté des Sciences Economiques et de Gestion
Center for Operations Research and Econometrics

et

Université de Namur

Faculté des Sciences Economiques et de Gestion
Center for Research in Finance and Management

Interbank networks and financial stability

Nicolas-Kirti SCHOLTES

Thèse présentée en vue de l'obtention du grade de:
docteur en sciences économiques et de gestion

Président du Jury:
Professeur Isabelle LINDEN (Université de Namur)

Promoteurs:
Professeur Jean-Yves GNABO (Université de Namur)
Professeur Sophie BEREAU (Université catholique de Louvain)

Membres du Jury:
Professeur Oscar BERNAL (Université de Namur)
Professeur Camille CORNAND (Université de Lyon, CNRS-GATE)
Professeur Jean-Charles DELVENNE (Université catholique de Louvain)

Soutenue le 06 Septembre 2018

Rempart de la Vierge, 13
B - 5000 Namur (Belgique)

ISBN : 978-2-39029-017-9
Dépôt légal: D/2018/1881/22

Acknowledgements

This PhD thesis marks the end of four eventful years which in retrospect, passed by in a whirlwind. It is no exaggeration to state that this would not have been possible without the support and encouragement of numerous individuals whom I will attempt to thank here.

First and foremost, I would like to thank my supervisor, Jean-Yves Gnabo for being a constant source of guidance and inspiration. Over the years, you were always ready to listen to my concerns and ideas and help me navigate the often murky world of academia. I am also eternally grateful to my co-supervisor, Sophie Béreau and the rest of the FiXS group, Oscar Bernal and Annick Castiaux for having taken a chance on a young researcher with his head full of ideas more than four years ago. My sincere thanks go to Camille Cornand, Isabelle Linden and Jean-Charles Delvenne for their invaluable comments and for taking the time to serve on my jury.

My sincere gratitude goes to the administrative staff at both institutions for all their help over the years and for ensuring that all documents were always signed and submitted on time. Thanks in particular to Pierrette Noël in Namur and Catherine Germain at CORE.

I was fortunate to spend six months at the European Central Bank, an institution I have enormous respect for. For this I would like to thank Michael Grill and my former colleagues at FRE for having provided such a welcoming atmosphere. I could not have asked for a better introduction to the policymaking world. Thanks to the "straight outta Ostend" crew: Joana, Lucilla, Katherine, Milou, Yvan, Ege and Fabio as well as my karaoke co-conspirators in the best office on 34: Iulia, Luis and Jacopo.

Coming now to my brothers and sisters in arms (i.e. PhD colleagues), I will always have fond memories of numerous discussions on academia, employment, life, politics and academia again. Special thanks to Manuela, my former co-author and Italian teacher, and Andras, with whom I shared an odd appreciation for cold war spy fiction and the intricacies of academic life. Thanks also to Keiti, Sabina, Sinem, Risa, Valeria, Jonas, Claudio, Cyrille, Marco, Ignacio, Andrea, Huan and the rest for all the good times. Outside the academic bubble, thanks to Iro and Pana for their friendship.

To Marie, I am thrilled to be sharing this milestone with you. Thank you for being a continuous source of encouragement and positive energy. You provided a much-needed stabilising influence as I dealt with the last stages of the PhD, job interviews and apartment hunting in Brussels. The equilibrium state of things now is in no small part thanks to you.

Finally, the most important support system of them all: My family. There are simply no words to express my gratitude for all that you have done for me and for always being there when I needed you. In the end, this thesis along with all I have accomplished is due to you, Maman, Papa and Gael.

Contents

List of Figures

List of Tables

General introduction

"As a result of the crisis, a hundred intellectual flowers are blooming"
– Olivier Blanchard (2015),

Overview

As the title suggests, this thesis explores the linkages between interbank markets and financial stability primarily through the application of tools from network theory. Following the 2007-2008 global financial crisis, the use of networks in assessing financial stability and systemic risk has grown in importance (Schweitzer et al., 2009) due to their inherent ability in capturing the externalities that the risk associated to a single institution poses for the entire financial system (Allen and Babus, 2009). Moreover, networks allow for a structural perspective comprising *nodes* and the *links* connecting them. In the case of interbank markets, nodes represent banks and the links the various types of interdependencies between them. To this end, I argue that interconnections between banks play a front-and-centre role in driving both individual bank behaviour and dynamics at the system level. With the primary focus being on the interbank market, each of the three chapters comprising the thesis is situated firmly within this narrative: Chapter 1 identifies the importance of banking sector dynamics in post-crisis macroeconomic modelling and posits an additional role for interconnectedness, Chapter 2 highlights the importance of network structure in driving financial contagion and Chapter 3 combines two approaches from the emerging field of *complexity economics* namely, network theory and Agent-Based Modelling to create a model in which interbank market tensions is an *emergent phenomenon* arising due to the interplay between counterparty and liquidity risk.

Interbank markets and the financial crisis

The global interbank market is defined as an Over-the-Counter (OTC) money market in which banks extend loans to one another at short maturities (with the majority being overnight). In the secured segment of the market, the loan is guaranteed by highly liquid, short term debt securities while unsecured transactions are settled without collateral. The market performs a key function in ensuring the smooth functioning and stability of the global financial system for two primary reasons: First, it provides a key source of liquidity for banks thereby allowing for the efficient channelling of funds from savers to investment in the face of unexpected liquidity imbalances. The second reason derives from the manner in which modern central banks conduct monetary policy. Taking the European Central Bank (ECB) and the US Federal Reserve as examples, both operate under the *inflation targeting* paradigm whereby the central bank targets a specific short-term interest rate in debt markets in order to achieve/maintain a desired inflation rate. Under this framework, the central bank buys or sells eligible government securities on the open market in order to steer short-term interest rates and indirectly expand or contract the total money supply in the economy. Since these open market operations are conducted with banks as the main counterparty, short-term money market rates (in the Eurozone, this rate is given by the EONIA or Euro Overnight Index Average rate) are the first to be affected by the central bank's policy rate. This in turn affects bank deposit and lending rates, credit supply and aggregate demand in a process known as the *transmission mechanism of monetary policy.*

Despite tensions in global financial markets going back to August 2007 when the French bank, BNP Paribas informed clients that it was suspending three of its funds exposed to US subprime mortgages, citing a "complete evaporation of liquidity" making it impossible to adequately value its assets, the watershed moment occurred on September 15^{th}, 2008 when the major US investment bank, Lehman Brothers filed for bankruptcy. This sent shockwaves through international financial markets due to the highly globalised and interconnected nature of the institution and resulted in a global widening of risk premia in unsecured interbank markets.

In the EU, one of the most common barometers of interbank market strains is the EURIBOR-OIS[1] spread which proxies banks' perception of the *default/credit risk* of other banks. The evolution of the 3m EURIBOR-OIS spread during the crisis is provided below:[2]

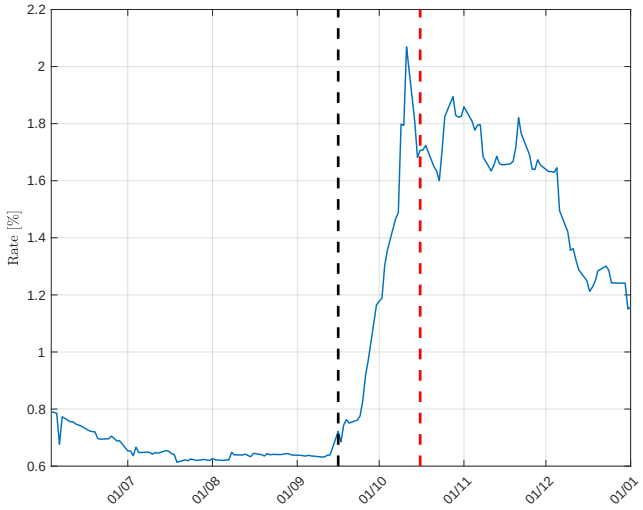

Figure 1: 3m EURIBOR-OIS Spread. Source: Bloomberg

Following a prolonged period of low spreads, the Lehman bankruptcy instigated a large jump, indicating a rapid accumulation of risks over a span of one month, eventually spiking at 200 bp after which the aggressive intervention by the ECB (as I will further detail below) succeeded in alleviating interbank market tensions.

In normal times, the ECB uses the various instruments at its disposal to steer short term interest rates in order to provide an anchor for the term structure of interest rates and achieve its inflation target of close to 2% as per its mandate. In doing so, the benchmark EU short-term interbank lending rate, the EONIA[3] fluctuates around the ECB's interest rate on its Main Refinancing Operations (MRO). However, as the crisis intensified following the Lehman Brothers bankruptcy on September 15th 2008, the ECB

[1]The EURIBOR (Euro Interbank Offered Rate) is a daily reference rate based on the average at which Eurozone banks lend unsecured funds to each other in the Euro wholesale money market. Comprising various maturities ranging from 1 week to 1 year, it is constructed by a panel of 23 major EU banks and is a key benchmark for pricing approximately EUR 150 trillion worth of financial products globally. Overnight Index Swaps (OIS) are considered risk-free, measuring the market's expectation of overnight rates over the term of the contract.

[2]Data between June and December 2008. Black dashed line represents the Lehman Brothers Bankruptcy (15/09/2008). Red dashed line represents ECB move from variable to fixed rate tender allotments (15/10/2008)

[3]Using a panel of 30 large EU banks, the rate is calculated on a daily basis by the ECB as a weighted average based on actual overnight, unsecured interbank transactions.

reacted by decreasing its main refinancing rate by 150 bp from 4.25 to 3.75% on October 15th followed by a further reduction to 2.5% by the end of the year in order to ease liquidity conditions on interbank markets where unfolding risks and information asymmetries led to a systemwide *crisis of confidence* characterised by a global retrenchment from money market funding (Trichet, 2010). Figure 2 below reports total trading volumes by EONIA-quoting banks as well as the associated rate and ECB policy rates. In order to highlight the growing redundancy of the conventional monetary policy framework, the EONIA rate is compared to the main refinancing and the deposit facility rate as well as the volume of bank deposits held by the ECB.

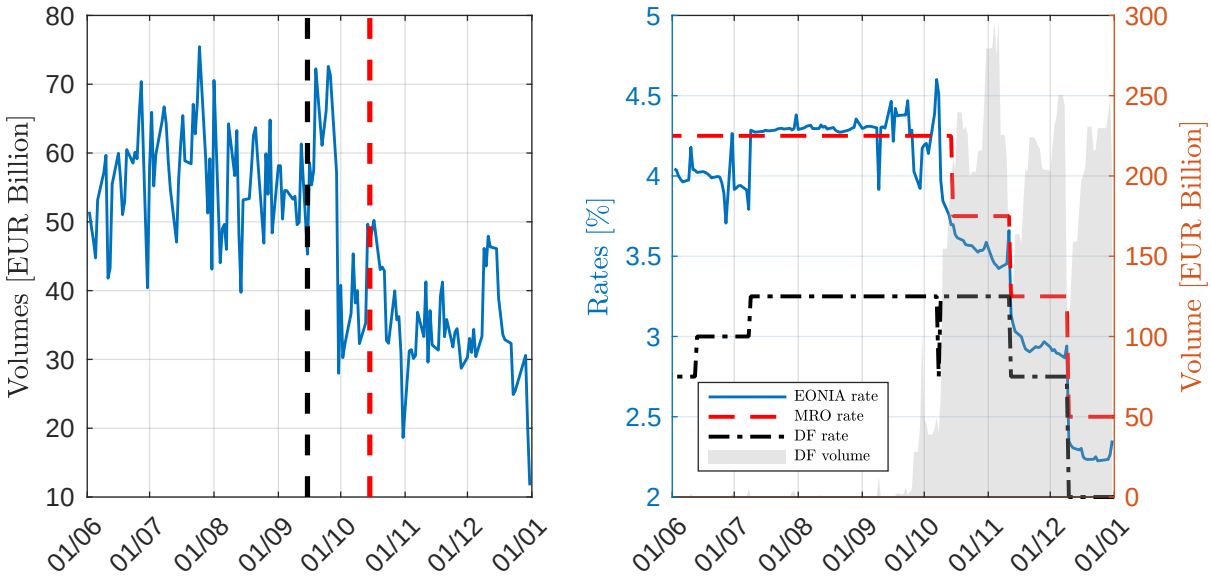

Figure 2: EONIA volumes (L) and various rates + recourse to deposit facility (R). Source: ECB.

Following the Lehman trigger, there is an immediate contraction of the interbank market, both in terms of volumes and rates. From a policy perspective, the MRO and EONIA rates diverged as the latter started to track the DF rate. This coincided with a sharp increase in the use of the ECBs deposit facility (heretofore unused due to the lower rate of return relative to wholesale funding). Recourse to the deposit facility can also be interpreted as an increase in excess reserves (above the minimum reserve requirement which until January 2012 was set at 2% of customer deposits) further highlighting banks' hoarding behaviour during the crisis.

Coinciding with the decrease in the policy rate, the ECB implemented further emergency measures by switching their liquidity-allotment policy from a variable rate tender to a

policy of *fixed rate full allotment* (FRFA) under which all liquidity requests by banks are met (against eligible collateral and under the condition of financial soundness) in order to meet their short-term funding needs and ensure the continued availability of credit to households and firms across the euro area. Figure 3 provides the allotment volumes (left panel) and the number of banks bidding for funding (right panel) under the ECBs weekly MRO tenders.

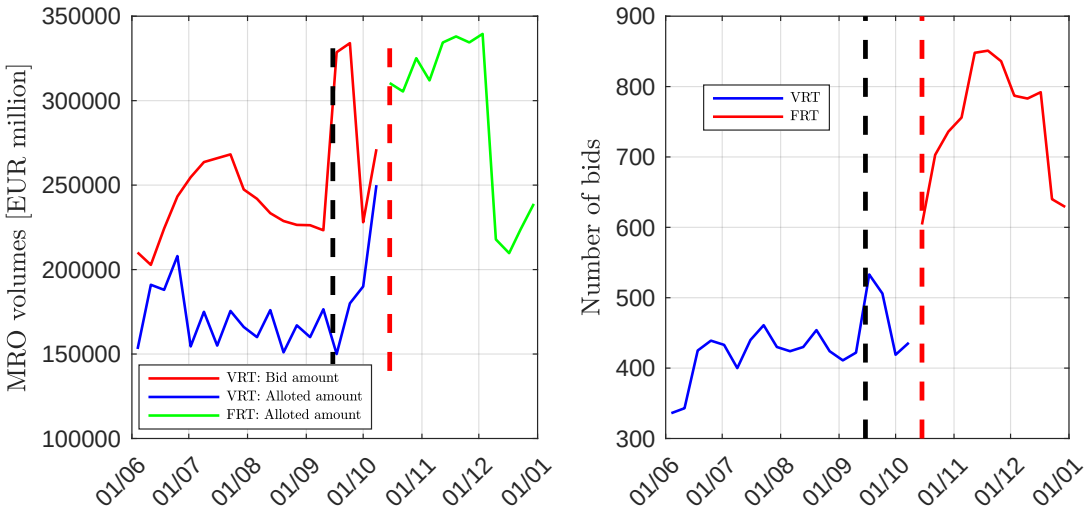

Figure 3: ECB Main Refinancing Operations. Weekly frequency and maturity. Allotted amounts calculated by the ECB such that banks are able to fulfil their reserve requirements. Source: ECB.

In line with the argument developed so far, the impact of the Lehman bankruptcy is immediately apparent. Faced with the onset of funding shortages, banks substantially increased their bids for ECB liquidity. Moreover, there is a clear increase in the *number* of bidding banks relative to the situation before the crisis. As shown in the Figure 2(a), interbank activity continued to decline combined with a concomitant increase in excess reserves.

Given that the aforementioned policy measures were focussed largely on mitigating the spillover of banking sector strains to the real economy, I end this section with a discussion on changes in bank credit provision activities. Using data from the consolidated balance

sheet of euro area MFIs[4] (Monetary Financial Institutions), Figure 4 reports bank loans to NFCs[5] (Non Financial Corporations) and households.

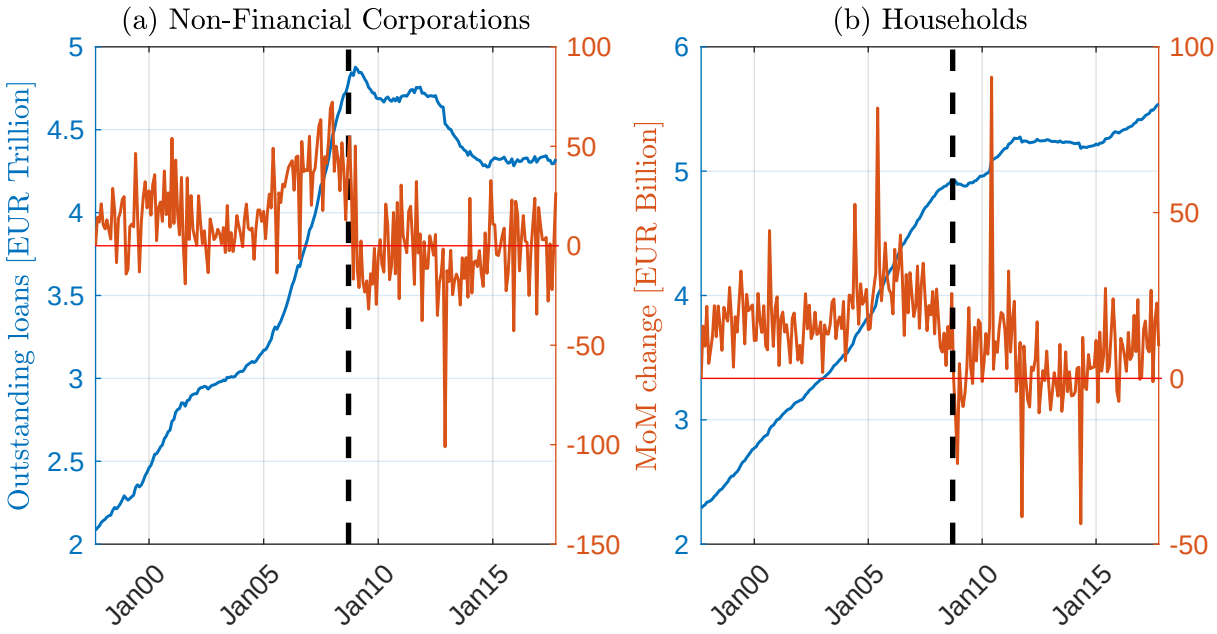

Figure 4: Loans vis-à-vis euro area NFC (L) and households (R) reported by MFI excluding ESCB in the euro area (stock). Source: ECB

In order to highlight the impact of the crisis on credit provision relative to normal times, a longer time series is provided. The impact of the Lehman bankruptcy is apparent: following eight years of continuous loan growth, the crisis resulted in a sharp drop for NFCs and a slowdown in loans to households. As I have shown in this section, the crisis had a marked impact on the EU interbank market and the wider economy via a contraction in credit. In response to this, the ECB entered uncharted territory by pumping large amounts of liquidity into the system and substantially altering its monetary policy framework in order to prevent a more widespread collapse.

[4]ECB Definition: Financial institutions which together form the money-issuing sector of the euro area. These include the Eurosystem, resident credit institutions (as defined in EU law) and all other resident financial institutions whose business is to receive deposits and/or close substitutes for deposits from entities other than MFIs and, for their own account (at least in economic terms), to grant credit and/or invest in securities.

[5]ECB Definition: Corporation or quasi-corporation that is not engaged in financial intermediation but is active primarily in the production of market goods and non-financial services.

The role of interconnectedness

As these events were unfolding, policymakers took note of the fact that what began as a localised shock to the US subprime mortgage and collateralised debt obligation (CDO) market ended up having global ramifications. Against this background, the *interconnectedness* of the financial system was identified as having played a central role in precipitating the crisis via a complex web of direct and indirect links between market participants. Notably, Giannone et al. (2012) highlight how in the years preceding the crisis, Euro area banks gradually replaced traditional retail funding i.e. deposits from households and firms with funding obtained from the financial sector via the wholesale money market. A similar trend was observed by Adrian and Shin (2010) for the US wherein other banks provided a significant source of funding, primarily through the use of repurchase agreements[6] and securitised assets. Moreover, both identify the buildup of procyclical intra-financial sector leverage via longer credit *intermediation chains* of financial institutions between ultimate creditors and savers as having played a key role in allowing systemic risks to develop and eventually unwind as distressed banks called in debt claims to shore up their own assets thereby adversely affecting the liability-side of connected institutions' balance sheets. Similarly, rapid globalisation over the past three decades resulted in growing cross-border exposures between banks, sovereigns and other market participants, adding an additional channel for the financial crisis to deepen and attain global proportions (International Monetary Fund, 2010).

[6] Also referred to as *repos*, repurchase agreements are a type of short-term loan consisting of the sale of an asset (typically fixed-income securities such as government bonds) combined with a forward agreement to repurchase it at maturity. Increasing repo haircuts and the cessation of repo lending against many forms of collateral was described by Gorton and Metrick (2012) as a "run on repo" and identified as having played a key role in exacerbating the subprime mortgage crisis.

As central banks responded to the seizing up of interbank credit by stepping in as the main intermediary across the banking sector, a number of key officials weighed in on the potential for systemic risk arising due to the excessive complexity and interconnectedness of the financial system. Notably, then-president of the ECB, Jean-Claude Trichet in a speech to the Eurofi financial forum on September 30th, 2009 stated that:

> *... One of the key lessons stemming from the financial crisis relates to the importance of understanding and assessing the degree of "interconnectedness" between market participants. In particular, the crisis demonstrated that the nature and magnitude of the systemic risk in the financial sector is related not only to the potential illiquidity or insolvency of large banks or other major regulated financial institutions, but it also depends on the close intertwining between financial institutions, markets and infrastructures*

A sentiment that was also echoed by his US counterpart, then-Federal Reserve Chairman Ben Bernanke on September 24th, 2010 in a speech given at Princeton University entitled "Implications of the financial crisis for economics":

> *... economists failed to predict the nature, timing, or severity of the crisis; and those few who issued early warnings generally identified only isolated weaknesses in the system, not anything approaching the full set of* ***complex linkages*** *and mechanisms that amplified the initial shocks and ultimately resulted in a devastating global crisis and recession*

More recently, Janet Yellen, his successor emphasised the link between studying interconnectedness and systemic risk and emerging research in *financial network analysis* in a speech to the American Economic and American Finance Associations on January 4th, 2013:

> *... Academic research that explores the relationship between network structure and systemic risk is relatively new. Not surprisingly, interest in this field has increased considerably since the financial crisis. A search of economics research focusing on "systemic risk" or "interconnectedness" since 2007 yields 624 publications, twice as many as were produced in the previous 25 years*

Viewing the world through a network lens

As interconnectedness wove itself into the policy discourse, researchers were turning to the use of network theory to better understand systemic risk and financial stability. In a comprehensive survey of the literature, Hüser (2015) highlights how the versatility of interbank network models allows them to capture the entirety of the '*financial fragility hypothesis*' posited by De Bandt et al. (2009) which outlines three interrelated features of the financial system that can undermine financial stability. These are: (*i*) The complex web of exposures amongst banks, (*ii*) the importance of balance sheet composition due to the maturity transformation role played by banks and (*iii*) the informational and control intensity of financial contracts. Against this background, the field of financial network analysis has gained traction amongst academics and central bankers due to the intuitive manner in which the various interdependencies between financial institutions are modelled and the flexibility of the modelling framework.

Before outlining the interbank network models comprising the thesis, I provide a brief overview of the *early* literature aimed at introducing networks into economic and financial modelling. These articles can be classified along two dimensions:

- **Financial contagion and network connectivity**: In the immediate aftermath of the crisis, there was a concerted effort amongst academics and policymakers to understand how interdependencies designed to share risks could simultaneously undermine financial stability by providing a channel for localised shocks to propagate through the system.
- **Understanding the architecture of financial systems**: Due to rapid advances in computing power and the increasing availability of data over the past decade, a prominent research avenue has opened up aimed at using granular exposure/transaction data to map the structure of various financial markets using networks in order to identify systemic vulnerabilities (e.g. banks who, by virtue of their centrality in the network are deemed *too-interconnected-to-fail*).

While these approaches helped cement the use of networks in financial stability analysis, the literature has since evolved to (*i*) focus on agent-behaviour, either embedded within a network or as a driver in network formation and (*ii*) incorporate increasingly sophisticated network topologies. These are expounded upon in the state-of-the-art section.

The robust-yet-fragile property of financial networks

Prior to the crisis, the increasingly intertwined nature of global financial markets was seen as a boon for the industry as it allowed for diversification of risks while providing greater investment and liquidity opportunities for savers. From an economic modelling perspective, the seminal theoretical contributions of Allen and Gale (2000) and Freixas et al. (2000) reached the same conclusion: That a highly interconnected network enhances the resilience of the system to the insolvency of an individual bank. By contrast Brusco and Castiglionesi (2007) develop an alternative theoretical model in which a larger number of interbank deposits promotes financial contagion. It was only after the crisis that the notion of phase transitions and tipping points entered the financial stability lexicon. Against this background, the higher connectivity is conducive to financial stability when the magnitude of the shock is *below* a certain threshold. For large shocks, the same links that allowed banks to diversify and dilute risks across multiple counterparties now act as a channel for the propagation (and potential amplification) of financial distress stemming from a small set of nodes/banks.

Initially elaborated by Haldane (2009) as the "*robust-yet-fragile*" property of financial networks, several early works (notably, the seminal papers of Nier et al. (2007) and Gai and Kapadia (2010)) explored the relationship between network structure and contagion, finding that while higher connectivity does indeed mitigate the likelihood of financial contagion (the robust aspect), the same set of linkages allow localised shocks of sufficient magnitude to propagate through the network (the fragile property). Acemoglu et al. (2015) add further nuance to the debate by identifying a shock magnitude threshold below which the assertion of Allen and Gale (2000) and Freixas et al. (2000) holds and above which interbank linkages facilitate financial contagion.

Mapping interbank networks

Parallel to the efforts aimed at exploring the impact of connectivity on financial contagion, another strand of research focussed on using data to empirically map real interbank networks. Given the high level of granularity required to reconstruct bilateral linkages combined with data confidentiality issues due to banks' reluctance in disclosing their positions vis-à-vis their counterparties/competitors, most of the current literature in this domain falls within two categories: (*i*) interbank *exposures* obtained from national credit registers[7] and (*ii*) payments transaction data from which the web of exposures is *inferred* using variations of an algorithm developed by Furfine (1999). As regards the actual *structure* of real-world networks, the literature has converged on two key features: (*i*) that interbank networks exhibit a *scale-free* topology[8] and (*ii*) that they exhibit a *core-periphery* structure.

Note that the concept of scale-free networks, stemming from the seminal article of Barabási and Albert (1999) aimed at classifying the network structure of several large datasets, needs to be taken with a grain of salt. Indeed, an article by Broido and Clauset (2018) tests the statistical fit of the scale-free paradigm applied to a wide variety of large datasets and compares it to several alternatives such as the exponential and log-normal distributions, finding that pure scale-free networks are poorly represented in the real world.[9]

Below, I classify the articles that confirm the two structural features outlined above, recalling the caveats mentioned in the previous paragraph.

[7] However, such data often suffers from reporting/completeness issues. Typically, researchers apply the *maximum entropy* (ME) method originating from physics and first applied to interbank network analysis by Sheldon and Maurer (1998). This features its own set of caveats including over/underestimation of exposures and an inability to account for key stylised facts associated to interbank markets such as sparseness or tiering (Upper, 2011).

[8] In this setup the degree distribution follows a *power law* whereby the fraction of nodes with degree k is proportional to $k^{-\alpha}$, where α is the so-called scaling parameter. The term scale-free indicates that there is no typical scale of the degrees, i.e. the mean may not be representative

[9] However, one of the originators of the model, Albert-László Barabási recently posted a rebuttal, entitled "Love is all you need" and available at https://www.barabasilab.com/post/love-is-all-you-need. In the piece, he argues for the existence of power laws in real-world networks, albeit subject to various corrective functions such as exponential cutoffs and logarithmic corrections.

Degree distribution

Boss et al. (2004) provide one of the first attempts to use interbank exposure data to map the national interbank network. Using the Austrian credit register and bank balance sheet data combined with ME to infer missing values, the reconstructed network is provided in Figure 5 below.

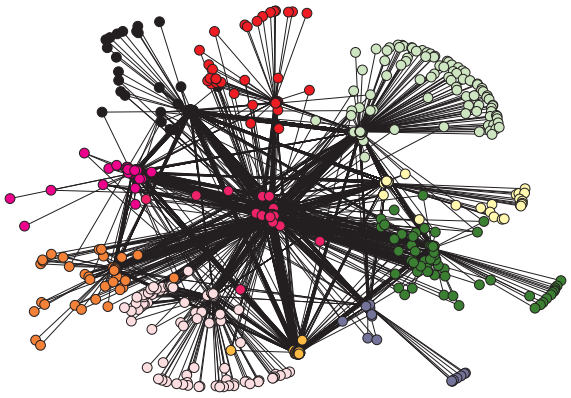

Figure 5: The Austrian interbank network in September 2002. Coloured nodes represent different *sectors*: agricultural banks, Volksbanken, joint stock banks, state mortgage banks, housing construction savings and loan associations, and special purpose banks

In addition to providing the first empirical mapping of an interbank network, Boss et al. (2004) were also the first to confirm the *scale-free* topology of interbank networks, a feature that has since been corroborated across various national markets. Using country-specific bilateral exposure data, a number of researchers followed suit in mapping their national interbank networks. Notable studies confirming the scale-free archetype include Soramäki et al. (2007) for the US Fedwire system, Alves et al. (2013) for large European banks, De Masi et al. (2006) for the Italian interbank market and León and Berndsen (2014) for the Colombian payment and settlement system.

Echoing the findings of Broido and Clauset (2018), another strand of the literature finds limited evidence for the scale-free representation. For example, Bech and Atalay (2010) identify the negative binomial distribution as providing the best fit for the out-degree distribution of the US Federal Funds Market. Studying the Italian e-MID market[10], neither Iori et al. (2008) or Fricke and Lux (2015) find direct evidence in favour of the scale-free degree distribution

[10]The e-MID electronic trading system was one of the first granular financial datasets that could be mapped and interpreted in a networks context. It is primarily used by Italian banks for unsecured, overnight interbank credit.

Core-periphery structures

A more recent development in the empirical literature has involved the classification of interbank networks as exhibiting a *core-periphery* wherein a small, densely-connected set of core banks extend credit amongst themselves and intermediate between a more populous set of peripheral banks that do not interact with each other. This representation has the added-value of being easier to interpret visually than the scale-free specification. Moreover, Craig and Von Peter (2014) confirmed the strong empirical fit of the core-periphery structure over the random and scale-free alternatives for the German interbank network. Similar analyses on the Dutch and U.K interbank networks by van Lelyveld et al. (2014) and Langfield et al. (2014) respectively also found a strong justification for the core-periphery structure.

Interbank networks are also known to exhibit strong *disassortative mixing* (Montagna and Lux, 2016) whereby high-degree nodes have a high tendency of connecting with low-degree nodes and vice versa. The link between disassortative mixing and the scale-free property has been identified by Fricke et al. (2013) while Craig and Von Peter (2014) highlights the link to the core-periphery property.

Complementary to the empirical literature on estimating core-periphery networks, a theoretical literature has emerged aimed at identifying the behavioural mechanisms by which such structures can develop *endogenously*. For example, van der Leij et al. (2014) develop a network formation game in which a stable core-periphery structure arises when agents are heterogeneous in terms of size. Lux (2015) allow banks to choose trading partners by forming preferential relationships via a reinforcement learning algorithm based on the degree of "*trust*" between banks. This concept of relationship lending plays a key role in interbank market dynamics, stating that banks form stable, long-term relationships between a small and stable set of counterparties, offerring them preferential treatment in terms of lower interest rates and higher loan availability. This was first observed by Cocco et al. (2009) for the Portuguese interbank market and has since been found to drive bilateral link formation in the German (Bräuning and Fecht, 2016) and US (Afonso et al., 2013) markets, both of whom identify the importance of relationships in minimising search frictions. Similarly, the stability of interbank relationships over time is confirmed by Affinito (2012) for the Italian interbank market.

Multilayer networks

The versatility of network analysis extends beyond the simple interbank credit exposures used to construct the above mapping. Using bilateral data on global CDS[11] (Credit Default Swap) trades, Peltonen et al. (2014) construct the following network mapping:

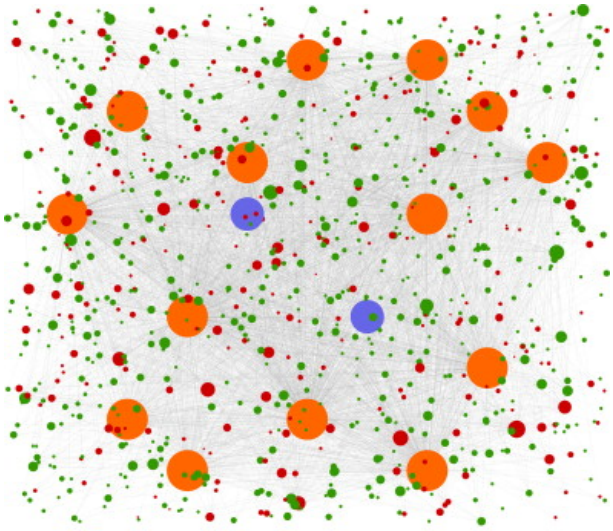

Figure 6: The global CDS network (Peltonen et al., 2014). Central clearing parties (CCPs) are in blue. Dealers are in orange. Customers in green (red) if they are net CDS buyers (sellers). Node size for customers is proportional to the square root of net notional exposure

The relative opacity of the OTC market for CDS has raised systemic risk concerns in recent years (Brunnermeier et al., 2013). By viewing the CDS market as a network, Peltonen et al. (2014) identify a number of important features for systemic risk measurement. Notably, the evident tiered structure combined with the concentration around 14 dealers who are the only members of the two CCPs.

In a recent report by the Office of Financial Research within the US Department of the Treasury, Bookstaber and Kenett (2016) highlight the need to recognise the numerous interdependencies (beyond simple credit exposures) that can exist between banks as well as the mechanisms through which risks can spread through the financial system. These concerns are at the heart of the recent drive in mapping and modelling *multilayer* networks (i.e. networks of networks). Two examples, based on the Mexican and UK interbank networks are provided below:

[11] These are financial derivatives designed as an insurance contract against the default of a particular entity. Historically, CDS facilitate risk-sharing amongst investors through improved price discovery and allocation of capital. At the same time, trading and speculation on CDS on MBS (Mortgage-Backed Securities) were at the heart of the financial crisis (Stulz, 2010).

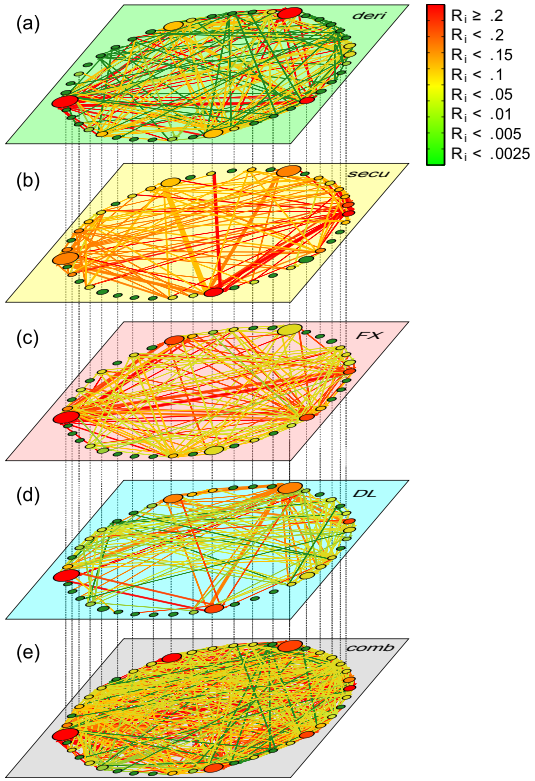

(a) Mexican banking network on September 30th 2013 (Poledna et al., 2015). Layers: (a) derivatives exposures, (b) securities cross-holdings, (c) foreign exchange exposures, (d) deposits and loans and (e) combined banking network. Nodes are coloured according to their systemic impact in the respective layer: from systemically important banks (red) to systemically safe (green). Node size proportional to total assets. Edge width proportional to exposure size between banks. Edge colour determined by counterparty.

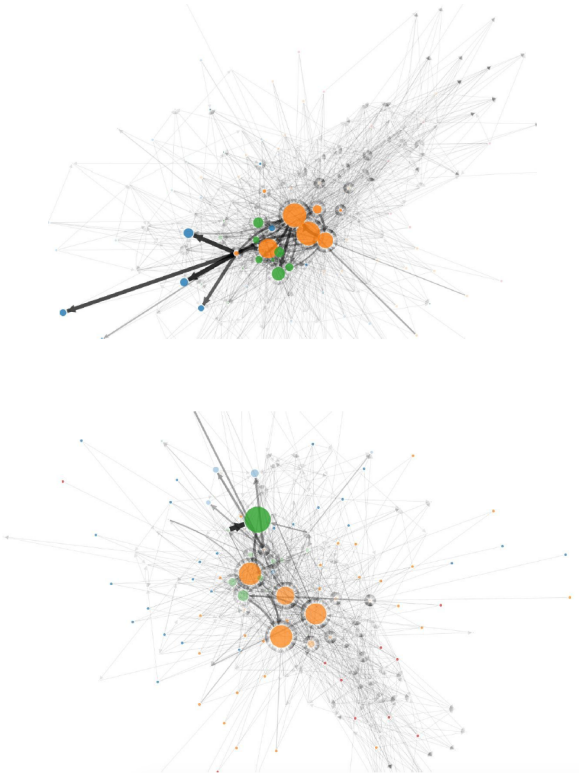

(b) UK interbank exposure (top) and interbank funding (bottom) network in 2011 (Langfield et al., 2014). Node size proportional to $\log(totalexposures)$ and $\log(receivedfunding)$ respectively. Orange circles represent selected large UK banks, green circles represent investment banks, blue circles represent overseas banks and red circles represent building societies. Edge width proportional to the value of the exposures and funding amounts.

Figure 7: **Multilayer network mapping**

Evidently, this domain of interbank network analysis is still in its infancy due to the high volume and granularity of the data required to reconstruct such maps. Other examples include Bargigli et al. (2015) using supervisory reports for the Italian banking sector organised by maturity and whether the contract is secured or unsecured and Aldasoro and Alves (2016) using exposure data for large European banks broken down by maturity and type of instrument.

Interconnectedness and macroprudential policy

The post-crisis regulatory landscape revolves around the Basel III reforms first released by the Basel Committee on Banking Supervision (BCBS) in December 2010. Recently finalised in December 2017, the reforms introduced *macroprudential policy* into the previous *micro*-prudentially oriented framework. Though the central aim of the package was to strengthen bank capital adequacy ratios and tighten liquidity and funding requirements, a number of aspects were aimed specifically at addressing systemic risk and interconnectedness. These are outlined in a report to the G20 prepared by the Basel Committee on Banking Supervision (2010):

- Capital incentives for banks to use central counterparties for OTC derivatives;
- Higher capital requirements for trading and derivative activities, as well as complex securitisations and off-balance sheet exposures
- Higher capital requirements for inter-financial sector exposures; and
- Introduction of liquidity requirements that penalise excessive reliance on short term, interbank funding to support longer-dated assets.

Interconnectedness also features strongly in the identification of Global Systemically Important Banks (G-SIBS). The methodology used to determine the systemic importance of a particular bank combines an indicator-based measurement approach with a bucketing/cutoff specification. In the first step, the five (equally-weighted at 20%) indicators are determined: cross-jurisdictional activity, size, *interconnectedness*, substitutability/financial institution infrastructure and complexity (BCBS, 2011). In this setup, interconnectedness comprises quantitative values associated to intra-financial system assets and liabilities and securities outstanding. The scores from this step are then assigned

to four equally-sized *buckets* to determine the *capital surcharge* i.e. the additional loss absorbing capital they are required to hold.

However, Espinosa-Vega and Sole (2014) point out that current stress testing methodologies and regulatory efforts to incorporate interconnectedness fail to harness the full complexity of financial sector interdependencies. As I have argued, networks provide the ideal framework to represent the structural complexity of the financial system. This has been recognised in the recent literature. For example, Halaj and Kok (2015) develop a network-based stress-testing model aimed at assessing the impact of regulatory large exposure limits and credit valuation adjustments. More recently, Poledna et al. (2017) develop an Agent-Based Model (ABM) in which an alternative to G-SIB surcharges is proposed, the so-called *systemic risk tax*. The authors argue that such an approach is inherently more efficient as it allows the financial network to self-organise into a topology such that cascading defaults do not occur. Within the context of multilayer networks and the bail-in regulation (part of the new EU-level bank resolution framework, applicable in binding form since 1 January 2016), Hüser et al. (2017) find a post-intervention rewiring of links across the different layers of the interbank network. Battiston and Martinez-Jaramillo (2018) survey the literature on financial networks and their current (and future) applicability to stress-testing and financial regulation.

State of the art

Langfield and Soramäki (2016) classify the research on interbank networks into three areas: Descriptions of interbank exposure networks, Simulation and modelling and the development of new network metrics to describe network topology and individual banks' relative importance. As mentioned, the first articles to study complex networks within the context of systemic risk and financial stability emerged about 10 years ago (following the crisis). The early literature focussed primarily on mapping the architecture of financial systems and understanding how shocks propagate through a network. As the field enters its adolescent phase, data quality and modelling specifications are continuing to increase in sophistication. Against this background, I identify the two subfields comprising the current state-of-the-art in financial network analysis below.

Complex, multilayer networks: Recognising that there exists a multiplicity of transaction types between banks, researchers have begun looking beyond simple exposure networks of national financial systems. In addition to providing a more realistic representa-

tion of financial interdependencies, multilayer networks are flexible enough to incorporate the finding by Glasserman and Young (2015) that credit exposures alone are insufficient to generate the widespread losses observed during the crisis. Complementary to the recent empirical exercises mentioned above (i.e. multilayer mappings of the Mexican, UK, Italian and EU banking sectors), Montagna and Kok (2016) developed a modelling framework for looking at contagion *within* and *across* the three different layers comprising the interbank market.

Agent behaviour on networks: Prior to the crisis, the dominant behavioural paradigm for answering policy questions at the macroeconomic level was the so-called New-Keynesian Dynamic Stochastic General Equilibrium (DSGE) class of models. Exemplified by the prototypical model of Smets and Wouters (2003), this approach allowed for nominal rigidities, methods for evaluating the effect of monetary and fiscal policies and most importantly, estimation using real data while also showing strong forecasting performance. However, such models came under heavy criticism following the crisis due to their inability to deal with nonlinearity and lack of a banking/financial sector (Blanchard, 2014). As summarised in the recent survey by Christiano et al. (2018), there has been a concerted effort to amend pre-crisis DSGE models by introducing various financial frictions and nonlinearities, an active banking sector and information asymmetries and heterogeneity into the canonical modelling framework. Blanchard et al. (2016) and Lindé (2018) adopt a similar viewpoint: That despite their flaws, DSGE models are still best suited for thinking about aggregate phenomena and policy. As a result, the New-Keynesian DSGE framework with financial frictions, such as the models of Gertler and Kiyotaki (2010) and Christiano et al. (2014) have retained their place within the modelling toolkit of almost all central banks.

However, a number of prominent academics argue that such models are erroneous by construction. Notably, then Chief Economist of the World Bank Paul Romer, in an essay entitled "*The trouble with macroeconomics*", argues that the excessive reliance on autocorrelated exogenous shocks to drive model dynamics precludes their usefulness as policy tools. The stochastic element (i.e. the treatment of uncertainty) in DSGE modelling is also highlighted as a key shortcoming by Stiglitz (2018) in addition to the "*wrong microfoundations which failed to incorporate key aspects of economic behaviour, e.g. incorporating insights from information economics and behavioural economics*".

The ensuing drive to redefine the behavioural foundations of macroeconomics led a number of researchers to the field of Agent-Based Modelling[12] which treats the economy as a complex, adaptive system in which the interaction of autonomous, heterogenous agents gives rise to macroeconomic regularities (Tesfatsion and Judd, 2006). Due to rapid advances in computing power in recent years, Colander et al. (2008), Farmer and Foley (2009) and Chan-Lau (2017) argue that ABMs provide an ideal framework for looking at macroeconomic dynamics due to the interactions of individual behaviours at the microeconomic level. Moreover, given that such models are essentially *computational* in nature and driven by simple behavioural rules of thumb (referred to as *heuristics*), they are unencumbered by the assumptions of neo-classical models such as representative agents, rational expectations and convergence to an equilibrium state that characterise the current workhorse DSGE models of most major central banks. This affords researchers the flexibility to incorporate a wide array of dynamics in order to understand the impact of various policies on economic performance and the manner in which risks can develop and spread in cases of widespread panic. Moreover, the modelling framework allows ABMs to be easily integrated into state-of-the-art network models.[13]

To date, ABMs have been developed to study the 1997-2008 housing boom and ensuing crash (Geanakoplos et al., 2012), the impact of network topology on systemic risk in interbank markets and the stabilising role played by the central bank (Georg, 2013) and the deleterious impact of high inflation on macroeconomic performance Ashraf et al. (2016). As mentioned previously, the ABMs developed by Halaj and Kok (2015) and Poledna et al. (2017) were also designed to answer key policy questions regarding the impact of large exposure limits on counterparty credit risk and the recent Basel III drive to classify banks as G-SIBS using an indicator/bucketing approach, respectively. Hałaj (2018) builds an ABM focussing on the relationship between bank solvency and liquidity combined with an analysis of the efficiency of two policy instruments aimed at mitigating systemic risk: banks' capital adequacy and the Basel III Liquidity Coverage Ratio (LCR).

[12]This debate was acknowledged in a July 2010 article in *The Economist* entitled "Agents of change" which highlighted the potential of ABMs to learn from the past crisis and develop an early-warning system for the next one. Insofar as real applications are concerned, Gode and Sunder (1993) show that non-rational behaviour of zero-intelligence traders yields allocation outcomes close to those predicted by neo-classical economics. Similarly, LeBaron (2001) builds on the famed Santa Fe artificial stock market ABM consisting of agent heterogeneity by trading rule and memory. Despite the parsimonious modelling framework, the author is able to generate return, volume, and volatility values remarkably similar to actual financial time series.

[13]Incorporating agent behaviour was recognised as the "next frontier" in network models by policymaker Jaime Caruana (General Manager, Bank for International Settlements) at a BIS research network meeting on global financial interconnectedness in October 2015

The present thesis is firmly situated at the nexus of these two subfields. Each chapter develops a novel methodology incorporating at least one of the two, with the third combining a *realistic* (in the topological sense) simulated bilayer network with an original Agent-Based Model of the interbank market.

Structure of the thesis

The thesis comprises three chapters revolving around a common narrative positing that the structural simplicity, granularity and holistic nature of network analysis can shed light on the most pressing policy issues of the day. Using the interbank market as a backdrop, we develop three theoretical models in which interconnectedness between banks, as represented by a network, plays a front-and-centre role in driving model dynamics. Each of the chapters is grounded in the application of networks to financial stability analysis in a different way, each time seeking to address a major policy-framed research question:

Chapter 1: To what extent did the *structure* of the interbank network impair the transmission mechanism of monetary policy and what was the impact on wholesale and retail markets?

Chapter 2: How does *network topology* affect systemic risk, defined as the ability of a localised shock to spread through the interbank market and engender widespread losses on bank balance sheets?

Chapter 3: Why did interbank markets freeze during the crisis despite an unprecedented level of policy intervention?

Definitions

Several interrelated concepts are repeated throughout the thesis and play an important role in developing the analytical framework of each chapter. In order to provide a unified framework for the thesis, key definitions, as well as their application in each chapter, are provided below.

Financial stability: Recognising the ambiguity of the term and the wide range of definitions in the literature, Schinasi (2004) of the IMF provides the following definition: "*A financial system is in a range of stability whenever it is capable of facilitating (rather than impeding) the performance of an economy, and of dissipating financial imbalances that arise endogenously or as a result of significant adverse and unanticipated events*". This is broadly in line with how the stability of the interbank networks in each chapter is treated. In chapter 1, financial stability encompasses reductions in bank lending, firm

credit and increasing policy intervention due to localised banking shocks. In chapter 2, similar local shocks threaten the stability of the network as they propagate via complex linkages in the interbank network. Finally, chapter 3 studies the stability of the interbank market in the face of endogenous shock propagation.

Systemic risk: A first comprehensive definition of the term was provided by The Group of Ten (2001), stating that "*Systemic financial risk is the risk that a [sudden or unexpected] event will trigger a loss of economic value or confidence in, and attendant increases in uncertainty about, a substantial portion of the financial system that is serious enough to quite probably have significant adverse effects on the real economy...generally seen as arising from disruptions to the payment system, to credit flows, and from the destruction of asset values*". Note that while the two definitions are intrinsically related (in that increasing systemic risk implies decreasing financial stability), systemic risk focusses on the contribution of individual financial institutions to potential financial (in)stability and gives rise to the concept of "too interconnected to fail" typically used in the financial regulation literature to indicate institutions that, due to the high number of systemic interlinkages, would cause widespread disruptions to the financial system if they failed. Applied to financial network analysis, it can be reinterpreted as the "robust yet fragile" property defined below.

Robust-yet-fragile property: As mentioned, this was a concept first articulated by Haldane (2009) within the context of financial network analysis. Though the original definition outlined a range of shock sizes within which "*connections serve as shock absorbers and connectivity engenders robustness*" and above which "*the system [flips to] the wrong side of the knife edge*" and above which fragility prevails, the article also makes the link between long-tailed degree distributions (i.e networks containing a small set of highly-connected hubs) and the susceptibility of the network to random vs. targeted shocks. Chapter 2 analyses all these aspects (network structure, shock size and random vs. targeted shocks) in turn, thereby providing a comprehensive analysis of the topic. By contrast, chapters 1 and 3 focus primarily on agent behaviour *within* the network.

Network structure: Throughout the thesis, the term is used along with 'network topology', the key difference between the two being that the latter refers either to specific *quantifiable* features of the network i.e. network measures such as the degree distribution, density etc or topological features such as the degree distribution or core-periphery structure. By contrast, network structure is used in a more general sense to describe the network as a whole.

Chapter summary

Network simulation

As mentioned above, each of the chapters uses a different methodology to answer a policy-relevant research question. However, they exhibit one common narrative namely, the use of realistic and exogenous simulated interbank networks where realistic refers to the following empirical findings outlined in the 'mapping interbank networks' section:

- **Disassortative mixing**: Both chapters 2 and 3 make use of a probabilistic simulation algorithm developed by Montagna and Lux (2016) to generate disassortative networks.
- **Scale-free degree distribution**: The algorithm mentioned above is capable of obtaining a power-law degree distribution with parameters in line with real-world findings.
- **Core-periphery structure**: Chapter 1 uses a highly-stylised representation of the core-periphery structure in order to isolate the transmission effects within a DSGE model. The more complex networks in Chapters 2 and 3 follow a core-periphery structure by virtue of the disassortative property.

I justify the assumption of an exogenous i.e. imposed network structure by citing the relationship lending literature documented above. That is, the core-periphery networks in which the three theoretical models are embedded can be said to be the result of the process of banks' optimising their interbank linkages prior to the running of the models.

Chapter 1

In the **first chapter**, we analyse the impairment of the transmission mechanism of monetary policy through the lens of an RBC-DSGE model featuring an active banking sector. Our contribution comes through the development of a novel methodology for combining the established field of DSGE modelling with the nascent field of financial network analysis. From a modelling perspective, this involves (*i*) incorporating the structure of the network into the microfounded behaviour of banks and (*ii*) establishing the framework through which aggregate fluctuations arise as the endogenous outcome of micro shocks propagating across interbank market linkages. As regards the latter point, our approach

is thus firmly embedded within the growing literature aimed at elucidating the "*network origins of aggregate fluctuations*" (Acemoglu et al., 2012).

The DSGE model is based on De Walque et al. (2010) whose microfoundations we modify to reflect banks' role as intermediaries between depositors and firms on the retail market. In addition, banks can request and provide wholesale funding on the interbank market, which is where we introduce the network. Building on the seminal models of Allen and Gale (2000) and Freixas et al. (2000), the economy comprises four *blocs* (which can be interpreted as countries or regions) each of which includes a local household, firm and bank. Each local bank combines wholesale (from connected banks) and retail funding (from depositors) to extend credit to firms for productive investment. The model includes a number of features that makes it relevant as a crisis-modelling tool and within a regulatory policymaking context. Firstly, it allows for endogenous loan defaults from banks as well as firms. In addition, macroprudential policy is considered via a capital requirement featuring endogenous risk weights and a number of disincentives to deviating from the regulatory requirement. Most importantly, the model incorporates a central bank who injects liquidity into the banking sector in order to correct liquidity imbalances on the interbank market, closely mirroring the refinancing operations used by all major inflation-targeting central banks to steer short-term interest rates.

Turning now to the main contribution of the paper, we propose four different structures for the underlying network of established lender/borrower interbank relationships: a *complete* network (i.e. maximally connected such that all banks lend to and borrow from all other banks), a *cyclical* network and two variations of the *core-periphery* topology. The core-periphery structure is central to the paper for two reasons: (*i*) it introduces a degree of realism into the model given that real-world interbank networks are known to exhibit such a *tiered* structure and (*ii*) it allows for heterogeneity derived from a bank's position in the network (i.e. as the core bank intermediating between peripheral banks or as a peripheral bank providing liquidity to or requesting liquidity from the core bank). System dynamics are driven by two types of negative shock: A standard aggregate productivity shock affecting firms in *each* bloc which we treat as the baseline and a localised banking shock hitting *one* of the four banks. The location of the shock in the network, combined with the network structure being used thus affects its propagation properties, the stability of the banking sector in the face of such a shock and finally, the impact on credit to the real economy.

Despite the novelty of the approach, the results assessing the impact of the different structures on network topology are largely intuitive. We find that the *complete network*

plays a stabilising role as banking sector shocks dissipate through the large number of linkages, ultimately reducing their effect. The *cyclical* network provides insights into shock propagation between indirectly connected nodes. However, the main focus is on the core-periphery structure given its real-world relevance. In line with the literature, we identify a robust-yet-fragile property associated to this structure: Shocks to the core create large and persistent fluctuations in interbank default rates and lending/borrowing volumes. Turning to the ability of the central bank to stabilise the system, core-periphery networks require the largest intervention. By contrast, complete networks again, act as a system stabiliser.

Chapter 2

Chapter 2 abstracts from a detailed representation of bank behaviour, instead shifting the focus to the implications of *network structure* on financial stability. Though numerous works have highlighted the impact of the "*robust-yet-fragile*" property of financial networks on systemic risk, they have typically relied on a simplistic representation of the interbank network. Against this backdrop, the models of Nier et al. (2007), Gai and Kapadia (2010) and May and Arinaminpathy (2010) were amongst the first to study financial contagion and systemic risk as well as the impact of random vs. targeted shocks within the context of complex networks. However their reliance on the *random* network archetype precludes their usefulness as policy tools due to the inability of random networks to replicate known topological features of interbank networks such as: the small-world effect, scale-free degree distribution, disassortative mixing and a core-periphery structure (Hüser, 2015).

Models of *cascading defaults*, initially derived from disciplines such as ecology and epidemiology (Haldane, 2009), are based on the concept that interbank exposures act as channels along which asset- or liability-side shocks are transmitted between banks. Their ability to *absorb* the shock depends on their capital buffer. Failure to absorb the shock implies further propagation through the pattern of interlinkages. This gives rise to the notion of *default cascades* in which the local shock can engender widespread systemic defaults as the shock propagates through then network. Central to this argument is the structure of the network and the predominance of risk-sharing vs. risk-spreading in financial networks, as discussed previously. I argue that a deeper topological analysis is needed in order to gauge the systemic potential of the network. Using the probabilistic network generation model developed by Montagna and Lux (2016) as a starting point, I calibrate

the range of parameters for the bank size distribution, balance sheet decomposition and network structure, taking observed topological properties of real interbank networks as a benchmark. These are then fed into a Latin Hypercube Design in order to produce a large sample of "realistic" interbank networks.

The first part of the analysis is theoretical in nature and entails running two variants of the cascading defaults model on each of the simulated networks. Specifically, I contribute to the study of the robust-yet-fragile property of financial networks by comparing a random (where the initial seed is any one of the nodes in the network) with a targeted shock. In the latter setup, the shock is restricted to an upper quantile of banks in terms of size (and by construction, interconnectedness). In order to keep the paper in line with the state-of-the-art in financial network analysis, I incorporate the observation by Upper (2011), Summer (2013) and Glasserman and Young (2015) that direct exposures alone are not a significant contributor to systemic risk by allowing for *liquidity effects* in which a bank's failure (occurring when the incoming shock wipes out its capital, rendering it insolvent) forces it to liquidate its assets, also referred to as a firesale. Acknowledging that that market's ability to absorb these assets is imperfect, firesales drive down asset prices which forces *all* banks in the system to revalue their portfolios. Where contagion via banks' interbank linkages can be considered a *direct* transmission channel, contagion through liquidity effects is indirect as its impact on other banks operates independently of the web of exposures.

The results of the theoretical model can be classified into two sets of variables. The first set describes the outcome of the cascading defaults model namely, the total capital wiped out as the shock propagates through the banking sector, number of failed banks, total losses on customer deposits and change in asset price (when liquidity effects are active). The second applies tools from the social network analysis discipline to ascribe numerical values to certain topological features of the network. This comprises *global* structural properties: density, diameter, reciprocity, assortativity, average path length and average clustering coefficient as well as *local* properties (applied to the set of initially shocked banks) via various *centrality measures* aimed at measuring node importance within the network. Similar to the global analysis, the centrality measures used (degree, closeness, betweenness and pagerank) capture different structural features of the network.

The results of the theoretical model described above constitute a dataset on which we develop an empirical model aimed at establishing a causal link between network topology and financial stability. From a policy perspective, this allows for an ex ante measurement of the *systemic risk* associated to a particular network structure. To my knowledge, this

paper provides a first attempt at identifying specific topological features of the network (in terms of the global and local measures proposed above) that pose a danger to financial stability. This builds on the literature studying the link between connectivity and systemic risk while also enhancing the real-world applicability of the cascading defaults model through our use of a realistic interbank network structure.

Chapter 3

The **third chapter** is a culmination of the first two and hence, offers a completely novel approach to studying the complex behavioural dynamics of the interbank market within a state-of-the-art network representation. As regards the latter point, the most recent interbank network models acknowledge that banks interact with one another in a variety of ways which are not captured by the simple directed exposure network. As a result, this paper contributes to the nascent literature on *multilayer* networks by considering two types of interdependency: direct exposures via interbank lending and borrowing and indirect exposures via banks' common holdings of certain securities (which I refer to as *overlapping portfolios*. However, unlike the previous chapter, the network structure is not the primary focus. Rather, the bilayer network houses an *Agent-Based Model of the interbank market* in which agents/banks interact according to a set of simple behavioural rules, referred to as *heuristics* or rules-of-thumb. Unlike the cascading defaults methodology described above these models are at an extremely early stage of development, given the additional computational complexity and the lack of a an established, concrete methodology for presenting the results of the simulations. The most relevant papers to date are Georg (2013), Iori et al. (2015) and Halaj and Kok (2015), all of whom also ground the ABM in a simulated network. However, this paper is the first to provide an encompassing model of interbank market dynamics. Against this background, this model develops *inter alia* a detailed representation of balance sheet movements due to bank behaviour, a thorough treatment of interbank market dynamics in terms of volumes as well as rates and a new approach to indirect contagion based on the relationship between the interbank market and external asset firesales.

Interbank market dynamics are driven primarily by two heuristics aimed at capturing the funding liquidity and counterparty risk of banks. The former is driven by banks' concern regarding their own ability to attract interbank funding while the second is associated to the creditworthiness of borrowers. All heuristics are constructed in the form of adaptive expectations based on actual definitions. In addition, all heuristics are grounded where

possible, on behavioural foundations from the established banking literature in order to reduce the *ad hoc* nature of the model. This flexibility is one of the main advantages of the ABM framework.

In line with the rest of the thesis, this chapter revolves around a concrete policy issue. Focussing on the period around the Lehman Brothers collapse in September 2008 (which triggered the global financial crisis), a puzzle has emerged asking why the interbank market underwent such severe strains despite an aggressive and unprecedented level of intervention by monetary authorities. Finding that the theoretical and empirical literature has, at present failed to each a consensus regarding the predominance of liquidity or counterparty risk in driving these tensions, I argue that ABMs offer the ideal modelling environment given their ability to encompass a wide variety of complex dynamics within a relatively simple behavioural specification.

To answer this question, I build a computational model in which banks go to the interbank market as lenders or borrowers in each period depending on the realisation of an idiosyncratic liquidity shock. Interbank volumes and weights are determined by the behavioural heuristics which are constructed to reflect banks' evolving funding and counterparty risk. As such, I construct an economy from the "*bottom-up*" in which autonomous agents, driven by these behavioural heuristics go about their daily business of making private sector investments, remunerating depositors and receiving return from their securities portfolios while using the interbank market to meet their daily liquidity needs. These actions are disrupted through the introduction of a *crisis period* imposed on the banking sector and characterised by falling asset prices and market liquidity. I present the results along the lines of two counterfactual *policy experiments*. In the first, the crisis is allowed to develop unchecked. The second introduces the extreme liquidity provision by the central bank in order to restore interbank market functioning and ensure continued credit to the private sector. This is constructed to mirror the *fixed rate full allotment policy* of the ECB.

The crux of my argument is based on the fact that these policies were deployed after a delay of about one month following the onset of the crisis (which I corroborate using actual data). As a result, funding liquidity and counterparty risks were allowed to develop and feedback on one another, thereby reducing the effectiveness of the policy. However, the counterfactual approach also reveals a complete breakdown of the interbank market followed by a credit crunch in the absence of any kind of intervention.

Computational Economics

In addition to providing a novel modelling framework for understanding financial stability and systemic risk, this thesis is also firmly situated in the *computational economics* tradition, defined by the Society for Computational Economics as a "*multidisciplinary field that uses advanced computing capabilities to understand and solve complex problems from all branches of economics*". Against this background, each chapter of the thesis uses computational methods to run the model and output relevant results. Given the growing importance of network analysis in the policy-sphere, I have developed an extensive and documented code base (primarily in MATLAB) written in a modular fashion for ease-of-use which I have placed in the public domain for end-users to calibrate and modify according to their specifications. Below, I provide the most relevant functions for each chapter.

Chapter 1 - https://github.com/nscholtes/NDSGE.: The code is written primarily on the Dynare platform (http://dynare.org) with each network structure requiring its own set of `.mod` files. Taking the complete network as an example, the top-level file, `compnet` contains the parameter values, steady state equations and first order conditions of the DSGE model and calls the following subfiles:

- `liqinjvardefs_ comp`, `liqinjvareqs_comp`, `liqinjvarinit_ comp`, `liqinjvarexo`: Liquidity injection variable definitions, equations and initialisation;
- `shockpardefs`, `shockpareqs`, `shockvardefs`, `shockvareqs`, `shockvarinit`: Parameter and variable specification under the two shock specifications.

Chapter 2 - https://github.com/nscholtes/Default-Cascades: Uses object-oriented programming to define a set of 'bank' structured arrays storing information on their balance sheet and location within the simulated network. The top-level file, `topsim2`, contains all exogenous parameters and calls the following subfiles:

- `createLH`: Latin Hypercube Design to sample from the parameter space;
- `netgen2`: Simulates the directed network;
- `networkmeasures`: Makes use of the brain connectivity toolbox located at https://sites.google.com/site/bctnet/ for various network measures;
- `cascadingdefaults`, `cascadealgorithm`: Initiates the random/targeted shock and provides the algorithm by which the shock propagates through the interbank network.

The results outputted by the `networkmeasures` and `cascadingdefaults` functions are combined and saved as a cross-sectional table. This is then called by a set of R codes, located at https://github.com/nscholtes/Cascading-defaults--regressions which provide the results of the empirical model.

Chapter 3 - https://github.com/nscholtes/Confidence-Crises. Similar object-oriented approach to Chapter 2. However, the behavioural heuristics and changing network structure create more complex bank objects. The top-level file, `topsim`, contains all exogenous parameters and calls the following subfiles:

- `netgen`: Simulates the undirected network;
- `phase0`, `phase1`, `phase2`, `phase3`: Contain the model dynamics developed in the chapter. The phases are run sequentially , with the output from one phase being passed as input to the next phase. The phases are looped over a fixed number of simulation periods;
- `Results_ balancesheet`, `Results_ IBM`, `Results_ failures`, `Results_ securitiesmarket`: Aggregates the bank-level results and outputs different sets of results over the simulation period.

Summary

Though each chapter views the networks-financial stability nexus from a different angle, there are a number of overlaps in the general modelling framework, which I summarise in the schematic below:

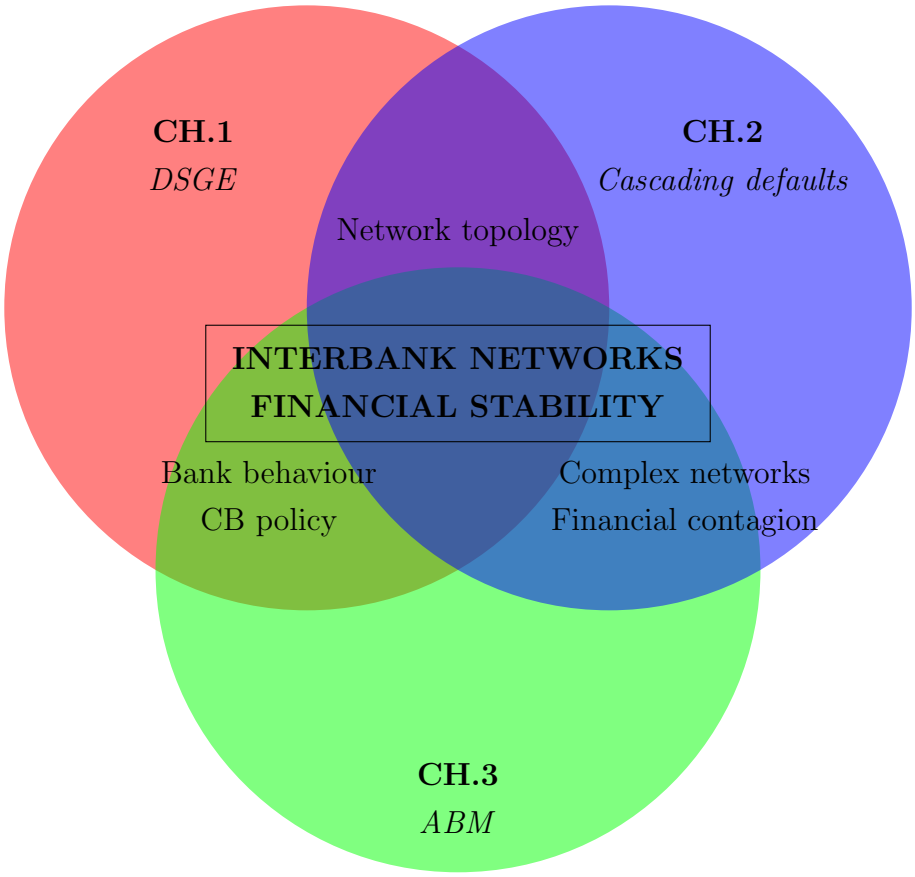

Starting with chapters 1 and 2, it is clear that both revolve around analysing the impact of network structure on financial stability and systemic risk. However, where chapter 1 couches a highly stylised four-node network within a sophisticated DSGE model featuring a microfounded banking sector, chapter 2 expounds upon the relationship between network topology and systemic risk through the use of network measures derived from statistical mechanics and social network analysis while abstracting from bank behaviour through the use of a mechanical cascading defaults model.

Chapters 2 and 3 make use of the same probabilistic network generation model in which the nodes are recast as heterogeneous bank balance sheets. Though the dynamic models of bank behaviour subsequently imposed on the networks are different in terms of scope and

complexity, a key difference is already built into the network generation stage. Specifically, chapter 2 simulates a *weighted, directed network* where lending/borrowing relationships and volumes are established ex ante. By contrast, the initial network in chapter 3 is *unweighted* and *undirected*, the purpose being to impose these features as the outcome of a complex model featuring idiosyncratic liquidity shocks and banks' use of heuristics to drive their behaviour on the interbank market. Thus the network in chapter 3 is introduced simply to house the Agent-Based Model. Unlike chapter 2, we do not attempt to derive the causal impact of network structure on model dynamics.

The comparison of chapters 1 and 3 is saved for the end given the competing philosophies underpinning DSGE and ABM. First and foremost, both are aimed primarily to shed light on banking sector dynamics in times of crisis and the role played by interconnectedness in exacerbating/mitigating these dynamics. However, where chapter 3 uses a topologically-realistic and complex multilayer to house the behavioural model, the network in chapter 1 is presented in a highly-stylised, four-node form due to limitations of the DSGE approach. Nevertheless, the novelty of introducing interconnectedness and financial contagion into a DSGE model provides an alternative canonical framework on which future work (for example, introducing nominal frictions into the model) can build. By contrast, chapter 3 develops a highly-computational model in which all data related to bank balance sheets, bilateral transactions, asset firesale volumes etc. are stored either as matrices (in the case of interactive variable such as interbank lending and repayment volumes) or structured arrays. Unlike DSGE modelling, where results are typically presented as Impulse Response Functions (IRFs), no such framework exists for ABM. Thus, despite both chapters incorporating bank balance sheets, interbank market activity and central bank policies, they differ substantially in the simulation methodology and the manner in which the results are presented.

Overall, the thesis makes the case for the use of networks in systemic risk modelling by highlighting the flexibility and versatility of these approaches. By attacking the problem on two fronts (network structure and behaviour on networks), the work is situated firmly within the state-of-the-art in financial stability analysis. Moreover, each chapter is framed as a theoretical response to a relevant policy question in order to highlight the tractability of the framework and place the thesis within the growing academic literature recognising the key role played by interconnectedness in the current economic and financial landscape.

Chapter 1

Assessing the role of interbank networks in business and financial cycle analysis

1.1 Introduction

In the aftermath of the global financial crisis, there was a strong drive amongst academics and policymakers alike to better understand the role of the financial sector as a source of macroeconomic fluctuations as well as the various amplification mechanisms associated to financial shocks (Adrian et al., 2013). Moreover, there has been a renewed interest in modelling the *supply*-side of credit markets in order to highlight the important role played by banks in driving the business cycle. From a macroeconomic modelling perspective, this has led to a reappraisal of the demand-side credit market frictions developed by Kiyotaki and Moore (1997) and Bernanke et al. (1999) while recognising the caveat related to the reliance on Modigliani and Miller (1958) irrelevance in assuming away supply-side conditions revolving around bank behaviour in credit markets. Finally, economic models post-crisis are being tailored to reflect the current economic climate, characterised by increasing financial system regulation and central bank interventions.

Parallel to these developments in macro-financial modelling, the notion that financial system *interconnectedness* can impair financial stability has opened up a research agenda seeking to apply tools from the *network theory* literature to study the threats to systemic risk posed by the various types of financial interdependence. Broadly speaking, the majority of papers in this literature aim to quantify the role of the network structure (commonly referred to as its *topology*) as a shock propagation and amplification mechanism. The seminal contribution by Allen and Gale (2000) finds that increasing the density of linkages between financial institutions has a mitigating effect on the propagation of liquidity shocks to individual banks. More recently, Elliott et al. (2014) and Acemoglu et al. (2015) develop models of cascading defaults wherein the network structure and the location of the shock in the network determine the extent of financial contagion.

This paper provides, to the best of our knowledge, a first attempt at reconciling these two seemingly unrelated developments by proposing a framework for combining the network structure of the interbank market with a macroeconomic model that *inter alia* allows for interactions between the banking sector and the wider economy as well as imperfections in interbank and credit markets. To this end, we develop a microfounded framework that incorporates an active banking sector and interbank market into a dynamic stochastic general equilibrium (DSGE) model. This is combined with the network interpretation of the interbank market by treating the pattern of interlinkages between banks as given. Consequently, the manner in which banks are connected in the network is mapped into the bank microfoundations by conditioning the set of variables associated to interbank transactions *viz.* lending, borrowing and endogenous default choices on the set of counterparties given by the network.

The macroeconomic framework is based on De Walque et al. (2010) (hereafter, WPR) who develop a DSGE model of the real business cycle (RBC)-variety while allowing for an endogenous banking sector, bank regulation (in the form of a capital requirement) and monetary policy through liquidity injections into the interbank market. Before introducing the networks dimension, we modify their construction of a heterogeneous banking sector, comprising deposit and merchant banks (interbank lenders and borrowers, respectively) by combining them into one bank who intermediates between households and firms. Following this, the key contribution of the paper is the application of the stylised four-node network methodology of Allen and Gale (2000) and Lee (2013), which we use to construct four representative interbank networks: 1) a complete network 2) a cyclical network and 3) two variations of the core-periphery topology. The structure is thus imposed exogenously and dictates the pattern of lending and borrowing counterparties.

As stated by Goodhart et al. (2006), the interactive dimension of bank behaviour is crucial from a financial stability perspective as well as for the design and implementation of monetary policy and (macro)prudential requirements.[1] The manner in which networks are introduced into the DSGE methodology is flexible enough that it factors into the policy aspect as well. Specifically, our regulatory framework consists of a capital requirement combined with a linear utility term for holding a capital buffer in excess of the regulator-imposed minimum. The network is featured via the dynamic risk-weights associated to interbank lending which are driven by banks' expectations on their (network-determined) counterparties loan repayment ability. In addition, the monetary authority injects liquidity on a bilateral basis wherever there is a mismatch between supply and demand of interbank funding. Consequently, each link in the network constitutes a market (in which a price, the interbank rate, is formed). As a result, the number and structure of the links in the network affects the impact of monetary policy.

Though the paper draws primarily from WPR, there is a growing literature incorporating a banking sector into DSGE models[2]. Within this framework, they introduce various endogenous financial frictions and an active interbank market. Notably, Gertler and Kiyotaki (2010) introduce credit market frictions in both the retail and wholesale financial markets as well as a comprehensive analysis of Federal Reserve credit policies. Another strand of research adds a layer of realism by introducing imperfect competition in the form of '*market power*' into bank behaviour. Such an approach has been applied by Gerali et al. (2010) and Dib (2010) and Pariès et al. (2011), who also incorporate regulation in the form of a capital-based measure. The role played by financial shocks in driving business cycle fluctuations is studied in Christiano et al. (2010).

[1] From a regulatory standpoint, the Basel III reforms identify interconnectedness as one of the five categories for determining global systemically important banks (BCBS, 2010).

[2] The interested reader is referred to Vlcek and Roger (2012) for a comprehensive survey of their use at various central banks.

Due to the growing availability of increasingly granular financial datasets, researchers have begun exploring the structure of real interbank networks in order to gain a better understanding of the shock propagation mechanisms at play along with the associated risks to financial stability. As documented in the introduction of the thesis, a common thread that has emerged across various studies is that interbank networks exhibit a *tiered* or *core-periphery* architecture wherein a small set of large 'core' banks intermediate between a larger set of smaller 'peripheral' banks who do not interact amongst themselves. The systemic implications of such a configuration are evident, as shown in the theoretical model of Freixas et al. (2000) who study the impact of central bank liquidity interventions in the presence of a large money center bank. Within the context of our modelling framework, the core-periphery topology allows us (*i*) to explore the implications of a real-world topology (*ii*) introduce heterogeneity (via banks' *position* in the network) into the system and (*iii*) explore dynamics related to the *location* of shocks in the network. In order to provide a benchmark for the core-periphery structure, the model is also run on the complete and cyclical topologies similar to Acemoglu et al. (2015). Despite the fact that such structures cannot be taken as indicative of real interbank networks, they allow us to compare the systemic impact of increasing connectivity, as done by Allen and Gale (2000) as well as the feedback effects of localised shock propagation. A similar structural analysis is undertaken by Roukny et al. (2016) within the context of a cascading defaults model (similar to chapter 2 in this thesis) wherein multiple equilibria give rise to uncertainty in systemic risk measurement.

Our choice of WPR as a modelling benchmark is driven by our desire to shed light on the macroeconomic impact of the *structure* of the interbank market. By abstracting from the more complex modelling approaches and frictions mentioned above, we are able to zoom in on the network drivers of economic and financial fluctuations. Broadly speaking, our model can be summarised as follows: We introduce four 'regions' that raise liquidity on the *inter*-regional wholesale market, characterised by a specific network structure, in order to complement *intra*-regional deposits used to finance *intra*-regional credit[3].

[3]In this regard, our model is similar to the region-specific DSGE with banking sector models developed by Brzoza-Brzezina et al. (2015) and Bokan et al. (2016).

The results of our model are presented in two steps: first we compare the effect of adding a regional banking shock to a baseline scenario consisting of four productivity shocks across all regions under the different network structures. Herein, we study the impact of each imposed network on the dynamics of *interbank* variables. The second step compares the networks directly by analysing the responses of aggregated (that is, summed across all four regions) variables from the real economy. In this section, we provide a policy perspective by comparing model dynamics when banks are subject to liquidity injections by the central bank.

Our results highlight the importance of taking the network into account when studying economic fluctuations, a key reason being that local shocks are easily transmitted via banks' interlocking exposures. Thus, a bank not itself subject to a shock can still be affected through its network of counterparties (and their counterparties etc.). This is made clear in the interbank dynamics under the cyclical and core-periphery topologies. The latter is prone to large potential instability when the core bank is constrained by the network structure, thereby limiting its ability to obtain wholesale funding. By contrast, the complete network performs a stabilising, *dissipative* role due to the large number of links. Turning to the policy side, we observe that the impact of liquidity injections varies depending on the network. The complete network is again, subject to relatively smaller downturns while the remaining structures require stronger central bank intervention.

The rest of the paper is structured as follows. Section 1.2 develops the model's micro-foundations, section 1.3 outlines the imposed network structures, section 1.4 provides the calibrations used, section 1.5 reports the results and section 1.6 concludes.

1.2 The Model Economy

Following Allen and Gale (2000), the economy is divided into four ex-ante identical regions $i = \{A, B, C, D\}$. Each region consists of a household and firm who act as lenders and borrowers of funds, respectively. In addition, we introduce a regional banking sector which finances lending to firms through access to two markets. In the retail financial market, banks obtain deposits from households within the same region while the wholesale financial market allows banks across regions to raise funds by borrowing and lending amongst themselves.

The microfoundations in our model are based primarily on De Walque et al. (2010). However, in addition to the aforementioned regional structure, our approach differs in a number of ways. Firstly, we depart from the notion that banks perform a specialised function as either originators or receivers of funding stemming from household deposit supply and firm credit demand, respectively. In this setup, the interbank market arises to restore equilibrium between banks with a liquidity surplus and those in deficit. By contrast, the banks in our approach perform a dual role by intermediating between regional households and firms and lending/borrowing on the wider interbank market. As such, each regional bank is subject to counterparty default on credit markets (by firms for whom the repayment rate is endogenous) as well as on the interbank market, where borrowing banks feature an endogenous repayment rate on past interbank loans. Other features of the banking sector include own funds commitment, insurance funds and portfolio diversification.

The second major contribution is our use of a stylised, tractable framework for modelling bank interconnectedness across regions. As detailed in section 1.3, the manner in which banks can exchange liquidity is constrained by the network structure. In this regard, two banks i, j can be connected such that i can only borrow from j or vice versa.

The economy is represented schematically in Figure 1.1. In addition to the three types of agents, all flows between them as well as the relevant interest rates are reported. Since our approach allows banks to both lend and borrow on the interbank market simultaneously[4], we compile bank i's lending and borrowing choice vis-à-vis counterparty j into the parameter $\Xi^{b,ij} = \left\{L^{b,ij}, B^{b,ij}\right\}$ for ease of exposition.[5]

[4]The concept that banks enter into long and short interbank positions has been observed empirically, using German balance sheet data, by Bluhm et al. (2016)

[5]Note that the interbank trading parameters given by Ξ capture the maximum number of exposures between banks as represented by the 'complete' network in Figure 1.3(a).

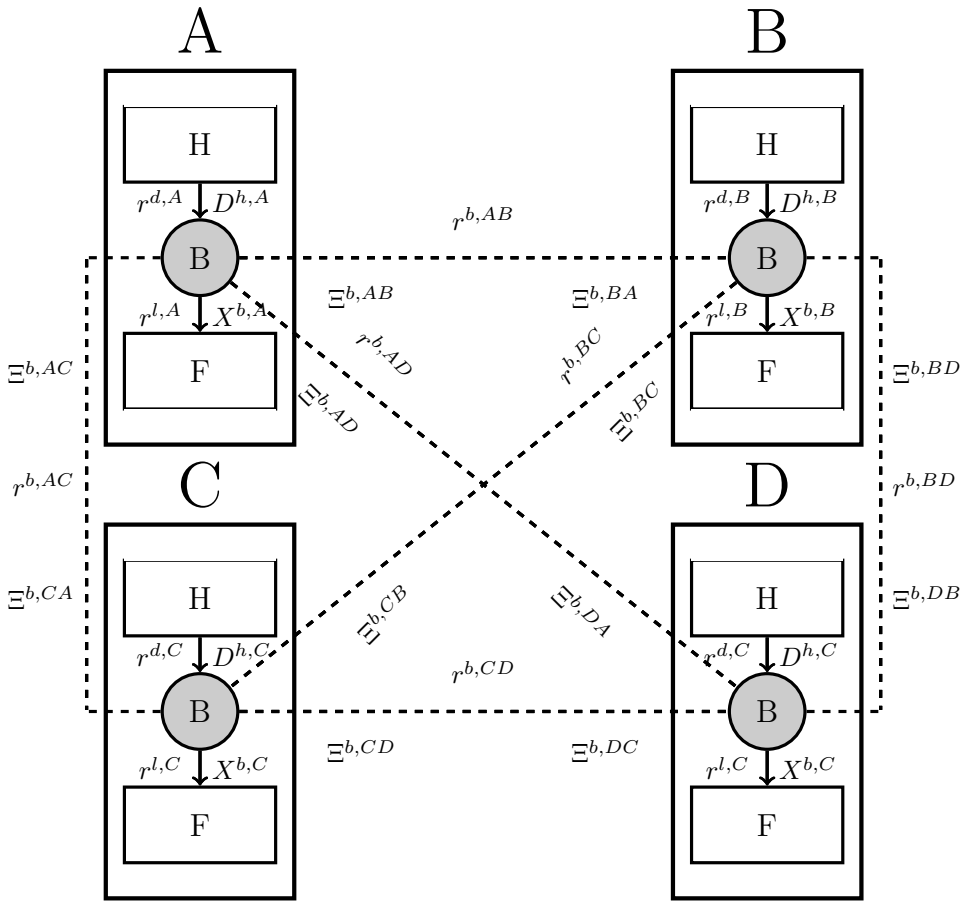

Figure 1.1: Flows between agents within and across regions

1.2.1 Households

The household in region i chooses consumption $C_t^{h,i}$ and deposit supply to its local bank $D_t^{h,i}$ to maximise a logarithmic utility function comprising a quadratic disutility term for deposits. This represents households' preference for a stable level of deposits around their long-run optimum.[6]

$$\max_{\{C_t^{h,i}, D_t^{h,i}\}} \sum_{s=0}^{\infty} \beta^s E_t \left[\ln\left(C_{t+s}^{h,i}\right) - \frac{\chi}{2}\left(\frac{D_{t+s}^{h,i}}{1+r_t^{d,i}} - \frac{\bar{D}^h}{1+r^d}\right)^2 \right] \tag{1.1}$$

[6]The reason for this non-standard convex disutility term is purely technical, as explained in footnote 10 of WPR. Briefly, calibrating a low, positive value for χ ensures that the steady state for $D_t^{h,i}$ is determined while having only a marginal impact compared to the standard setup where $\chi = 0$.

The household budget constraint is given by

$$T_t + C_t^{h,i} + \frac{D_t^{h,i}}{1 + r_t^{d,i}} = w_t N_t + D_{t-1}^{h,i} \tag{1.2}$$

where T_t denotes a lump-sum tax levied on households to finance both liquidity injections into the banking sector by the central bank and an insurance fund that allows banks to recover a fraction of non-performing loans on the interbank and credit market. Finally, we impose an exogenous labour supply $N_t = \bar{N}$.[7] Solving the dynamic problem yields the following Euler equation for consumption (augmented with the deposit target term):

$$\frac{1}{C_t^{h,i}} = \beta E_t \left[\frac{1}{C_{t+1}^{h,i}} \right] - \frac{\chi}{1 + r_t^{d,i}} \left(\frac{D_{t+s}^{h,i}}{1 + r_t^{d,i}} - \frac{\bar{D}^h}{1 + r^d} \right) \tag{1.3}$$

1.2.2 Banks

The primary function of bank i in each region $i = \{A, B, C, D\}$ is the intermediation of funds between depositors (households) and ultimate borrowers (firms). This comprises the retail market of the national financial market. In addition, we allow banks to obtain and provide wholesale funding on the interbank market. Counterparty information is provided by the sets $\mathcal{S}_i$ (*suppliers*) and $\mathcal{D}_i$ (*demanders*) which determine from whom i can obtain funds and to whom i can provide funds, respectively. The expected payoff function of bank i consists of a concave representation of profits, $\pi_t^{b,i}$ less a non-pecuniary disutility cost d_b associated to the endogenous default decision vis-à-vis its interbank creditors, $j \in \mathcal{S}_i$. On the interbank market, the set of endogenous variables for each i thus consists of the default rate $\delta_t^{b,ij}$ on past borrowing as well as current borrowing, $B_t^{b,ij}$ from creditors $j \in \mathcal{S}_i$ and bilateral lending, $L_t^{b,ij}$ to debtor banks $j \in \mathcal{D}_i$. In their role as financial intermediaries, banks choose fund allocation from amongst deposits from households $D_t^{b,i}$ and credit to firms in region i, $X_t^{h,i}$ as well as investment in risky securities, $S_t^{b,i}$. Finally, banks are subjected to a positive linear utility d_{F^b} for the buffer of own funds chosen by the bank

[7] Again, we maintain the assumption of WPR. Though this is contrary to the the majority of the RBC literature wherein labour supply is endogenous, the authors found that the wealth effects generated on impact of the market book shock resulted in countercyclical employment. In order to avoid this counterintuitive result, endogenous employment was considered out of scope.

$F_t^{b,i}$ above the minimum regulatory capital requirement represented by the coverage ratio k as well as the respective risk weights $w_t^{f,i}$, $\left\{w_t^{b,ij}\right\}_{j\in\mathcal{D}_i}$, w_t^S on firm credit, interbank loans and the bank's securities portfolio. The balance sheet of each bank can thus be represented as:

Assets	**Liabilities**
Firm credit (X^i)	Deposits (D^i)
Interbank lending ($\sum L^i$)	Interbank borrowing ($\sum B^i$)
Market book (S^i)	Own funds (F^i)

Figure 1.2: Bank balance sheet

Putting these together yields the following bank maximisation programme:

$$\max_{\left\{\left\{\delta_t^{b,ij},B_t^{b,ij}\right\}_{j\in\mathcal{S}_i},\left\{L_t^{b,ij}\right\}_{j\in\mathcal{D}_i},\ D_t^{b,i},X_t^{b,i},F_t^{b,i},S_t^{b,i},\pi_t^{b,i}\right\}} \sum_{s=0}^{\infty} E_t\left\{\beta^s\left[\ln\left(\pi_{t+s}^{b,i}\right) - d_b\sum_{j\in\mathcal{S}_i}\left(1-\delta_{t+s}^{b,ij}\right) + d_{F^b}\left(F_{t+s}^{b,i} - k\left(w_{t+s}^{f,i}X_{t+s}^{b,i} + \sum_{j\in\mathcal{D}_i} w_{t+s}^{b,ij}L_{t+s}^{b,ij} + w_t^S S_{t+s}^{b,i}\right)\right)\right]\right\}, \tag{1.4}$$

subject to constraints on the profit function, the law of motion of own funds and the dynamic evolution of the capital requirement risk weights:

$$\begin{aligned}\pi_t^{b,i} &= \frac{D_t^{b,i}}{1+r_t^{d,i}} - \frac{X_t^{b,i}}{1+r_t^{l,i}} + (1+\Gamma_t)\,S_{t-1}^{b,i} - S_t^{b,i} \\ &+ \sum_{j\in\mathcal{S}_i}\frac{B_t^{b,ij}}{1+r_t^{b,ij}} + \sum_{j\in\mathcal{D}_i}\delta_t^{b_{ji}}L_{t-1}^{b,ij} + \zeta_b\sum_{j\in\mathcal{D}_i}\left(1-\delta_{t-1}^{b_{ji}}\right)L_{t-2}^{b,ij} + \alpha_t^{f,i}X_{t-1}^{b,i} + \zeta_f\left(1-\alpha_{t-1}^{f,i}\right)X_{t-2}^{b,i} \\ &- \left[D_{t-1}^{b,i} + \sum_{j\in\mathcal{D}_i}\frac{L_t^{b,ij}}{1+r_t^{b,ij}} + \sum_{j\in\mathcal{S}_i}\delta_t^{b,ij}B_{t-1}^{b,ij} + \frac{\omega_b}{2}\left(\sum_{j\in\mathcal{S}_i}\left(1-\delta_{t-1}^{b,ij}\right)B_{t-2}^{b,ij}\right)^2\right]\end{aligned} \tag{1.5}$$

$$F_t^{b,i} = (1-\xi_b)\,F_{t-1}^{b,i} + \nu_b\pi_t^{b,i} \tag{1.6}$$

$$w_t^{f,i} = \tilde{w}^f \left[\left(\frac{\alpha}{\alpha_{t+1}^{f,i}} \right)^{\eta_f} \right] \tag{1.7}$$

$$w_t^{b,ij} = \tilde{w}^b \left[\left(\frac{\delta}{\delta_{t+1}^{b,ij}} \right)^{\eta_b} \right] \text{ for each } j \in \mathcal{D}_i \tag{1.8}$$

Equation 1.5 defines the period profits of bank i. The first line collects the bank's activity on the retail and credit market namely, deposits remunerated at rate $r_t^{d,i}$ less credit to firms at the rate $r_t^{l,i}$ as well as the stochastic return on past securities investment, denoted by Γ_t which follows an AR(1) process, less current purchases. The second line collects the parameters pertaining to an *inflow* of funds in period t. The first two terms outline interbank borrowing from all creditors $j \in \mathcal{S}_i$ and repayment by debtor banks $j \in \mathcal{D}_i$ on past interbank loans. Note that this includes the repayment rate $\delta_t^{b,ji}$ which is featured in counterparty j's optimisation programme and thus, taken as given by i. The insurance fund allows banks to recover a fraction ζ_b of each borrowing counterparty's default on the interbank market. Similarly, each bank is subject to the default of regional firms on credit extended in the previous period. Similar to interbank lending, the repayment rate is exogenous to the bank while an insurance fund allows it to recover a fraction ζ_f of the firm's defaulted amount. Finally, the third line collects all *outflows* of funds. This includes lending on the interbank market as well as repayment on past interbank loans. The latter features the repayment rate parameter $\delta_t^{b,ij}$ which is now endogenous to i. The last term represents the quadratic pecuniary penalty associated to interbank loan default and reflects *inter alia* the reputation costs of defaulting.

Equation 1.6 provides the law of motion of own funds. This consists of contributions to the insurance fund managed by the government (represented by the parameter ξ_b, this is used to recover losses from counterparty defaults) and an exogenous fraction of profits ν_b redirected towards own funds. Equations 1.7 and 1.8 reflect the risk-sensitive credit weights on loans to firms and banks, respectively. Set by the supervisory authority, the risk weights increase as expectations of default increase.

A key feature of our microfounded network model is that the pattern of interlinkages between banks maps into the *number* and *composition* of the policy functions. To be precise, given that each banks' optimisation programme features three bilateral interbank vari-

ables (those superscripted by ij namely, lending, borrowing and default), each additional interbank link thus gives rise to three additional first-order conditions.

The above characterises the relationship between the network and the number of policy functions. The difference in composition occurs when imposing an *asymmetric*[8]network structure where banks differ in the manner in which they're connected to their counterparties. For example, if bank i only lends to bank j, this is reflected in the interbank components of i profit function comprising only $L^{b,ij}$ while removing the borrowing variables $B^{b,ij}$ and $\delta^{b,ij}$ (with the inverse holding for bank j). Another bank in the same network that both lends and borrows would feature all interbank variables.

For the sake of brevity, we compute the first-order conditions assuming the (symmetric) cyclical network topology shown in Figure 1.3(b) wherein each bank i has two distinct counterparties, one from which it borrows (indexed by j) and another to which it lends (indexed by k):[9]

$$\lambda_t^\pi B_{t-1}^{b,ij} = E_t\left[\beta\lambda_{t+1}^\pi\omega_b\left(1-\delta_t^{b,ij}\right)\left(B_{t-1}^{b,ij}\right)^2\right]+d_b \tag{1.9}$$

$$\frac{\lambda_t^\pi}{1+r_t^{b,ik}} = E_t\left[\beta\lambda_{t+1}^\pi\delta_{t+1}^{b,ik}+\beta^2\lambda_{t+2}^\pi\zeta_b\left(1-\delta_{t+1}^{b,ki}\right)\right]-d_{F_b}k\bar{w}_t^{b,ik}E_t\left[\left(\frac{\delta}{\delta_{t+1}^{b,ki}}\right)^{\eta_b}\right] \tag{1.10}$$

$$\frac{\lambda_t^\pi}{1+r_t^{b,ij}} = E_t\left[\beta\lambda_{t+1}^\pi\delta_{t+1}^{b,ij}+\beta^2\lambda_{t+2}^\pi\omega_b\left(1-\delta_{t+1}^{b,ij}\right)^2B_t^{b,ij}\right] \tag{1.11}$$

$$\frac{\lambda_t^\pi}{1+r_t^{l,i}} = E_t\left[\beta\lambda_{t+1}^\pi\alpha_{t+1}^{f,i}+\beta^2\lambda_{t+2}^\pi\zeta_f\left(1-\alpha_{t+1}^{f,i}\right)\right]-d_{F_b}k\bar{w}_t^{f,i}E_t\left[\left(\frac{\alpha}{\alpha_{t+1}^{f,i}}\right)^{\eta_f}\right] \tag{1.12}$$

$$\frac{\lambda_t^\pi}{1+r_t^{d,i}} = E_t\left[\beta\lambda_{t+1}^\pi\right] \tag{1.13}$$

$$d_{F_b}\nu_b = \left(\lambda_t^\pi-\frac{1}{\lambda_t^\pi}\right)-E_t\left[\beta\left(1-\xi_b\right)\left(\lambda_{t+1}^\pi-\frac{1}{\lambda_{t+1}^\pi}\right)\right] \tag{1.14}$$

where λ_t^π is the Lagrange multiplier associated to bank profits and Equations 1.9-1.12 are the Euler equations for interbank lending, borrowing and firm lending respectively.

[8]Throughout the paper, we refer to symmetric networks as those in which each bank features the same number of incoming and outgoing links. In this case, the choice of optimising bank is arbitrary as their interbank policy functions will be identical albeit with different counterparty superscripts.

[9]Appendix 1.A reports the relevant equations for all networks.

1.2.3 Firms

Each firm maximises the discounted sum of expected payoffs by choosing employment, borrowing from its regional bank in the current period and the repayment rate on previous period borrowing, $\alpha_t^{f,i}$ (the default rate from the point of view of the bank). Similar to the bank, defaulters are subject to both a linear disutility cost, d_f as well as a quadratic pecuniary cost on profits, represented by the parameter ω_f. The firm maximisation programme is then given by

$$\max_{\left\{N_t, X_t^{f,i}, \alpha_t^{f,i}, K_t,\right\}} \sum_{s=0}^{\infty} E_t \left\{ \beta^s \left[\pi_{t+s}^{f,i} - d_f \left(1 - \alpha_{t+s}^{f,i} \right) \right] \right\} \tag{1.15}$$

subject to the following constraints

$$\pi_t^{f,i} = A_t Y_t^i - w_t^i N_t^i - \alpha_t^{f,i} X_{t-1}^{f,i} - \frac{\omega_f}{2} \left[(1 - \alpha_{t-1}^{f,i}) X_{t-2}^{f,i} \right]^2 \tag{1.16}$$

$$K_t^i = (1 - \tau) K_{t-1}^i + \frac{X_t^{f,i}}{1 + r_t^{l,i}} \tag{1.17}$$

where Equation 1.16 represents period profits of the firm. A_t is a stochastic AR(1) total factor productivity shock. Each firm produces output using an identical CRS Cobb-Douglas production function with capital and labour as inputs, $K_t^{\mu} N_t^{1-\mu}$. Equation 1.17 is the law of motion of capital with depreciation rate τ and expansion of capital stock financed by firm borrowing from its regional bank.

The first-order conditions are given by:

$$w_t^i = (1-\mu)A_t\left(\frac{K_t^i}{N_t^i}\right)^{\mu} \tag{1.18}$$

$$\frac{\lambda_t^K}{1+r_t^{l,i}} = E_t\left[\beta\alpha_{t+1}^{f,i} + \beta^2\omega_f\left(1-\alpha_{t+1}^{f,i}\right)^2 X_t^{f,i}\right] \tag{1.19}$$

$$X_{t-1}^{f,i} = \beta\omega_f\left(1-\alpha_t^{f,i}\right)\left(X_{t-1}^{f,i}\right)^2 + d_f \tag{1.20}$$

$$\mu A_t\left(\frac{K_t^i}{N_t^i}\right)^{\mu-1} = \lambda_t^K - E_t\left[\beta\lambda_{t+1}^K(1-\tau)\right] \tag{1.21}$$

1.2.4 Central bank and government

Government

As mentioned, the government levies a lump-sum tax on households which is used to fund the insurance scheme (in addition to the period contributions into the fund by banks and firms) against interbank counterparty and regional firm default. We assume that central bank money creation is not financed by the immediate lump-sum tax on households. Rather, we assume that the central bank is not balance-sheet constrained and can thus create real cash balances by itself.

In addition to the standard Ricardian equivalence assumption of fiscal policy, we also assume that each of the four regions is responsible for its own taxation scheme. For the interbank market, this implies that each regional government provides insurance to its own local bank against default to its counterparties in other regions. Thus, each regional government is tasked with minimising outgoing spillovers due to local financial strains. Finally, by treating taxation in a disaggregated manner, we abstract from consideration of the redistributive effects of taxation. The government budget constraint thus comprises four equations (one for each region) of the form:

$$T_t = \zeta_b\sum_{i\in\mathcal{S}}\sum_{j\in\mathcal{D}_i}\left(1-\delta_{t-1}^{b,ij}\right)B_{t-2}^{b,ij} + \sum_{i\in\mathcal{N}}\left(1-\alpha_{t-1}^{f,i}\right)X_{t-2}^{b,i} - \xi_b\sum_{i\in\mathcal{N}}F_{t-1}^{b,i} \tag{1.22}$$

The first two terms in Equation 1.22 collect all payments to banks out of the insurance fund. The last term (in parentheses) denotes payments into the insurance fund (taken out of banks' own funds).

Central bank

Since we restrict our attention to a purely real model, the standard approach to short-term nominal rate setting via a Taylor policy-rule does not apply in this context. In our framework, the central bank injects liquidity into the banking system in order to equalise supply and demand of interbank funding between each pair of connected banks[10]. The general form of central bank liquidity injections is thus given by

$$M_t^{ij} = B_t^{ij} - L_t^{ji}, \quad \forall i, j \in \mathcal{E} \tag{1.23}$$

where $M_t^{ij} > (<)0$ represents an injection (withdrawal) of liquidity by the central bank into (from) the bilateral transfer between banks i and j. We assume no liquidity injections at steady state, $M_t^{ij} = 0$, $\forall i, j \in \mathcal{N}$.

While the above equation signifies how the monetary policy instrument in our setup features in banking sector dynamics, it does not provide the main objective of monetary policy. Following WPR, liquidity injections serve to smooth interbank rate fluctuations relative to their long run value[11] via the following rule:

$$M_t^D = \nu \left(\bar{r}^b - r^b \right) \tag{1.24}$$

As M_t is also driven by autoregressive shocks, we use the superscript D to denote the deterministic component of liquidity injections. The variable $\bar{r}^b$ denotes the average interbank rate. From a network perspective, each directed edge between banks constitutes a

[10] The identity of connected banks depends on the particular network structure applied to represent the interbank market, as will be made clear in Section 1.3

[11] Though highly stylised, this methodology closely mirrors central banks' use of the overnight rate to signal the policy stance and launch the monetary policy transmission mechanism. An early study by Bernanke and Blinder (1992) confirms the importance of the US federal funds rate as an indicator for monetary policy. More recently, Linzert and Schmidt (2011) study the drivers of the widening spread between the EONIA and ECB MRO rate.

market for which a price is determined either purely through market forces (setting $\nu = 0$) or through a combination of market forces and central bank liquidity injections. In this case, the value of $\nu > 0$ represents the responsiveness of the central bank to deviations in the average interbank rate from its steady state value.

1.2.5 Closing the model

Structural shocks

The model features three types of autoregressive shocks, total factor productivity shocks, shocks to bank profits (represented by an unexpected change in the market book) and a liquidity shock. All three follow stochastic AR(1) processes. The productivity shock is applied to firms in all four regions and is given by:

$$A_t^i = \left(A_{t-1}^i\right)^{\rho_A} \exp\left(\varepsilon_t^A\right) \tag{1.25}$$

where $i = \{A, B, C, D\}$. In the first section of our impulse response analysis (see section 1.5.1), we treat the aggregate productivity shock scenario as a benchmark against which we study the *additional* impact of a localised banking shock on variable dynamics[12]. Including the benchmark provides a common basis for comparison between the dynamics of shocked and non-shocked banks in each network structure, thus highlighting the propagation profile of the shock. Moreover, the banking shock is applied on a *regional* rather than aggregate basis in order to highlight how the shock is transmitted across the network via banks' interlocking interbank asset and liability structures. The banking shock specification is as follows:

$$\Gamma_t^A = \left(\bar{\Gamma}\right)^{1-\rho_\Gamma} \left(\Gamma_{t-1}\right)^{\rho_\Gamma} \exp\left(\varepsilon_t^\Gamma\right) \tag{1.26}$$

where $\bar{\Gamma} > 0$ is the (calibrated) average market book return of banks. In this case, the shock is applied only to bank A. As will be made clear in section 1.3, the choice of A as the target for a banking shock is arbitrary for two of the structures, the complete and cyclical networks, due to their symmetry. By contrast, for the (asymmetric) core-periphery topologies, the *location* of the shock has a marked impact on its propagation dynamics.

[12] From a modelling perspective, this implies taking advantage of the linearity of the policy functions to add the impulse responses under the two shocks.

Similar to the above scenario in which a regional banking shock is compared to a benchmark comprising an aggregate productivity shock, section 1.5.2 maintains the banking and productivity shock scenario as a benchmark against which to compare the impact of central bank liquidity injections. Recall that these consist of a deterministic component given by Equation 1.24 as well as a stochastic AR(1) component given by:

$$M_t^S = \rho_M M_{t-1} + \exp\left(\varepsilon_t^M\right) \tag{1.27}$$

The central bank policy rule is then obtained by adding the stochastic and deterministic (i.e. liquidity injection) components:

$$M_t = M_t^S + M_t^D \tag{1.28}$$

Finally, all innovations are assumed to be i.i.d-normally distributed i.e. $\varepsilon_t^Z \sim \mathcal{N}(0, \sigma_Z^2)$ where $Z = \{A, \Gamma, M\}$.

Market clearing

Note that the central bank liquidity injections given in Equation 1.23 provide the clearing conditions for the interbank market. In order to bridge the gap between the policy rule (Equation 1.28) and central bank interventions, we simply divide M_t by the number of links of the network being considered. This yields the individual M_t^{ij} values, thereby assuming equal treatment by the central bank of the interbank market constituents.[13]

In the simulations that do not feature liquidity injections, interbank market clearing is simply given by:

$$B_t^{ij} = L_t^{ji}, \quad \forall i, j \in \mathcal{E} \tag{1.29}$$

[13]Though this stylised approach is an abstraction from reality, it bears some similarity to the pre-crisis allotment policies of the major central banks who fix the aggregate volume of open market operations (OMOs) at their discretion (Blenck et al., 2001).

1.3 Interbank network structures

An interbank *network* consists of a set of banks connected by interbank claims on one another. In Section 1.2, we outlined banks' optimisation programmes subject to the optimising behaviour of regional households and firms as well as other banks to whom they are connected (constituting the interbank market). The latter revolves around the lending and borrowing counterparty sets $\mathcal{S}_i$ and $\mathcal{D}_i$ respectively which constrain to (from) whom banks can provide (request) liquidity. Up to now, these sets remain undefined. Following Allen and Gale (2000), this section proceeds to defining several stylised network structures, classified based on completeness and interconnectedness. Consequently, the interbank network provides the foundation on which the DSGE microfoundations are superimposed.

1.3.1 Complete and cyclical topologies

In the complete (i.e. perfectly interconnected) network, each bank has exposures to all other banks in the system. Though unrealistic, the complete network structure allows us to study the case where banks are maximally connected. In our stylised model of four banks, each bank thus lends to and borrows from the three remaining banks corresponding to six directed edges per banks for a total of 12 edges in the network. This is captured in Figure 1.3(a) below[14]:

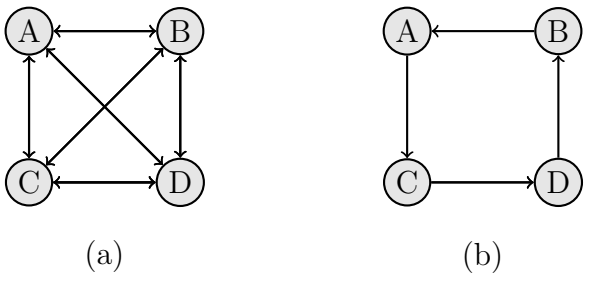

(a) (b)

Figure 1.3: (a) Complete and (b) Cyclical network topologies

[14]For simplicity, we combine the ingoing and outgoing edges between bank pairs. A double-headed arrow between nodes i and j indicates that i both lends to and borrows from j and vice versa.

The cyclical structure in Figure 1.3(b) assumes that each bank has one borrowing and one lending relationship to two distinct adjacent banks. Notice that both topologies are symmetric across banks. Depending on the interbank network structure in place, the support of the bank optimisation programme given in Equation 1.4 consisting of interbank market transactions (lending, borrowing and defaults) will vary. For example, under a cyclical network, the set of bilateral transactions consists of the following set of optimal lending and borrowing choices and the interbank rate that clears each market:[15]

$$\begin{aligned} \Xi &= \left\{\left\{L^{b,AC}, B^{b,CA}\right\}, \left\{L^{b,CD}, B^{b,DC}\right\}, \left\{L^{b,DB}, B^{b,BD}\right\}, \left\{L^{b,BA}, B^{b,AB}\right\}\right\} \\ R &= \left\{r^{b,AC}, r^{b,CD}, r^{b,DB}, r^{b,BA}\right\} \end{aligned}$$

1.3.2 Core-periphery topologies

Though the aforementioned network topologies are interesting cases for the study of the implications of financial interconnectedness, they are somewhat unrealistic and cannot be seen to represent the structure of real interbank networks. By contrast, mounting empirical evidence points towards the tiered/core-periphery topology as representative of the *form* and *function* of the interbank market. Here, the form refers to the densely interconnected core connected to a sparsely interconnected periphery while the function refers to the fact that larger core banks act as money centre banks who intermediate between smaller peripheral banks who do not exchange liquidity amongst themselves (Craig and Von Peter, 2014). While maintaining the same stylised 4-bank structure, we provide the following two core-periphery configurations:

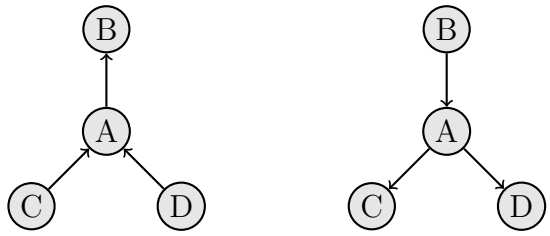

Figure 1.4: Core-periphery network with (a) core bank as a net borrower and (b) core as a net lender

[15]For bilateral rates $r^{b,ij}$, we adopt the following convention: The first superscript i denotes the lending counterparty (located at the tail of the link connecting them in the network) while the second corresponds to the interbank borrower.

Unlike the previous setup, the core-periphery topology features more distinct roles for banks vis-à-vis each other. Under both configurations, bank A acts as a market-maker, redistributing liquidity across the banking system. However, in configuration (a), the core relies on two banks (C and D) for wholesale funding compared to one (bank B) in configuration (b).

This asymmetry between banks depending on their position in the network implies that the location of the banking shock is no longer arbitrary as in the complete and cyclical frameworks. To account for this in our analysis, we target the banking shock according to the following three configurations:

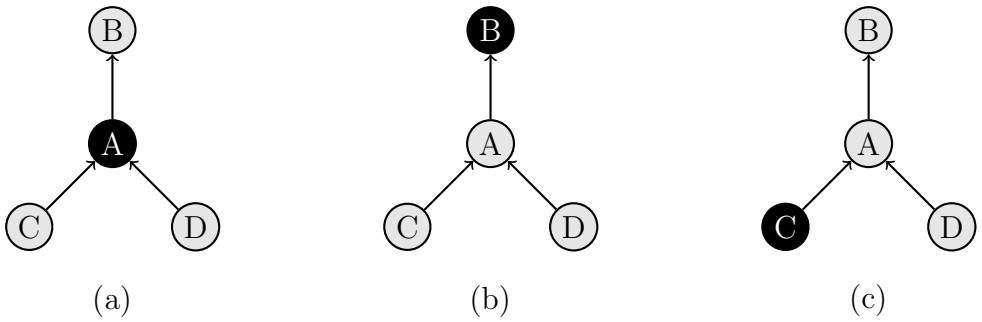

Figure 1.5: Shock configurations under core-periphery net borrower network.

In configuration (a), the core bank is subject to a market book shock. By virtue of its centrality in the network, the shock is then transmitted to *all* remaining banks due to the core optimally changing its portfolio composition in response to the shock. Note however, that banks B and C will be impacted differently due to their different roles as core borrower and core lender, respectively. By contrast, D will face the same impact as C. In the results, we thus only report the impulse responses for C for the sake of brevity.

The same set of shocks are applied to the net-lender setup given in Figure 1.4(b). In this case, a shock to bank B (Figure 1.5(b)) will have a different impact due to B's role as the sole provider/recipient of interbank funding.

1.4 Calibration

We calibrate our model following WPR who use average historical real quarterly US data from 1985Q1 to 2008Q2. However, our modelling methodology differs along two dimensions: (i) we combine their heterogeneous banking sector into one representative, regional bank who intermediates directly between households and firm in the same region and (ii) the interbank market is represented as a form of intra-regional transfers of funds between banks. Consequently, the parameter values *inferred* at steady state will not only differ from those in their contribution (due to the difference in modelling framework) but will also differ across the imposed network structures in our own approach.

Relative to WPR, we maintain the same base weight values on risky asset exposures. However in their approach, bank exposures are *either* to the interbank market (in the case of the deposit bank) or to the credit market (in the case of the merchant bank) while our intermediary is exposed to firm as well as interbank default risk on the asset side of its balance sheet. In addition, the steady states values for various flow variables obey the following ratios as per WPR: $L = 0.5X$, $B = L$ and $D = 2X$ while the steady state interbank and firm repayment rates are given by $\delta = 0.99$ and $\alpha = 0.95$, respectively. Table 1.1 below reports the remaining banking sector calibrations:

Table 1.1: Parameter calibration: Banks

Parameter	Definitions	Value
	Capital requirement	
k	Minimum own funds ratio	0.08
$\tilde{w}^{f,i}$	Risk weight: loans to firms	0.8
$\tilde{w}^{b,ij}$	Risk weight: interbank loans	0.05
$\tilde{w}^{S}$	Risk weight: market book	1.20
	Insurance fund	
ζ_b	Insurance coverage: interbank default	0.80
ζ_f	Insurance coverage: firm default	0.80
ϑ_b	Insurance fund contributions from profits	0.5

We collect the parameters implied at steady state in Tables 1.2 and 1.3 in order to study how they differ depending on the network structure. The first table provides the inferred values for the complete and cyclical networks. The three rates were set in order to minimise the differences between the two sets of parameters.

Table 1.2: Inferred parameters: Banks (Symmetric networks)

Parameter	Definition	Network structure	
		Complete	**Cyclical**
r^d	Deposit rate	0.5%	0.5%
r^l	Prime lending rate	0.1%	0.5%
r^b	Interbank rate	1.2%	1%
d_b	Interbank default disutility	3773	3642
d_{F^b}	Own funds utility	7849	9148
ξ_b	Insurance fund contribution	0.0548	0.0640
ω_b	Interbank default cost	326	532

As shown in Appendix 1.A, the manner in which nodes are connected in the core-periphery structure imposes a degree of asymmetry which affects the set of variables in banks' optimisation programmes (depending on their location in the network).

Table 1.3: Inferred parameters: Banks (Asymmetric networks)

Parameter	Definition	Network structure					
			CP-nb			**CP-nl**	
		A	B	C/D	A	B	C/D
r^d	Deposit rate	”	0.05%	”	”	0.05%	”
r^l	Prime lending rate	”	0.04%	”		0.04%	”
r^b	Interbank rate	”	0.09%	”	”	0.09%	”
d_b^i	Interbank default disutility	3760	5233	-	2325	-	5233
$d_{F^b}^i$	Own funds utility	10462	12458	9290	8131	150150	12458
ξ_b^i	Insurance fund contribution	0.0480	0.0403	0.0540	0.0617	0.0540	0.0403
ω_b	Interbank default cost		637			637	

Tables 1.4 and 1.5 report the parameters associated to the real economy (firms and households) and the stochastic processes specified in the model.

Table 1.4: Parameter calibration: Real economy

Parameter	Definitions	Value
	Households	
χ	Deposit gap disutility	0.01
$\bar{N}$	Labour supply	0.20
$\bar{D}^h$	Deposit target	0.38
	Firms	
d_f	Firm default disutility	0.163
ω_f	Firm default cost	15
μ	Capital share	0.333
τ	Capital depreciation rate	0.03

Table 1.5: Parameter calibration: Exogenous processes

Parameter	Definition	Value
ρ_A	AR parameter: productivity shock	0.95
σ_A	Standard deviation: productivity shock	0.1
ρ_Γ	AR parameter: banking shock	0.5
σ_Γ	Standard deviation: banking shock	0.1
ρ_M	AR parameter: liquidity shock	0.5
σ_M	Standard deviation: liquidity shock	0.1

1.5 Results

In this section, we discuss the results of the model. In order to analyse how the network structure contributes to financial stability, we provide two simulation studies.[16] Both take the form of a '*crisis simulation*' whereby the innovations of the relevant stochastic processes are set to one negative standard deviation. All impulse responses are reported as variations from the steady state, in % points for the repayments and in % for the other variables.

1.5.1 Responses to a banking shock

In the first simulation, we focus on the effect of adding a banking shock to the baseline productivity shock as outlined in Section 1.2.5. Given that all banks are ex-ante homogenous and the regional productivity shocks are identical, impulse responses across the four banks in the benchmark scenario will not vary. The banking shock introduces ex-post heterogeneity into the system. As this is calibrated to hit only one of the four banks, analysing the impact on the remaining banks via the different network structures (i.e. those in regions only hit by productivity shocks to firms) will provide an indication of its shock transmission properties. To this effect, our impulse response analysis in this section focuses specifically on the evolution of banking sector variables namely, interbank rates, lending and borrowing and bank repayment rates.

Cyclical network

Recall that the cyclical network given in Figure 1.3*(b)* entails one interbank lending and one borrowing relationship for each bank. In order to simplify the interpretation of the bilateral variables, the region to which a particular IRF is associated is given in bold font above the y-axis. Figures 1.6-1.7 below report the impulse responses of banking sector variables under the cyclical network topology.

[16] We are grateful to the authors of De Walque et al. (2010) for providing us with their Dynare codes.

As shown in Figure 1.6, interbank volumes experience a small increase on impact following the baseline aggregate productivity shock. This is immediately followed by a larger-magnitude decrease wherein the exposures for all banks decrease relative to the steady state before gradually converging 20 periods into the simulation.

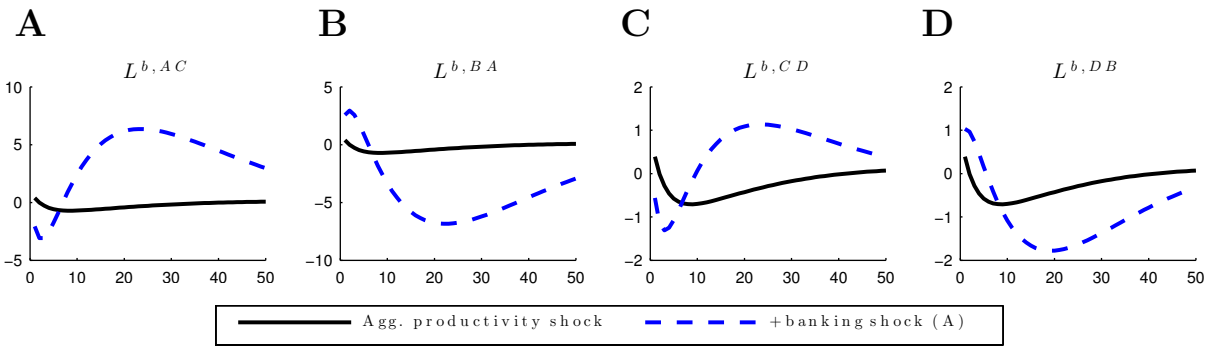

Figure 1.6: Interbank lending and borrowing volumes - Cyclical network

By contrast, the addition of a regional banking shock is not only larger in magnitude for all exposures, but exhibits more persistent dynamics as well. For example, bank A's lending to C $(L^{b,AC})$[17] shows an initial decrease of approximately 4% followed by an increase to a peak of 6% (with the transition from negative to positive occurring eight periods into the simulation).

Comparing this with $(L^{b,BA})$ i.e. the volume of interbank liquidity *borrowed* by A, we see that the dynamics (and corresponding magnitudes) are inverted but identical. Thus changes in the shocked bank's lending behaviour are offset by changes in its borrowing behaviour. The interbank repayment rates, given in Figure 1.7 below further highlight this symmetry between the shocked bank's *immediate* counterparties. Namely, A's repayment rate on borrowing from B, $\delta^{b,AB}$ features the same offsetting effect relative to C's repayment on borrowing from A, $\delta^{b,CA}$. Furthermore, comparing the loan volumes to their corresponding repayment rate[18] reveals that the initial decrease in lending from A to C results in a corresponding decrease in C's repayment to A and vice versa. This *quid pro quo* mechanism also applies to B's initial increase in lending to A.

Network effects come into play when observing the same intermediary dynamics for non-shocked banks as any banking dynamics herein occur solely due to the outward propagation from the source through the network. As before, analysis of $L^{b,DB}$ and $L^{b,CD}$ wherein

[17] Due to the market clearing conditions under no liquidity injections, studying both the lending and borrowing components of a bilateral exposure is redundant. We thus restrict our focus to interbank lending.

[18] Note that insofar as the network links represent a flow of liquidity from a lender to a borrower, repayment rates flow in the opposite direction as they are undertaken by borrowers towards their lenders.

the intermediary D is not subject to a banking shock, reveals a similar but *imbalanced* offsetting effect, with the trough in D's lending being smaller than the corresponding peak in borrowing.

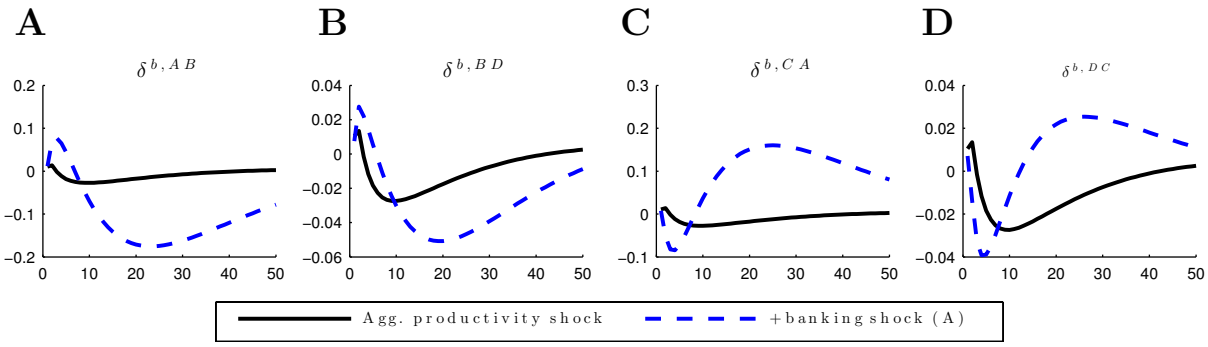

Figure 1.7: Interbank repayment - Cyclical network

The same asymmetry is present in the corresponding repayment rates (though the two still follow the same general trajectory as before). We explain these dynamics within the context of the network as follows: A's financial distress is propagated to B through increased loan delinquencies which then drives B to increase its borrowing and repayment from D. Given that the initial default is only transmitted in this direction due to the network (and not from A to C, as this entails a lending relationship), this accounts for the observed asymmetry.

The notion that the cyclical network transmits banking shocks outwards is further corroborated through analysis of the interbank rates. We begin by reporting the spread between the market rate on each bank's lending subtracted by the market rate of borrowing in Figure 1.8 below

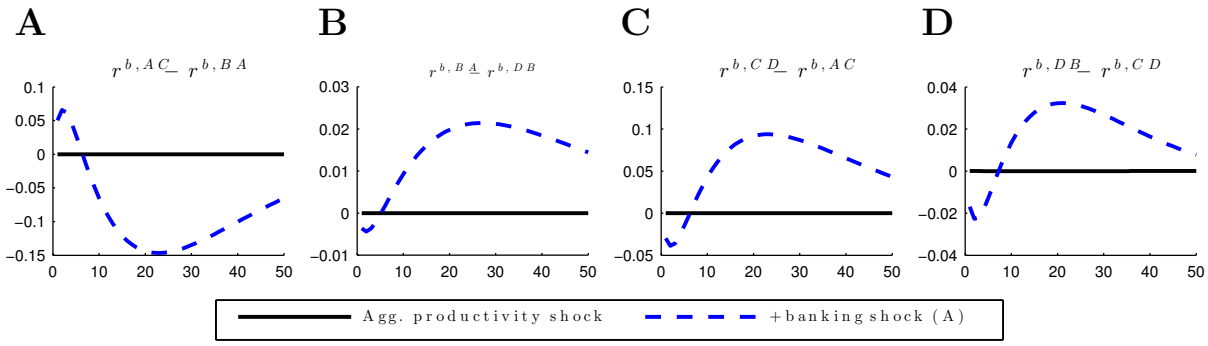

Figure 1.8: Interbank rate spreads - Cyclical network

At first glance, it is apparent that strains in the regional productive sector do not affect (what can loosely be interpreted as) the bid-offer spread on wholesale funding. By contrast, the banking shock produces persistent dynamics across all banks' spreads. The leftmost figure reports the spread between the rate at which A provides liquidity (to C) and the rate at which it receives liquidity (from B). The initial widening on impact is contrasted by the remaining spreads which experience a small decline followed by an increase in their lending relative to their borrowing rate. Analysis of the superscripts in panels B and C reveal that only one of the variables in the spreads stems from the shocked bank, which explains their smaller magnitudes. Panel D reports the spread for interbank rates not *directly* connected to A. As expected, the magnitude is smaller compared to the previous cases, indicating that while the shock does propagate through the network, its impact dissipates as proximity to the source decreases. Though less indicative than spreads, Appendix 1.B provides a further decomposition of interbank rates. Specifically, Figure 1.B.1 shows that the dynamics of standalone rates are largely driven by the decline due to the aggregate productivity shock. Isolation of the banking shock in Figure 1.B.2 shows an initial increase in interbank rates across all regions. The magnitudes follow the cyclical structure with the initial rate increase being the largest for r^{AC} followed by r^{CD}, r^{DB} and finally, r^{BA}.

Complete network

The complete network is characterised by a high density of linkages which makes a market-by-market analysis similar to the above more complex due to the large number of endogenous variables associated to each (interbank) link. However, the symmetry of the complete network (combined with the asymmetry introduced due to the localised banking shock) allows us to restrict our attention to a few key cases. These are provided above the relevant plots as 2- or 3-node schematics to indicate the counterparties being analysed. As before, we begin by looking at the impulse responses of interbank lending and borrowing volumes:

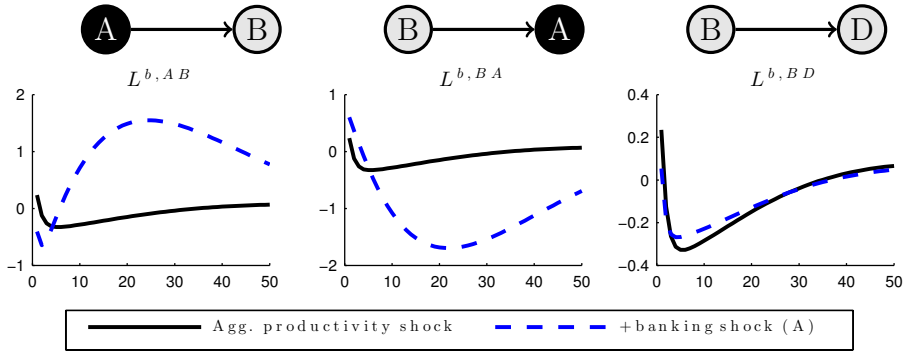

Figure 1.9: Interbank lending and borrowing volumes - Complete network

where the three scenarios correspond to (i) shocked bank lending to a non-shocked bank, (ii) non-shocked bank lending to a shocked bank and (ii) exposure between two non-shocked banks. Initial comparison with the interbank exposures under cyclicality provided in Figure 1.6 shows a smaller impact of the baseline under completeness. The same applies when a banking shock is incorporated. This highlights the dissipative characteristics of complete networks, as documented by Allen and Gale (2000). Under this structure, banks are maximally exposed to the wholesale market, allowing them to more efficiently redistribute risk across counterparties and limit individual exposures.[19] Analysis of the rightmost panel indicates that as the shock propagates outwards from A, the impact on lending between non-shocked banks is minimal, having almost the same trajectory as the baseline.

The interbank repayments behave in a similar manner, as shown in Figure 1.10 below with a smaller increase in banks' defaults under completeness than their cyclical counterparts. Comparing A's repayment on borrowing from B and B's default on borrowing from D, we obtain the intuitive result that the former exhibits a higher default rate due to the shock than the latter.

[19] A counterargument in which the same links can exacerbate interbank tensions by acting as a channel for financial contagion for large shocks is well documented in the literature (Acemoglu et al., 2015). However, such mechanisms are not included in our theoretical model and thus, are outside the scope of this paper.

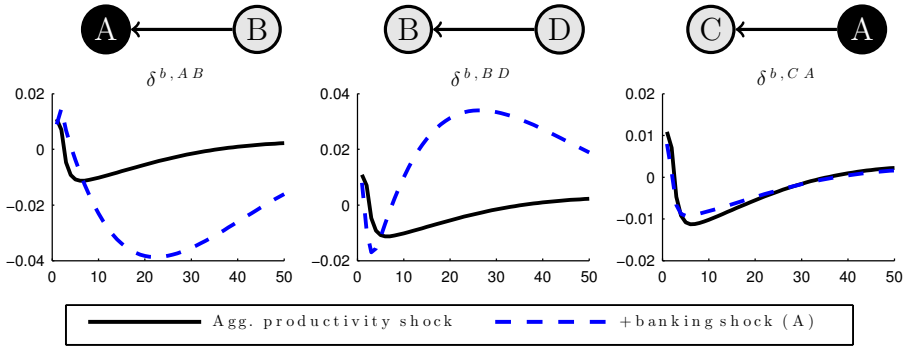

Figure 1.10: Interbank repayments - Complete network

We now proceed to the analysis of interest rate spreads. These involve three banks of which the intermediary is located in the middle of the three-node linear networks given below:

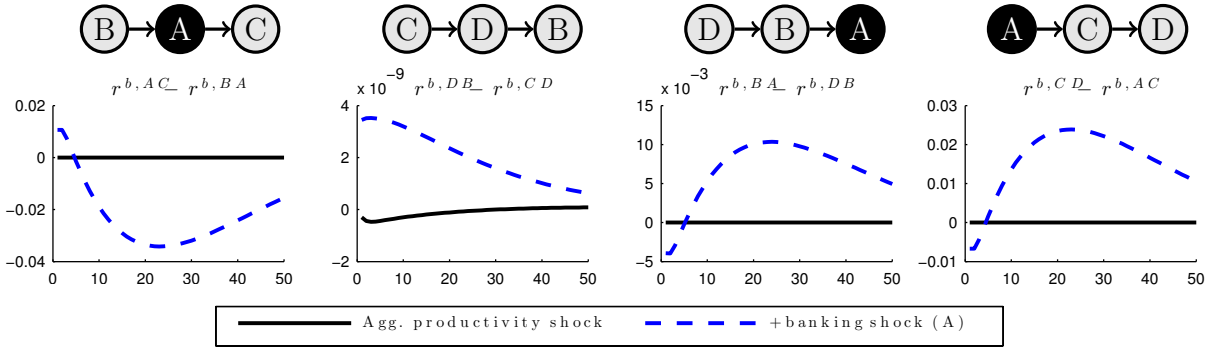

Figure 1.11: Interbank rate spreads - Complete network

As before, aggregate productivity shocks have minimal impact on interbank spreads. The largest swings occur when A is the intermediary whereas the smallest occurs when none of the banks involved is shocked, both of which are intuitive results. Moreover, there is a substantial difference in magnitudes (but not dynamics) between the scenarios where A is the first bank in the intermediation chain (third panel) compared to when it is the last (rightmost panel). Specifically, the magnitudes of the initial decline and peak 20 periods into the situation are both smaller when A is the terminal node in the chain compared to when it is the initial node, which further highlights the ability of the network to transmit local shocks beyond their immediate vicinity.

Another interesting case study involves the degree of *reciprocity* between bank pairs who simultaneously lend to and borrow from one another. This is captured in Figure 1.12 for the cases when one of the two banks or neither is subject to a banking shock:

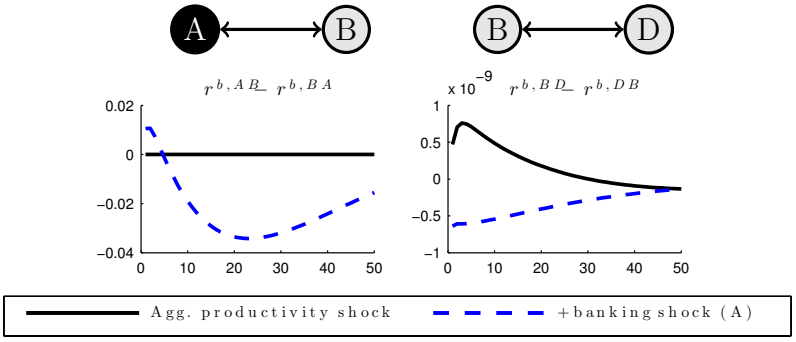

Figure 1.12: Interbank rate spreads (reciprocity) - Complete network

As expected, the spread is negligible in the absence of a shock to either of the banks. By contrast, the lack of reciprocity is manifested in the left panel through an increase in A's lending rate to B relative to its borrowing rate. This lends further weight to the argument that complete networks are stability-enhancing: In the event of a shock to bank A, it benefits from preferential treatment vis-à-vis its counterparty via a higher lending rate and/or a lower borrowing rate. This is also in line with the 'relationship lending' argument made in the general introduction.

We end our discussion of interbank dynamics under the complete network by referring to Figures 1.B.3 and 1.B.4 in Appendix 1.B which, unlike the cyclical dynamics, do not show any marked heterogeneity in interbank rates. This further exemplifies the stabilising role of the complete network.

Core-periphery networks

We end this section by reporting the IRFs under two variations of the core-periphery topology: one in which the core is a *net borrower* and one in which the core is a *net lender* on the interbank market as outlined in Figure 1.4. Given the inherent asymmetry of the structure, we expand the set of banking shock configurations from one to three in order to show how the *location* of the shock can affect inter-bank dynamics (see Figure 1.5).

Core bank as net borrower As in the previous cases, we begin our treatment by reporting the response of interbank volumes to an aggregate negative productivity shock and regional negative banking shock.

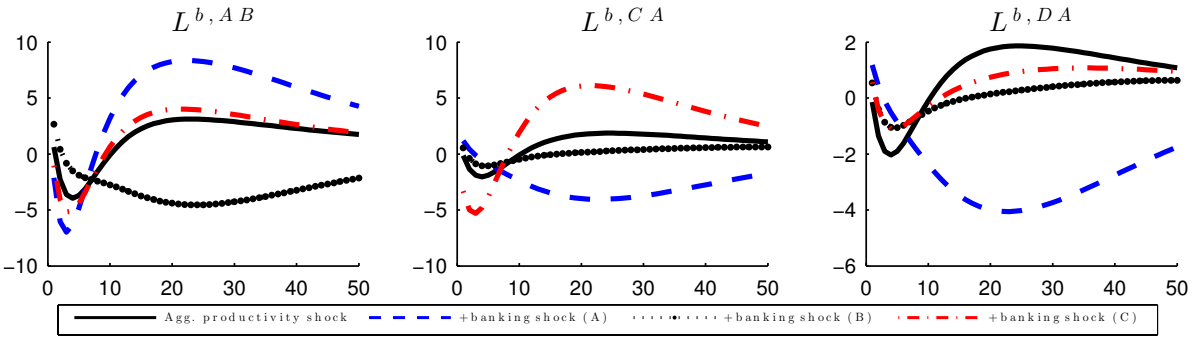

Figure 1.13: Interbank volumes under CP network - net borrower case.

As expected, a negative shock to the core bank A results in the largest and most persistent fluctuations by virtue of its high centrality in the system. Upon impact, A reduces lending to B (its only borrower in this setup) while increasing its borrowing from C and D. Another intuitive result arises when C is subject to the banking shock: given its role as one of the main providers of funding for A and ultimately B, we observe a large decrease in lending from C to A followed by a slightly smaller decrease in lending from A to B. In this case, A's role as an inter-bank intermediary dampens the pass-through of the shock. Interestingly, the same shock also produces a small reduction in D's lending to A. This shows that shock propagation in a core-periphery network is not necessarily linear and can impact banks off the direct transmission path. Finally, we observe that the shock to B produces (relative to the other configurations) subdued dynamics due to its relatively less important role in the interbank market compared to the intermediary and initial providers of funding.

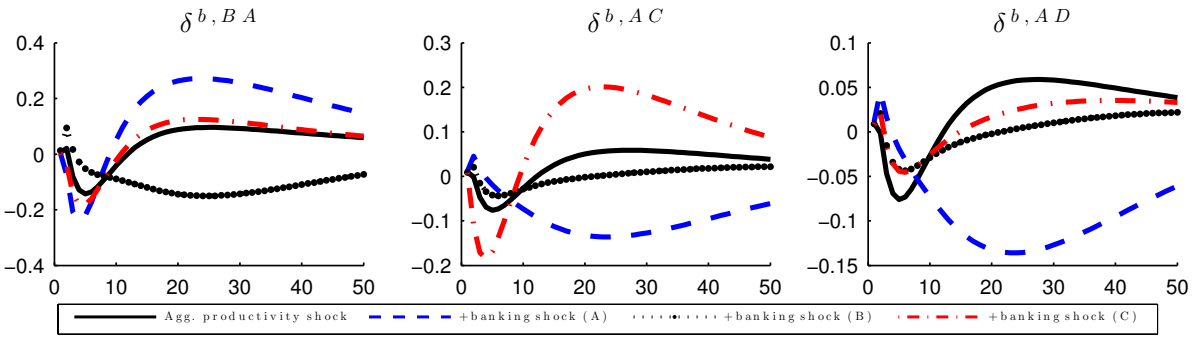

Figure 1.14: Interbank repayment rates under CP network - net borrower case.

As in the previous cases, repayment dynamics closely mirror interbank volumes. Closer observation of the impulse response magnitudes reveals that the initial increase in B's default when A is shocked is similar to A's default rate when C is shocked. This highlights that shocks to the 'periphery' can also drive interbank market tensions (compared to core shocks) when core banks are dependant on them for funding.

Due to its structure, the core-periphery network only permits two spreads, reported in Figure 1.15 which are symmetric around A for most of the shock specifications the exception being the shock to C which has a much smaller (but not zero) impact on the spread between B and D via bank A compared to the case given in the left figure.

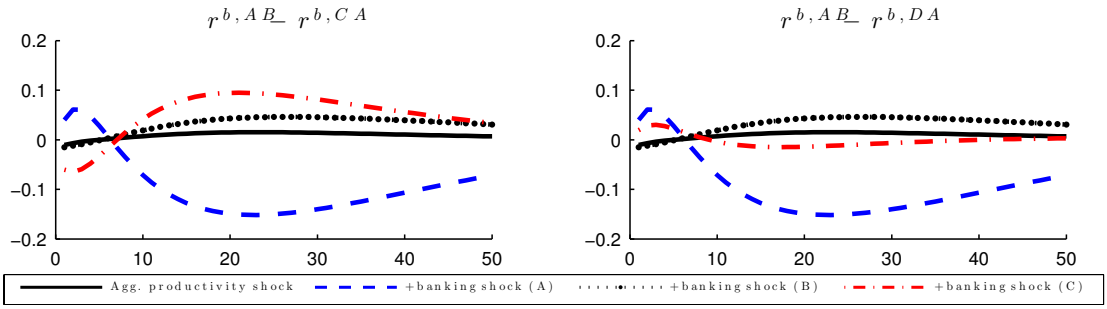

Figure 1.15: Interbank rate spreads under CP network - net borrower case.

The isolated banking shock reported in the Appendix (Figure 1.B.6) shows an across the board increase in interbank rates. However, unlike the previous cases (complete and cyclical), where the initial increases were between 0.2 and 0.3 percentage points, several of the initial rate spikes were between 0.1 and 0.15 p.p. Closer analysis reveals that the shock to B results in (comparatively) smaller increases due to its non-central role in the network. By contrast, the core shock in the first row is followed by increases greater than 0.2 p.p with the largest occurring on A's lending to B.

Core bank as net lender Under this setup, the core bank now has two banks that depend on it for interbank lending along with one sole source of wholesale funding.

Despite having the same base-structure as the net-borrower case, the IRFs follow different trajectories with large differences in magnitude. For example, a banking shock to B results in a 20% decline in lending to A which then translates (via A) to a 10% decrease in lending to both C and D. This contrasts with the much smaller decline in volumes due to a shock to B under the net borrower case. As mentioned, the core-periphery specification imbues the network with a function in addition to the basic form. Under the net lender case, A is reliant on B for funding followed by both C and D being reliant on A. Thus a negative

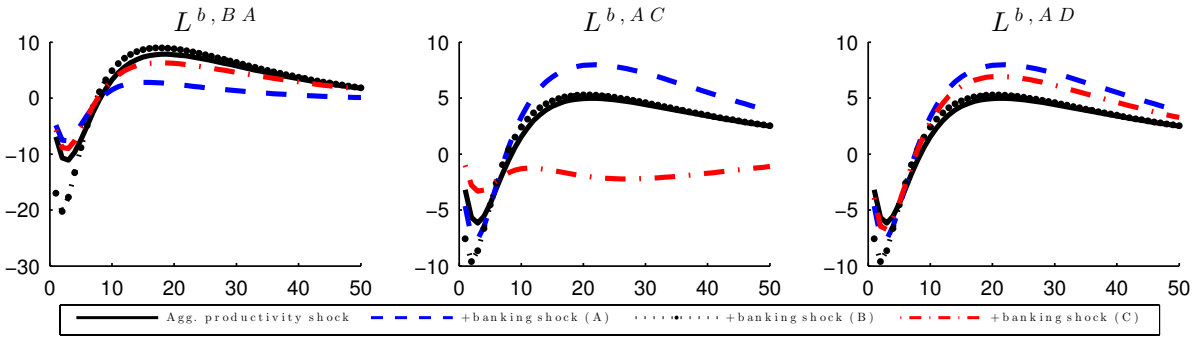

Figure 1.16: Interbank volumes under CP network - net lender case.

shock to the only source of funds will have a more pronounced effect than a shock to the ultimate recipient of funds. Similar to lending volumes, interbank repayments fare much worse under the net lender case than their net borrower counterparts

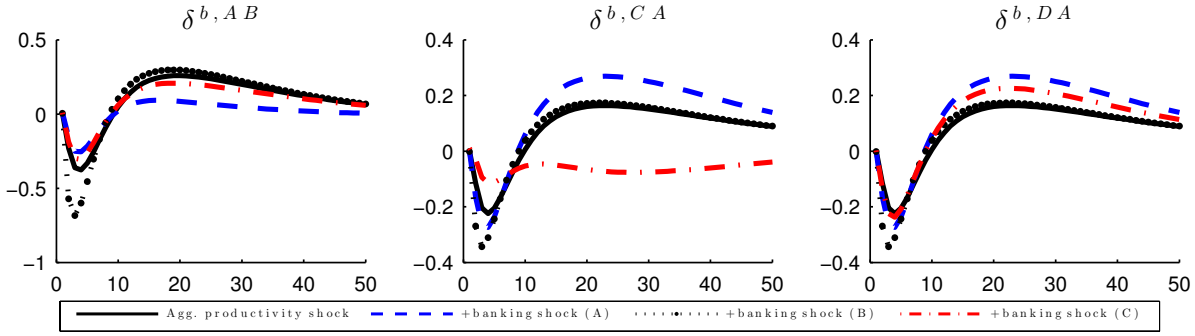

Figure 1.17: Interbank repayment rates under CP network - net lender case.

The shock to B also has a strong impact on the interbank rate spreads, showing a relative increase in A's cost of borrowing. Interestingly, the shock to A exhibits much more subdued dynamics than its counterpart. We posit that this occurs due to the interbank market dynamics playing out in strong fluctuations in volumes and repayment rates rather than in the interest rate. This is justified by Figure 1.B.8 wherein the rate increase in the first column is smaller in magnitude than the second and third. The higher spike due to the B shock is consistent with the dynamics explored thus far.

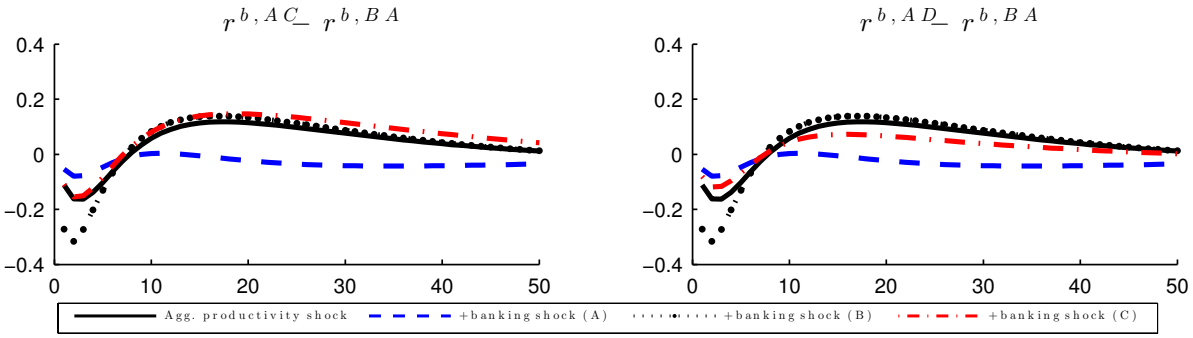

Figure 1.18: Interbank rate spreads under CP network - net lender case.

The main takeaway from the core-periphery analysis is that a small-variation in the pattern of linkages can have wide-ranging effects on the system's ability to withstand certain shocks. We have shown, in a stylised manner, that when a core bank is limited in its ability to obtain funding, this is easily transmitted to downstream banks who are themselves dependent on the core.

We end our discussion of banking sector dynamics by observing that the impulse responses to a market book shock resulted in fairly large swings above and below the steady state prior to converging. This is likely due to general equilibrium effects associated to the comprehensive manner in which banking sector specificities are taken into account in banks' maximisation programmes. Notably, the nonlinear pecuniarity penalty associated to interbank loan defaults as well as the countercyclical capital buffer are likely to engender large movements and countermovements in the impulse response functions. As we will highlight below, this can lead to counterintuitive results when paired with the ex-ante heterogeneity arising due to the two core-periphery structures.

1.5.2 Real economy effects

The second simulation study provides the policy dimension of the paper. Specifically, we analyse how central bank liquidity injections (given by Equation 1.24) can alleviate strains to the *real economy* brought on by the banking shock and its transmission through the network. We now treat the second scenario from the first simulation (aggregate productivity and regional banking shock[20]) as the benchmark and toggle on the central bank policy function.

We begin by comparing the total volume of liquidity injections (m, whose dynamic process is given in Equation 1.28) across the different network structures. In order to provide a basis for comparison, we normalise m by dividing by the number of links which yields:

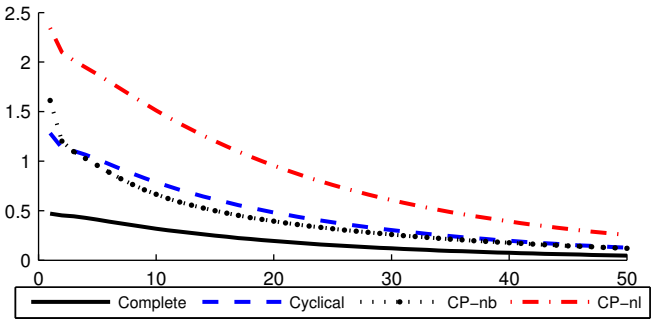

Figure 1.19: Total normalised central bank liquidity injections

As expected, our crisis simulation prompts the central bank to action, injecting liquidity into the banking sector across all imposed networks. However, despite the same shock calibration, the central bank response varies widely across networks. As has been shown in the paper, the complete network is highly stable due to the shock-dissipative effect of its high interconnectedness. Interestingly, the core-periphery network in which the core bank is a net borrower requires the second lowest aggregate central bank intervention over time. We posit that this occurs due to the relative stability that having two sources of funding and only one source of default risk can provide. This argument is strengthened by the relatively inferior performance of the net lender case, in which the central bank had to intervene more aggressively. In this case, the core is subject to two sources of default risk and only one source of retail funding. As a result, it increases its reliance on wholesale funding.

[20]In the case of the core-periphery networks, we restrict our attention to the first configuration in which the core bank A is subject to the banking shock.

Having compared the effect of interbank network structure on the dynamics of interbank variables in section 1.5.1, we now analyse how a negative banking shock, within the context of our model, affects total credit to firms and total output. Note that the former provides the link by which interbank market tensions are transmitted to the real economy namely, through a reduction in *credit availability*:

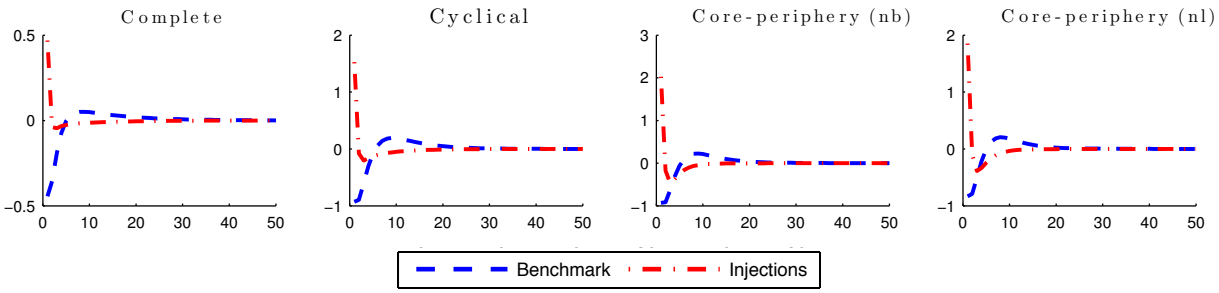

Figure 1.20: Total credit

The figure above confirms that the initial banking shock and its transmission through the network results in a reduction in credit provision to firms. The stability-enhancing properties of the complete network are again evident given the lower reduction in credit it exhibits. However, we notice that the increase in total output following central bank interventions is comparatively smaller. Thus, the positive impact of liquidity injections are also subject to dissipative effects, resulting in a lower total impact.

Though difficult to observe, the CP-nl network exhibits a slightly smaller decrease in credit than the cyclical and CP-nb cases. This puzzling feature seems to contradict the relative instability of this network observed in the previous section along with the larger central bank interventions reported above. As mentioned at the end of the last section, the various adjustments present in the bank maximisation programme, combined with heterogeneity in terms of the interbank variables (and associated disutilities) can create unexpected effects within a general equilibrium framework.

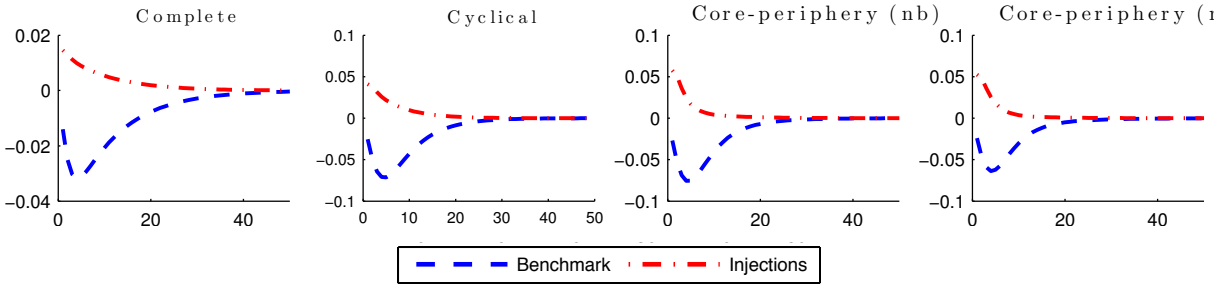

Figure 1.21: Total output

Analysing the variation in total output across the four networks, it is evident that liquidity injections into the banking sector play a positive role in stabilising economic output. Again, the complete network features the smallest decrease while the remaining structures are more difficult to distinguish.

Throughout the analysis, the complete network has revealed itself to be conducive to financial stability, both in terms of interbank market dynamics and within the context of spillovers to the real economy. In order to provide the first step towards a normative analysis of the impact of network structure, Figure 1.22 below provides the impulse response functions for total household consumption when moving *from* the complete network to the three remaining alternatives. In this way, we analyse the impact on global welfare in the event of shocks that forces the network to self-organise into a less stable configuration. Consequently, this provides a first glimpse into possible future analyses aiming to *endogenise* the network structure. Note that IRFs below are without liquidity injections.

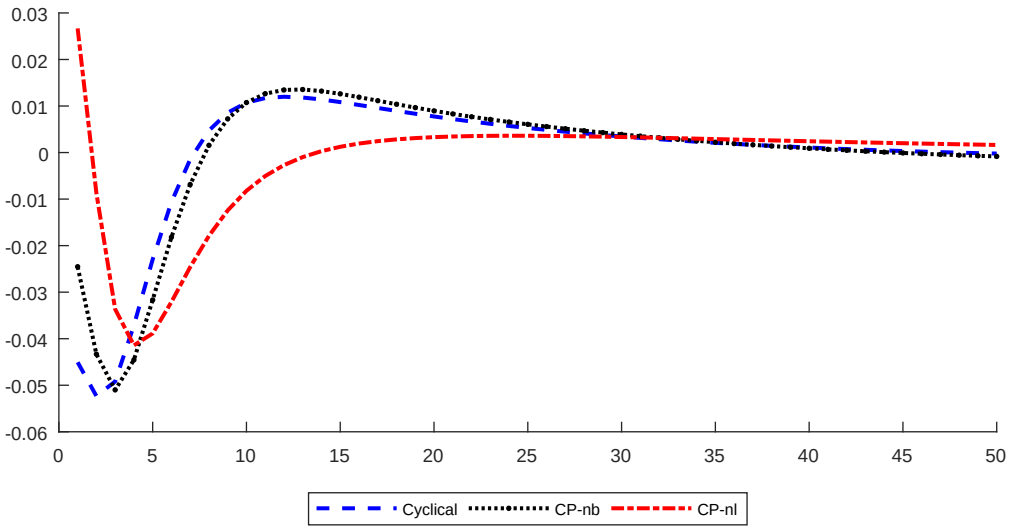

Figure 1.22: Change in total consumption with complete network benchmark

Interestingly, both the cyclical and the CP-nb networks exhibit a decreases in total consumption when moving from the complete network. By contrast, the CP-nl (which recall, is the most prone to interbank market instability) shows an instantaneous increase when compared to the complete network. Similar to the total credit case, we argue that these unusual dynamics arise due to general equilibrium effects related to bank heterogeneity in terms of optimisation programmes.

1.6 Concluding remarks

In this chapter, we develop a novel methodology for taking into account financial system *interconnectedness* within the framework of a DSGE model. The RBC-DSGE model we use as a benchmark is part of a recent but growing literature that recognises the importance of the banking sector for the transmission and propagation of shocks. Before developing the crux of our modelling framework, we modify the bank microfoundations in our benchmark model by allowing for *one* regional, representative bank intermediating funds between households and firms. We then assume four regions, each comprising the three agents just mentioned.

Our main contribution arises in the manner in which these four regions interact. Specifically, we assume that banks are connected in an interbank *network* which provides them access to inter-regional wholesale funding to complement intra-regional retail funding from households. We vary the structure of this network across a set of stylised but suitably varied configurations namely, the complete, cyclical and core-periphery network topologies. This structure is then imposed on the microfounded model and the effect of the network is analysed using two simulation studies.

In the first simulation, we study how interbank market dynamics are driven by the network structure. We do this by first establishing a benchmark consisting only of aggregate productivity shocks. Since transmission through the interbank network is minimal (occurring only *indirectly* through changes in firm credit demand), it provides a basis for comparing the propagation of a regional banking shock which is transmitted directly through the network. Following this, we study how central bank liquidity injections directly into the banking sector can alleviate the spillover of banking sector shocks to the real economy via decreases in credit provision to firms.

Our results highlight the important role played by the network structure in driving economic fluctuations. We show that the complete network acts as a system stabiliser by allowing shocks to dissipate across the large number of linkages. Further evidence of this is provided when analysing central bank liquidity injections and the real economy. Unlike the complete network, the cyclical setup allows for a more in-depth analysis of the transmission of the banking shock through the network since it features nodes that are not *directly* connected to the source of the shock. A recurring result is that IRF magnitude decreases as distance from the source of the shock increases. However this decrease is never negligible which highlights the importance of accounting for interconnectedness. The core-periphery topology introduces a degree of reality into the model given that real

interbank networks are known to exhibit such a structure. Moreover, from a modelling perspective, it allows for heterogeneity in banks' microfoundations and a more complete view of how shock *location* (which was redundant in the symmetric structures treated above) can drive system dynamics.

We now turn to a comparison of our modelling framework with the two pillars on which it is based namely, the benchmark DSGE model of De Walque et al. (2010) and the optimal risk sharing model of Allen and Gale (2000). Regarding the former, our combination of WPR's single purpose deposit and merchant banks and the resulting interbank markets into one bank accepting deposits and extending credit better aligns the model with the intermediating role played by real banks. Moreover, the additional *structural* realism gained through the use of core-periphery networks also adds a level of *behavioural* realism due to the heterogeneity between peripheral banks, who are either borrowers or lenders on the interbank market and the core bank, who plays the role of intermediary. It should also be noted that by keeping to WPR's microfoundations, we could replicate their analysis while adding additional research avenues due to the additional banks and network structure (as outlined below). Compared to Allen and Gale (2000), the main advantage is the move from a partial to a general equilibrium setup and the addition of a productive firm sector allowing for the analysis of macroeconomic fluctuations. Moreover, several elements of our model are contained in their discussion (section IX) namely, *point D* on allowing for stochastic returns on the illiquid asset which is taken into account in our market book shock and *point E* on the addition of a central bank, a key element of our model that is intrinsically linked to the network given its intervention in the interbank market.

We end our discussion by pointing out a number of caveats in our modelling framework along with potential directions for future research. As mentioned, this chapter is to our knowledge, the first to combine networks and DSGE modelling in this way. As such, we have relied on very simple models along both fronts. Our use of WPR as a benchmark model was driven primarily by our desire to focus on the role played by the *network* in transmitting and propagating shocks while abstracting from the more complex frictions present in New-Keynesian DSGE models à-la Smets and Wouters (2003). From a pure modelling standpoint, we believe that the banking sector developed by WPR includes a number of realistic features (heterogeneity, endogenous defaults, adherence to capital requirements etc.) and thus, provides a relevant benchmark.

Having said that, our approach for incorporating the network is flexible enough to incorporate an alternative set of microfoundations. One possibility would thus be to study how the network could be included in the canonical BGG financial accelerator model

and whether interesting insights could be gained from their interaction. Alternatively, researchers could experiment with relaxing the assumptions on convex deposit disutility and exogenous labour supply to provide a more holistic macrofinancial analysis. This would then allow for the pinpointing of the general equilibrium effects that could generate counterintuitive impulse responses, especially in a heterogeneous framework.

From a policy perspective, the model highlights the effectiveness of direct intervention by the central bank via changes to its monetary policy framework to inject liquidity directly into the banking sector . This is reflected in the figures for credit and output in which central bank intervention successfully averts temporary decreases in those variables. An important feature of the model in this context is that it shows how the structure of the interbank network affects the volume of liquidity injections required to stabilise interbank rates with core-periphery networks, due to the instability inherent in their structure, requiring the highest level of intervention. Consequently, the chapter recommends that central banks *incorporate the network structure into their monetary policy framework* in order to ensure that interventions on the interbank market take into account its structural specificities . An extension along this dimension (for example by allowing for heterogeneous liquidity injections conditional on the network structure) would constitute an important addition to the literature on incorporating financial stability into the objective function of central banks and the separability of price and financial stability.[21]

Insofar as policy-relevant extensions are concerned, the model features a number of parameters whose further study could provide relevant insights into the tools available to regulators to mitigate systemic risk. For example, combining our core-periphery network study with a more in-depth treatment of the capital requirements would provide an interesting analysis of capital surcharges for banks deemed 'too big to fail'.

[21] The importance of such an analysis for policymakers was discussed by ECB executive board member Peter Praet at the 14th Annual Internal Banking Conference on 10 November 2011 (https://www.ecb.europa.eu/press/key/date/2011/html/sp111110.en.html) and BIS General Manager Jaime Caruana on 06 June 2014 (https://www.bis.org/speeches/sp140606.pdf).

In order to align our methodology with the state-of-the-art in DSGE modelling, future work would revolve around developing a valid estimation strategy. Central to this is the need for a data-driven underpinning of the interbank linkages in our model. As granularity remains an issue, one possibility would be to turn to country-level cross-border interbank holdings. Within the context of our model, the four regions would thus represent countries. Given that the purpose of this chapter was to develop the methodology by which two distinct fields, DSGE and financial network analysis, could be combined into one coherent framework, we chose to remain as close to the behavioural benchmark as possible and considered estimating or developing a more realistic calibration framework out of scope.

Turning now to the network, it is clear that four nodes is the minimum required to provide a reasonably varied set of structures on which to conduct our analysis. However, this belies the complexity of real financial networks. A next step would be to increase the number of nodes and links, allowing for example for an interbank core comprising more than one bank. This would then allow researchers to apply tools from network science such as the analysis of network centrality and distribution. Incorporating a less stylised network would also allow for an analysis of common/correlated shocks. This adds another degree of realism into the model as banking sector shocks are unlikely to hit only one bank in the event of a crisis.

Though a number of extensions are possible, we believe that our approach provides a promising and intuitive benchmark for considering how banks' behaviour is affected by the structure of the system in which they reside. The intuitive aspect is largely due to the four-node network structure which has the advantage of providing a simple and visual representation of the network while allowing for a holistic view of financial system and the manner in which institutions are connected.

Chapter 1 Appendices

1.A Computations

1.A.1 Cyclical network

In the cyclical network topology of Figure 1.3(b), each bank $i = \{A, B, C, D\}$ lends to and borrows from two distinct banks. Thus, this network is *symmetric* and the interbank components of the profits function are identical across banks. We thus report one bank profit function. Interconnectedness is captured in Table 1.A.0:

Table 1.A.0: Counterparties of i in cyclical network topology

i	$j \in \mathcal{S}_i$	$k \in \mathcal{D}_i$
A	B	C
B	D	A
C	A	D
D	C	B

where i denotes the bank of interest with lending and borrowing counterparties given by j and k, respectively. With respect to bank i's optimisation programme given in Section 1.2.2, Figure 1.A.2 below provides the basis for the first-order conditions given in Equations 1.9 - 1.14:

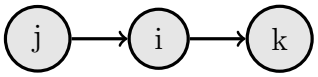

Figure 1.A.1: Local interbank market for each bank i under cyclical network

We begin with the observation that while the interbank component of bank profits vary depending on the network structure, the remaining components namely deposits, lending and market book exposures remain constant. In order to focus on cross-network heterogeneities, we extract the following 'constant' (C) terms from banks' profit function:

$$\pi_t^{b,i}(C) = \frac{D_t^{b,i}}{1+r_t^{d,i}} - D_{t-1}^{b,i} - \frac{X_t^{b,i}}{1+r_t^{l,i}} + \alpha_t^{f,i} X_{t-1}^{b,i} + \zeta_f \left(1 - \alpha_{t-1}^{f,i}\right) X_{t-2}^{b,i} + (1+\Gamma_t)\, S_{t-1}^{b,i} - S_t^{b,i}$$

The remaining terms in $\pi_t^{b,i}$ comprise the interbank (IB) components of bank profits under cyclicality:

$$\pi_t^{b,i}(IB) = \frac{B_t^{b,ij}}{1+r_t^{b,ji}} - \delta_t^{b,ij} B_{t-1}^{b,ij} - \frac{L_t^{b,ik}}{1+r_t^{b,ik}} + \delta_t^{b,ki} L_{t-1}^{b,ik} + \zeta_b \left(1-\delta_{t-1}^{b,ki}\right) L_{t-2}^{b,ik} - \frac{\omega_b}{2}\left(\left(1-\delta_{t-1}^{b,ij}\right) B_{t-2}^{b,ij}\right)^2$$

At the steady state, $\pi^{b,i}(C)$ is also constant across the different networks while $\pi^{b,i}(IB)$ will vary depending on the number of borrowing and lending counterparties. Under cyclicality, we obtain:

$$\pi^{b,i}(IB) = \left(\frac{1}{1+r^b} - \delta^b\right) B^b + \left(\delta^b + \zeta_b\left(1-\delta\right) - \frac{1}{1+r^b}\right) L^b - \frac{\omega_b}{2}\left[\left(\left(1-\delta^b\right) B^b\right)^2\right]$$

Recall that $B = L$ at steady state. Plugging this in and simplifying terms, the steady state interbank component of bank profits under cyclicality is given by:

$$\pi^{b,i}(IB) = \zeta_b\left(1-\delta\right) L^b + \frac{\omega_b}{2}\left[\left(\left(1-\delta^b\right) L^b\right)^2\right]$$

1.A.2 Complete network

In the complete network topology of Figure 1.3(a), each bank $i = \{A, B, C, D\}$ lends to *and* borrows from the three remaining banks in the economy. Despite the increasing complexity, the network remains symmetric vis-à-vis the number of counterparties (six for each bank as opposed to two under the cyclical topology). Similar to the above example, we represent bank profits for an arbitrary bank i and its lending and borrowing counterparties, $\{j, k, l\}$:

Table 1.A.1: Counterparties of i in complete network topology

i	$j \in \mathcal{S}_i = \mathcal{D}_i$	$k \in \mathcal{S}_i = \mathcal{D}_i$	$l \in \mathcal{S}_i = \mathcal{D}_i$
A	B	C	D
B	A	C	D
C	A	B	D
D	A	B	C

Figure 1.A.1 below represents the table in (local) network form:

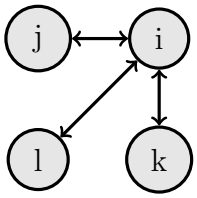

Figure 1.A.2: Local interbank market for each bank i under cyclical network

Derivation of the interbank component of bank i's profits under completeness gives:

$$
\begin{aligned}
\pi_t^{b,i}(IB) &= \frac{B_t^{b,ij}}{1+r_t^{b,ji}} + \frac{B_t^{b,ik}}{1+r_t^{b,ki}} + \frac{B_t^{b,il}}{1+r_t^{b,li}} - \delta_t^{b,ij} B_{t-1}^{b,ij} - \delta_t^{b,ik} B_{t-1}^{b,ik} - \delta_t^{b,il} B_{t-1}^{b,il} \\
&- \frac{L_t^{b,ij}}{1+r_t^{b,ij}} - \frac{L_t^{b,ik}}{1+r_t^{b,ik}} - \frac{L_t^{b,il}}{1+r_t^{b,il}} + \delta_t^{b,ji} L_{t-1}^{b,ij} + \delta_t^{b,ki} L_{t-1}^{b,ik} + \delta_t^{b,li} L_{t-1}^{b,il} \\
&+ \zeta_b \left[\left(1 - \delta_{t-1}^{b,ji}\right) L_{t-2}^{b,ij} + \left(1 - \delta_{t-1}^{b,ki}\right) L_{t-2}^{b,ik} + \left(1 - \delta_{t-1}^{b,li}\right) L_{t-2}^{b,il} \right] \\
&- \frac{\omega_b}{2} \left[\left(\left(1 - \delta_{t-1}^{b,ij}\right) B_{t-2}^{b,ij} \right)^2 + \left(\left(1 - \delta_{t-1}^{b,ik}\right) B_{t-2}^{b,ik} \right)^2 + \left(\left(1 - \delta_{t-1}^{b,il}\right) B_{t-2}^{b,il} \right)^2 \right],
\end{aligned}
$$

which, at steady state, is equal to:

$$\pi^{b,i}(IB) = 3\left(\frac{1}{1+r^b} - \delta^b\right) B^b + 3\left(\delta^b + \zeta_b\left(1-\delta\right) - \frac{1}{1+r^b}\right) L^b - \frac{3\omega_b}{2}\left[\left(\left(1-\delta^b\right) B^b\right)^2\right].$$

Simplifying terms as before, we arrive at:

$$\pi^{b,i}(IB) = 3\zeta_b\left(1-\delta\right) L^b + \frac{3\omega_b}{2}\left[\left(\left(1-\delta^b\right) L^b\right)^2\right]$$

1.A.3 Core-periphery networks

The link asymmetry inherent in the core-periphery network precludes the kind of symmetric analysis (i.e. $\pi_t^{b,i}(IB)\,\forall i \in \mathcal{N}$) undertaken above. Moreover, there are substantial differences between the two core-periphery networks considered.

Net-borrower case

Beginning with the case where i is a net *borrower* of funds, we provide the set of counterparties for each bank in the table below:

Table 1.A.2: Counterparties of i in core-periphery network topology (net borrower case)

i	$j \in \mathcal{S}_i$	$k \in \mathcal{D}_i$
A	C,D	B
B	A	$\emptyset$
C	$\emptyset$	A
D	$\emptyset$	A

where $\emptyset$ indicates that the bank does not have any counterparties with whom it has a lending or a borrowing relationship. As a result, the profit equation will vary across banks:

$$\begin{aligned}
\pi_t^{b,A}(IB) &= \frac{B_t^{b,AC}}{1+r_t^{b,CA}} + \frac{B_t^{b,AD}}{1+r_t^{b,DA}} - \delta_t^{b,AC} B_{t-1}^{b,AC} - \delta_t^{b,AD} B_{t-1}^{b,AD} - \frac{L_t^{b,AB}}{1+r_t^{b,AB}} + \delta_t^{b,BA} L_{t-1}^{b,AB} \\
&+ \zeta_b \left(1-\delta_{t-1}^{b,BA}\right) L_{t-2}^{b,AB} - \frac{\omega_b}{2}\left(\left(1-\delta_{t-1}^{b,AC}\right) B_{t-2}^{b,AC}\right)^2 - \frac{\omega_b}{2}\left(\left(1-\delta_{t-1}^{b,AD}\right) B_{t-2}^{b,AD}\right)^2 \\
\pi_t^{b,B}(IB) &= \frac{B_t^{b,BA}}{1+r_t^{b,AB}} - \delta_t^{b,BA} B_{t-1}^{b,BA} - \frac{\omega_b}{2}\left(\left(1-\delta_{t-1}^{b,BA}\right) B_{t-2}^{b,BA}\right)^2 \\
\pi_t^{b,C}(IB) &= -\frac{L_t^{b,CA}}{1+r_t^{b,CA}} + \delta_t^{b,AC} L_{t-1}^{b,AC} + \zeta_b \left(1-\delta_{t-1}^{b,AC}\right) L_{t-2}^{b,CA}
\end{aligned}$$

We omit the equation for bank D as this will have the same form as that for bank C. Depending on the interbank role played by each bank, certain components of the general specification do not appear. For example, C and D lend exclusively to A and do not borrow on the interbank market. Consequently, the pecuniary cost of default (parametrised by ω_b) does not appear in their profit function. From this, it is apparent that the core-periphery network will feature heterogenous profits at steady state which, after simplification, are given by:

$$\begin{aligned}
\pi^{b,A}(IB) &= \left(\frac{1}{1+r^b} - \delta^b + \zeta_b\left(1-\delta\right)\right) L^b - \omega_b\left[\left(\left(1-\delta^b\right) L^b\right)^2\right] \\
\pi^{b,B}(IB) &= \left(\frac{1}{1+r^b} - \delta^b\right) L^b - \frac{\omega_b}{2}\left[\left(\left(1-\delta^b\right) L^b\right)^2\right] \\
\pi^{b,C}(IB) &= \left(\delta^b + \zeta_b\left(1-\delta\right) - \frac{1}{1+r^b}\right) L^b
\end{aligned}$$

Net-lender case

The set of counterparties for each i when A is a net *lender* of funds is given by:

Table 1.A.2: Counterparties of i in core-periphery network topology (net lender case)

i	$j \in \mathcal{S}_i$	$k \in \mathcal{D}_i$
A	B	C,D
B	$\emptyset$	A
C	A	$\emptyset$
D	A	$\emptyset$

Which gives rise to the following profit equations:

$$\begin{aligned}
\pi_t^{b,A}(IB) &= \frac{B_t^{b,AB}}{1+r_t^{b,BA}} - \delta_t^{b,AB} B_{t-1}^{b,AB} - \frac{L_t^{b,AC}}{1+r_t^{b,AC}} - \frac{L_t^{b,AD}}{1+r_t^{b,AD}} + \delta_t^{b,CA} L_{t-1}^{b,AC} + \delta_t^{b,DA} L_{t-1}^{b,AD} \\
&+ \zeta_b \left(1-\delta_{t-1}^{b,CA}\right) L_{t-2}^{b,AC} + \zeta_b \left(1-\delta_{t-1}^{b,DA}\right) L_{t-2}^{b,AD} - \frac{\omega_b}{2}\left(\left(1-\delta_{t-1}^{b,AB}\right) B_{t-2}^{b,AB}\right)^2 \\
\pi_t^{b,B}(IB) &= -\frac{L_t^{b,BA}}{1+r_t^{b,BA}} + \delta_t^{b,AB} L_{t-1}^{b,BA} + \zeta_b \left(1-\delta_{t-1}^{b,AB}\right) L_{t-2}^{b,BA} \\
\pi_t^{b,C}(IB) &= \frac{B_t^{b,CA}}{1+r_t^{b,AC}} - \delta_t^{b,CA} B_{t-1}^{b,CA} - \frac{\omega_b}{2}\left(\left(1-\delta_{t-1}^{b,CA}\right) B_{t-2}^{b,CA}\right)^2
\end{aligned}$$

At steady state, these reduce to:

$$\begin{aligned}
\pi^{b,A}(IB) &= \left(\frac{1}{1+r^b} - \delta^b + \zeta_b\left(1-\delta\right)\right) L^b - \omega_b \left[\left(\left(1-\delta^b\right) L^b\right)^2\right] \\
\pi^{b,B}(IB) &= \left(\frac{1}{1+r^b} - \delta^b\right) L^b - \frac{\omega_b}{2}\left[\left(\left(1-\delta^b\right) L^b\right)^2\right] \\
\pi^{b,C}(IB) &= \left(\delta^b + \zeta_b\left(1-\delta\right) - \frac{1}{1+r^b}\right) L^b
\end{aligned}$$

1.B Figures

1.B.1 Additional impulse response functions: Cyclical network

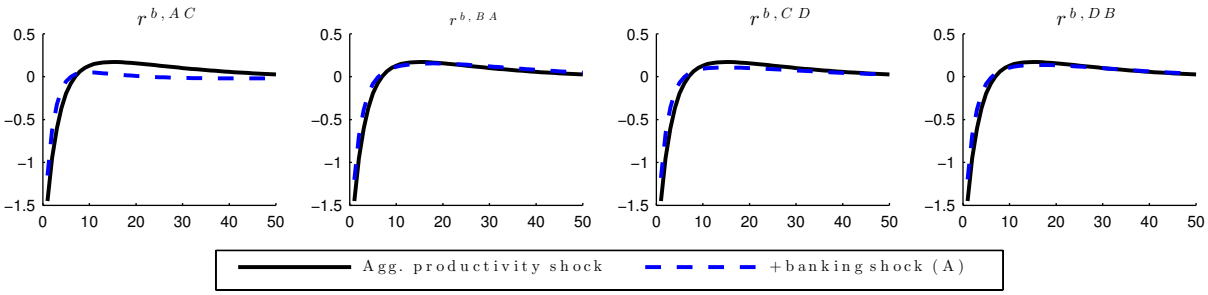

Figure 1.B.1: Interbank rates - Cyclical network

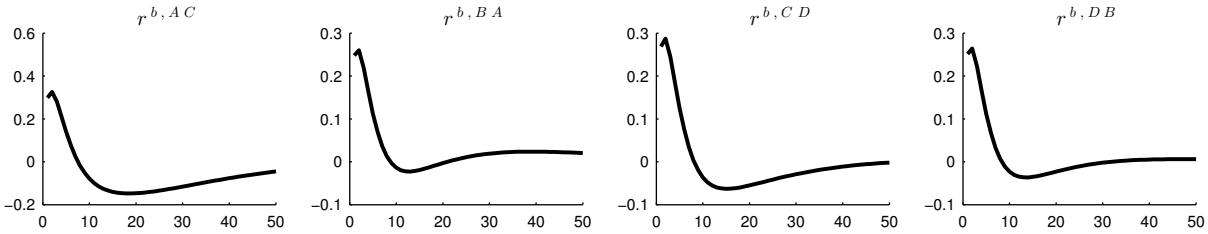

Figure 1.B.2: Interbank rates (Isolated banking shock) - Cyclical network

1.B.2 Additional impulse response functions: Complete network

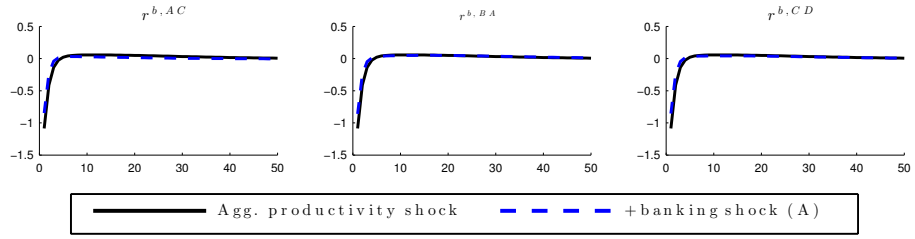

Figure 1.B.3: Interbank rates - Complete network

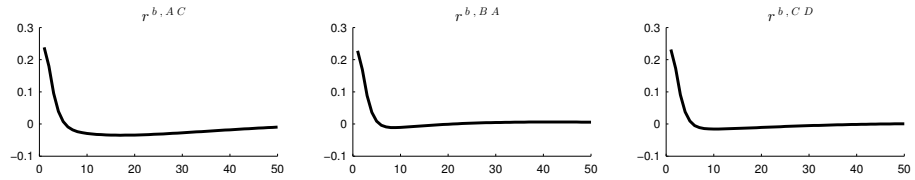

Figure 1.B.4: Interbank rates (Isolated banking shock) - Complete network

1.B.3 Additional impulse response functions: Core-periphery networks

Net borrower case

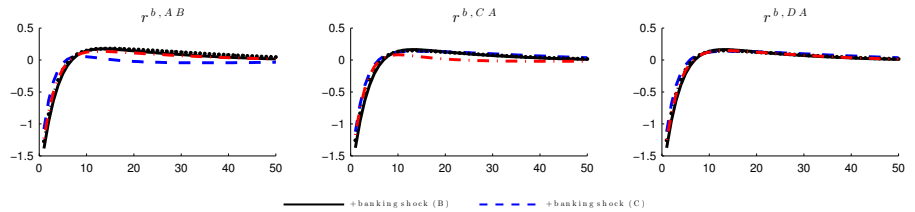

Figure 1.B.5: Interbank rates - CP network (net borrower case)

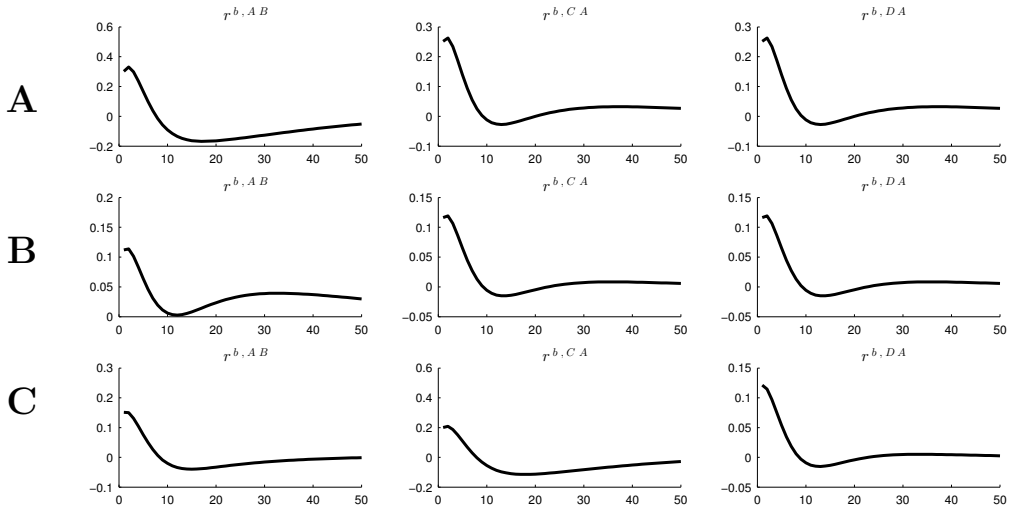

Figure 1.B.6: Interbank rates (Isolated banking shock) - CP network (net borrower case)

Net lender case

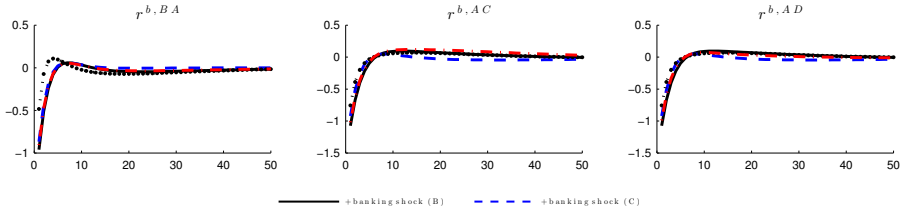

Figure 1.B.7: Interbank rates - CP network (net lender case)

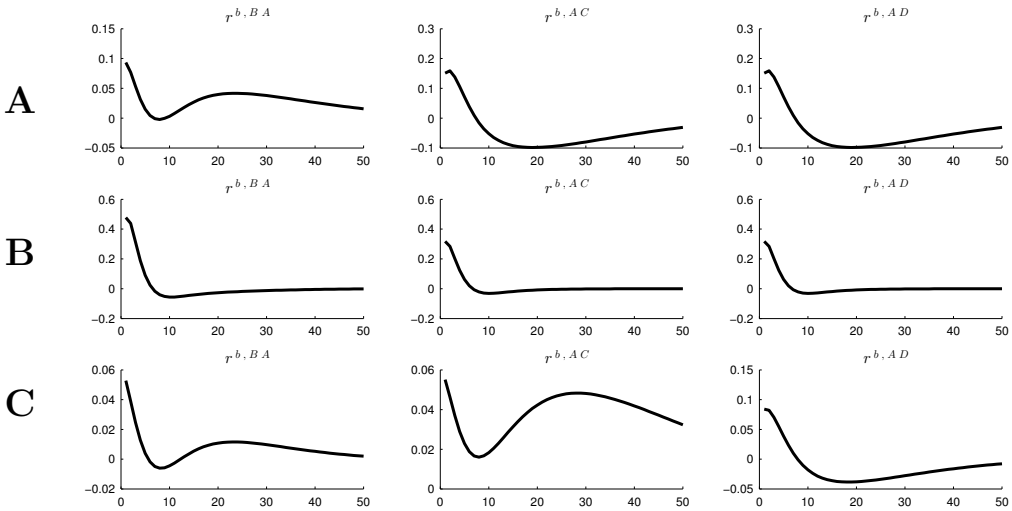

Figure 1.B.8: Interbank rates (Isolated banking shock) - CP network (net lender case)

Chapter 2

Default cascades and systemic risk on different interbank network topologies

2.1 Introduction

In a recent policy brief, Battiston et al. (2016) argue that "*network effects matter to financial-economic stability because shock amplification may occur via strong cascading trends*". This reflects a growing consensus on the importance of financial sector interconnectedness that has permeated both the research and policy[1] worlds. Within the latter, there has been a concerted effort by policymakers to introduce insights from network theory into stress testing (Anand et al., 2013; Espinosa-Vega and Sole, 2014) and identification of Globally Systemically Important Banks (G-SIBS) (BCBS, 2011). By contrast, academic research has been more multifarious, revolving broadly around two research domains namely (*i*) use of granular bank-level data from a variety of sources to reconstruct real-world interbank networks and (*ii*) simulation studies focussing on the relationship between financial contagion and network structures (and the role of connectivity) across different shock specifications and distress channels.

[1] A notable example being a 2013 speech by then Vice-Chairperson of the Federal Reserve, Janet Yellen in which "*...complex interactions among market actors may serve to amplify existing market frictions, information asymmetries, or other externalities*" (Yellen, 2013). This sentiment has been echoed by policymakers at the Bank of England (Haldane, 2009), European Central Bank (ECB, 2009) and the International Monetary Fund.(International Monetary Fund, 2010).

As is apparent, the two are intrinsically related and potentially mutually reinforcing. That is, realistic network topologies (derived from real data) can be used as a basis for counterfactual simulations aimed at assessing the likelihood and drivers of contagious defaults. Empirically-grounded networks thus lends this approach further credence as a stress-testing and systemic risk measurement device. Subsequently, these analyses enable policymakers to identify potential structural vulnerabilities in financial systems and construct adequate early-warning systems (Squartini et al., 2013). Our paper is placed firmly at this nexus. Using state-of-the-art techniques in probabilistic network simulation, we generate a variety of network structures that reflect a number of topological properties of real interbank networks. On the basis of this, we conduct a simulation study using a combination of random and targeted shocks which are propagated across the network via a *direct* and an *indirect* contagion channel. By doing so, we provide a holistic viewpoint on the systemic risk associated to a wide class of network structures.

Against this background, the first part of our analysis requires us to determine what topological features constitute a "realistic" interbank network. In a general sense, the three key findings mentioned in the general introduction of this thesis come into play: That real interbank networks feature a degree distribution following a power law, a core-periphery structure and disassortative mixing. It is important to note that these structural features are derived from *interbank exposure* data wherein interbank linkages are represented exclusively as credit flows between banks. This representation was called into question by Upper (2011), Summer (2013) and Glasserman and Young (2015) who argue that interbank exposures alone do not provide a sufficient channel for widespread default propagation[2]. With this in mind, alternate transmission channels are being explored. Chief among these is the notion that financial markets have a limited capacity to absorb the illiquid external assets due to inelastic demand in the event of a panic-driven firesale (Shleifer and Vishny, 2011; Greenwood et al., 2015; Duarte and Eisenbach, 2015). To highlight the importance of asset price dynamics, Cifuentes et al. (2005) develop a theoretical model in which sales by distressed banks depress the market price of such assets. In a mark-to-market framework, this can then induce a further round of endogenously generate firesale which further depresses asset price etc. Consequently, liquidity effects provide an *indirect channel* for shock transmission (where the direct channel arises due to interbank exposures as described earlier). Indirect contagion, defined by Clerc et al. (2016) as a situation when " *firms' actions generate externalities that affect other firms through non-contractual channels*" thus represents the next frontier in systemic risk

[2]An obvious caveat is that this may have been due to ex-post government intervention due to importance of interbank markets for liquidity reallocation and the transmission mechanism of monetary policy.

analysis. While chapter 3 of this thesis considers an 'overlapping portfolio' network à-la Caccioli et al. (2014), we restrict our analysis here to the topology of the interbank exposure network and incorporate liquidity effects via a single asset following Cifuentes et al. (2005). Comparison with the base case absent these effects reveals large systemic risk differences and motivates the multilayer network analysis undertaken in chapter 3.

Parallel to these developments in data-driven interbank network reconstruction, an alternative stream of the literature focussed on the development of simulation studies aimed at delineating the systemic implications of heterogeneous bank balance sheets and varying network structure/connectivity[3]. Early network contagion studies, inspired by epidemiological and ecological models, sought to establish theoretical relationships between and understand the conditions under which the system can undergo a *phase transition* from stability to instability. Pioneering examples within this literature are Nier et al. (2007), Gai and Kapadia (2010), May and Arinaminpathy (2010), Haldane and May (2011) and Gai et al. (2011). Key findings include: A non-monotonic impact of connectivity on financial stability (Nier et al., 2007), and a "*Robust-yet-fragile*" property in which despite low probabilities of occurrence, shocks can be extremely widespread when problems occur (Gai and Kapadia, 2010).

While these studies opened up a new field of research, as Hüser (2015) points out, they relied primarily on the random network archetype which has since been shown to be a poor fit when compared to more realistic structures (Craig and Von Peter, 2014). Moreover, current state-of-the-art models on interbank dynamics have focussed primarily on developing behavioural foundations of interbank market behaviour, the lack of which which was one of the key shortcomings of network contagion models (Upper, 2011)[4]. For example, Georg (2013) compares three different networks (random, scale free and small-world) in a dynamic model featuring portfolio-optimising banks and normal to crisis period regime switches. The robust-yet-fragile hypothesis is revisited by Acemoglu et al. (2015) who propose a variety of highly stylised topologies ranging from a complete to a ring network, identifying a phase transition below which complete networks are stabilising and above which more connections facilitate contagion. Similarly, Arinaminpathy et al. (2012) propose a random network model benchmark and fat-tailed/geometric degree distribution as a realistic alternative followed by endogenous liquidity hoarding behaviour by banks.

[3]Stemming from the seminal paper by Allen and Gale (2000) who augment the bank run model of Diamond and Dybvig (1983) to allow for interregional linkages. Their key finding is that the *complete* network is stability enhancing.

[4]Alves et al. (2013) elaborate further on the difference between *mechanical* propagation models, such as those mentioned above and those with *behavioural foundations*.

They find that the geometric network is stable when shocks occur at random but susceptible to widespread failures under a targeted shock regime.

We argue that while such models contribute to our understanding of systemic risk and contagion dynamics, they fail to harness the full power of network analysis in providing an empirically-grounded basis for their simulations. Our paper aims to fill this gap by proposing a model taking the "*best of both worlds*" through the development of a simulation study based on a topologically realistic representation of the direct exposure network combined with an encompassing shock regime (random vs. targeted shocks as well as varying shock magnitudes) and incorporation of liquidity effects. Moreover, where the canonical models focus on the relationship between network connectivity (measured either by network density or average degree) via a sensitivity analysis of the parameters, our paper is firmly grounded in network theory through our use of state-of-the-art measures aimed at capturing various dimensions of network topology. Against this background, we aim to identify what structural characteristics of interbank networks induce widespread knock-on defaults and endanger the stability of the financial system.

Using a wide array of stylised facts on real interbank network structures as a benchmark, we apply the Latin Hypercube methodology developed by McKay et al. (1979) which provides a more stratified sample compared to traditional Monte Carlo sampling. As a result, the Latin Hypercube Design (LHD) allows us to explore more of the parameter and ultimately, create a more representative sample of networks based on the fixed input parameters[5]. LHDs have recently been applied to financial Agent-Based Models by Salle and Yıldızoğlu (2014) and Bargigli et al. (2018) to create *metamodels* whose simulated moments are taken to the data. The LHD produces a large set of parameters which are subsequently fed into the *fitness-based model with mutual benefit* (Caldarelli et al., 2002), recently applied to contagion analysis by Montagna and Lux (2016) to create realistic simulated interbank networks (where realistic refers to the three structural features mentioned above). The contagion model run on the simulated networks closely follows Nier et al. (2007), Gai and Kapadia (2010) and May and Arinaminpathy (2010). However, we depart from their setup by allowing for heterogenous banks, weighting of bilateral loans dependent on the degree of similarity between connected banks and multiple random or targeted external asset shocks.

[5]From a statistical standpoint, LHD also results in efficiency gains over MC as it reduces the sampling error and increases the convergence rate of computed statistics to their theoretical values. The interested reader is referred to chapter 10.3 of Owen (2013) for the relevant mathematical proofs.

After running the default cascade model on each of our networks generated via the Latin Hypercube design, we develop an empirical specification whereby various measures of the extent of financial contagion are regressed on (*i*) global network measures, (*ii*) aggregate balance sheet variables and (*iii*) various *network centrality* measures associated to the set of initially shocked banks. Our results highlight the important role played by the network structure in explaining the extent of the default cascades. Absent liquidity effects, a number of global network measures have a significant impact on the number of failures during the simulation. Similarly, the strong explanatory power of the network is preserved when moving to the local scale via the various centrality measures associated to the shocked bank(s). Specifically, nodes with higher incloseness and betweenness centralities induce a larger default cascade as opposed to nodes with higher outcloseness and pagerank centralities which are shown to be stability enhancing. Allowing for liquidity effects reduces the explanatory power of the network on the number of failures which is intuitive given that these effects are not wholly propagated through the network. However, we observe an improved role played by the network at both scales when analysing the impact on asset price changes.

Though our approach provides the most comprehensive treatment on the impact of network topology on systemic risk (via a large number of global and local network measures), a number of related studies recognize the importance of moving towards more realistic representations of the interbank market. Notably, Temizsoy et al. (2017) study the impact of network centrality on interbank funding rates using e-MID data, finding *inter alia* that at the local scale, having more links increases borrowing costs for borrowers and reduces premia for lender. Globally, they find that banks perceived to be better connected can borrow at lower rates (echoing an earlier finding by Gabrieli and Georg (2015)). The concept of 'systemic centrality' is revisited by Chan-Lau (2018) in combination with a community detection framework to analyse groups of firm that can play a 'too important to fail' role in financial stability.

The paper is structured as follows. Section 2.2 introduces the necessary tools and definitions from network theory used in the subsequent analysis. Section 2.3 outlines the network generation algorithm and latin hypercube design for producing the replicates for the empirical analysis, Section 2.4 develops the cascading default model run on each simulated network. Section 2.5 provides the calibrated parameter bounds fed into the LH design. Section 2.7 develops the empirical model and Section 2.8 concludes and provides policy recommendations.

2.2 Network theory

2.2.1 Basic definitions

A directed graph $\mathcal{G}\left(\mathcal{N}, \vec{\mathcal{E}}\right)$ consists of a nonempty set $\mathcal{N}$ of nodes and a set of ordered pairs of nodes called edges where $\vec{\mathcal{E}} \subseteq \mathcal{N}^2$. The graph structure can be represented by the *adjacency matrix*, $A(\mathcal{G}) = [a_{ij}]_{N\times N}$ where $a_{ij} = 1$ when there exists a directed edge from node i to node j and 0 otherwise[6]. For the sake of brevity, any measure associated to a network will use the shorthand form $\vec{\mathcal{G}}$.

A useful property of directed networks that can be derived from the adjacency matrix is the in- and out-degree of each node which represent the number of incoming and outgoing links, respectively:

Definition 1. *The in- and out- degree, d_i^{in} and d_i^{out} of a node, $i \in \mathcal{N}$ are given by:*

$$d_i^{in} = \sum_{j=1}^{N} a_{ji} = (\mathcal{A}^\top)_i \cdot \mathbf{1} \quad d_i^{out} = \sum_{j=1}^{N} a_{ij} = (\mathcal{A})_i \cdot \mathbf{1}$$

Where $A^\top$ is the transpose of A[7], $(\mathcal{A})_i$ is the i^{th} row of $\mathcal{A}$ and $\mathbf{1}$ is an N-dimensional column vector $(1, \dots 1)^\top$.

For each node i, we distinguish between its in- and out-degree as this determines its initial neighbourhood of counterparties for whom i serves as a lender or borrower, denoted by the sets $\mathcal{N}_i^l(\mathcal{G}) = \{j : a_{ij} = 1\}$ and $\mathcal{N}_i^b(\mathcal{G}) = \{j : a_{ji} = 1\}$ whose cardinalities are given by the out- and in-degree, respectively.

Another node-specific property is the total number of nodes $j \in \mathcal{N}_i$ (the neighbourhood of i) for which a *bidirectional* edge exists i.e. for which $a_{ij} = a_{ji} = 1$. This can be expressed as:

$$d_i^{\leftrightarrow} = \sum_{j\neq i} a_{ij}a_{ji} = A_{ii}^2$$

[6]Furthermore, we restrict our attention to graphs containing no self-loops $a_{ii} = 0$ or multiple edges $a_{ij} \in \{0, 1\}$.

[7]We adopt the convention that the i^{th} row (column) represents node i's outgoing (incoming) links.

2.2.2 Global network measures

The set of measures[8] provided below aim to quantify different topological characteristics of the network *as a whole* (as opposed to individual nodes' importance as will be developed in the next section)[9]. These measures take the form of real-valued functions $f : \mathcal{G} \to \mathbb{R}$ ascribing a numerical value to some complex feature of the entire network structure. Following, Gabrieli and Georg (2014), we argue that these measures lend themselves to an intuitive economic interpretation within the context of interbank liquidity flows.

Density measures how *connected* the network $(\mathcal{N}, \vec{\mathcal{E}})$ is relative to the complete graph constructed on $\mathcal{N}$ (i.e. the graph with the maximum number of edges). In the directed case, this is given by:

$$D = \frac{E}{N(N-1)}$$

where $E = |\vec{\mathcal{E}}|$ denotes the number of edges in the network.

Assortativity measures the tendency of nodes with similar number of edges to connect to one another and, following Foster et al. (2010), is defined as:

Definition 2. *For a directed network, $G(\mathcal{N}, \vec{\mathcal{E}})$, a set of four assortativity measures can be computed. Let $\mu, \nu \in \{in, out\}$ denote the degree-type and j_i^μ, k_i^ν denote the μ- and ν-degree associated respectively to the source and terminal node of edge i. Then the assortativity of G is given by the Pearson correlation coefficient:*

$$\rho(\mu, \nu) = \frac{\frac{1}{E}\sum_i \left(j_i^\mu - \bar{j^\mu}\right)\left(k_i^\nu - \bar{k^\nu}\right)}{\sigma^\mu \sigma^\nu}$$

[8] These are computed using the MATLAB programming language, making heavy use of the Brain Connectivity Toolbox developed by Rubinov and Sporns (2010) for various network measures.

[9] Many of these techniques stem from the field of Social Network Analysis which coopts tools from graph theory and statistical mechanics to the analysis of human interaction via networks. The interested reader is referred to Marin and Wellman (2011) for a thorough overview of the field.

Where $\bar{j}^{\mu}(\bar{k}^{\nu})$ denotes the mean $\mu(\nu)$ degree of the source (terminal) nodes over all edges in $\mathcal{G}$. $\sigma^{\mu}(\sigma^{\nu})$ are the standard deviations of the $\mu(\nu)$-degree associated to the to the source and terminal nodes, respectively.

Reciprocity is a feature of directed networks measuring the tendency of nodes to form mutual connections (i.e. the existence of an ij and a ji edge between nodes i and j). A robust measure of reciprocity, developed by Garlaschelli and Loffredo (2004) is given by:

$$r = \frac{\sum_{i \neq j} (a_{ij} - D)(a_{ji} - D)}{\sum_{i \neq j} (a_{ij} - D)^2}$$

where, D denotes the density of the network and a_{ij} the adjacency matrix element ij.

Average path length captures the ability of the network to efficiently transfer information between nodes. Within the context of interbank networks, it measures the average length of liquidity intermediation chains. Given a directed network $\vec{\mathcal{G}}$, a path between nodes i and j is defined as a sequence of edges $\{i_1, i_2\}, \{i_2, i_3\} \ldots \{i_{N-1}, i_N\}$ such that $i_1 = i$ and $i_N = j$ and each node in the sequence $i_1 \ldots i_N$ is distinct. When multiple paths exist from node i to node j, the shortest path is referred to as the *geodesic*) and denoted d_{ij}. The average path length is then computed by taking the average of d_{ij} over each node in the network as follows:

$$\bar{l}_{\vec{\mathcal{G}}} = \frac{1}{N(N-1)} \cdot \sum_{i \neq j} d_{ij}$$

Diameter Similar to the previous measure, network diameter makes use of the geodesic to construct a value representing the network structure. However, while the average path length averages the geodesics between all node pairs in the network, the diameter simply measures the length of the *longest* geodesic.

Clustering coefficient is defined in Watts and Strogatz (1998) as the probability that two incident edges, $ij \in \vec{\mathcal{E}}$ are completed by a third one to form a triangle. Fagiolo (2007) extends the framework to binary (i.e. unweighted) directed networks. Given a node i, the product $a_{ij}a_{jk}a_{ik}$ denotes any one of the 8 possible triangles that i can form with its neighbours j and k. Consequently, the *local clustering coefficient* of i is defined as the number of directed triangles *actually* formed by i (t_i^D) divided by the total number of *potential* triangles i could form (T_i^D) . This is expressed mathematically as:

$$\begin{aligned} C_i^D(A) &= \frac{t_i^D}{T_i^D} = \frac{\frac{1}{2}\sum_j\sum_k (a_{ij}+a_{ji})(a_{ik}+a_{ki})(a_{jk}+a_{kj})}{[d_i^{tot}(d_i^{tot}-1)-2d_i^{\leftrightarrow}]} \\ &= \frac{(A+A^\top)^3_{ii}}{2\,[d_i^{tot}(d_i^{tot}-1)-2d_i^{\leftrightarrow}]} \end{aligned}$$

Our variable of interest however, is the *average clustering coefficient* which defines clustering at the network level. This is obtained by simply averaging the local C_i^D values across all nodes $i \in \mathcal{N}$.

2.2.3 (Local) centrality measures

Unlike the above measures that ascribe a numerical value to some global structural feature of the network, centrality focuses primarily on the question of what characterises an important *node*. The centrality measures described below take the form of real-valued functions whose output provides a ranking of all nodes based on varying interpretations of node importance. Many of the definitions provided below make implicit assumptions on the way information flows in through the network. Borgatti (2005) classifies the measures based on the characteristics of the flow processes into the following categories: measures based on shortest paths/geodesics between nodes (betweenness and closeness centralities) and measures based on number of walks[10] (Eigenvector, Katz and PageRank centralities) between nodes. With regard to economic interpretations, the degree of variation in the different network measures used implies that when conducting our empirical analysis on the main drivers of default cascades, we capture a variety of interpretations of what constitutes an *important node*. Against this background, these measures aim to determine the *systemic importance* of the node. As mentioned by Bramoullé et al. (2016), the policy relevance of conducting such an analysis is clear.

[10] A walk is a generalisation of a network path (see the definition of average path length) in which the the nodes in the sequence do not have to be distinct.

Degree centrality is based on the assumption that a node's importance in the network is driven purely by the number of connections it has to other nodes in the network. As such a node i's in- and out-degree centralities, $C_i^{D,in}$ and $C_i^{D,out}$ are determined by the number of incoming and outgoing edges, respectively.

Closeness centrality measures the average distance from one particular node to all other nodes in the network. Using the concept of the geodesic path (see the definition of average path length), node i's closeness centrality is given by:

$$C_i^{C,\mu} = \frac{N-1}{\sum_{j \neq i} d_{ij}^{\mu}}$$

where $\mu \in \{in, out\}$ indicates that this measure is defined both for incoming (incloseness centrality) as well as outgoing (outcloseness centrality) edges. Thus, a node with a high incloseness centrality can be reached by other nodes in the network in relatively few steps. Similarly, increasing outcloseness increases the influence exerted by that node via its ability to reach the other nodes in the network in few steps.

Betweenness centrality was first defined by Freeman (1978) and measures, in a broad sense, the share of times that any node i needs to use node k (whose centrality we are trying to measure) to access any node k. Formally, it is defined as the fraction of all shortest paths between $i, j \in \mathcal{N}$ passing through k and is expressed as:

$$C_k^B = \frac{\sum_{j \in \mathcal{N}^b} \frac{\sigma_{ij|k}}{\sigma_{ij}}}{(N-1)(N-2)}$$

where $\sigma_{ij|k}$ denotes the number of geodesics between i and j passing through k and σ_{ij} is the total number of geodesics between the two nodes. Note that this is different to the length of the geodesic paths, d_{ij} used to compute closeness centrality. The denominator is a normalisation factor denoting the total number of node pairs. The applicability of this measure to financial network analysis is apparent: a bank with high betweenness centrality exerts greater control in the intermediation chain and thus, its failure can put significant pressure on dependant banks.

PageRank centrality is derived from the *Eigenvector centrality* measure developed by Bonacich (1987) which is based on the notion that a node's relative importance in the network is determined by the importance of its immediate neighbours. Specifically, given the adjacency matrix $\boldsymbol{A}$, the standard eigenvector equation $\boldsymbol{Ax} = \lambda_1 \boldsymbol{x}$ is used to populate the $N \times 1$ vector $\boldsymbol{x}$ of node centrality scores where λ_1 denotes the largest eigenvector of $\boldsymbol{A}$. However, as pointed out by Newman (2010), its power as a centrality measure is limited in the case of directed networks due to uncertainty over the relative importance of incoming vs. outgoing edges as well as the occurrence of null centralities arising when selecting the left or right eigenvectors. These shortcomings are addressed in the centrality measure developed by Katz (1953) by giving each node a small amount of centrality "for free" via the parameter β in the equation $\boldsymbol{x} = \alpha \boldsymbol{Ax} + \beta \boldsymbol{1}$ where $\alpha \in (0, 1/\lambda_1)$ is an attenuation factor that penalises indirect connections made with distant neighbours.

The PageRank[11] centrality measure is a variation of the Eigenvector and Katz measures that conditions a node's centrality score not only the scores of its neighbours, but also on the *number* of neighbours with the logic being that the centrality contribution from each connected node should be diluted in proportion to the amount that is shared with other nodes.

$$\boldsymbol{x} = \alpha \boldsymbol{A} \boldsymbol{D}^{-1} \boldsymbol{x} + \beta \boldsymbol{1}$$

where $\boldsymbol{A}, \boldsymbol{x}$, α and β are as described above. The key difference is the inclusion of the diagonal matrix $\boldsymbol{D}$ with elements $D_{ii} = \max\{d_i^{out}, 1\}$ which ensures that nodes that point to many others pass only a small amount of centrality on to each of those others, even if their own centrality is high. To summarise, pagerank centrality is driven by three distinct factors: (i) the number of incoming links, (ii) the link propensity of the linkers, and (iii) the centrality of the linkers. Within the context of our study, the pagerank measure is distinct from degree centrality in that it conditions a node's centrality on its ability to influence nodes beyond its immediate neighbours. Moreover, it does not rely on the assumption that information flows along a geodesic, as is the case for the betweenness and closeness centrality measures.

[11] This is actually the trade name for the algorithm developed by Brin and Page (1998) to rank web pages in the original Google search engine.

2.2.4 Network structures

Erdős-Renyi networks

Given that our objective is to compare contagion dynamics across a wide variety of network topologies, the Erdős-Renyi or *random* network archetype provides a useful benchmark for our simulations. The basic premise of the model is that nodes form links randomly with independent probability p. The degree distribution is given by:

$$p_k = \binom{n-1}{k} p^k (1-p)^{n-1-k}$$

which is a binomial distribution. This property limits the applicability of the random graph model since real-world networks typically possess right-skewed degree distributions with most vertices having low degree but with a small number of high-degree "hubs" (Newman et al., 2001). Another unrealistic feature of Erdős-Renyi networks is their low clustering coefficient.

Small-world networks

In order to grow random graphs exhibiting more realistic clustering, Watts and Strogatz (1998) developed an algorithm to generate so-called small-world networks (Milgram, 1967), interpolating between a regular ring lattice (a type of network in which each node has the same degree) and an Erdős-Renyi network assuming a fixed number of nodes, and edges. The algorithm works by visiting each node in the lattice sequentially and rewiring it (i.e. taking one of the edges and connecting it to a random node in the lattice) with probability β or leaving it in place with probability $1 - \beta$ and proceeding to the next node. Barrat and Weigt (2000) provide the full degree distribution arising from the algorithm as a function of the rewiring probability, β, finding that as $\beta \to 0$, the distribution approaches the Dirac delta function of the lattice graph while as $\beta \to 1$, it approaches the Poisson distribution of the random graph.

Scale-free networks

While the Watts-Strogatz model generates networks possessing the high clustering and low average path length of real-world networks, it is unable to produce a realistic degree distribution. Barabási and Albert (1999) observe that many real-world networks exhibit a *scale-free* degree distribution characterised by a power law: $p_k \sim k^{-\gamma}$ where γ is a scaling parameter typically taking values between 2 and 3. In order to generate such networks, the authors developed the "*preferential attachment*" algorithm that features two key ingredients (*i*) *network growth* whereby, starting with a small number m_0 of nodes, a new node with $m \leq m_0$ edges is linked to the m nodes already present in the system and (*ii*) *preferential attachment* which states that the probability that a new node is connected to an existing one is proportional to the degree of the existing node.

Ultimately, the algorithm produces a scale-free network with scaling parameter $\gamma = 3$. In addition to this restrictive result, the clustering coefficient predicted by the BA model are often orders of magnitude lower than in the real-world (Klemm and Eguiluz, 2002). Caldarelli et al. (2002) develop a "*fitness*-based model" that eschews the notion of growing networks via preferential attachment in favour of the idea that two nodes form a link as a function of some intrinsic value describing their individual fitness/importance. In addition to the fact that this algorithm is capable of generating scale-free networks with realistic clustering, we argue that this approach is ideally suited towards the generation of interbank networks due to the key role played by node fitness heterogeneity in driving the network structure. This allows us to incorporate bank balance sheet heterogeneity (a key driver of interbank contagion according to Glasserman and Young (2015)) directly into our generative model, which we develop in the next section.

2.3 Network simulation

We begin by establishing the modelling approach for generating a wide variety of network topologies. This then serves as the basis for our cascading defaults contagion model. The key components of our network simulation approach involve (*i*) Setting up the probabilistic methodology for creating the network with the desired topological properties, (*ii*) establishing how these properties are driven by model parameters and (*iii*) Applying the Design-of-Experiments (DOE) framework to create an ensemble of network structures encompassing known topological properties of real interbank networks.

2.3.1 Directed network: interbank exposures

Bank size distribution

Prior to launching the fitness-model for generating the network, we develop the probability distribution from which bank balance sheet heterogeneity is derived. Following Clauset et al. (2009), we start with the power law probability density function: $p(x)\,\mathrm{d}x = Cx^{-\gamma}\,\mathrm{d}x$ where C is a normalising constant. The truncated power-law is obtained by applying the identity $\int_{a_{min}}^{a_{max}} Cx^{-\gamma}\,\mathrm{d}x = 1$ to compute C. This results in a pdf of the form:

$$p\left(a;\gamma_a,a_{min},a_{max}\right) = \frac{(1-\gamma_a)}{a_{max}^{1-\gamma_a} - a_{min}^{1-\gamma_a}} a^{-\gamma_a} \tag{2.1}$$

where $\{\gamma_a, a_{min}, a_{max}\}$ is the parameter set associated to the bank size distribution.

Fitness-based model with mutual benefit

The N-dimensional vector, $\boldsymbol{a}$ of bank sizes are now assumed to represent the node's intrinsic *fitness* i.e. its ability to attract edges in the generative model. Following Caldarelli et al. (2002), the probability that two nodes form a link is jointly driven by their fitness values:

$$p_{ij} = d \cdot \left(\frac{a_i}{a_{max}}\right)^{\alpha} \cdot \left(\frac{a_j}{a_{max}}\right)^{\beta} \tag{2.2}$$

where a_{max} denotes the largest bank in $\boldsymbol{a}$. An important feature of Equation 3.2 is the relationship between the parameters α and β and in and out degree distributions. Specifically, Caldarelli (2007) prove that Equation 3.2 yield power laws for both distributions, given by:

$$g\left(k_{in}\right) \propto k_{in}^{-\frac{1+\beta}{\beta}}, \quad g\left(k_{out}\right) \propto k_{out}^{-\frac{1+\alpha}{\alpha}} \tag{2.3}$$

Moreover, the parameter d can be adjusted to target different network densities, D:

$$D = \frac{2\sum_{i,j=1}^{N} p_{ij}}{N(N-1)} \Rightarrow d = \frac{D \cdot N(N-1) a_{max}^{\alpha+\beta}}{\sum_{i,j=1}^{N} a_i^{\alpha} a_j^{\beta}} \tag{2.4}$$

2.3.2 Latin hypercube sampling

Latin hypercube designs (LHD), developed by McKay et al. (1979) provides a robust alternative to the classical Monte Carlo approach to generating a sequence of random draws from a given probability distribution. Specifically, it addresses the issue of inefficiency whereby the Monte Carlo algorithm generates redundant sampling points while leaving other parts of the parameter space unexplored (Salle and Yıldızoğlu, 2014). By contrast, latin hypercubes stratify the random draws equally across the sample space, thereby generating a sample with good *space-filling* properties. Assuming an experimental design with p runs and d input variables/dimensions, we provide the following definition:

Definition 3. *An experimental design is expressed as a* $p \times d$ *matrix*

$$\boldsymbol{X} = \begin{bmatrix} x_1^1 & \dots & x_1^d \\ \vdots & \ddots & \vdots \\ x_p^1 & \dots & x_p^d \end{bmatrix}$$

in which each column represents a variable and each row represents a sample. The experimental design is a latin hypercube if each column is a random permutation of $\{1,2,\dots p\}$.

To illustrate our approach, we provide a toy example below comprising five random draws over two variables i.e. $(p, d) = (2, 5)$. The two-dimensional structure allows us to visualise the hypercube as a space-filling *latin square*:

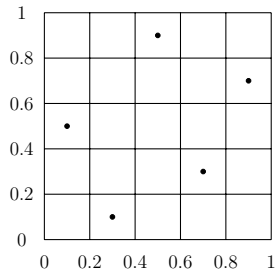

$$\boldsymbol{X} = \begin{bmatrix} 3 & 5 \\ 4 & 2 \\ 2 & 1 \\ 1 & 3 \\ 5 & 4 \end{bmatrix}$$

Figure 2.1: A space-filling latin hypercube design (source: (Santner et al., 2013))

2.4 Contagion model

Following the counterfactual simulation of p random networks via latin hypercube design, we now develop the cascading defaults model featuring *inter alia*: (i) heterogenous bank balance sheets, (ii) nonlinear liquidity effects (iii) weighted bilateral loan and shock transmission derived from bank pairs' link probability given by Equation 3.2 and (iv) a varying shock regime that drives the cascading dynamics.

2.4.1 Initialisation

We consider an interbank market comprising $N = |\mathcal{N}|$ banks linked together by their claims on one another (where the exact pattern of interbank assets and liabilities is driven by the edge structure of the simulated network). Recall that the networks are *directed*. Following convention, we assume that an edge from i to j constitutes an interbank relationship where i lends to j, with the contrary resulting from a j to i edge. Each bank/node is then imbued with the following balance sheet structure: assets, A_i comprising interbank lending, l_i and external asset holdings, e_i and liabilities, I_i comprising interbank borrowing b_i and customer deposits, d_i:

$$A_i = l_i + e_i \tag{2.5}$$

$$I_i = b_i + d_i \tag{2.6}$$

where A_i is drawn from a truncated power law distribution. This provides the first of two sources of bank heterogeneity (the second being derived from the network structure). The balance sheet identity, which fixes bank capital, η_i is then expressed as the difference between i's assets and liabilities:

$$\eta_i \equiv (l_i + e_i) - (d_i + b_i) \geq 0 \tag{2.7}$$

where $\eta_i \geq 0$ is the solvency condition for bank i. In our conceptual framework, a shock (either exogenous or transmitted from connected banks) that forces a bank's capital into negative territory results in that bank being declared insolvent. This entails removing the bank from the system while propagating any residual shock onwards to connected banks, which forms the crux of our contagion model. The specifics of the contagion mechanism will be provided in Section 2.4.2. Following Nier et al. (2007) and Montagna and Lux (2016), we define the parameters θ and γ which determine, respectively, the external asset to asset and capital to asset ratio.

$$\begin{aligned} e_i &= \theta A_i \\ l_i &= (1-\theta) A_i \\ \eta_i &= \gamma A_i \end{aligned} \tag{2.8}$$

Note that i's aggregate interbank assets are fixed ex ante, determining the magnitude of its exposure to counterparty defaults. Up to now, we have been dealing with an *unweighted*, *directed* network. In order to specify the magnitude of *bilateral* exposures, we introduce the following specification for specifying individual loan amounts l_{ij} based on i's aggregate interbank lending:

$$l_{ij} = \frac{p_{ij}}{\sum_{j \in \mathcal{N}_i^l} p_{ij}} l_i \tag{2.9}$$

Recall that p_{ij} is the probability that banks i and j form a directed edge which is driven by their similarity in size (resulting in a disassortative graph). Equation 2.9 states that banks will weight bilateral lending as an increasing function of counterparties' relative similarity in terms of size. Note that both l_i and l_{ij} are nonzero for banks that have at least one outgoing edge in the simulated network.

Similarly, for banks that borrow on the interbank market (i.e. have at least one incoming edge), aggregate interbank liabilities, b_i are determined by summing over l_{ji}

$$b_i = \sum_{j=1}^{N} l_{ji} \tag{2.10}$$

Lastly, we treat customer deposits as a residual, populated after total assets and interbank liabilities have been fixed.

$$d_i = (e_i + l_i) - (\eta_i + b_i) \tag{2.11}$$

2.4.2 Cascading defaults model

Once the network has been simulated and heterogenous balance sheets created, we proceed to defining the shock that triggers potential default propagation through the network. We begin by fixing the following notation: In each iteration, the set of shocked banks is given by the set $\mathcal{N}^{S,t} \subseteq \mathcal{N}$. As we will show in this section, this set is updated as the initial shock propagates outwards through the chain of interbank exposures. Following Nier et al. (2007), we assume that the initial shock, s_i wipes out a fraction f of a bank, or set of banks' external assets such that $s_i = f \cdot e_i^0$. In this setting, the first iteration of the model, i's external asset entry on its balance sheet is updated as:

$$e_i^1 = (1 - f)e_i^0 \tag{2.12}$$

where e_i^0 corresponds to the initial value obtained from i's total assets and the parameter θ. The loss is first absorbed by bank capital η_i followed by interbank liabilities and lastly

by deposits as the ultimate sink. Mathematically, if $s_i < \eta_i$, the shock is absorbed by bank capital and is not transmitted to i's creditors. Otherwise, the shock wipes out i's capital and the shock residual $s_i - \eta_i > 0$ is propagated onwards. If $s_i - \eta_i > b_i$, bank i's aggregate borrowing cannot absorb the entire shock. In this case, depositors face a loss of $s_i - \eta_i - b_i$. Otherwise, the residual $s_i - \eta_i$ is transmitted to i's creditors and b_i is reduced by the same amount. We assume that bilateral shock transmission is conducted on an equally-weighted basis across i's creditors. This entails dividing the residual by bank i's in-degree, d_i^{in}. Once the shock has been transmitted, the updated set of shock banks perform the same exercise, checking whether they hold sufficient capital to absorb the shock.

As described above, the asset-side shock is then compared to capital and interbank liabilities to determine whether the shock is halted or propagated onwards. We summarise these dynamics in Figure 2.2 below

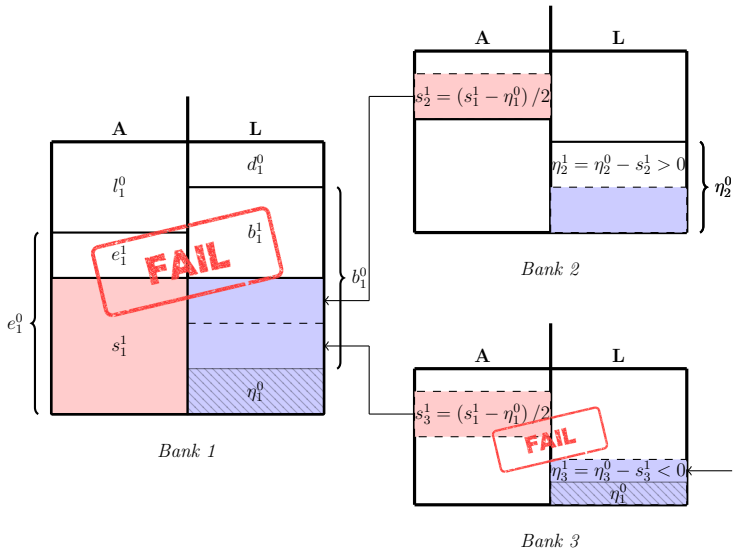

Figure 2.2: Cascading defaults model

In this simplified setup, the model is launched with a shock of magnitude s_1^1 to bank 1's external assets. It is clear that bank 1's initial capital η_1^0 is insufficient to absorb the shock. The shock residual is then divided equally across creditors 2 and 3. Where bank 2 has sufficient capital to absorb the shock (and curtail further propagation), bank 3 does not, resulting in the non-absorbed component of the initial residual being transmitted onward to its creditors.

Liquidity effects

In order to incorporate the finding that direct interbank exposures do not generate default cascades of sufficient size, we introduce liquidity risk via the firesale mechanism developed by Cifuentes et al. (2005) and introduced into the network contagion framework by Nier et al. (2007) and Gai and Kapadia (2010). In this framework, liquidity effects arise due to the limited ability of the market to absorb failed banks' assets.

The mechanism by which liquidity effects are introduced into the contagion dynamics of the model is as follows: if the asset-side shock (either to external assets in the initial case or via interbank claims in subsequent rounds) forces bank i into insolvency in iteration round t, all remaining external assets of this bank are sold off in the market, inducing a decline in market price according where the law of motion of market price is given by the following inverse demand function

$$p_{t+1} = p_t \cdot \exp\left(-\omega \cdot \frac{\sum_{\left\{i \in \mathcal{N}^S : \eta_i^t < 0\right\}} e_i^t}{\sum_{i \in \mathcal{N}} e_i^t} \right) \tag{2.13}$$

Equation 2.13 shows how the external asset price declines from p_t to p_{t+1} as a function of the relative amount of external assets sold in iteration t. The parameter ω measures the the speed at which market price declines as external assets are sold. Following Gai and Kapadia (2010), we calibrate ω such that the asset price falls by 10% when 10% of system assets have been sold.

For each insolvent bank, additional losses to capital are imposed, equal to $(p^t - p^{t+1})$ per unit of external assets sold. Thus, liquidity effects are transmitted to creditors in an additive manner via the direct channel of interbank exposures. However, assuming that external assets are marked-to-market, an *indirect channel* emerges whereby all other banks incur an additional loss brought about by the revaluation of their assets from price p_t to p_{t+1}.

Cascade algorithm

In order to demonstrate how shocks propagate through the interbank network, the pseudocode for the cascading defaults models provided in Algorithm 1. For simplicity, we do not include liquidity effects in the algorithm.

Algorithm 1 Default cascade

```
Require: ActiveBanks
stop = False
FailedBanks ← 0
while not stop do
    FailureCount ← 0
    AbsorbCount ← 0
    for (CurrentBank in ShockedBanks) do
        if CurrentBank.Shock <= CurrentBank.Capital then
            AbsorbCount = AbsorbCount + 1
            CurrentBank.Capital ← CurrentBank.Capital - CurrentBank.Shock
            Shockpropagate = 0
        else
            FailureCount = FailureCount + 1
            FailedBanks → append(CurrentBank)
            ShockedBanks ← CurrentBank.Lenders
            Shockpropagate = (CurrentBank.Shock - CurrentBank.Capital)/length(CurrentBank.Lenders)
        end if
    end for
    ActiveBanks → remove(FailedBanks)
    ActiveBanks.Lenders → remove(FailedBanks)
    ActiveBanks.Borrowers → remove(FailedBanks)
    if (AbsorbCount == length(ShockedBanks)) or (length(ShockedBanks) == 0) or ((length(FailedBanks) == NumBanks) then
        stop = True                ▷ Stop conditions: 1) Shock is absorbed 2) No further creditors 3) All banks failed
    end if
end while
```

2.5 Simulations

2.5.1 Parameter bounds for Latin Hypercube design

Before constructing the Latin Hypercube Design, we assume that each parameter from the set $\Theta = \{a_{min}, a_{ratio}, \gamma_a, \alpha, \beta, d, \theta, \gamma\}$ is drawn from a uniform distribution whose support is given in Table 2.1:

Table 2.1: Calibration bounds for simulation parameters

Parameter	**Lower bound**	**Upper bound**
Network		
a_{min}	10	50
a_{ratio}	10	50
γ_a	2	3
α	0.5	1
β	0.5	1
d	0.1	0.5
Balance sheet		
θ	0.5	0.9
γ	0.01	0.1

Following this, we implement a Latin hypercube design where the matrix $\hat{\boldsymbol{X}}$ comprises $p = 1000$ samples of the $d = 8$ parameters by defining the following vectors:

$x_{LB} = \begin{bmatrix} 10 & 10 & 2 & 0.5 & 0.5 & 0.1 & 0.5 & 0.01 \end{bmatrix}$, $x_{UB} = \begin{bmatrix} 50 & 50 & 3 & 1 & 1 & 0.5 & 0.9 & 0.1 \end{bmatrix}$, $\boldsymbol{X_{LB}} = x_{LB} \cdot \mathbf{1}$ and $\boldsymbol{X_{UB}} = x_{UB} \cdot \mathbf{1}$ where $\mathbf{1}$ is a $p \times 1$ vector of ones. These are used to construct the final latin hypercube that is used to generate our ensemble of networks.

$$\boldsymbol{X} = \boldsymbol{X_{LB}} + (\boldsymbol{X_{UB}} - \boldsymbol{X_{LB}}) \circ \hat{\boldsymbol{X}} \tag{2.14}$$

where $U \circ V$ denotes the Hadamard product of U and V. A subset of the latin hypercube is provided in Appendix 2.A.2. Each row provides the parameters used to generate the realistic interbank networks and heterogenous balance sheets using the methodology provided in Sections 2.3 and 2.4. Lastly, the model also features directly calibrated parameters for which we do not explore the impact of heterogeneity via a latin hypercube design. The first is the parameter ω which, as mentioned, measures the ability of the market to absorb assets sold in a firesale. We calibrate this as $\omega = 1.054$ following the definition given in the previous section. The fraction of shocked banks' external assets that initialises the model's cascade dynamics, $f = 0.35$ following Caccioli et al. (2014).

2.6 Instability dynamics

Before running the empirical model, we extract the median network (in terms of density, an exercise we will repeat in chapter 3) and associated cascading default model run and report the evolution of total system capital and the number of active banks under the four shock specifications with and without liquidity effects. Starting with the latter in Figure 2.3, we can immediately identify the five-bank targeted shock which not only takes longer to pass through the system, but also wipes out more capital. By contrast, the one-bank targeted shock exhibits relatively subdued dynamics. As we will show later, this can most likely be attributed to the densely-connected core; A shock hitting a bank within this set will propagate across the core-core linkages without spilling over to the wider interbank market.

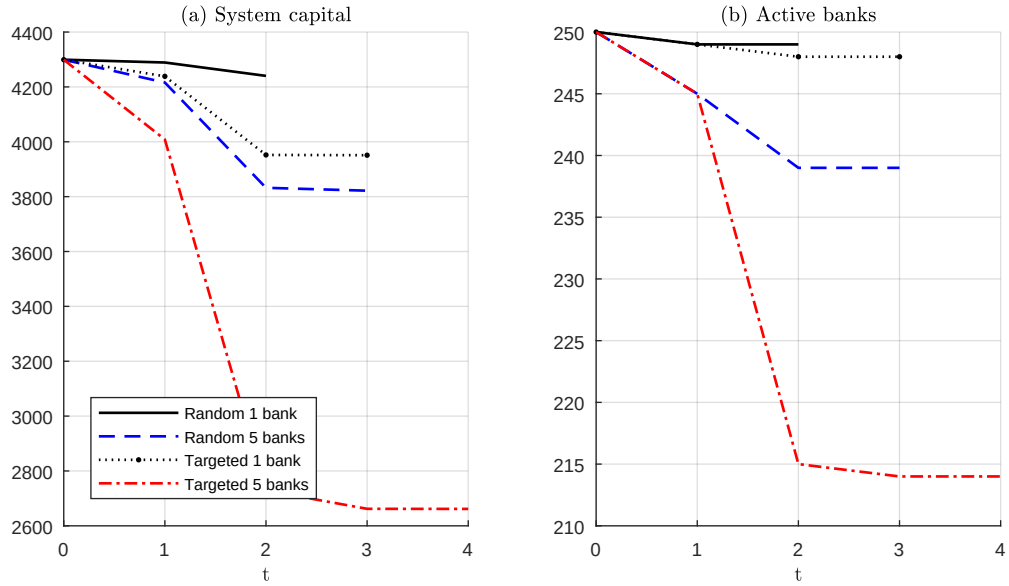

Figure 2.3: Model dynamics without liquidity effects.

Allowing for liquidity shocks significantly alters the dynamics, as shown below. While the network remains resilient to one-bank random shocks, the five bank shocks produce the largest capital losses. In terms of number of failed banks, all configurations but the one-bank random shock completely wipe out the banking sector, with the five-bank targeted shock doing so the most quickly.

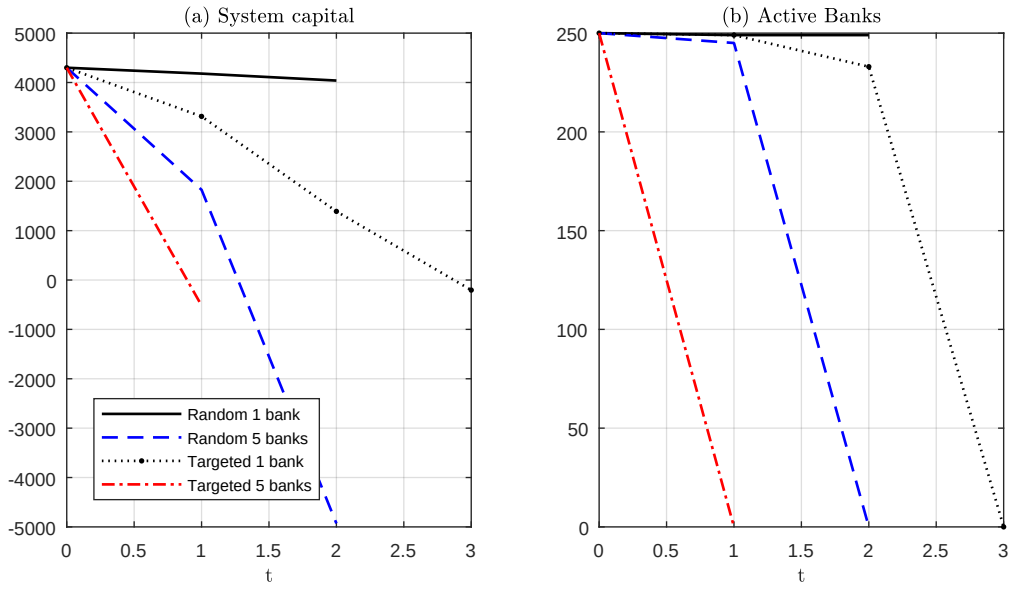

Figure 2.4: Model dynamics with liquidity effects.

The second set of results reveal the unpredictability of systemic risk dynamics when a second contagion channel is introduced. As we will demonstrate in the empirical section, this is due to the fact that liquidity effects operate *independently* of the network, transmitting via market-wide price declines rather than bilateral exposures.

2.7 Empirical Analysis

2.7.1 Simulated network properties

As stated in Section 2.2, we identify a set of six global measures that ascribe a particular value to some topological feature of the network. Throughout the current section, we will use the following shorthand forms for density ($DSTY$), diameter ($DIAM$), reciprocity ($RPTY$), assortativity ($ASTY^{\mu\nu}$), average path length (APL) and average clustering coefficient (ACC). Note that these measures capture the topology of *unweighted*, *directed* networks. Consequently, we abstract from the weights (corresponding to interbank claims) along each link set in Equation 2.8 in order to focus exclusively on the structural properties of the network.

Given that our objective in using the latin hypercube design is to create an ensemble of networks displaying a wide variety of topological characteristics, we begin our analysis by providing a set of summary statistics of the network measures of interest in Table 2.2 below. Note that since the fitness algorithm developed in Section 2.3 does not provide a closed-form relationship between the parameters and our network measures of interest, we aim to produce an ensemble of networks that reproduce key topological features of real interbank networks as closely as possible. To assess this, we compare the means of various network measures across the ensemble of simulated networks with a set of measures obtained *directly* from mappings of real interbank networks, summarised in Appendix 2.A.

Table 2.2: Summary statistics - Global network measures

Statistic	**Data**	Mean	St. Dev.	Min	Max
$DSTY$	*0.003 - 0.007*	0.071	0.039	0.010	0.221
$DIAM$	*6.6 - 7.3*	5.057	1.395	3	12
$RPTY$		0.092	0.046	0.015	0.204
$ASTY^{oi}$		−0.049	0.026	−0.141	−0.006
$ASTY^{io}$		−0.027	0.013	−0.091	−0.003
$ASTY^{oo}$		−0.038	0.019	−0.101	−0.003
$ASTY^{ii}$		−0.035	0.013	−0.107	−0.010
APL	*2.26 - 2.62*	2.451	0.468	1.782	4.549
ACC	*0.12 - 0.53*	0.166	0.076	0.020	0.328

Given the larger size and dynamic nature of the real interbank networks, a direct reproduction is infeasible. However, we observe that our algorithm creates similarly sparse networks (as evidenced by the low density value). Another topological feature successfully

replicated is the disassortativity of real interbank networks, given by the negative $ASTY$ values. The simulated values for diameter, average path length and clustering are also within the range of observed values. In order to complement the summary statistics of our network measures of interest, we provide the correlation matrix below.

Table 2.3: Correlation Matrix - Global network measures

	$DSTY$	$DIAM$	$RPTY$	$ASTY^{oi}$	$ASTY^{io}$	$ASTY^{oo}$	$ASTY^{ii}$	APL	ACC
$DSTY$	1								
$DIAM$	-0.865	1							
$RPTY$	0.723	-0.649	1						
$ASTY^{oi}$	0.214	-0.266	0.142	1					
$ASTY^{io}$	0.777	-0.710	0.665	0.130	1				
$ASTY^{oo}$	0.769	-0.787	0.639	0.557	0.810	1			
$ASTY^{ii}$	0.406	-0.446	0.299	0.661	0.367	0.467	1		
APL	-0.875	0.947	-0.722	-0.237	-0.759	-0.825	-0.448	1	
ACC	0.906	-0.818	0.941	0.160	0.759	0.740	0.365	-0.869	1

Immediately, we observe that certain network measures are *highly* correlated. For example, average clustering and density and average clustering and reciprocity. Given that these measures are all derived from the number of links in the network, a certain level of comovement is expected, however inclusion in the regression specification can pose multicollinearity concerns, resulting in large standard errors.[12] Thus, we use this exercise purely to build the regression specification that minimises the extent of correlation between independent variables.

To rectify the multicollinearity issue, we apply *variance inflation factors* which we use as a diagnostic tool to remove highly correlated predictors from the model. The VIF tables for each regression (whose dependant variables we will describe below) are provided in Appendix 2.A.4. On this basis, we propose the following candidates for removal from the model:

- Average clustering
- Indegree and outdegree centralities
- Initial interbank lending and borrowing of shocked banks

In order to express the extent of contagion in the system as a numerical value, we define the following terms: Cascade size ($CASCSIZE$) as the total capital wiped out due to the

[12] As shown in the correlation matrices in Appendix 2.A.3, multicollinearity is prevalent for the local centrality measures of the shocked banks as well. Again, this is expected given the similarity in the calculation methodologies for certain measures. For example, recall that both the closeness and betweenness centrality measures are computed using the geodesic of the network.

propagation of the shock through the system, the number of failed banks ($NUMFAIL$) over the course of the simulation and the total deposit loss ($DEPOSITLOSS$) occurring when the shock is too large to be absorbed by bank capital and interbank liabilities.Another variable $SIMTIME$, indicates the average number of iteration steps before the simulation loop is terminated due to one of the following occurrences: (i) complete absorption of the shock by bank capital implying no further propagation (ii) the current set of insolvent banks have no creditors to whom the shock can be propagated and (iii) insolvency of all banks in the system.

Recall that $CASCSIZE$ comprises losses due to insolvency (in which case the entirety of the failed bank's capital is included in the measure) as well as shock absorption. In this case, capital is reduced by the relevant amount with the difference added to $CASCSIZE$. In addition, we define the following additional variable:

$$DIFFUSION = \frac{CASCSIZE}{SHOCKSIZE}$$

where $SHOCKSIZE$ is the total capital wiped out due to the initial shock (i.e. prior to further propagation through the network). By dividing total lost capital after propagation by the exogenous initial capital loss, we obtain a variable that measures the extent to which the shock has spread through the network. The variable is, by construction, bounded above by 1 in the absence of amplifying liquidity effects since all capital losses are driven by the size and propagation of the initial shock. Thus, lower values indicates that the shock has not propagated through the network, instead remaining at or close to the initially shocked node(s). This can arise due to poor connectivity of the shocked banks and/or the relative amounts of interbank liabilities, external assets and capital.

Formally, our empirical strategy consists of estimating various versions of the following general linear regression model for each network i

$$y_i = (\beta^N)' X_i^N + (\beta^B)' X_i^B + (\beta^S)' X_i^S + \varepsilon_i \tag{2.15}$$

where y_i can be any one of the cascade variables, $CASCSIZE$, $NUMFAIL$ or $DIFFUSION$, X_i^N collects the global network measures ($DSTY$, $DIAM$, $RPTY$, $ASTY^{\mu\nu}$, APL and ACC), X_i^B collects variables associated to *aggregate* bank balance sheets and X_i^S collects the centrality measures associated to the *shocked nodes* that initialise the cascade. Consequently, our empirical framework studies the relative importance of balance sheet properties and the network from both a global and local perspective.

Regarding the empirical specification, we employ the *beta regression* model for the dependant variables expressed in normalised form by dividing by aggregate initial values. For example, $NUMFAIL$ which recall denotes the number of failed banks due to the shock, is normalised by dividing by the total number of banks initially present (250). These variables are thus constrained to the *closed* unit interval by construction. Given that beta regression applies to dependant variables in the *open* unit interval, we follow the suggestion of Smithson and Verkuilen (2006) and manually rescale the dependent variable y such that $y'' = n^{-1}(y(n-1) + 0.5)$ where n is the sample size (1000).

We end this section by discussing the dependant variables used to measure default cascades: $DIFFUSION$, $NUMFAIL$ and $DEPOSITLOSS$. Each measures a different dimension of financial contagion through the network. As already mentioned, diffusion measures the degree to which the initial shock has spread through the network. The number of failed banks is the most typically used indicator in financial contagion models, measuring the magnitude of the shock. Lastly, the total amount of deposits lost due to banks' capital and liabilities inability to absorb shocks can be interpreted as the ability of the banking sector to contain strains and not pass them onto the real economy. As such, our empirical framework encompasses a very broad definition of default cascades.

2.7.2 Baseline approach

Recall that model dynamics are driven by idiosyncratic shocks to one or more banks' external assets. In this section, we compare cascade dynamics under the random and targeted shock regimes, each consisting of two scenarios: a shock to one or five banks. In the former, the shocked banks are randomly selected across the entire set of 250 banks. By contrast, the targeted shock framework identifies the 10 largest banks out of which the shocked banks are randomly selected. In order to control for extreme events, we run the model (comprising the random draw of initially shocked banks and cascade model) `100` times for random shocks and `10` times for targeted shocks and average the simulation results. We begin by conducting the empirical analysis absent liquidity effects, which we treat as the baseline. With respect to the cascading defaults model, this implies that the market is sufficiently liquid to absorb the external assets of insolvent banks. As such, asset prices remain constant, additional losses are not imposed on creditors and external asset portfolios are not marked to market and subsequently devalued. Summary statistics of the results of the cascading defaults model over the set of networks are provided in Table 2.4 below for random shocks

Table 2.4: Summary statistics - Random shock, liquidity effects off

Statistic	Mean	St. Dev.	Min	Max
		1 bank		
$NUMFAIL$	2.018	1.377	1.000	9.230
$CASCSIZE$	60.739	28.954	10.442	163.308
$DEPOSITLOSS$	10.325	15.922	0.000	124.461
$SIMTIME$	2.293	0.270	2.000	3.400
$DIFFUSION$	0.877	0.148	0.357	1.000
		5 banks		
$NUMFAIL$	10.735	7.780	5.000	60.390
$CASCSIZE$	302.032	138.501	54.962	732.575
$DEPOSITLOSS$	51.943	79.208	0.000	659.021
$SIMTIME$	2.787	0.525	2.000	4.860
$DIFFUSION$	0.870	0.148	0.326	0.996

Focussing on the mean values, we immediately observe a strong linearity between the two shock magnitudes for random and targeted shocks (provided in Table 2.5 below) for the cascade variables $CASCSIZE$ and $DEPOSITLOSS$. Specifically, total capital and deposit loss increase approximately fivefold when moving from one to five shocked banks under both shock regimes. While this rule is obeyed for the $NUMFAIL$ variable under random shocks, it is clearly violated for targeted shocks, where moving from one to five shocked banks results in an increase by a factor of eight.

Table 2.5: Summary statistics - Targeted shock, liquidity effects off

Statistic	Mean	St. Dev.	Min	Max
		1 bank		
$NUMFAIL$	5.814	5.819	1.000	33.900
$CASCSIZE$	220.021	108.319	35.725	550.700
$DEPOSITLOSS$	19.630	43.468	0.000	372.484
$SIMTIME$	2.812	0.552	2.000	4.900
$DIFFUSION$	0.932	0.123	0.348	1.000
		5 banks		
$NUMFAIL$	40.521	47.305	5.000	250.000
$CASCSIZE$	1,054.590	518.857	175.557	2,666.553
$DEPOSITLOSS$	101.892	216.981	0.000	1,886.960
$SIMTIME$	3.636	0.982	2.000	7.700
$DIFFUSION$	0.896	0.133	0.303	0.993

As regards the $SIMTIME$ variable, we observe a much smaller increase when increasing shock magnitude under both regimes. From a policy perspective, this imposes a larger burden on regulatory bodies to prevent widespread losses as quickly as possible given that larger shocks propagate through the network (and inflict commensurately larger losses) in roughly the same time.

We now turn to the main set of results which aim to identify the key drivers of cascade dynamics through a realistic (in the topological sense) interbank network. Though we have established that targeted shocks result in higher losses and a larger number of bank failures than their random counterparts, the objective of our empirical study is *inter alia* to determine whether targeted shocks result in different aspects of the network/bank balance sheets having a significant impact on cascade dynamics.

Shock diffusion

In Table 2.6, the dependent variable of interest is $DIFFUSION$ which recall, measures the extent to which the shock has spread through the network. Given that shock diffusion is expressed as a ratio, we normalise the relevant RHS variables accordingly. Thus, where K^0 and L^0 denote aggregate initial capital and interbank exposures, their normalised forms, $\hat{K}^0$ (N.B. this can also be interpreted as the systemwide leverage ratio[13]) and $\hat{L}^0$ are obtained by dividing by aggregate initial assets. The positive coefficient of $\hat{K}^0$ indicates that system leverage plays an important role in promoting diffusion across all shock magnitudes and regimes. This is intuitive as a larger capital base implies a lower likelihood that the shock 'exits' the network by being absorbed into bank deposits after wiping out both capital and interbank liabilities. The same logic applies to the impact of $\hat{L}^0$ on diffusion. However, notice that the difference between the impact of $\hat{K}^0$ and $\hat{L}^0$ increases when moving to the targeted shock regime. As the shocked banks in this setup are larger and by construction, more connected and knowing that bank capital is affected before interbank liabilities in the shock propagation mechanism, it stands to reason that the role played by bank capital in spreading the shock through the network increases relative to interbank liabilities.

[13]We refer here to the Basel III definition of the leverage ratio (BIS, 2014) rather than financial leverage. The former is given by a bank's T1 capital over total exposures. Consequently, a higher leverage ratio implies a better-capitalised bank.

Table 2.6: Regression results - liquidity effects off

	Random shock		**Targeted shock**	
	1 bank	*5 banks*	*1 bank*	*5 banks*
$DSTY$	3.920^{**}	4.059^{**}	-4.703^{*}	-5.204^{**}
$DIAM$	-0.041	-0.042	0.006	-0.017
APL	-0.221	-0.058	-0.307	-0.030
$RPTY$	-5.601^{***}	-4.541^{***}	2.909^{*}	1.617
$ASTY^{oi}$	2.894	3.676^{**}	-1.338	-0.214
$ASTY^{io}$	12.509^{***}	10.663^{***}	-4.544	-0.421
$ASTY^{oo}$	-14.044^{***}	-11.831^{***}	2.039	-2.028
$ASTY^{ii}$	5.743^{**}	1.180	5.184	3.440
$\hat{K}^0$	15.535^{***}	15.100^{***}	19.026^{***}	23.426^{***}
$\hat{L}^0$	12.449^{***}	11.406^{***}	9.967^{***}	7.875^{***}
$INCLOSE^S$	$-1,849.971^{**}$	$-4,941.711^{***}$	$1,297.129$	722.980
$OUTCLOSE^S$	$2,065.829^{***}$	$4,338.452^{***}$	-432.176	-51.507
$BTWN^S$	-0.001	-0.003^{***}	-0.00002	-0.0005
$PAGERANK^S$	417.700^{***}	762.561^{***}	24.599	126.121
k^S	0.001	0.001	-0.002^{**}	-0.002^{***}
Constant	-2.498	-2.046	-1.672	-2.320
R^2	0.771	0.848	0.728	0.755

Notes: $^{\star}p < 10\%$; $^{\star\star}p < 5\%$; $^{\star\star\star}p < 1\%$. RHS: Aggregate capital and interbank claims divided by relevant initial values. Estimated via beta regression using the following rescaling: $y'' = n^{-1}(y(n-1) + 0.5)$ to account for 0,1 occurrences.

Turning now to the impact of global network measures, we first observe the significant impact of *network density* on shock diffusion, noting that the impact is positive for random and negative for targeted shocks. Given that higher density (i.e. number of links) implies that the shock can spread more easily through the network, the random shock results are intuitive. By contrast, increasing network density under targeted shocks decreases the shock's tendency to propagate through the network. This can be attributed to the fact that a larger density also implies that the density of links amongst the largest banks is higher. Consequently, the initial shock is quickly dissipated across the set of densely-connected large banks and fails to spread out further through the network. The assortativity variable $ASTY^{io}$ is defined as the correlation between the number of incoming edges (i.e. number of lenders) of each source node and the number of outgoing edges (number of borrowers) of each terminal node. Recalling the manner in which shocks are transmitted via interbank borrowing (i.e. from terminal to source nodes), this finding is intuitive as a higher in-out assortativity optimises the degree of contagion between the terminal (borrower) and source (lender) nodes.

Our results show that the *local* centralities of the shocked nodes significantly influence shock diffusion through the entire network under the random shock regime. Specifically, closeness centrality plays an important role in diffusing the random shock. Again the signs of the coefficients follow from the definitions of the network measures and the shock transmission mechanism. For example, incloseness centrality measures a node's reachability via incoming links. Thus, given that the shocked node transmits via its interbank liabilities (incoming links), it stands to reason that a higher incloseness centrality, indicating that the node is reachable via few links, will mitigate the ability of the shock to transmit outwards. Lastly, shocked banks with a higher *pagerank* centrality increase the spread of the shock through the network. Recall that this measure classifies a bank as "important" depending on the number of *incoming links*. Similar to the incloseness case, the significance of the measure can be attributed to the fact that shocks propagate via these links.

Number of failed banks

Table 2.7 provides the results for the second dependant variable measuring the extent of contagion through our network: the total number of failed/insolvent banks. We observe a negative impact of system leverage, lending further credence to the notion that a better capitalised banking sector is conducive to financial stability. Interestingly, under the targeted regime featuring one shock, system leverage becomes relatively more important in mitigating contagion while five shocks display a similar effect to the random shock regime. We conclude that, under the targeted 5-shock regime, bank failures are so widespread that system capital is less capable of mitigating the impact of financial contagion compared to the 1-shock regime.

Recall from Table 2.6 that the network density coefficient switched from positive to negative when going from a random to a targeted shock. We see a similar effect for $NUMFAIL$ within the targeted shock framework: For small shocks, a higher density mitigates the severity of the default cascade. By contrast, these same links serve as propagation channels for larger shocks. Regarding the assortativity coefficients, we observe that when the terminal node measure consists of incoming links $ASTY^{ii}$ and $ASTY^{oi}$, all coefficients are significant across all specifications with the former having a negative impact on $NUMFAIL$ and the latter having a positive impact. Increasing in-in assortativity decreases the number of failures as the shock is dissipated over the large number of incoming links.

Table 2.7: Regression results - Number of failed banks (liquidity effects off)

	Random shock		**Targeted shock**	
	1 bank	*5 banks*	*1 bank*	*5 banks*
$DSTY$	-0.370	1.733	-2.684^{**}	4.056^{*}
$DIAM$	0.026	0.032^{*}	0.053^{*}	0.045
APL	-0.354^{**}	-0.712^{***}	-0.663^{**}	-0.981^{*}
$RPTY$	-1.011^{***}	-1.288^{***}	-0.314	-0.883
$ASTY^{oi}$	2.226^{**}	2.716^{***}	4.143^{***}	6.121^{***}
$ASTY^{io}$	1.209	1.773	2.567	6.428
$ASTY^{oo}$	-2.871	-2.958	-8.624^{***}	-14.099^{***}
$ASTY^{ii}$	-3.148^{***}	-3.903^{***}	-6.808^{***}	-6.660^{**}
$\hat{K}^0$	-9.666^{***}	-10.336^{***}	-22.256^{***}	-10.317^{***}
$\hat{L}^0$	1.229^{***}	1.486^{***}	1.159^{***}	2.463^{***}
$INCLOSE^S$	567.262	687.248	$1,102.078^{**}$	$1,720.287^{**}$
$OUTCLOSE^S$	-659.774^{***}	$-1,127.850^{***}$	$-1,082.014^{***}$	$-1,894.556^{***}$
$BTWN^S$	0.001^{***}	0.002^{***}	0.001^{***}	0.001^{***}
$PAGERANK^S$	-122.751^{**}	-330.345^{***}	-118.706^{***}	-188.852^{**}
k^S	0.001	0.002	0.001^{**}	0.001
$\hat{S}$	11.767^{***}	3.050^{***}	4.241^{***}	2.984^{***}
Constant	-4.024^{***}	-0.821	-2.081	-1.038
R^2	0.823	0.837	0.782	0.791

Notes: $^{*}p < 10\%$; $^{**}p < 5\%$; $^{***}p < 1\%$. LHS: $NUMFAIL$ normalised by dividing by total number of banks (250). RHS: Aggregate capital and interbank claims divided by relevant initial values. Estimated via beta regression using the following rescaling: $y'' = n^{-1}(y(n-1) + 0.5)$ to account for 0,1 occurrences.

Regarding the importance of *local* network structure, we again observe an important role played by closeness centrality. Note however that the coefficient signs for these measures are reversed relative to Table 2.6. Moreover, increasing the incloseness centrality of shocked banks increases the number of failures under targeted shocks only while increasing outcloseness decreases the number of failures across all specifications. The positive incloseness coefficient indicates that since the shocked node can be easily reached via interbank borrowing chains, it will induce a larger number of defaults. By contrast, increasing outcloseness of the shocked bank(s) results in a reduced number of channels for the shock to propagate outwards. The positive coefficient for betweenness centrality suggests that increasing a bank's intermediating role (following the definition of the measure) allows for easier shock propagation resulting in a larger cascade. By contrast, shocked nodes with a higher pagerank centrality mitigate the spread of the shock through the system. As pagerank is driven by a node's incoming links, this appears to conflict with the positive coefficient of $INCLOSE^S$.

However, recalling that the pagerank measure also takes neighbours' centrality and outgoing link propensity into account, we conjecture that the stabilising role played by the pagerank centrality of the shocked node arises due to the high pagerank of its immediate neighbours implicit in the measure. As a result, once the shock propagates to these neighbours, there is a greater dissipation of the shock thereby dampening its further propagation through the network.

Deposit loss

The final dependant variable analysed in this section is the loss of customer deposits due to bank insolvencies and insufficient interbank exposures to absorb total capital losses. Compared to the previous dependant variables studied (diffusion and number of failed banks) which measure the extent to which the initial shock has spread *within* the network, deposit loss measures the amount of shock that has *escaped* the network i.e. exceeded its capacity to restrict losses to the banking sector. From a policy perspective, our analysis sheds light on the variables that, although derived from the network (i.e. the interbank market), have an impact *beyond* the network (in this case, the real economy).

Table 2.8: Regression results - Deposit loss (liquidity effects off)

	Random shock		**Targeted shock**	
	1 bank	*5 banks*	*1 bank*	*5 banks*
$DSTY$	0.080	−1.753	2.909***	2.375
$DIAM$	−0.004	0.009	0.004	0.036
APL	−0.043	−0.087	0.209	−0.432
$RPTY$	0.678***	2.185***	−1.511**	0.087
$ASTY^{oi}$	−0.435	−1.932*	0.010	−0.375
$ASTY^{io}$	−0.831	−4.260**	2.884	1.401
$ASTY^{oo}$	2.302**	5.747***	−0.357	0.468
$ASTY^{ii}$	−1.652**	−0.662	−1.916	−3.559
$\hat{K}^0$	−2.101***	−6.404***	−3.520***	−10.065***
$\hat{L}^0$	−2.191***	−5.744***	−3.695***	−7.471***
$INCLOSE^S$	103.659	2,437.583***	−609.722	−737.440
$OUTCLOSE^S$	−367.997***	−2,270.915***	383.325*	−412.517
$BTWN^S$	0.0002	0.002***	−0.0001	0.0001
$PAGERANK^S$	17.187	−232.774***	−6.700	−108.458
k^S	−0.0001	−0.0002	0.001*	0.002***
$\hat{S}$	1.160***	0.092	1.205***	0.215***
Constant	−6.229***	−4.716***	−6.089***	−0.149
R^2	0.798	0.846	0.618	0.684

Notes: $^{*}p < 10\%$; $^{**}p < 5\%$; $^{***}p < 1\%$. LHS: $DEPOSITLOSS$ normalised by dividing by total initial deposits. RHS: Aggregate capital and interbank claims divided by relevant initial values. Estimated via beta regression using the following rescaling: $y'' = n^{-1}(y(n-1) + 0.5)$ to account for 0,1 occurrences.

As the results in Table 2.8 show, system leverage and normalised interbank exposures continue to play an important role in mitigating the impact of financial shocks on agents outside the system. Amongst the global network measures, the only variable to maintain a significant impact is network reciprocity under random shocks. This is likely due to the the fact that the $DEPOSITLOSS$ variable occurs outside the network (i.e. after the network transmission channels have been used up). As a result, it is less likely that the network structure will have an impact on its magnitude.

Similar logic applies to the set of centrality measures. As shown in Table 2.7, the closeness, betweenness and pagerank centralities of the shocked banks all had a significant impact on $NUMFAIL$, with the sign of the coefficient following from the definition of the measure. By contrast, only outcloseness remains significant across the random shock regime.

The empirical analysis conducted above lends itself to a set of key findings across all dependent variables under the baseline approach. First, it is clear that amongst the three dependant variables analysed, the network structure (at both global and local scales) provides the strongest explanatory power for the number of failed banks. This is expected as bank failures serve as the triggering effect for shock propagation. By contrast, $DIFFUSION$, which is driven by $CASCSIZE$ (i.e. total capital lost by banks over the simulation) also includes capital losses of banks who absorbed the shock through capital and did not propagate via the network. Similarly, $DEPOSITLOSS$, measures the impact of the shock on customer deposits, which are affected *after* capital and interbank liability adjustments and thus, occur outside the network.

2.7.3 Liquidity effects

We now activate the liquidity effects developed in Section 2.4.2 in which the market's demand for illiquid assets is less than perfectly elastic, resulting in sales by distressed institutions depressing the market price of such assets. As mentioned, this comprises a direct channel whereby insolvent banks' losses due to firesales are added to the shock transmission via interbank liabilities and an indirect channel due to marked-to-market accounting forcing all banks (even those not directly connected to the insolvent bank) to revalue their asset portfolios.

Note that we now consider a new dependant variable, $\Delta ASSETPRICE$ denoting the endogenous change in asset price (due to firesales) from its initial value of 1. Moreover, we remove the diffusion variable from our analysis as it is no longer restricted to the closed unit interval as capital losses can now arise due to external asset firesales in addition to the propagation of the initial shock via interbank exposures. As a result, it is not feasible from an empirical standpoint to compare shock diffusion with and without liquidity effects.

Beginning with the random shock, comparison of Table 2.4 and Table 2.9 below reveals substantially increased indicators of financial distress in the presence of liquidity effects. Notably, a random shock to 1 bank resulted in an average of two failures without liquidity effects, increasing to 25 when liquidity effects are included. A similar twelvefold increase is observed when five banks are initially shocked. Though less extreme, total capital losses more than doubled under liquidity effects. By contrast, deposit losses remain more or less constant under both setups. The twofold increase in shock diffusion further highlights the important role played by liquidity effects. However, the low value of $\Delta ASSETPRICE$ suggests that marked to market accounting (indirect channel) plays a much smaller role than the additive contribution of firesales to direct interbank contagion.

Table 2.9: Summary statistics - Random shock, liquidity effects on

Statistic	Mean	St. Dev.	Min	Max
		1 bank		
$NUMFAIL$	25.371	38.791	1.000	201.490
$CASCSIZE$	123.095	113.071	10.650	599.400
$DEPOSITLOSS$	10.402	15.688	0.000	121.753
$SIMTIME$	2.258	0.181	2.000	2.880
$DIFFUSION$	1.735	1.254	0.497	6.343
$\Delta ASSETPRICE$	0.009	0.010	0.003	0.063
		5 banks		
$NUMFAIL$	128.750	87.679	5.030	250.000
$CASCSIZE$	746.024	455.710	76.341	2,644.463
$DEPOSITLOSS$	52.806	78.914	0.000	617.373
$SIMTIME$	2.394	0.419	1.100	3.310
$DIFFUSION$	2.097	0.774	0.711	4.386
$\Delta ASSETPRICE$	0.060	0.049	0.019	0.232

Turning now to model dynamics under targeted shocks, comparison of Tables 2.5 and 2.10 below reveals that the combination of targeted shocks and liquidity effects results in more widespread financial distress relative to the baseline. Comparing the increase in the number of failed banks for random shocks without and with liquidity effects ($2.018 \rightarrow 25.371$) to the the targeted shock setup ($5.814 \rightarrow 100.339$) reveals another nonlinearity under targeted shocks as the former involves an increase by a factor of 12 compared to 17 for the latter.

Table 2.10: Summary statistics - Targeted shock, liquidity effects on

Statistic	Mean	St. Dev.	Min	Max
		1 bank		
$NUMFAIL$	100.339	112.630	1.000	250.000
$CASCSIZE$	536.730	558.070	37.892	3,664.604
$DEPOSITLOSS$	20.380	43.909	0.000	398.570
$SIMTIME$	2.531	0.489	1.000	3.800
$DIFFUSION$	2.224	1.788	0.213	8.337
$\Delta ASSETPRICE$	0.043	0.057	0.012	0.398
		5 banks		
$NUMFAIL$	249.911	1.439	220.600	250.000
$CASCSIZE$	2,287.057	1,516.877	114.748	7,950.257
$DEPOSITLOSS$	105.975	218.149	0.000	1,766.362
$SIMTIME$	1.619	0.576	1.000	3.000
$DIFFUSION$	1.956	0.936	0.237	4.638
$\Delta ASSETPRICE$	0.179	0.153	0.060	0.652

Lastly, the $SIMTIME$ variables when considering liquidity effects are also lower than their counterparts. Combined with the larger shock impact, this is particularly important from a financial stability perspective as it indicates that when taking liquidity effects into account, shocks pass through the system faster *and* induce higher losses on banks.

Number of failed banks

As in the baseline approach, we now provide the results of the empirical model when the dependant variable is the (normalised) number of failed banks in Table 2.11 below. At first glance, we observe that the explanatory variables under targeted shocks exhibit a *much* lower level of significance, contrary to Table 2.7 wherein many of the variables had a significant impact across all specifications (with others, such as network density and incloseness centrality being significant only for targeted shocks). Moreover, the targeted shocks to 5 banks specification exhibits an extremely low R^2 value relative to the other three. Combined with the low level of significance, this suggests that our variables have very low predictive power in the face of large shocks. This is supported by the summary statistics table for targeted shocks in which all banks fail very quickly. Thus, the network is unable to drive dynamics in a meaningful way.

Table 2.11: Regression results - Number of failed banks (liquidity effects on)

	Random shock		**Targeted shock**	
	1 bank	*5 banks*	*1 bank*	*5 banks*
$DSTY$	1.253	0.771	−2.660	−0.041
$DIAM$	0.086**	−0.004	0.084	−0.005
APL	−0.526	0.009	−0.041	0.260
$RPTY$	−1.624***	−1.447***	−0.800	−0.076
$ASTY^{oi}$	3.967**	2.614	2.567	−2.171
$ASTY^{io}$	5.964*	4.509	6.024	−2.720
$ASTY^{oo}$	−4.593	−5.479	−3.550	3.566
$ASTY^{ii}$	−7.004***	−4.351	−6.920	2.472
$\hat{K}^0$	−55.565***	−58.516***	−62.830***	−2.431
$\hat{L}^0$	0.288**	−1.694***	−1.454***	−0.279
$INCLOSE^S$	−1,789.284**	238.350	−527.476	384.458
$OUTCLOSE^S$	866.543*	−174.728	183.999	−22.366
$BTWN^S$	0.002***	0.004***	−0.0001	0.0001
$PAGERANK^S$	42.199	62.384	74.830	−31.083
k^S	0.004	0.001	0.001	0.001
$\hat{S}$	17.754***	9.515***	3.124***	−0.102
Constant	0.894	1.071	3.444	5.630*
R^2	0.878	0.913	0.822	0.034

Notes: $^{\star}p < 10\%$; $^{\star\star}p < 5\%$; $^{\star\star\star}p < 1\%$. LHS: $NUMFAIL$ normalised by dividing by total number of banks (250). RHS: Aggregate capital and interbank claims divided by relevant initial values. Estimated via beta regression using the following rescaling: $y'' = n^{-1}(y(n-1) + 0.5)$ to account for 0,1 occurrences.

As regards the impact of the aggregate balance sheet variables, we observe that higher system leverage continues to play a strong stabilising role across all shock configurations. Furthermore, comparison of the magnitudes with Table 2.7 shows that capital becomes more important in containing the number of failed banks when allowing for liquidity effects.

Amongst the global network measures, we see a stabilising role played by link reciprocity for random shocks, as was the case under the baseline. Moreover, the magnitude of the coefficient is similar. By contrast, the impact of assortativity as well as average path length and density on the number of failed banks is reduced compared to the baseline. This allows us to summarise that global networks hold less predictive power when taking liquidity effects into account. Given that a large part of these effects (i.e. marked to market updating of all banks' external asset portfolios due to the firesale of one bank) do not propagate through the network via interbank liabilities, it stands to reason that the network structure does not drive model dynamics.

The same finding (less significant impacts of variables on the number of failed banks) can be deduced from the impact of the local centrality measures. Where betweenness had a consistent significant positive impact on the number of failed banks absent liquidity effects, it is now only significant for random shocks. In addition, the ability of closeness and pagerank centrality to predict the number of failed banks is diminished under liquidity effects. However, comparing the $BTWN$ coefficient with its baseline counterpart in Table 2.7, we see that the value has doubled. As a result, under the scenario where shocks spread rapidly through the network and inflict large losses on banks, the ability of a shocked node's betweenness in the network to predict large default cascades is improved relative to the baseline.

Deposit loss

Recall that under the baseline approach, the coefficients of the global network measures with $DEPOSITLOSS$ as the dependant variable showed a lower level of significance than the results for $NUMFAIL$, especially for targeted shocks. This finding is maintained when liquidity effects are present. Moreover, unlike $NUMFAIL$, the magnitudes and signs of the coefficients do not change dramatically when moving from the baseline. A key example is system leverage $\hat{K}^0$ which, for $NUMFAIL$, goes from a a magnitude of approx. -10 under the baseline (random shock 1 and and 5 banks as well as the targeted shock to 5 banks) to -60 in Table 2.11. By contrast, the marginal impact of the same variable on $DEPOSITLOSS$ remains within the -2 to -7 range across both setups in Table 2.12 below.

Table 2.12: Regression results - Deposit loss (liquidity effects on)

	Random shock		**Targeted shock**	
	1 bank	*5 banks*	*1 bank*	*5 banks*
$DSTY$	-0.196	-2.553^{**}	2.254^{**}	-1.834
$DIAM$	-0.007	0.009	0.015	0.033
APL	0.063	-0.006	0.138	0.692
$RPTY$	0.810^{***}	2.057^{***}	-0.071	-0.293
$ASTY^{oi}$	-0.739	-1.161	-0.765	-1.076
$ASTY^{io}$	-1.907^{*}	-3.480^{**}	1.032	-0.064
$ASTY^{oo}$	2.890^{**}	4.254^{**}	2.035	-2.275
$ASTY^{ii}$	-0.976	-1.641	-2.239	-0.247
$\hat{K}^0$	-2.107^{***}	-7.155^{***}	-4.241^{***}	0.130
$\hat{L}^0$	-2.179^{***}	-5.735^{***}	-3.622^{***}	-7.028^{***}
$INCLOSE^S$	453.682^{**}	$2,394.289^{***}$	176.290	$1,425.974^{*}$
$OUTCLOSE^S$	-528.463^{***}	$-2,110.757^{***}$	-232.661	-219.269
$BTWN^S$	0.0003^{*}	0.001^{***}	0.0003^{***}	0.0003
$PAGERANK^S$	-71.731^{**}	-109.768	-118.891^{***}	-227.224^{***}
k^S	0.0002	-0.0002	0.001^{**}	0.002^{***}
$\hat{S}$	1.274^{***}	-0.179	1.095^{***}	0.357^{***}
Constant	-6.494^{***}	-5.297^{***}	-5.871^{***}	-7.179^{***}
R^2	0.802	0.844	0.632	0.574

Notes: $^{*}p < 10\%$; $^{**}p < 5\%$; $^{***}p < 1\%$. LHS: $DEPOSITLOSS$ normalised by dividing by total initial deposits. RHS: Aggregate capital and interbank claims divided by relevant initial values. Estimated via beta regression using the following rescaling: $y'' = n^{-1}(y(n-1) + 0.5)$ to account for 0,1 occurrences.

While the impact of global network measures on deposit losses remained constant relative to the baseline, we observe the opposite effect for the centrality measures: several coefficients exhibiting low levels of significance improved when adding liquidity effects. Notably, betweenness centrality showed a significant positive impact for three of the four specifications with liquidity effects compared to one under the baseline. Similarly, pagerank centrality continues to play a strong preventative role in shock propagation, now extending beyond the confines of the network.

Change in asset price

The last dependant variable in our analysis is the change in asset price due to external asset fire sales driven by bank insolvencies. Note that $\Delta ASSETPRICE$ is not available under the baseline approach as asset price does not deviate from its initial value of 1. One of the first notable features of Table 2.13 below is the high level of significance across all variables under the random shock to 1 bank regime. Second, where the previous tables (i.e with $NUMFAIL$ and $DEPOSITLOSS$ as dependant variables) showed a reduced explanatory power of global network measures relative to their baseline counterparts, the

network structure appears to exert a stronger influence on $\Delta ASSETPRICE$. For example, increasing average path length induces smaller asset price spirals. Similar dynamics were observed under the basline model in Table 2.7 with the number of failed banks as the dependant variable. Similarly, network reciprocity plays a stabilising role under both setups.

Again, we observe a lower R^2 value under the large shock (i.e. targeted shock to 5 banks) regime combined with a lower level of significance across all variables as in Table 2.11. This further highlights the limited explanatory power of the network in the face of very large shocks.

Table 2.13: Regression results - Change in asset price (liquidity effects on)

	Random shock		**Targeted shock**	
	1 bank	*5 banks*	*1 bank*	*5 banks*
$DSTY$	2.607^{**}	0.431	5.282^{***}	-1.519
$DIAM$	0.055^{**}	0.061^{**}	0.036	-0.061
APL	-1.382^{***}	-0.666^{*}	-1.726^{***}	0.442
$RPTY$	-1.597^{***}	-1.005^{**}	-0.837	-0.627
$ASTY^{oi}$	4.233^{***}	-0.232	3.273	-2.866
$ASTY^{io}$	5.238^{***}	0.658	-1.174	-5.673
$ASTY^{oo}$	-4.642^{**}	-0.972	-2.820	3.881
$ASTY^{ii}$	-7.031^{***}	-0.107	-8.652^{***}	6.088
$\hat{K}^0$	-7.078^{***}	-35.923^{***}	-17.384^{***}	-5.319^{***}
$\hat{L}^0$	1.232^{***}	-0.510^{***}	0.606^{***}	-0.891^{***}
$INCLOSE^S$	-917.883^{**}	$-1,713.057^{**}$	-945.944	$1,012.980$
$OUTCLOSE^S$	-535.230^{**}	$1,139.284^{**}$	-952.562^{**}	-143.643
$BTWN^S$	0.002^{***}	0.001	0.001^{***}	0.0004
$PAGERANK^S$	-97.700	368.465^{**}	-58.060	-87.382
k^S	0.001	0.003^{*}	0.001	0.001
$\hat{S}$	23.528^{***}	-2.091^{***}	3.889^{***}	-1.555^{***}
Constant	-0.549	-0.124	3.824	-2.438
R^2	0.865	0.759	0.694	0.208

Notes: $^{\star}p < 10\%$; $^{\star\star}p < 5\%$; $^{\star\star\star}p < 1\%$. LHS: $\Delta ASSETPRICE$ constrained on [0,1] interval. Larger value indicates a larger deviation from initial value of 1. RHS: Aggregate capital and interbank claims divided by relevant initial values. Estimated via beta regression using the following rescaling: $y'' = n^{-1}(y(n-1)+0.5)$ to account for 0,1 occurrences.

While the impact of global network measures exhibited increased explanatory power on the change in asset price relative to the other dependant variables when allowing for liquidity effects, this finding is less conclusive when considering the impact of node centrality. However, betweenness centrality continues to play a destabilising role, a consistent finding throughout the analysis.

2.8 Concluding remarks

In this paper, we have extended the canonical cascading defaults model along two dimensions. First, we recognise that the use of *random networks* represents an unrealistic assumption given the growing consensus that real interbank networks exhibit a number of common features namely, a power-law degree distribution, disassortative mixing and a tiered/core-periphery structure. With this in mind, we apply a state-of-the-art probabilistic network simulation methodology capable of generating realistic (in the topological sense) interbank networks.

Then, rather than restricting our analysis to the standard approach of conducting comparative statics around the various balance sheet parameters at play, we apply a sophisticated Monte Carlo simulation methodology known as *Latin Hypercube Sampling* to obtain a stratified sample of networks on which the same cascading defaults model is run. Taking each replicate as an observation, we develop an empirical model by which various representative measures of the shock cascade are regressed on three categories of variables: (*i*) Global network measures representing various topological features of the network as a whole, (*ii*) aggregate balance sheet properties and (*iii*) local measures associated to the set of initially shocked banks. This last category comprises balance sheet variables associated to the shocked banks as well as various *network centrality* measures widely used in the social network analysis literature. Note that while we used variance inflation factors to control for multicollinearity, one possible extension would be to apply the rank transformation methodology (Iman and Conover, 1979) to the variables and rerun the same empirical exercise.

Our empirical strategy is built on comparing the magnitude of the default cascade when initial shocks are *random* or *targeted* and with or without liquidity effects. Given that several studies have highlighted the relatively minor contribution of interbank exposures to systemic risk, allowing for asset firesales and endogenous price spirals adds further realism to our contagion model.

As shown in the results of our empirical model, the impact of the balance sheet and network-related variables varies significantly depending on the default cascade measure used as well as the presence of liquidity effects and whether the shock is random or targeted. However, one common finding across all specifications is the important role played by *system capital* in mitigating the spread of the initial shock. From a policy perspective, this makes a case for a *macroprudential* viewpoint of bank leverage.

In the baseline model without liquidity effects, we find that amongst the three explanatory variables used to measure the magnitude of the default cascade, the number of failed banks is better explained by the structure of the network at both the global and local levels compared to deposit losses and shock diffusion. In this setup, we find that average path length plays a mitigating role in the default cascade. This finding follows from the definition of the measure. Amongst the global measures, network density is shown to shift from playing a stabilising role to promoting default cascades when moving from one to five banks. This echoes the "*robust-yet-fragile*" property of financial networks. Within the same setup, we also observed an important role played by the local centralities of the shocked banks.

We then allow for liquidity effects i.e. endogenous price spirals triggered by failure-induced asset firesales and a limited ability of the market to absorb these assets. This comprises a direct channel whereby additional losses due to firesales are compounded on to losses from interbank assets and an indirect channel stemming from banks' marking to market their external asset portfolios. While the former is propagated via the interbank network, indirect contagion is largely independent of the network, affecting all banks simultaneously. The existence of effects occurring *outside* the propagation capabilities of the network is reflected in the results of our empirical model which shows a significantly reduced role played by the network in predicting default cascades (as measured by the number of failed banks) at both the global and local levels. However, allowing for liquidity effects also introduces a new measure of the extent of the default cascade namely, the change in asset price. Unlike the number of failed banks measure, the asset price factors liquidity effects into its computation. Consequently, we expect the network to have greater explanatory power for this measure, which we observe in the results. At the global level, the same stabilising role is played by average path length while increasing network density induces larger price spirals. Amongst the centrality measures, betweenness continues to have a positive impact on the dependant variable, thereby mitigating financial stability.

Throughout the analysis, we have shown that the network structure has an important role to play in systemic risk analysis and financial system stability. This applies to the topology of the network as a whole as well as via the the use of local centrality measures to identify systemically important banks. To our knowledge, this paper is the first to not only consider cascading defaults within the context of *realistic* simulated interbank networks but also the first to posit a link between a variety of topological measures of the network and the extent of the default cascade, which we then identify empirically.

The approach developed in this paper also opens up several avenues to future work. Starting with specific modelling features, a more in-depth treatment of liquidity effects would be highly relevant within the systemic risk literature. For example, limiting the banks impacted by a marked-to-market decline in their assets as a function of the number of edges from the shocked node(s). Similarly, recognising the feedback loops present in fire sales and asset price spirals and the high volatility this engenders from an accounting perspective would make for an interesting study of *informational contagion*. Another possible extension lies in allowing for alternative shock propagation mechanisms within the same directed, weighted network. Note that the present framework entails a borrower defaulting on its liability and impacting the asset side of the lenders balance sheet. Switching the directionality of shock propagation (assets to liabilities) introduces *liquidity hoarding* into the system, whereby funding constraints limit lenders' participation in the interbank market. The following chapter of the thesis operates within this framework, using the same simulated network approach combined with an Agent-Based Model incorporating both funding and counterparty risks.

Coming now to more general research avenues, recall that the cascading defaults model features banks passively receiving and propagating shocks absent any behavioural considerations. As mentioned, the development of models of bank behaviour across a variety of markets represents a fruitful area of research which could be incorporated into our analysis. Another promising area still in its infancy is the use of granular bank data to construct financial networks. Then, rather than relying on simulation methods as we have done, researchers could compute the various topological measures associated to the financial system of a particular country, sector etc. The combination of these two dimensions into one coherent approach would constitute a powerful addition to the systemic stress testing toolbox. In this idealised setup, policymakers possess a dashboard consisting of a large set of financial institutions and interdependencies. Then, highly central nodes could be identified and subjected to a set of exogenous shocks which spread through the network following the model specification. Based on the results of this exercise, *microprudential* tools could be applied accordingly. From a *macroprudential* perspective, we have shown that the structure of the network as a whole also affects financial stability. Through early identification of such global vulnerabilities, policymakers could then implement the necessary macroprudential tools to ensure a more resilient financial system.

Chapter 2 Appendices

2.A Tables

2.A.1 Empirical basis

Table 2.A.1: Collected measures of the Austrian, US and EU interbank networks

	Austrian	US	US	EU
Descriptive				
Dataset	MAUS, GKE[a]	Fedwire RTGS[b]	Federal funds[c]	Interbank exposures[d]
Source	(Boss et al., 2004)	(Soramäki et al., 2007)	(Bech and Atalay, 2010)	(Alves et al., 2013)
Timeframe	2000-2003	Q1 2004	April 1997 - Dec 2006	31-Dec-11
Frequency	Quarterly	Daily	Daily	
Number of observations	10	64		1
Number of nodes	883	5086	470	53
Number of edges		76614	8660	1737
Total value		USD 1.3 trillion	USD 338 billion	EUR 1.7 trillion
Network measures				
Density		0.003	0.007	0.60
Reciprocity		0.22	0.065	0.71
Average path length	2.26	2.62		1.38
In	2.59		2.4	
Out	2.59		2.7	
Diameter		6.6	7.3	
Average clustering	0.12	0.53		
In			0.10	
Out			0.28	
Average degree		15.2	3.3	
Average in-degree				
Average out-degree				
Power law scaling parameter	2.01			
in-degree scaling	1.73	2.15		3.5
out-degree scaling	3.11	2.11	2.00	3.5

[a] MAUS refers to the Austrian bank balance sheet database and GKE to the major loan register (interbank loans > EUR 360,0000). Local entropy maximisation used to fill in missing values.
[b] Operated by the US Federal Reserve, the Fedwire RTGS (Real Time Gross Settlement) funds transfer system encompasses a variety of transactions between numerous participants (including government agencies). The authors restrict their focus to payment flows between commercial banks.
[c] Where Fedwire is a large value interbank electronic payment system, the federal funds market is the market for immediately available reserve balances at the Federal Reserve in which participating depository institutions can lend funds (typically at overnight maturity) at a rate referred to as the *federal funds rate*. Monetary policy implementation by the federal reserve is conducted via open market operations on this market.
[d] The dataset collected by national supervisory authorities, the EBA and the ESRB, comprises bilateral/counterparty exposures of 53 large EU banks. This consists of assets, derivatives and off-balance sheet exposures all broken down by residual maturity.

2.A.2 Latin hypercube parameter draws

Table 2.A.1: Random draws from Latin Hypercube Design

a_{min}	a_{ratio}	γ_a	α	β	d	θ	γ
36.916	49.433	2.802	0.692	0.981	0.757	0.620	0.025
48.179	35.443	2.849	0.536	0.617	0.525	0.644	0.098
37.146	36.189	2.358	0.944	0.684	0.704	0.665	0.078
28.628	21.755	2.501	0.827	0.534	0.922	0.534	0.085
37.037	34.937	2.688	0.671	0.973	0.851	0.512	0.049
17.780	34.487	2.380	0.923	0.895	0.800	0.659	0.047
28.785	32.633	2.726	0.524	0.686	0.754	0.805	0.038
36.639	30.380	2.821	0.897	0.859	0.960	0.698	0.018
27.480	21.645	2.002	0.593	0.644	0.747	0.774	0.099
13.304	31.890	2.498	0.733	0.656	0.656	0.514	0.035
11.109	20.354	2.960	0.794	0.865	0.935	0.692	0.078
38.066	25.014	2.277	0.548	0.740	0.768	0.847	0.093
21.835	47.717	2.839	0.971	0.949	0.540	0.699	0.044
15.891	26.037	2.512	0.819	0.659	0.514	0.741	0.041
40.869	48.358	2.863	0.877	0.958	0.514	0.794	0.045
31.717	45.980	2.713	0.907	0.984	0.783	0.745	0.052
48.688	42.263	2.374	0.959	0.694	0.882	0.862	0.062
42.433	34.907	2.240	0.898	0.866	0.739	0.809	0.069
35.245	32.205	2.435	0.576	0.725	0.508	0.897	0.088
18.109	39.196	2.958	0.522	0.985	0.813	0.683	0.051
15.011	35.206	2.947	0.925	0.654	0.542	0.716	0.077
23.013	32.794	2.754	0.547	0.551	0.597	0.636	0.067
41.941	21.663	2.496	0.875	0.549	0.613	0.894	0.020
15.925	31.599	2.979	0.849	0.713	0.887	0.673	0.021
37.210	20.117	2.410	0.784	0.862	0.824	0.527	0.035
28.857	30.726	2.207	0.570	0.762	0.820	0.691	0.089
22.478	32.618	2.061	0.586	0.626	0.983	0.645	0.094
23.619	24.579	2.889	0.898	0.549	0.729	0.589	0.019
47.949	20.080	2.468	0.999	0.971	0.907	0.522	0.072
41.991	23.675	2.281	0.653	0.698	0.644	0.806	0.041
32.864	27.624	2.099	0.720	0.616	0.645	0.829	0.028
49.746	41.044	2.098	0.754	0.751	0.772	0.865	0.084
32.459	43.137	2.519	0.674	0.558	0.827	0.628	0.019
37.459	42.985	2.361	0.841	0.748	0.960	0.633	0.068
17.671	20.327	2.631	0.887	0.515	0.715	0.807	0.100
12.629	23.465	2.100	0.840	0.571	0.731	0.732	0.019
45.066	27.292	2.760	0.618	0.849	0.534	0.680	0.076
47.774	46.495	2.740	0.896	0.713	0.792	0.519	0.046
30.980	49.755	2.356	0.915	0.884	0.890	0.661	0.026
20.643	34.603	2.844	0.530	0.916	0.604	0.839	0.014
24.342	32.826	2.144	0.815	0.542	0.856	0.659	0.085
47.695	47.034	2.735	0.600	0.519	0.867	0.818	0.054
11.331	36.943	2.043	0.763	0.688	0.556	0.737	0.069
36.756	30.701	2.872	0.638	0.606	0.656	0.775	0.084
19.673	26.371	2.828	0.841	0.609	0.549	0.837	0.055
29.619	43.549	2.248	0.845	0.862	0.594	0.740	0.014
14.957	33.394	2.734	0.651	0.745	0.996	0.665	0.060
43.409	38.892	2.993	0.998	0.742	0.584	0.615	0.096
12.372	43.165	2.121	0.712	0.510	0.623	0.648	0.041
42.834	38.677	2.886	0.572	0.978	0.926	0.646	0.056

2.A.3 Correlation matrices - Centrality measures

Baseline approach

Random shocks

Table 2.A.1: Correlation Matrix - centrality measures (1 bank, liquidity effects off)

	$INDEG^S$	$OUTDEG^S$	$INCLOSE^S$	$OUTCLOSE^S$	$BTWN^S$	$PAGERANK^S$	S
$INDEG^S$	1						
$OUTDEG^S$	0.998	1					
$INCLOSE^S$	0.932	0.931	1				
$OUTCLOSE^S$	0.919	0.921	0.994	1			
$BTWN^S$	-0.746	-0.744	-0.861	-0.861	1		
$PAGERANK^S$	-0.175	-0.186	-0.315	-0.339	0.694	1	
S	-0.079	-0.079	-0.117	-0.128	0.212	0.296	1

Table 2.A.1: Correlation Matrix - centrality measures (5 banks, liquidity effects off)

	$INDEG^S$	$OUTDEG^S$	$INCLOSE^S$	$OUTCLOSE^S$	$BTWN^S$	$PAGERANK^S$	S
$INDEG^S$	1						
$OUTDEG^S$	1.000	1					
$INCLOSE^S$	0.936	0.937	1				
$OUTCLOSE^S$	0.923	0.925	0.996	1			
$BTWN^S$	-0.869	-0.870	-0.962	-0.963	1		
$PAGERANK^S$	-0.405	-0.412	-0.561	-0.597	0.703	1	
S	-0.092	-0.094	-0.115	-0.126	0.115	0.175	1

Targeted shocks

Table 2.A.1: Correlation Matrix - centrality measures (1 bank, liquidity effects off)

	$INDEG^S$	$OUTDEG^S$	$INCLOSE^S$	$OUTCLOSE^S$	$BTWN^S$	$PAGERANK^S$	S
$INDEG^S$	1						
$OUTDEG^S$	0.901	1					
$INCLOSE^S$	0.935	0.878	1				
$OUTCLOSE^S$	0.856	0.933	0.939	1			
$BTWN^S$	-0.679	-0.687	-0.665	-0.675	1		
$PAGERANK^S$	0.387	0.173	0.422	0.223	0.311	1	
S	-0.022	-0.028	-0.040	-0.051	0.165	0.162	1

Liquidity effects

Random shocks

Table 2.A.1: Correlation Matrix - centrality measures (1 bank, liquidity effects on)

	$INDEG^S$	$OUTDEG^S$	$INCLOSE^S$	$OUTCLOSE^S$	$BTWN^S$	$PAGERANK^S$	S
$INDEG^S$	1						
$OUTDEG^S$	0.998	1					
$INCLOSE^S$	0.930	0.931	1				
$OUTCLOSE^S$	0.916	0.920	0.994	1			
$BTWN^S$	-0.747	-0.748	-0.867	-0.867	1		
$PAGERANK^S$	-0.110	-0.124	-0.259	-0.286	0.644	1	
S	-0.067	-0.067	-0.106	-0.114	0.164	0.204	1

Table 2.A.1: Correlation Matrix - centrality measures (5 banks, liquidity effects on)

	$INDEG^S$	$OUTDEG^S$	$INCLOSE^S$	$OUTCLOSE^S$	$BTWN^S$	$PAGERANK^S$	S
$INDEG^S$	1						
$OUTDEG^S$	1.000	1					
$INCLOSE^S$	0.937	0.938	1				
$OUTCLOSE^S$	0.924	0.926	0.996	1			
$BTWN^S$	-0.874	-0.876	-0.962	-0.963	1		
$PAGERANK^S$	-0.430	-0.438	-0.571	-0.607	0.708	1	
S	-0.093	-0.092	-0.111	-0.121	0.111	0.163	1

Targeted shocks

Table 2.A.1: Correlation Matrix - centrality measures (1 bank, liquidity effects on)

	$INDEG^S$	$OUTDEG^S$	$INCLOSE^S$	$OUTCLOSE^S$	$BTWN^S$	$PAGERANK^S$	S
$INDEG^S$	1						
$OUTDEG^S$	0.904	1					
$INCLOSE^S$	0.935	0.878	1				
$OUTCLOSE^S$	0.859	0.933	0.940	1			
$BTWN^S$	-0.693	-0.699	-0.691	-0.707	1		
$PAGERANK^S$	0.377	0.168	0.410	0.214	0.301	1	
S	-0.027	-0.029	-0.043	-0.052	0.165	0.164	1

Table 2.A.1: Correlation Matrix - centrality measures (5 banks, liquidity effects on)

	$INDEG^S$	$OUTDEG^S$	$INCLOSE^S$	$OUTCLOSE^S$	$BTWN^S$	$PAGERANK^S$	S
$INDEG^S$	1						
$OUTDEG^S$	0.907	1					
$INCLOSE^S$	0.936	0.880	1				
$OUTCLOSE^S$	0.861	0.934	0.941	1			
$BTWN^S$	-0.743	-0.740	-0.726	-0.735	1		
$PAGERANK^S$	0.390	0.185	0.437	0.239	0.240	1	
S	-0.025	-0.031	-0.041	-0.053	0.170	0.165	1

2.A.4 Variance Inflation Factors

Baseline approach

Table 2.A.1: Variance Inflation Factors for $DIFFUSION$ regression (liquidity effects off)

	Random shock		**Targeted shock**	
	1 bank	*5 banks*	*1 bank*	*5 banks*
Density	207.485	874.094	229.933	359.100
Diameter	11.797	12.071	13.560	13.857
Average_Path_Length	159.659	197.790	230.638	241.639
Average_Clustering	282.021	291.794	325.399	402.851
Reciprocity	102.234	105.195	104.762	111.238
OutIn_Assortativity	12.466	13.065	12.241	12.729
InOut_Assortativity	11.946	12.280	11.113	11.357
OutOut_Assortativity	28.494	30.762	28.110	28.485
InIn_Assortativity	6.551	7.209	7.200	7.248
Norm_Init_Capital	4.149	4.323	4.197	4.195
Norm_Init_IB_exp	3.637	3.580	3.738	3.341
Indeg_cent_SB	437.579	1784.132	131.632	269.378
Outdeg_cent_SB	297.469	1434.463	145.990	275.287
Inclose_cent_SB	335.005	540.207	314.668	415.860
Outclose_cent_SB	148.236	286.657	113.999	133.108
Btwn_cent_SB	27.765	59.831	19.882	43.699
Pagerank_cent_SB	11.927	11.251	26.924	50.051
Init_capital_SB	6.098	6.297	6.386	6.151
Init_IBB_SB	192.280	979.614	27.017	29.005
Init_IBL_SB	196.125	984.768	27.664	29.184

Table 2.A.1: Variance Inflation Factors for $NUMFAIL$ regression (liquidity effects off)

	Random shock		**Targeted shock**	
	1 bank	*5 banks*	*1 bank*	*5 banks*
Density	204.269	805.269	208.132	328.787
Diameter	12.271	12.375	12.916	12.595
Average_Path_Length	153.748	190.842	221.588	252.111
Average_Clustering	286.922	293.093	303.188	401.550
Reciprocity	99.417	100.332	103.536	115.062
OutIn_Assortativity	11.710	12.406	12.089	14.684
InOut_Assortativity	10.774	11.362	10.952	12.829
OutOut_Assortativity	27.107	29.620	26.116	30.243
InIn_Assortativity	5.824	6.313	6.849	7.443
Norm_Init_Capital	6.540	7.177	6.828	6.876
Norm_Init_IB_exp	2.903	2.921	2.834	2.908
Indeg_cent_SB	431.845	1911.526	121.969	257.178
Outdeg_cent_SB	327.636	1541.187	132.864	240.046
Inclose_cent_SB	321.004	535.415	281.091	401.398
Outclose_cent_SB	151.111	295.020	102.556	134.905
Btwn_cent_SB	29.777	60.783	19.000	52.274
Pagerank_cent_SB	12.424	9.722	26.610	62.333
Init_capital_SB	6.542	6.786	6.312	6.381
Init_IBB_SB	212.870	1024.626	28.858	30.583
Init_IBL_SB	216.354	1026.871	27.488	29.498
Norm_Shock_size	3.508	3.620	3.655	3.777

Table 2.A.1: Variance Inflation Factors for $DEPOSITLOSS$ regression (liquidity effects off)

	Random shock		**Targeted shock**	
	1 bank	*5 banks*	*1 bank*	*5 banks*
Density	203.071	871.763	227.311	382.836
Diameter	11.882	12.656	14.422	15.345
Average_Path_Length	153.681	195.161	231.779	258.805
Average_Clustering	288.132	291.511	334.507	410.585
Reciprocity	101.930	103.934	107.076	111.837
OutIn_Assortativity	12.851	13.008	12.694	12.615
InOut_Assortativity	11.930	12.616	11.534	11.820
OutOut_Assortativity	28.879	31.529	29.427	30.825
InIn_Assortativity	6.469	7.383	7.381	7.665
Norm_Init_Capital	5.962	6.580	6.180	6.509
Norm_Init_IB_exp	3.514	3.770	3.482	3.782
Indeg_cent_SB	416.549	1810.574	129.315	285.919
Outdeg_cent_SB	301.806	1466.887	146.036	299.277
Inclose_cent_SB	323.754	546.832	326.844	462.535
Outclose_cent_SB	148.070	284.471	111.609	128.565
Btwn_cent_SB	28.865	59.098	19.162	41.659
Pagerank_cent_SB	12.079	11.318	25.919	44.952
Init_capital_SB	6.280	6.366	6.254	6.409
Init_IBB_SB	207.888	1005.394	27.014	28.151
Init_IBL_SB	212.776	1009.657	27.461	28.888
Norm_Shock_size	3.333	3.527	3.398	3.519

Liquidity effects

Table 2.A.1: Variance Inflation Factors for $DIFFUSION$ regression (liquidity effects on)

	Random shock		**Targeted shock**	
	1 bank	*5 banks*	*1 bank*	*5 banks*
Density	235.262	712.371	203.029	308.772
Diameter	11.472	11.617	12.159	12.252
Average_Path_Length	153.083	192.315	224.038	238.552
Average_Clustering	295.206	294.578	333.573	411.549
Reciprocity	103.903	103.719	109.156	113.478
OutIn_Assortativity	13.432	13.786	13.571	13.985
InOut_Assortativity	12.382	12.688	12.020	12.417
OutOut_Assortativity	29.949	31.150	28.884	29.847
InIn_Assortativity	6.357	6.951	7.398	7.590
Norm_Init_Capital	4.142	4.222	3.939	3.943
Norm_Init_IB_exp	3.188	3.210	2.988	3.006
Indeg_cent_SB	474.434	1770.632	123.699	237.386
Outdeg_cent_SB	324.916	1406.214	120.246	220.544
Inclose_cent_SB	313.538	536.691	283.005	389.287
Outclose_cent_SB	145.097	309.667	110.904	136.580
Btwn_cent_SB	28.341	54.877	25.083	51.573
Pagerank_cent_SB	10.623	9.876	34.894	63.101
Init_capital_SB	6.718	6.622	6.325	6.351
Init_IBB_SB	252.538	1051.234	27.603	30.474
Init_IBL_SB	254.306	1045.181	28.145	30.223

Table 2.A.1: Variance Inflation Factors for $NUMFAIL$ regression (liquidity effects on)

	Random shock		**Targeted shock**	
	1 bank	*5 banks*	*1 bank*	*5 banks*
Density	242.105	681.100	201.503	309.689
Diameter	12.506	11.809	12.174	12.149
Average_Path_Length	159.891	192.788	225.209	244.371
Average_Clustering	281.931	304.296	332.601	412.582
Reciprocity	96.677	108.261	108.958	113.747
OutIn_Assortativity	12.431	13.909	13.530	13.925
InOut_Assortativity	11.027	13.309	11.971	12.415
OutOut_Assortativity	28.464	31.783	28.876	29.905
InIn_Assortativity	5.904	7.203	7.371	7.583
Norm_Init_Capital	7.507	5.525	6.906	6.045
Norm_Init_IB_exp	2.907	3.990	3.189	3.190
Indeg_cent_SB	480.480	1812.102	122.999	238.393
Outdeg_cent_SB	341.801	1486.386	119.149	221.266
Inclose_cent_SB	314.225	548.964	282.521	393.040
Outclose_cent_SB	144.530	307.480	110.783	138.499
Btwn_cent_SB	26.445	56.798	25.354	52.136
Pagerank_cent_SB	10.652	10.463	35.133	63.628
Init_capital_SB	6.356	6.344	6.353	6.352
Init_IBB_SB	242.451	1061.344	27.715	30.757
Init_IBL_SB	242.176	1051.434	28.128	30.463
Norm_Shock_size	3.592	3.513	3.461	3.410

Table 2.A.1: Variance Inflation Factors for $DEPOSITLOSS$ regression (liquidity effects on)

	Random shock		**Targeted shock**	
	1 bank	*5 banks*	*1 bank*	*5 banks*
Density	223.380	743.676	211.387	348.572
Diameter	11.902	12.473	14.571	15.462
Average_Path_Length	156.636	198.817	227.526	238.896
Average_Clustering	290.187	284.117	344.227	428.343
Reciprocity	102.709	101.979	105.645	111.754
OutIn_Assortativity	12.820	12.506	12.305	12.698
InOut_Assortativity	12.056	12.029	10.950	12.190
OutOut_Assortativity	29.163	30.016	28.445	32.245
InIn_Assortativity	6.467	7.319	7.416	7.390
Norm_Init_Capital	6.319	6.539	6.209	6.200
Norm_Init_IB_exp	3.555	3.763	3.475	3.885
Indeg_cent_SB	465.421	1829.949	128.759	265.281
Outdeg_cent_SB	330.494	1380.450	133.901	267.563
Inclose_cent_SB	320.419	572.782	304.832	452.416
Outclose_cent_SB	143.928	295.953	113.220	129.664
Btwn_cent_SB	27.695	47.721	23.116	46.510
Pagerank_cent_SB	10.516	10.620	29.944	53.537
Init_capital_SB	6.547	6.351	6.223	6.352
Init_IBB_SB	242.498	943.372	26.437	28.733
Init_IBL_SB	245.162	935.723	27.495	29.741
Norm_Shock_size	3.448	3.498	3.438	3.463

Table 2.A.1: Variance Inflation Factors for $\Delta ASSETPRICE$ regression (liquidity effects on)

	Random shock		**Targeted shock**	
	1 bank	*5 banks*	*1 bank*	*5 banks*
Density	248.598	708.394	202.932	311.508
Diameter	12.584	11.862	12.606	12.027
Average_Path_Length	153.330	203.995	227.511	237.453
Average_Clustering	283.404	292.451	311.158	413.830
Reciprocity	97.026	102.447	104.605	114.117
OutIn_Assortativity	11.340	13.625	13.140	13.947
InOut_Assortativity	10.788	11.821	11.840	12.722
OutOut_Assortativity	27.311	30.100	27.878	30.052
InIn_Assortativity	5.560	6.553	7.092	7.578
Norm_Init_Capital	7.391	6.855	6.650	5.895
Norm_Init_IB_exp	2.948	3.075	2.899	3.350
Indeg_cent_SB	475.317	1778.091	124.825	237.634
Outdeg_cent_SB	339.091	1387.879	120.779	221.399
Inclose_cent_SB	314.630	534.904	282.585	385.308
Outclose_cent_SB	132.991	310.855	109.126	136.704
Btwn_cent_SB	25.248	55.428	26.546	51.802
Pagerank_cent_SB	10.695	9.965	34.545	63.682
Init_capital_SB	6.760	6.373	6.170	6.447
Init_IBB_SB	247.828	1121.925	28.502	29.891
Init_IBL_SB	247.640	1114.903	27.797	30.289
Norm_Shock_size	3.917	3.523	3.620	3.433

Chapter 3

Central bank policy experiments using a multilayer network and an embedded agent-based model of the interbank market

3.1 Introduction

A key feature of the 2007-2008 financial crisis was the resulting impairment of global money markets (Brunnermeier, 2009). Beginning in August 2007, risk premia on the unsecured, interbank market rose to unprecedented levels in both the EU (Brunetti et al., 2010) and US (Taylor and Williams, 2009). This was accompanied by a sharp reduction in interbank lending volumes (Afonso et al., 2011). In light of the ongoing turmoil, and given the importance of the interbank market in facilitating private sector credit provision and as the first step in the transmission mechanism of monetary policy, central banks were quick to intervene by increasing the stock of aggregate bank reserves and lowering short-term interest rate targets to near zero in order to restore interbank market functioning and minimise spillovers to the real economy. Despite an unprecedented level of policy intervention in both the US (Sarkar, 2009) and EU (Giannone et al., 2012) in the early stages of the crisis, the unsecured interbank market in both these jurisdictions remained severely impaired and credit conditions tightened (Iyer et al., 2013). Following successive rounds of unconventional monetary policy, interest rates stabilised (Abbassi and Linzert, 2012) as central banks, in their capacity as lenders of last resort, gradually replaced the interbank market in allocating liquidity across the banking sector (Garcia-de Andoain et al., 2016).

This puzzling disconnect between aggressive liquidity provision by monetary authorities and continued hoarding behaviour by banks has spawned a rich research agenda attempting to identify the drivers of interbank market tensions. To date, two opposing viewpoints have emerged, without consensus. The first revolves around increases in *counterparty risk* as banks, unsure of the creditworthiness of borrowers, require higher risk premia (taking the form of higher interbank rates) to participate in the market. The opposing viewpoint points to increases in *liquidity risk* driven by banks' uncertainty regarding their ability to attract funding in the future.

Counterparty risk is defined as "*the risk that a party to an contract may fail to perform on its contractual obligations, causing losses to the other party*" (Canabarro and Duffie, 2003). Intuitively, it involves banks using private information[1] to form an assessment on their counterparties which in turn, may incentivise liquidity hoarding. This is the case in Heider et al. (2015) who develop a model in which the interplay between endogenous liquidity and asymmetric information about the risk of banks' assets exacerbates *counterparty credit risk* and can lead to hoarding behaviour. In their model, intervention by the central bank crowds out private liquidity supply thereby impeding price discovery and peer monitoring. Similarly, Acharya and Bisin (2014) identify a counterparty risk externality arising due to the opacity of bilateral financial transactions.

In contrast to counterparty risk, the liquidity risk driver of interbank market dynamics states that bank behaviour on the interbank market is driven primarily by concerns over their own ability to attract funding (Diamond and Rajan, 2011). Turning to the interbank market, Eisenschmidt and Tapking (2009) argue that counterparty risk alone cannot account for the increased spreads in the unsecured interbank market. They identify a *funding liquidity risk premium* whereby banks lend at elevated rates in term money markets in order to account for the risk of borrowing in the overnight segment while Drehmann and Nikolaou (2013) develop an empirical model in which the liquidity risk premium is based on banks' bidding behaviour in central bank open market operations (OMOs). The impact on liquidity hoarding is explored by Acharya and Skeie (2011) who develop a model in which lenders' willingness to provide term funding is driven by the risk of being unable to roll over their own maturing debt. Acharya and Merrouche (2012) hypothesise and confirm, using UK Sterling Money Market data, a *precautionary motive* to liquidity hoarding by banks during the crisis. The precautionary aspect of liquidity hoarding is corroborated by Berrospide (2013) and De Haan and van den End (2013) for

[1]Seen as one of the key elements of decentralised interbank markets by Rochet and Tirole (1996) in that it motivates effective peer monitoring between banks.

the U.S and Dutch banking sectors, both finding that increased funding liquidity risk puts downward pressure on bank lending.

A number of articles, recognising the importance of disentangling credit and liquidity effects, propose empirical models to this effect. Notably, Taylor and Williams (2009) find that increased counterparty risk played a predominant role in driving the widening LIBOR-OIS spread during the crisis. By contrast, Michaud and Upper (2008) find a significant role played by interbank bid-ask spreads which are commonly used as liquidity measures. More recently, Schwarz (2015) develops a robust set of liquidity and credit risk measures which, when applied to the Italian e-MID dataset during the crisis, shows that market liquidity effects explain more than three times the variation in interbank rate spreads relative to credit. Within the literature applying term-structure models to interbank spreads, both Filipović and Trolle (2013) and Dubecq et al. (2016) confirm the significance of credit and liquidity effects at various stages of the crisis.

Thus, while the empirical literature is converging on the notion that interbank rate dynamics are driven by a combination of liquidity and credit factors, current theoretical models remain firmly entrenched within the two camps. This is due to the fact that such models lack the flexibility to concretely incorporate *both* counterparty and liquidity risk concerns into bank behaviour let alone study the implications of the interactions and feedback effects between them on financial stability and central bank policy. With these concerns in mind, we argue that Agent-Based Modelling (ABM) provides a flexible environment in which the various types of risk can be incorporated into a dynamic, behavioural model in a tractable manner. At their core, ABMs are essentially computerised simulations of autonomous agents interacting in a *bottom-up* fashion through a set of prescribed heuristics. According to Farmer and Foley (2009) and Haldane (2016), the inclusion of agent heterogeneity and interaction makes such models particularly useful towards the study of complex economic dynamics. Similarly, Bookstaber et al. (2017) argues that agent heuristics and interactions must be considered in parallel in order to properly model financial crises.

Operating at the nexus of individual bank behaviour and inter-bank interactions, our approach entails embedding an Agent-Based Model (ABM) inside a network calibrated to replicate certain topological features of real interbank networks. Where the network determines the initial set of interdependencies between banks, the ABM dictates how banks interact with one another in this environment by fixing interbank borrowing/lending volumes as well as interest rates. Our model makes use of the *bounded rationality* paradigm whereby agents/banks form expectations based on observable quantities

which are updated in each period as additional observations become available. Moreover, bank decision-making on the interbank market is characterised by simple heuristics which determine *inter alia* lenders' willingness to provide interbank funding, their setting of interbank risk premia along with borrowers' firesale of securities to meet interbank obligations. Against this background, we incorporate counterparty, market and funding liquidity risk into the behavioural specification of banks in a tractable framework wherein each driver features in the different heuristics throughout the simulation.

The model proceeds in two steps. The first step involves simulating a *core-periphery* network following the empirical literature documented in the general introduction of the thesis. To do this, we make use of the generative algorithm developed by Montagna and Lux (2016) also used in chapter 2. However, where the previous chapter assumed the directionality of the interbank linkages, we now simulate an *undirected* network where edge directions and weights arise due to bank behaviour, resulting in a *dynamic representation of the interbank market*. In this way, we also partially endogenise the network structure. Similarly, abstracting from directionality *ex ante* provides a stronger alignment with the notion of a bank 'relationship' that can be mobilised to provide/request liquidity as needed.

In addition, we incorporate the findings by Upper (2011), Summer (2013), Clerc et al. (2016) and Caccioli et al. (2018) that direct exposures alone are not a significant contributor to systemic risk by also allowing banks to hold overlapping portfolios of securities, thus providing a form of *indirect* dependency between banks via the endogenous price and firesale dynamics of the securities within their portfolios. This extends the single-asset framework (where portfolio overlap is maximal by definition) used in chapter 2 where allowing for liquidity effects via a combination of firesale-induced price spirals and marked-to-market accounting created large systemic risks in the network. Our simulation methodology in the current chapter is based on Caccioli et al. (2014) who develop a model to simulate a *random bipartite network* representing banks' asset holdings. Note that unlike the direct exposure layer, we remain agnostic about the structure of the overlapping portfolio layer, relying on the random network structure. We justify this by recognising that empirical studies along this dimension are still in their nascent stage. For example, Huang et al. (2013) uses US balance sheet data and the bipartite formulation in a cascading defaults model but does not elucidate the topology of the network. A more recent article by Fricke and Roukny (2018) examines banks' diversification incentives in terms of firm credit via a bipartite representation of Japanese bank-firm data.

Combining the direct exposures and overlapping portfolio networks, we obtain a *multi-layer* structure comprising two forms of interdependency between the same set of banks whereby interbank dynamics occur not only *within* the two layers, but *across* them as well. In this way we align the chapter with the state of the art in interbank network modelling. Moreover, it extends the complex network structure developed in chapter 2 while developing a comprehensive behavioural framework for interbank dynamics, as was done in chapter 1.

Once the network has been generated, we embed the ABM using the approach developed by Lux (2015) where the balance sheet elements of each heterogeneous bank are initialised using the bank sizes (populated in the network generation step) and a set of calibrated weight parameters. The ABM then proceeds sequentially over a fixed simulation time, with each period comprising three *phases* in which various aspects of interbank trading occur. In *phase 1*, a deposit shock determines whether banks go to the interbank market as *lenders* or *borrowers*. The interbank market arises when borrowers (those hit by a negative shock) make funding requests to their local neighbourhood of counterparties. This reallocation of funds from excess to deficit banks as the prime motivation for interbank markets forms part of the standard banking model developed by (Allen and Gale, 2004). Furthermore, similar to Acemoglu et al. (2015), our model incorporates the real economy via an illiquid investment made both by liquidity-long and short banks. A key modelling assumption throughout the paper is that bank decisions vis-à-vis the size and composition of their balance sheet revolve around the adjustment of assets/leverage rather than capital.[2]

After borrower requests have been transmitted to the counterparties in their local neighbourhood (within the network), lenders first allocate available liquidity across their local counterparties and then proceed to fixing the interbank rate offered to each borrower. Funding liquidity risk is incorporated in the first step: Each lender chooses how much of their available reserves to allocate to interbank lending (conversely, how much to *hoard* in that period) based on its perception of its own past ability to attract wholesale funding the last time a negative shock cast it into a borrowing role. This is broadly in line with the definition given by Brunnermeier (2009) regarding borrowers' perceived difficulties in rolling over short-term debt. Mathematically, this heuristic is expressed as a scaling factor applied to lenders' available reserves. Following the decision on total interbank volumes, lenders set a counterparty risk premium for each borrower based on their past repayment

[2]This follows the observation by Adrian and Shin (2011) who relate this to the costs associated to equity issuance (for example, due to the opacity of bank balance sheets and business models)

behaviour. Similar to the funding liquidity case, we define the heuristic around a stylised fact associated to interbank market dynamics namely, the finding by Babus (2011) and Bräuning and Fecht (2016) that banks engage in repeated interactions with a small set of counterparties (in order to minimise search frictions and information asymmetries) which in turn, enables them to infer borrowers' default risk on the basis of past reneging of interbank loan repayments. Against this background, the heuristic is intuitive: Lenders observe their history with each borrower, locating periods in which a loan was provided and setting a counterparty risk premium that increases with the default rate. By allowing banks to alternate between lending and borrowing on the basis of their liquidity needs, we follow the seminal model of **?**. Moreover, conditioning current dynamics on both lending and borrowing histories imbues the model with a high-degree of complexity, albeit in a stylised and tractable framework.

Following the transferral of liquidity from lenders to borrowers, *phase 2* begins with a system-wide liquidity shock to banks' external asset portfolios. Immediately afterwards, borrowers are required to repay their interbank loans. This comprises both the principal and interest which, recall respectively incorporate lenders' funding liquidity and counterparty risk. In order to meet their interbank obligations in full, borrowers first allocate available reserves after which they sell begin to liquidate external assets at the current market price. As a result, defaults (either partial or full) will only occur if, given low reserves, asset prices are sufficiently depressed such that the required volume of firesales exceeds the holdings of the bank. By proceeding in this manner (i.e. bank defaults after reserves and asset holdings have been exhausted), we incorporate the finding by Glasserman and Young (2015) that interbank contagion due to pure spillover/domino effects are rare. Moreover, conditioning banks' firesale behaviour on short-term debt obligations is in line with what was observed during the crisis (Shleifer and Vishny, 2011)[3]. Note that firesale activity by borrowers influences their ability to repay creditors in full, which is exacerbated as the market becomes more illiquid. Consequently, mounting defaults set in motion by illiquid borrowers will be reflected in higher risk premia on future loans (using the mechanism developed in phase 1). Thus our model incorporates a positive feedback effect between firesales and counterparty risk following the model of Caballero and Simsek (2013).

[3]An alternative motivation for firesales, based on meeting a predefined *leverage target* is provided by Greenwood et al. (2015) and Cont and Schaanning (2017). This is implicit in our model, where the target is borrowers' leverage prior to taking on the loan.

Using the mechanism developed by Cifuentes et al. (2005) and expanded in Montagna and Kok (2016), second-round price spirals are triggered endogenously using an inelastic demand function reflecting the market's imperfect absorption ability[4]. While this has no *direct* impact on borrower repayments in the current period, the combination of overlapping portfolios and mark-to-market accounting provides an *indirect* transmission channel in which all banks holding the distressed assets (as determined by the bipartite network) revalue their portfolios on the basis of the updated price.

To the best of our knowledge, this paper is the first to combine a realistic, multilayer network and a comprehensive behavioural model of interbank market dynamics. As regards the latter, the flexibility of ABM and the power of computer simulations allows us to imbue our model with a large amount of detail by recasting well-established methodologies within the context of the heuristics driving bank behaviour and interactions. From a modelling perspective, our paper is most closely related to Georg (2013) in which dynamic interbank behaviour is derived from portfolio optimisation. Also closely related are the ABMs of Halaj and Kok (2015), and Iori et al. (2015), whose modelling of *trust* between banks based on repeated interactions is closely related to our counterparty risk argument.

Within the literature studying financial contagion/stability through the lens of network theory, such models combining bank behaviour and network structure constitute the state-of-the-art, addressing the criticism of Upper (2011) that *static* network models' lack of behavioural foundations precludes their usefulness as policy tools. This refers to models operating either within the *clearing payment vector* paradigm developed by Eisenberg and Noe (2001) (notably, Cifuentes et al. (2005) and Montagna and Kok (2016), whose market impact function is applied to model endogenous asset price movements in this paper) or those based on a mechanistic contagion process via *cascading defaults* such as Nier et al. (2007), Gai and Kapadia (2010) and May and Arinaminpathy (2010).

As our ABM entails "*growing a society from the bottom-up*" (Epstein and Axtell, 1996) no established methodology exists *prima facie* for presenting the results. While this lack of a harmonised framework constitutes a shortcoming of ABMs, it also affords practitioners a certain degree of flexibility to decide what features of agent behaviour to report in order to motivate a particular research question. We start by recalling the core argument of the paper: that strains in the interbank market persisted despite aggressive policy intervention by the central bank due to the combination of unfolding counterparty and

[4]The link between market liquidity and asset prices is well-documented in the literature. The seminal paper by Allen and Gale (1994), posits a link between limited market participation and asset price volatility. Brunnermeier (2009) puts *firesale externalities* arising due to falling lending standards and tightening margins at the heart of the crisis.

funding liquidity risk. Against this background, we construct two counterfactual *policy experiments*, each of which includes a fixed crisis period in which market liquidity declines and asset prices are subject to negative shocks. Starting with the baseline model in which unconventional central bank policy is not present, these risks are allowed to to develop unchecked. In the second experiment, the central bank intervenes with a short delay following the onset of the crisis. As we will demonstrate in the next section, this was largely the case.

Our simulation results are in line with the findings of Afonso et al. (2011) and Gabrieli and Georg (2014): while the crisis put significant strain on the interbank market, it did not freeze entirely. Similarly, while credit conditions did tighten as banks adjusted to decreased wholesale liquidity and rising counterparty defaults, the unprecedented policy intervention by the central bank was able to avert a full-scale credit crunch. Again, this is in line with the empirical findings of Giannone et al. (2012) and Ciccarelli et al. (2015). Our finding on the importance of funding liquidity risk as a key driver of interbank market tensions is in line with de Haan et al. (2017).

Regarding the emergency liquidity provision role played by the central bank, our findings are in line with Garcia-de Andoain et al. (2016), that between 2008 and 2010, the ECB "took over' the liquidity provision role of the interbank market. Moreover, policymakers recognised that such interventions were unsustainable within the monetary policy framework of the ECB as they promote the misalignment between the ECB's policy rate and the yield curve. Notably, ECB executive board member Lorenzo Bini Smaghi in a 2008 speech[5] stated that "*When considering possible further measures to revive the money market, the ECB must carefully balance the objective of steering short-term money markets and ensuring sufficient liquidity in the banking sector, on the one hand, and its wish to foster a reactivation of the money market, on the other hand.*"

The paper is organised as follows: Section 3.2 describes the simulation methodology for the bilayer network, Section 3.3 develops the ABM, Section 3.4 outlines the calibrations used to generate the network and run the ABM, Section 3.5 provides the results of our two policy experiments and Section 3.6 concludes and provides policy recommendations.

[5]Available at https://www.ecb.europa.eu/press/key/date/2008/html/sp081201.en.html.

3.2 Simulating the bilayer network

Before developing the dynamic portion of the model, we first outline the methodology for simulating a bilayer network while satisfying the topological properties of interbank networks mentioned earlier. Bilayer networks consider two *different* types of interdependency connecting the *same* set of nodes. In our model, the two forms of bank interdependency are (i) direct exposures due to short-term, unsecured interbank lending/borrowing and (ii) indirect exposures arising due to overlapping portfolios and firesales of securities held within those portfolios. Moreover, our framework allows for transmission and feedback effects between the two layers as banks' activities vis-à-vis their counterparties on the interbank market condition their need to firesale assets in their portfolio and vice versa. A simple toy model is provided in Figure 3.1 below:

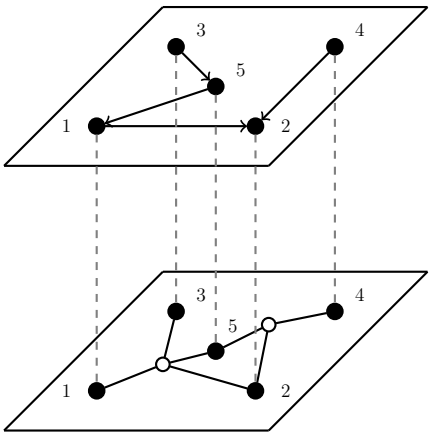

Figure 3.1: Toy bilayer network with 5 banks (black circles) and 2 external assets (white circles). Top layer = direct exposures (directed graph). Bottom layer = indirect exposures (bipartite graph)

3.2.1 Interbank network

Definitions

The initial direct exposure network is an *unweighted, undirected* graph (also referred to as a *simple* graph), $\mathcal{G}^{IB}(\mathcal{N}, \mathcal{E})$ comprising node set $\mathcal{N}$ and the edge set $\mathcal{E}$ containing all unordered pairs of connected nodes, $\mathcal{E} \subseteq \mathcal{N}^2$. The number of nodes in the network N is given by the cardinality of $\mathcal{N}$. In our model, nodes represent banks while the edges determine the presence of a pre-existing lending/borrowing relationship. Intuitively, such

a relationship should be *directed* in order to reflect the difference between node i lending to or borrowing from j. Indeed, our model allows for oriented edges between banks though we incorporate these into the ABM wherein an undirected edge between banks is transformed to a directed one depending on the bank's role as a supplier or demander of liquidity in the transaction[6]. In this way, our approach is more flexible than those assuming fixed directed edges between banks.

The network is represented by the symmetric, binary *adjacency* matrix $[a_{ij}]_{N\times N} = \mathcal{A}(\mathcal{G}^{IB})$ where $a_{ij} = 1$ if there exists an edge connecting i and j and $a_{ij} = 0$ otherwise. Similarly, our simple graph model precludes the presence of self-loops ($a_{ii} = 0$) and multi-edges ($a_{ij} > 1$). Consequently, the maximum number of edges possible in such a network is given by $N(N-1)/2$.

Simulation

We assume that intrinsic fitness of each bank $i \in \mathcal{N}$ stems from the total assets a_i, of the bank. Consequently, large banks (that is, banks holding a large number of assets on their balance sheets) are more likely to connect with large banks than small banks due to the aforementioned fitness-based model. The first step is thus to populate the node set with N banks. This is done using the following *truncated power law*:

$$f(a; \gamma_a, a_{min}, a_{max}) = \frac{(1-\gamma_a)}{a_{max}^{1-\gamma_a} - a_{min}^{1-\gamma_a}} a^{-\gamma_a} \tag{3.1}$$

Where γ_a is an exogenous parameter dictating the shape of the power law distribution and a_{min} and a_{max} represent the smallest and largest banks in the system, respectively. This determines the initial (i.e. at time $t = 0$) size of each bank i in the system. We denote this by a_i^0. These values are then passed to the following function which gives the probability, p_{ij} of an undirected edge existing between i and j Dropping the 0 superscript for simplicity, the probability function is given by:

$$p_{ij} = P(a_i, a_j) = d \cdot \left[\left(\frac{a_i}{a_{max}} \right) \cdot \left(\frac{a_j}{a_{max}} \right) \right]^{\gamma_p} \tag{3.2}$$

[6]Moreover, undirected edges can also be interpreted as being *bidirectional* i.e. encompassing a directed edge from i to j and from j to i.

Two additional parameters, d and γ_p are introduced. These are calibrated to control the density of the network (by affecting the probability that two nodes will form a link). Note that the original fitness-based model with mutual benefit proposed in Caldarelli et al. (2002) and applied in Montagna and Lux (2016) simulates a directed network with the network structure relying on two calibrated exponents, $\{\alpha, \beta\}$. The undirected version in our model involves setting $\alpha = \beta = \gamma_p$ The adjacency matrix is then constructed according to the following rule:

$$a_{ij} = \begin{cases} 1, \text{ with probability } p_{ij} \\ 0, \text{ with probability } 1 - p_{ij} \end{cases} \tag{3.3}$$

Moreover, the model is known to produce a scale-free degree distribution with the value of the exponent depending on the α and β. Under our calibration, we obtain a theoretical degree distribution, $p(k) \propto k^{-2}$ which is consistent with numerous empirical findings of interbank network structure.

3.2.2 Overlapping portfolio network

Definitions

The network given by $\mathcal{G}^{\mathcal{OP}}(\mathcal{N}, \mathcal{M}, \mathcal{E})$ comprises the same set of nodes $\mathcal{N}$ whose interdependence in this layer arises *indirectly* via the degree of overlap in their external asset portfolios. The set of external assets is given by $\mathcal{M}$ whose cardinality, M is the total number of assets across all banks. The notion of a *bipartite network* from the graph theory literature offers an ideal representation. Specifically, this framework allows for two distinct types of nodes (defined by the disjoint sets $\mathcal{N}$ and $\mathcal{M}$ above) where edges are only permitted between nodes in different sets. A graphical representation is provided in Figure 3.2.

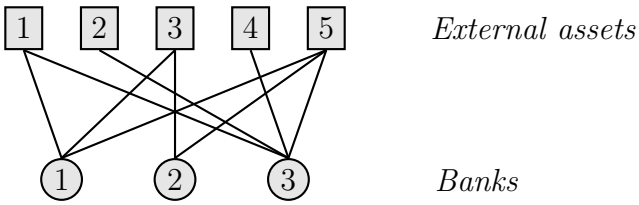

Figure 3.2: Bipartite graph representing banks' common holdings of external assets

Given the structure of a bipartite graph, the *biadjacency* matrix $A\left(\mathcal{G}^{\mathcal{OP}}\right) \in \mathbb{R}^{(N+M)\times(N+M)}$ is symmetric and expressed in block-matrix form:

$$A\left(\mathcal{G}^{\mathcal{OP}}\right) = \begin{bmatrix} 0_N & B \\ B^\top & 0_M \end{bmatrix}$$

where B is an $N \times M$ block representing all bank-asset edges and 0_N and 0_M are $N \times N$ and $M \times M$ zero matrices representing the null graphs of interbank and interasset edges. Mathematically, the elements of the biadjacency matrix $\left[a_{ij}^{OP}\right]_{N\times M} = A\left(\mathcal{G}^{\mathcal{OP}}\right)$ are equal to 1 if there exists a link between $i \in \mathcal{N}$ and $j \in \mathcal{M}$ and 0 otherwise.

Following Caccioli et al. (2014), we provide a set of parameters associated to the bipartite network. First, the *average diversification* of the banks is the average number of assets held by each bank $i \in \mathcal{N}$ given by its degree, deg_i^{OP}.

$$\mu_b = \frac{1}{N}\sum_{i=1}^{N} deg_i^{OP} \tag{3.4}$$

Similarly, the degree of each asset $k \in \mathcal{M}$ represents the number of banks holding it in their portfolio. The average degree is thus given by:

$$\mu_a = \frac{1}{M}\sum_{k=1}^{M} deg_j^{OP} \tag{3.5}$$

Since the total degrees of both banks and external assets must match, the following condition must hold: $\mu_b N = \mu_a M$.

In order to define the degree of overlap between banks, the *crowding parameter*, $n = N/M$ measures the extent to which banks' portfolios contain the same assets. Finally, We denote the total value of external assets held by bank i in period t by

$$e_i^t = \sum_{\text{J}=1}^{M} s_{ij}^t \cdot p_j^t, \quad \forall i \in \mathcal{N} \tag{3.6}$$

Where s_{ik}^t denotes the number of shares of asset k held by bank i and p_k^t the price of asset j at time t. Note that s_{ik}^t is nonzero if bank i holds asset j in its portfolio and zero otherwise. We define the $1 \times M$ asset vector of bank i, $\boldsymbol{s}_i^t = [s_{i1}^t, \dots s_{iM}^t]$ along with the $1 \times M$ price vector $\boldsymbol{p}^t = [p_1^t, \dots p_M^t]$. Equation 3.6 can thus be expressed in vector notation as $e_i^t = \boldsymbol{s}_i^t \cdot (\boldsymbol{p}^t)^\top$.

Simulation

Keeping to the framework developed by Caccioli et al. (2014), we consider random networks with Poisson degree distribution for both banks and external assets. Consequently, the probability of a link being formed between each bank-asset pair is given by $\frac{\mu_b}{M}$. The result is an Erdős-Renyi graph with average degrees for banks and assets given by μ_b and $\mu_a = \mu_b \cdot \frac{N}{M}$, respectively. For simplicity, we denote the number of assets held in i's portfolio by M_i.

3.3 The Model

3.3.1 Initialisation

Following Lux (2015), we create the initial entries of the balance sheet using the N bank size values drawn in the previous section:

$$\begin{aligned} e_i^0 &= \alpha a_i,\ c_i^0 = (1-\alpha)a_i^0 \\ d_i^0 &= \beta a_i^0,\ k_i^0 = (1-\beta)a_i^0 \end{aligned}$$

Where e_i^0 and c_i^0 respectively represent external asset and cash holdings on the asset-side of i's balance sheet at $t = 0$ while initial liabilities comprise deposits d_i^0 and capital k_i^0. α, β are calibrated parameters representing the initial fraction of external assets and deposits respectively. The above implies that $l_i^0 = b_i^0 = 0$ i.e. no interbank lending exists ex-ante. Rather, the interbank market arises endogenously due to the shocks and ensuing liquidity positions of banks in the network.

Recall that our assumption of relationship between banks involves each $i \in \mathcal{N}$ having a *local neighbourhood* of counterparties with whom it engages in lending/borrowing on the interbank market. We denote i's set of counterparties by $\mathcal{N}_i$. The number of i's counterparties is determined from node i's *degree*, $|\mathcal{N}_i| = N_i = deg_i^{IB} = \sum_{j=1}^{N} a_{ij}$.

In order to allow for heterogeneity as well as overlap in banks' asset portfolios, we assume that initially, the market prices of the M assets held by each bank are identical and equal to one viz. $\boldsymbol{p}^0 = \mathbf{1}$ where $\mathbf{1}$ is an M-dimensional vector. Assuming an initially equally-weighted portfolio, we obtain the following individual asset holdings: $s_{ik}^0 = \frac{e_i^0}{M}$ for each $k \in \mathcal{M}$. This formulation implies that larger banks will ex ante have larger securities portfolios as a whole as well as hold a larger amount of each of the securities.

3.3.2 Balance sheet

The asset side of the stylised balance sheet, a_i comprises cash reserves, c_i, interbank loans, l_i and securities holdings, e_i. At each period, the balance sheet identity requires that this equals total liabilities, i_i comprising customer deposits d_i, interbank borrowing b_i and bank capital k_i. That is,

$$\begin{aligned} a_i &= e_i + l_i + c_i \\ i_i &= d_i + b_i + k_i \end{aligned}$$

Figure 3.3 provides a simple schematic with 3 banks of differing size in which a core bank (bank 2) intermediates between two peripheral banks. Despite banks 1 and 3 not having a direct lender/borrower relationship, an indirect relationship arises due to their common holdings of a particular security.

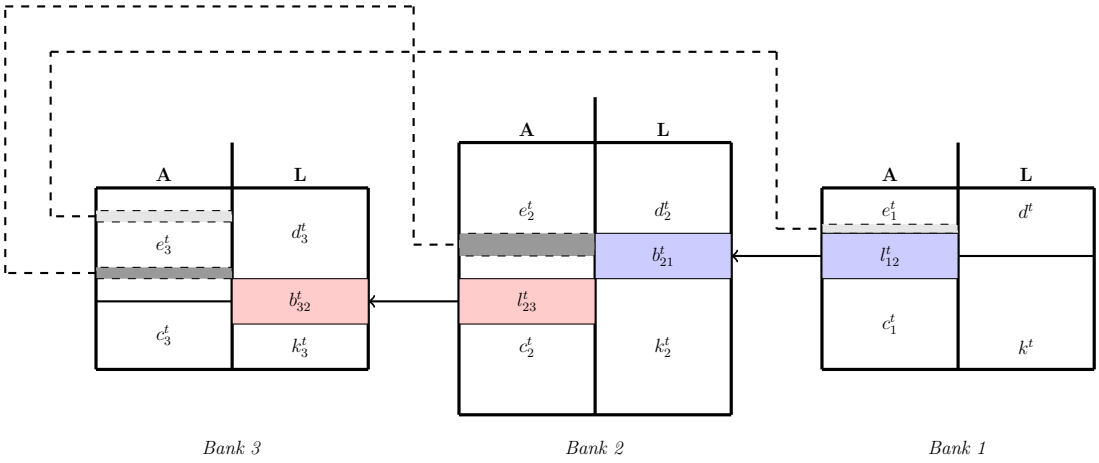

Figure 3.3: Interlocking balance sheets with 3 banks

3.3.3 Dynamic model

In order to simplify the exposition of the model, we adopt a set of conventions that will remain constant throughout the model. First, all bilateral parameters (involving a lender and a borrower) are subscripted by ij or ji where i refers to the lending and j refers to the borrowing counterparty. Second, a variable x that is *provisional* (i.e. whose final value is fixed at a later stage) is denoted by $\tilde{x}$.

One of the key points of the dynamic model is the evolution of the balance sheet over time. In order to provide a realistic depiction of interbank market activity, we consider a temporal structure consisting of $t = 1, \dots T$ *periods* in simulation-time, each of which comprises $\tau = 3$ *phases*. In order to highlight how certain parameters evolve over time, each variable is defined by a period-phase 2-tuple $\{t, \tau\}$. Figure 3.10 below outlines the main dynamics of the ABM as well as the ordering in which agents interact with one another.

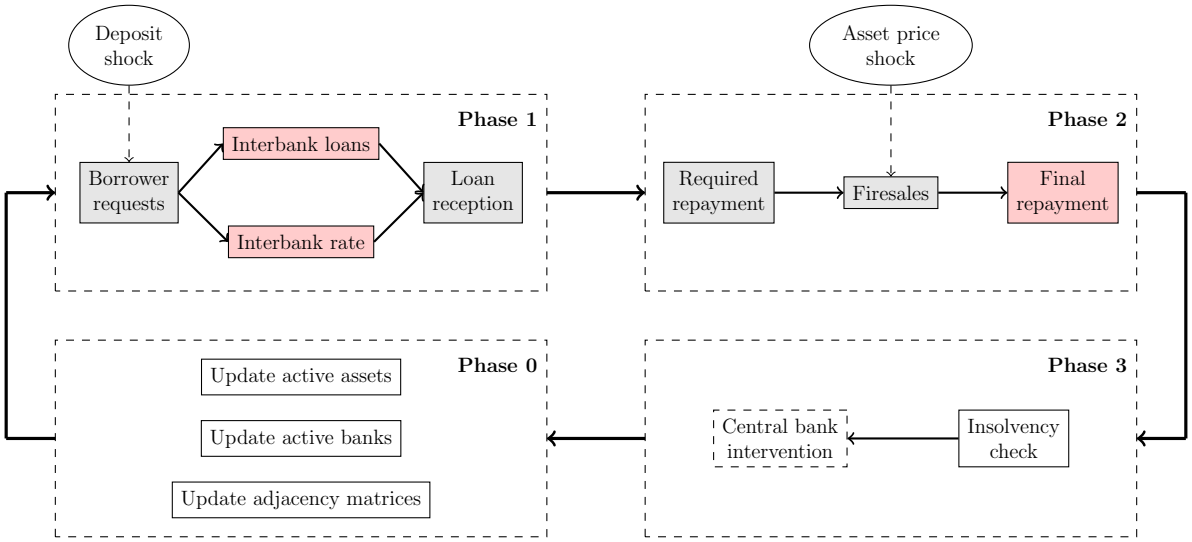

Figure 3.4: Model dynamics

As the above indicates, the basic framework of the model is simple: Borrowers initiate short-term loans on the basis of their liquidity needs. Observing these requests, lenders decide how much to allocate to interbank lending and at what rate to provide the funds. The red boxes indicate a behavioural component. Specifically, loan volumes are conditioned on lenders' perception of their own funding liquidity risk while the interbank rate is determined by the counterparty risk associated to a specific borrower. In phase 2, the loan becomes due. Borrowers will first try to settle their obligations using available reserves. If these are insufficient to cover the principal + interest, the borrower sells of a portion of its external assets at the prevailing market price. However, a negative asset price shock increases the stock of external assets that need to be sold to cover the shortfall between reserves and obligations. As we will show, asset prices also develop endogenously, leading to rising market liquidity risk and prospective price spirals. After phase 2, all obligations are settled. Depending on the outcomes of interbank trading and the magnitude of the liquidity shocks, certain banks will come up insolvent ($k_i^t < 0$), prompting their removal from the system. We then introduce the central bank, who has perfect information on the

liquidity situation in the banking sector and intervenes by providing refinancing to banks as needed. This concludes one period of the model (after which the system passes to the next period of interbank trading).

Preliminaries

At the beginning of each period (phase 0), each bank's balance sheet comprises only variables carried over from the previous period (except at $t = 0$). All debt contracts are assumed to have been settled (fully or partially) in the previous period i.e. $l_i^{t,0} = b_i^{t,0} = 0$. As a result, the balance sheet in phase 0 of period t is given by:

$$\begin{aligned} a_i^{t,0} &= c_i^{t-1,2} + e_i^{t-1,2} \\ i_i^{t,0} &= d_i^{t-1,1} + \tilde{k}_i^{t,0} \end{aligned}$$

Note that the first superscript in the two equations above indicates that the parameter was carried over from the previous period while the second indicates the intra-period phase in which the parameter was updated. Bank capital $\tilde{k}_i^{t,0}$ is a residual value, set such that $a_i^{t,0} = i_i^{t,0}$. Consequently, it can be expressed as:

$$\tilde{k}_i^{t,0} = c_i^{t-1,2} + e_i^{t-1,2} - d_i^{t-1,1} \tag{3.7}$$

Phase 1: Liquidity shock and move to interbank markets

Deposit shock: Phase one begins with an idiosyncratic *liquidity shock* to bank deposits. The shock specification, based on Lux (2015), consists of both a random and a mean-reverting component in order to ensure that deposits are stationary. Consequently, bank deposit evolution over time is given by

$$\delta_i^t = \theta \left(\bar{d}_i - d_i^{t-1} \right) + \phi_i^t \epsilon_i^t, \quad \text{where } \bar{d}_i = \beta a_i^0 \tag{3.8}$$

where $\epsilon_i^t \sim \mathcal{N}(0, 1)$, and the parameters $\{\theta,\ \bar{d}_i\}$ denote the mean reversion speed and long-run value of deposits, respectively. ϕ_i^t is assumed to be proportional to balance sheet size in order to tailor the deposit shock magnitude to each bank. Finally, the mean across all banks is subtracted from the ensemble of deposit shock realisations in order to render

the system completely conservative in terms of aggregate deposits. The shock is then incorporated in an additive manner into bank balance sheet dynamics

$$d_i^{t,1} = d_i^{t-1,1} + \delta_i^t \tag{3.9}$$

Investment decision - Lenders: In our model banks play the traditional role of *maturity transformers*, using short-term deposits to finance long-term, illiquid investments. To this end, interbank market activity is initially driven by the magnitude and sign of the deposit shock, δ_i^t. If i experiences a positive liquidity shock ($\delta_i^t > 0$), it uses that amount first to finance an illiquid investment z_i^t which lasts for one period and pays a fixed interest rate r^z, realised at the *end* of phase 3. The standard maturity mismatch is incorporated by placing payments on deposits (remunerated at the calibrated rate r^d) in phase 1, prior to the realisation of returns from illiquid investments.

In each period, banks seek to maintain a constant level of investment relative to the previous periods. Specifically, they use the average over all previous periods to fix current-period *desired* investment levels, $\tilde{z}_i^t = \bar{z}_i^{1:t-1}$, reflecting committed lines of credit between banks and the private sector. As the size of the investment is driven by the magnitude of the shock, we develop a *balance sheet adjustment* heuristic by which lender banks adjust their balance sheet in response to a positive deposit shock. Beginning with the investment entry, we identify three cases:

$$z_i^t = \begin{cases} \tilde{z}_i^t \text{ if } \delta_i^t \geq \tilde{z}_i^t \\ \tilde{z}_i^t \text{ if } \delta_i^t < \tilde{z}_i^t \wedge \tilde{z}_i^t - \delta_i^t \leq (1-\psi)\, c_i^{t-1,2} \\ \tilde{z}_i^t - (1-\psi)\, c_i^{t-1,2} + \delta_i^t \text{ if } \delta_i^t < \tilde{z}_i^t \wedge \tilde{z}_i^t - \delta_i^t > (1-\psi)\, c_i^{t-1,2} \end{cases} \tag{3.10}$$

In the first (and simplest) case, the deposit shock is sufficient to make the desired investment. Cases 2 and 3 arise when the deposit shock is smaller than the desired investment, implying that the bank must finance the investment using another source of funds. Throughout the paper, we assume that cash reserves, c_i^t are used primarily for this purpose. The parameter ψ represents the minimum reserve requirement set by the central bank which states that banks are obliged to maintain reserves greater than or equal to $\psi\%$ of total reserves on their balance sheet in each period. The value $\psi c_i^{t-1,2}$ is thus the cash balance sheet entry such that this constraint becomes binding. Conversely,

$(1-\psi)c_i^{t-1,2}$ are the reserves available to the bank to fund the investment. In case 2, the reserve requirement is still satisfied following the cash outflow and the bank is able to make the desired investment. In case 3, the required funds would cause banks to violate the minimum requirement. We thus assume that banks transfer the maximum amount possible, leaving current cash holdings at the regulatory minimum (plus the positive but insufficient amount of deposits).

In cases 1 and 2, current period cash reserves are both updated as: $c_i^{t,1} = c_i^{t-1,2} + \delta_i^t - z_i^{t-1}$. Note that in the first scenario, reserves increase (as $\delta_i^t \geq \tilde{z}_i^t$) while in the second, they decrease by the same increment. The decrease in reserves is more pronounced in case three, wherein $c_i^{t,1} = \psi c_i^{t-1,2}$. The balance sheet dynamics in Equation 3.10 are summarised in Figure 3.5, where panels (a), (b) and (c) correspond respectively to lines 1,2, and 3.

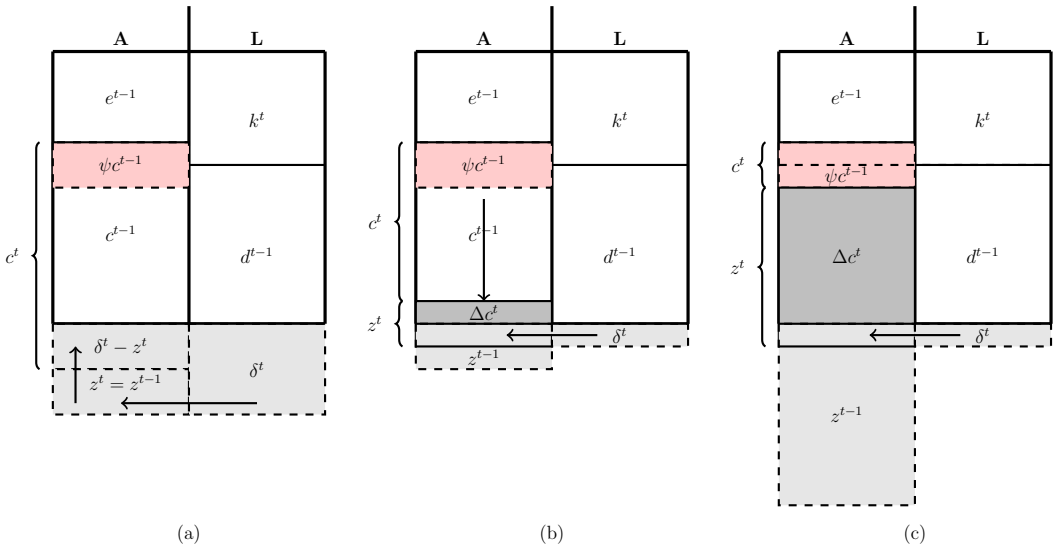

Figure 3.5: Banks hit by a positive shock: Investment decision and balance sheet adjustments

For ease of exposition, we simplify to one-period, resulting in a desired investment level of z^{t-1}. Starting with panel (a), we see that the magnitude of the shock δ^t is more than sufficient to make the desired investment, allowing the bank to subsequently redirect the additional liquidity $\delta^t - z^t$ towards its cash reserves. In panel (b) $\delta^t < z^{t-1}$. However, by allocating Δc^t from available reserves, the investment can be made. By contrast, the desired investment in panel(c) is sufficiently large such that the bank is forced to reduce its reserves by Δc^t to the regulatory minimum.

Interbank market - Borrower requests: Banks hit by a *negative* deposit shock also seek to smooth investment levels over time. However, in the absence of an influx of retail funding from deposits, these banks turn to wholesale funding by requesting liquidity on the interbank market equal to average of past investments:

$$\tilde{b}_i^t = \bar{z}_i^{1:t-1} \tag{3.11}$$

Recall that $\tilde{b}_i^t$ indicates that these are *provisional* values. Since the actual interbank credit is decided by lenders (as will be seen), the final balance sheet component for interbank borrowing, b_i^t will depend on the loan-provision activities of lenders.

After fixing their aggregate liquidity needs, each borrower i now redistributes this value across their local neighbourhood of counterparties. The network structure comes into play at this point as the number of local counterparties of i, N_i determines the number of banks from whom they can request liquidity. Before proceeding with the model, we define a set of variables conditional on the realised shock distribution. First, the set of banks hit by a negative shock in t, $\mathcal{N}_-^t = \{i \in \mathcal{N} : \delta_i^t < 0\}$ and its complement corresponding to banks hit by a positive shock, $\mathcal{N}_+^t = \mathcal{N} \backslash \mathcal{N}_-^t$. This allows us to refine the set of each bank's local counterparties according to their status *viz.* $\mathcal{N}_-^t \supseteq \mathcal{N}_{i,-}^t = \left\{j \in \mathcal{N}_i : \delta_j^t < 0\right\}$ and $\mathcal{N}_{i,+}^t = \mathcal{N}_i \backslash \mathcal{N}_{i,-}^t$ correspond to i's counterparties subject to a negative and positive shock respectively.

In our framework, the realisation of the liquidity shock imposes directed edges on the previously undirected network (hence the t superscripts on the aforementioned sets) as a request from bank j to bank i for liquidity implies a directed edge from i to j. Since interbank transactions are *borrower-initiated* in our model, the head of a directed edge is placed *ex-post* at each node hit by a negative shock conditional on there being an undirected edge there *ex-ante* (signifying a pre-existing relationship between two banks). Taking these rules into account, we populate the adjacency matrix of the directed network in period t[7] as follows:

$$\vec{a}_{ji}^{t,A} = \begin{cases} 1 \text{ if } j \in \mathcal{N}_-^t \wedge i \in \mathcal{N}_{j,+}^t \\ 0 \text{ if } j \in \mathcal{N}_-^t \wedge i \in \mathcal{N}_{j,-}^t \\ 0 \text{ otherwise} \end{cases}, \quad \forall i, j \in \mathcal{N} \tag{3.12}$$

[7]Note that the structure of the directed network depends on the realisation of the liquidity shock and thus, will vary from period-to-period.

where $\vec{a}^t_{ji}$ denotes each element of the adjacency matrix associated to the directed graph $\mathcal{G}^{IB}\left(\mathcal{N}^t, \vec{\mathcal{E}}^t\right)$. Figure 3.6 below illustrates this using a simple six-node network.

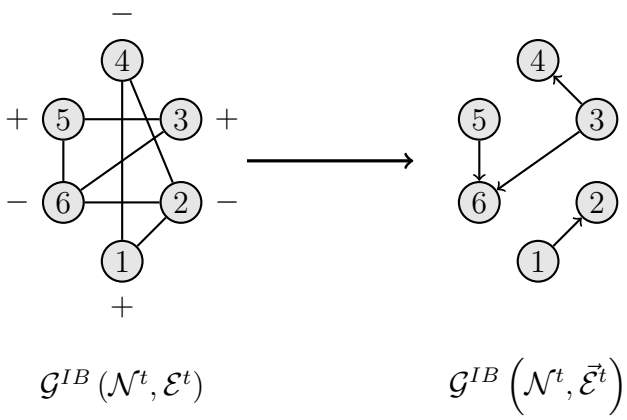

$\mathcal{G}^{IB}\left(\mathcal{N}^t, \mathcal{E}^t\right)$ $\mathcal{G}^{IB}\left(\mathcal{N}^t, \vec{\mathcal{E}}^t\right)$

Figure 3.6: Revealing the directed network conditional on shock sign distribution

Finally, in order to determine bilateral loan requests, we assume that each borrower redistributes its aggregate loan requests, *equally* across their lending counterparties:

$$\tilde{b}^t_{ji} = \left(\frac{1}{N^t_{j,+}}\right) \cdot \tilde{b}^t_j, \quad \forall i \in \mathcal{N}^t_{j,+} \tag{3.13}$$

Interbank market - Lender offers: These requests are then transmitted to creditors who (i) following the investment made prior, examine how much liquidity they have on hand to lend out on the interbank market, (ii) decide on how much to allocate towards interbank lending and (iii) fix the *counterparty risk premium* on extended interbank loans. In step one, banks compare the sum of loan requests from their local neighbourhood of borrowers with their available cash. Provisional loans are thus given by

$$\tilde{l}^t_i = \min\left\{c^t_i\left(1-\psi\right); \sum_{j \in \mathcal{N}^t_{i,-}} \tilde{b}^t_{ji}\right\} \tag{3.14}$$

We now develop the *funding liquidity risk* heuristic that drives lenders' final loan volumes. Specifically, each lender looks through their history to the last period in which a negative shock cast it as a borrower. They then compare the ratio of total received to total requested loans in that period which is used as a proxy for funding tensions and drives a

precautionary motive whereby lenders hoard a fraction of available liquidity in anticipation of future difficulties in obtaining funding, based on realised past observations. Denoting the last period where the current lender i borrowed on the interbank market by $\hat{t}_i^B$, the following scaling factor is applied to $\tilde{l}_i^t$:

$$\hat{l}_i^t = \frac{b_i^{\hat{t}_i^B}}{\tilde{b}_i^{\hat{t}_i^B}} \tilde{l}_i^t \tag{3.15}$$

The numerator refers to the total loans received from lenders (defined later in Equation 3.16) while the denominator indicates total requests (Equation 3.11). Given that the latter is constructed as an upper bound for the former, the scaling factor is constrained in $[0, 1]$. A smaller scaling factor thus implies that lender i faced difficulties in obtaining wholesale funding in the past. Consequently, it adjusts current lending behaviour downward in response to a perceived higher funding liquidity risk.

Finally, bilateral loan supply is obtained in the same matter as loan demand: $\hat{l}_{ij}^t = \left(\frac{1}{N_{i,-}^t}\right) \cdot \hat{l}_i^t$. Borrowers then aggregate the loans received in period t:

$$b_i^t = \sum_{j \in \mathcal{N}_i / \mathcal{N}_{i,+}^t} \hat{l}_{ji}^t \tag{3.16}$$

In the final step of phase 1, lenders now set the bilateral interbank rates associated to each loan. Where loan volumes were assumed to be driven by lenders' concerns over their own funding, interbank risk premia are assumed to be driven by the *counterparty risk* associated to each borrower. To achieve this, we use a similar type of backwards-looking heuristic in which the lender i observes its history relative to *each* borrower in its local neighbourhood $j \in \mathcal{N}_{i,-}^t$, locating the last period in which they were also connected in a lender-borrower relationship. We denote this period by $\hat{t}_{ij}^L$. Note that it is not limited to being the same period for each borrower.

We illustrate this with the following example whereby lender 2 is required to compute the counterparty risk premium for borrowers 7,13,19 and 20 in period 5:

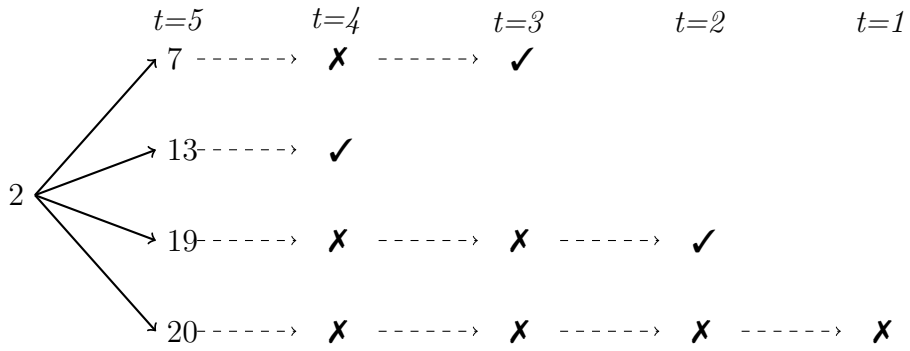

Figure 3.7: Lender backwards-looking heuristic for counterparty risk premium setting

As Figure 3.7 shows, when lender i and borrower j were connected in a lender-borrower relationship in the past, the search is halted and bilateral loan provision and repayment activities in that period recorded (indicated by the ✓-sign). For all current borrowers with whom a past lender-borrower relationship existed, lenders proceed to computing the bilateral counterparty risk premium according to the following equation:

$$\rho_{ij}^{t} = 1 + \left(l_{ij}^{\hat{t}_{ij}^{L}} - x_{ji}^{\hat{t}_{ij}^{L}} \right) \frac{\bar{l}_{i}^{\hat{t}_{i}^{L}}}{\bar{x}_{j}^{\hat{t}_{i}^{L}}} \tag{3.17}$$

where $l_{ij}^{t} = \left(1 + r_{ij}^{t}\right) \hat{l}_{ij}^{t}$ specifies the loan principal and interest i.e. the amount lender i expects to receive from borrower j in phase 2 of the current period[8] and x_{ji}^{t} refers to the final amount repaid by borrower j.

The risk premium is subsequently applied as a scaling factor to the interest rate set for borrower j in period $\hat{t}_{ij}^{L}$ to obtain the current interbank rate:

$$r_{ij}^{b,t} = \rho_{ij}^{t} r_{ij}^{b,\hat{t}_{ij}^{L}} \tag{3.18}$$

[8]To avoid confusion over the different specifications for lending, recall that $\tilde{l}_{i}^{t}$ refers to lenders' available liquidity and is defined in the aggregate only. $\hat{l}_{i}^{t}$ and $\hat{l}_{ij}^{t}$ refer to loan volumes adjusted for funding liquidity risk as well as the final amounts extended to borrowers.

Equation 3.17 is derived from a simple graphical argument[9] stating that lenders 'punish' past deviations from their expected return, equal to the principal plus interest. As shown in the inverse demand graph below, full repayment of the loan to counterparty j in period $\hat{t}^L_{ij}$ ($x^{\hat{t}^L}_{ji} = l^{\hat{t}^L}_{ij}$) maps to a risk premium of 1 which, when substituted into Equation 3.18, implies no change in the interbank rate.

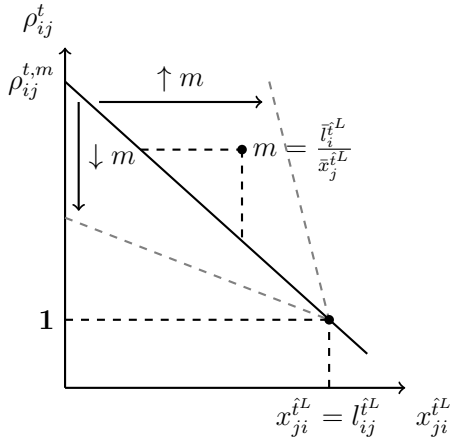

Figure 3.8: Lender risk premium setting heuristic

By contrast, as the difference between $x^{\hat{t}^L}_{ji}$ and $l^{\hat{t}^L}_{ij}$ increases (recall that $x^{\hat{t}^L}_{ji} \in [0, l^{\hat{t}^L}_{ij}]$), the risk premium increases at a rate equal to the ratio of i's average loan provision to the average repayment in period $\hat{t}^L_{ij}$. This allows the lender to compare each individual borrower's behaviour to its loan-competitors. Consequently, in periods where average repayment was high relative to loans ($\uparrow m$: the rightmost grey dashed line in Figure 3.17), small deviations from full repayment will be penalised. Similarly, keeping the slope constant and shifting $l^{\hat{t}^L}_{ij}$ to the right results in a higher risk premium associated to partial defaults. From a behavioural standpoint, this shows that lenders' counterparty risk concerns increase with the volume of loans.

[9]The relationship between Figure 3.8 and Equation 3.17 is provided in Appendix 3.A.

Phase 2: Loan repayment and borrower deleveraging

Phase dynamics: Phase 2 begins with a subset of system-wide external assets subjected to an external asset shock, updating asset prices from $p_k^{t-1} \to \tilde{p}_k^t$. Following this, borrower repayments on interbank loans become due, prompting potential firesales as borrowers seek to satisfy interbank obligations. In the case of firesales, a downward shift in external asset holdings occurs: $s_k^{t-1} \to s_k^t$. Finally, we introduce a *market impact function* whereby total firesales engender further decreases in asset prices: $\tilde{p}_k^t \to p_k^t$. Recall that portfolio value of external asset k, e_k is given by $p_k \cdot s_k$. Figure 3.9 below tracks the variation in e_k during phase 2.

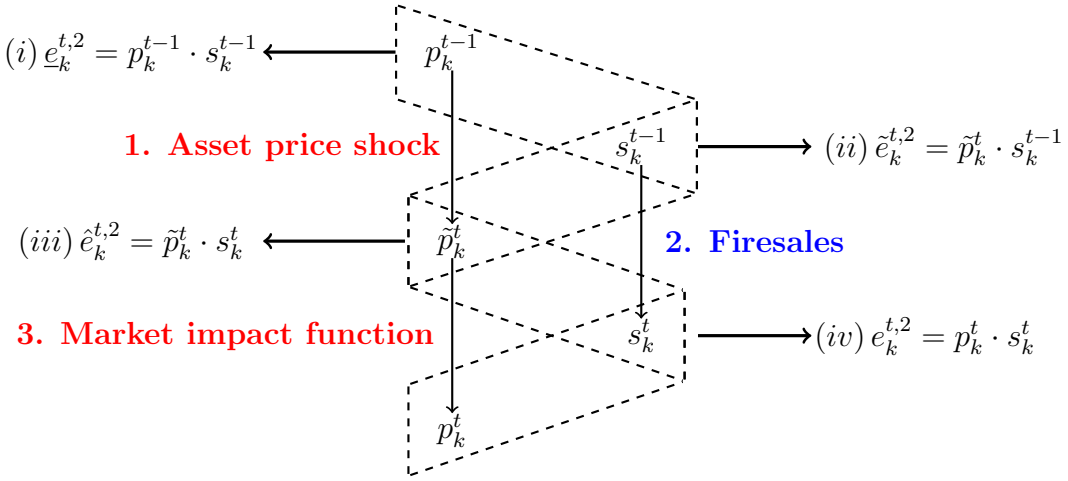

Figure 3.9: Phase 2 portfolio dynamics

Prior to the shock, asset prices and holdings are carried over from the previous period, yielding the following ex-ante portfolio value:

$$\underline{e}_i^{t,2} = \sum_{k \in \mathcal{M}^t} p_k^{t-1} \cdot s_{ik}^{t-1}$$

External asset shock: Where phase 1 of the model involved banks opening interbank positions vis-à-vis one another due to an exogenous (liability-side) liquidity shock, In the current phase, banks are now required to close these positions (since we are examining short-term lending).

Recall that each bank initially holds an equally-weighted portfolio of M_i^0 securities which overlap according to a random bipartite network. In what follows, we develop a negative, exogenous shock to a subset of the price vector that occurs in each period. The first step of the external asset shock is thus to select the number of securities to shock as well as the identity of the securities subject to the shock. Where the magnitude of the deposit shock in phase 1 was expressed as a function of the bank's size, we assume that external asset shock size is driven by the financial state $\mathcal{F}$ of the economy, calibrated as 'stable' or 'crisis' $\mathcal{F} = \{s, c\}$. In the normal state, the initial number of assets shocked is low. Switching from the normal to the crisis state thus implies an increase in the number of shocked assets.

Denoting the set of shocked assets in period t by $\mathcal{M}^{t,S}$, the *number* of shocked assets in period t is computed according to: $|\mathcal{M}^{t,S}| = M^{t,S} \sim \lfloor \mathcal{U}(1, \nu(\mathcal{F}) \cdot M) \rfloor$ where $\lfloor \cdot \rfloor$ denotes the floor function ensuring that the shock realisation is rounded down to the nearest integer. $\nu(\mathcal{F}) \in [0, 1]$ represents the fraction of total external assets held by the banking sector that undergo an exogenous shock. As mentioned above, this is calibrated to the current financial state such that $\nu(c) > \nu(s)$.

Having identified the number of securities to shock, we now turn to the magnitude of the shock i.e. the effect on the marked-to-market price of the selected securities. We incorporate both first-round and second-round effects arising due to the aforementioned exogenous shock. The first-round effects are simply the shift in market price from, p_k^{t-1} to the ex post price $\tilde{p}_k^t$ in period t given by:

$$\tilde{p}_k^t = f_k p_k^{t-1}, \quad \forall k \in \mathcal{M}_s^t \tag{3.19}$$

where $f_k \sim \mathcal{U}(f_{min}, f_{max})$ denotes the exogenous shift in the market price of shocked asset $k \in \mathcal{M}_s^t$. The lower and upper bounds of the price shock distribution are given by $f_{min}(\mathcal{F})$ and $f_{max}(\mathcal{F})$, indicating that asset price fluctuations are determined by the financial state. Note that this shock is idiosyncratic since its effect on individual banks will depend on which of the shocked assets it holds in its external assets portfolio. Defining this set as $\mathcal{M}_i^{t,S} \subseteq \mathcal{M}^{t,S}$, we can express i's ex-post balance sheet entry for external assets as:

$$\tilde{e}_i^{t,2} = \sum_{k \in \mathcal{M}_i^{t,S}} \tilde{p}_k^t \cdot s_{ik}^{t-1} + \sum_{k \in \mathcal{M}^{t,S} \setminus \mathcal{M}_i^{t,S}} \tilde{p}_k^t \cdot s_{ik}^{t-1}$$

where the first term consists of the assets whose market price varies due to the shock.

Firesales: Following the external asset shock, borrower banks are now contractually obligated to repay their interbank loans plus interest from the previous phase. It is here that we incorporate the securities firesale mechanism. Specifically, in order to reduce the possibility of default, we allow borrowers to make up for the difference between available liquidity and repayment obligations by liquidating a portion of their external asset portfolios. First, we define the required repayment, $\tilde{x}_{ji}^t$ of each borrower j to its lending counterparties $i \in \mathcal{N}_{j,+}^t$:

$$\tilde{x}_{ji}^t = l_{ij}^t = \left(1 + r_{ij}^t\right) \hat{l}_{ij}^t \tag{3.20}$$

Observing their aggregate interbank obligations $\tilde{x}_j = \sum_{i \in \mathcal{N}_{j,+}^t} \tilde{x}_{ji}^t$, borrowers proceed to comparing this with available reserves for loan repayment. Equation 3.21 below provides the mechanism by which borrowers compute the total *value* of external assets that need to be sold to account for any shortfall in available reserves:

$$\nu_j^t = \min\left\{0; (1-\psi)\, c_j^{t,1} - \tilde{x}_j^t\right\} \tag{3.21}$$

As the above shows, when $(1-\psi)\, c_j^{t,1} \geq \tilde{x}_j^t$, reserves are sufficient to cover all interbank obligations resulting in a zero firesale requirement. By contrast, when $(1-\psi)\, c_j^{t,1} < \tilde{x}_j^t$, nonzero firesale of assets occur to account for the shortfall.

Thus borrower j needs to sell off v_j^t worth of assets to meet its interbank obligations. We assume that this deleveraging process is spread equally over its portfolio, resulting in a per-asset value of $\nu_{jk}^t = \frac{v_j^t}{M_j^t}$. In order to arrive at the *amount* of shares sold, we need to take into account both the current market price $\tilde{p}_k^t$ and the fact that potential firesales are constrained by banks' current asset holdings s_{jk}^{t-1}. For each asset $k \in \mathcal{M}_j^t$, the number of shares sold at firesale is given by

$$\xi_{jk}^t = \min\left\{s_{jk}^{t-1}; \frac{\nu_{jk}^t}{\tilde{p}_k^t}\right\} \tag{3.22}$$

Note that when j's holding of asset k is insufficient to cover the required firesale amount, the entire position s_{jk}^{t-1} is sold off. From this, external asset holdings are updated according to

$$s_{jk}^{t} = s_{jk}^{t-1} - \xi_{jk}^{t} \tag{3.23}$$

Finally, the value of loans repaid by interbank borrowers following the firesale mechanism described above is given by:

$$x_{ji}^{t} = \tilde{x}_{ji}^{t} - \sum_{k \in \mathcal{M}_i^t} \tilde{p}_k^t \cdot \xi_{jk}^t \tag{3.24}$$

Note that when Equation 3.24 evaluates to $x_{ji}^t = \tilde{x}_{ji}^t$, borrower j's loans are repaid in full, even if it possesses insufficient reserves to do so. This is due to Equation 3.22 evaluating to $\tilde{p}_k^t \cdot \xi_{ji}^t = \nu_{jk}^t$ for each $k \in \mathcal{M}_i^t$, implying that j has sufficient holdings of *each* asset at the current market price to make the required repayment.

Second round effects: Following Montagna and Kok (2016), we assume that the asset firesales induce further reductions in asset prices via the following inverse demand curve, which we refer to as the *market impact function*:

$$p_k^t = \tilde{p}_k^t \cdot \exp\left\{ \frac{-\omega_k \cdot \sum_{j \in \mathcal{N}_-^t} \xi_{jk}^t}{\sum_{j \in \mathcal{N}_-^t} s_{jk}^{t-1}} \right\} \tag{3.25}$$

Where ω_k is a positive constant representing the market depth of asset k. Consequently, higher firesales across all borrowers holding asset k will result in a larger downward price adjustment. Notice that Equation 3.22 incorporates the asset's marked-to-market price into j's ability to meet its interbank obligations. Thus we introduce an additional source of intertemporal feedback in which firesales in the current period result in future difficulties in repaying interbank loans.

Phase 3: Insolvency check and central bank intervention

Where phases 1 and 2 developed individual banks' interbank market behaviour, phase 3 focusses on the banking system as a whole. Specifically, as interbank positions have closed and banks' liquidity deficits and surpluses are revealed, it is at this point that the central bank intervenes, using information on imbalances between (i) Loan requests by borrowers and loan provision by lenders (after hoarding) and (ii) expected loan repayment (i.e. the principal plus interest) by lenders and the final loan repayment (after firesales, if required) by borrowers. Using this information, the central bank calculates the *aggregate* amount of liquidity that needs to be injected into the banking sector to correct the aforementioned imbalances:

$$\Omega^B = \sum_{j \in \mathcal{N}_-^t} \left(\tilde{b}_j^t - b_j^t \right)$$

$$\Omega^L = \sum_{i \in \mathcal{N}_+^t} \left(\tilde{l}_i^t - x_i^t \right)$$

where Ω^B and Ω^L denote aggregate *borrower* and *loan* refinancing. For simplicity, we assume that the aggregate amounts are redistributed such that each bank's liquidity shortfall is met. This is modelled as an increase in each bank's cash reserves equivalent to the relevant value. Note that this additional liquidity does not guarantee that each bank will be solvent following the intervention. In order to ground our model in reality as best as possible, we assume that refinancing operations occur at a set frequency t^Ω which we will calibrate to mirror the weekly main refinancing operations of the ECB. Consequently, the above equations are only applied during a refinancing period.

As regards the last point above, we now introduce the policy of fixed rate full allotment, which is activated in crisis times and has the aim of providing refinancing to counteract rising bank insolvencies due to heavy pressure on the asset-side of their balance sheet.

Thus, for a bank i entering phase 3 in an insolvent condition ($k_i^{t,3} < 0$), cash reserves are updated according to:

$$c_i^{t,3} = c_i^{t,2} + \left(|k_i^{t,3}| + k_i^0\right) \tag{3.26}$$

This equation states that the central bank injects enough additional liquidity (indicated by the term in parentheses) such that the bank returns to solvency *and* attains its initial capital level.

Note that when the FRFA policy is activated, bank insolvencies do not occur by construction. As mentioned, this is not the case for the normal refinancing operations. In this case, when a bank is declared insolvent, the following steps are taken: (*i*) It is removed from the network as both an autonomous agent and as a counterparty to the remaining active banks and (*ii*) Its remaining external assets are sold off at the prevailing market price and distributed amongst its counterparties (as dictated by the direct exposure layer of the network).

3.3.4 Summarising feedback dynamics

The causal-loop diagram below illustrates the impact of past occurrences on banks' present behaviour. Using a minimum working example comprising two banks (a lender, 1 and a borrower 2), we outline the feedback dynamics governing: loan repayment (LR_{21}), interbank rate setting (IBR_{12}), interbank loan volumes (IBV_1) and the market impact function (MIF_2).

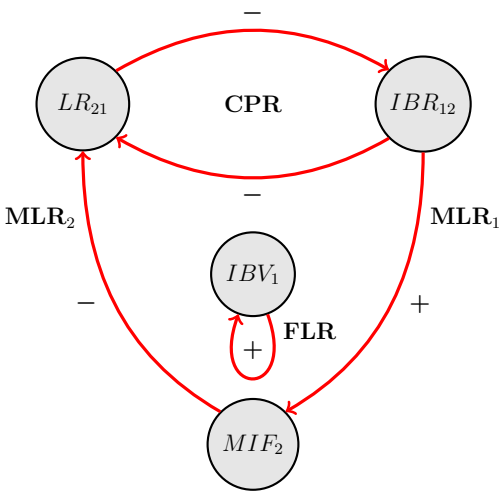

Figure 3.10: feedback loops

Counterparty risk: The CPR loop, expressed mathematically in Equations 3.17 and 3.18, is a negative loop in which lower loan repayment by borrower 2 in the past engenders a higher bilateral risk premium in the premium, which in turn increases the likelihood of future default.

Funding liquidity risk: Unlike the CPR loop, where current lenders observed past periods where they were also lenders, the FLR loop in our model involves current lenders observing their past as interbank borrowers in order to form a proxy over their future ability to attract funding in times of need. That is, a higher success rate in obtaining loans (IBV) in the past, given by Equation 3.15, maps to higher loan provision in the present.

Market liquidity risk: The MLR loop provides an additional channel between the current interbank rate and borrowers' future loan repayment. Specifically, a higher rate can lead to a higher firesale requirement which results in a larger downward price adjustment via Equation 3.25. In the case of future firesales, lower market prices imply that banks have to sell off more shares to achieve the same value, increasing the probability of default.

3.4 Calibration and network generation

Our calibration methodology is split into two stages: First we set the parameters used to generate the direct exposure and overlapping portfolio layers of the multilayer network. We then provide the parameters used in the ABM simulation. Recall that our approach entails embedding the latter in the former. Throughout this section, we provide justification for our choice of parameter values, either based on known properties or derived from the related literature

3.4.1 Network generation

Table 3.1 below provides the calibrations used to generate the bilayer network structure on which the ABM runs.

Table 3.1: Network parameters

Parameter	*Value*	*Definition*	*Notes*
		Interbank network	
a_{min}	5	Minimum bank size	Source: (Montagna and Lux, 2016)
a_{max}	100	Maximum bank size	–
γ_a	2	Power law exponent (size distribution)	–
$\gamma_p^\star$	1.2	Scaling exponent (probability function)	Source: (Alves et al., 2013)
$d^\star$	3	Density adjustment factor	–
N	50	Number of banks	–
		Overlapping portfolio network	
M	50	Number of securities	
p	0.2	Erdős-Renyi index	Source: (Montagna and Kok, 2016) (Caccioli et al., 2014)
μ_b	20	Average bank diversification	Source: (Caccioli et al., 2014)

Notes: Dashed line in notes column indicates that the parameter value is derived from the same source as above. Starred values are calibrated in order to match the network topology of the European interbank market reported in Alves et al. (2013).

Passing the N-element vector of bank sizes (sampled from the truncated power law distribution given in Equation 3.1 as arguments to the probability function (Equation 3.2) populates the N^2 element probability matrix denoting the probability that a given pair of nodes i and j will form an edge[10]. Though the focus of this paper is bank behaviour rather than the financial stability implications of interbank network topology, we nevertheless seek to simulate as realistic a network as possible. Though this is achieved in part by using an algorithm allowing for disassortative mixing, we calibrate certain parameters to recreate as best as possible the structure of European Interbank market reported by Alves et al. (2013). The highly granular dataset consists of the bilateral interbank exposures of 53 large EU banks (hence our use of 50 banks) at the end of 2011. The total exposure value is EUR 1.7 trillion. In addition, the authors highlight a number of network properties derived from the data. Of interest to us are the network density, average path length, assortativity and number of links. Through calibration of the starred parameters in Table 3.1, we are able to generate a direct exposure network possessing similar topological features as the EU interbank market. These are reported in Table 3.2 below:

Table 3.2: Replicating the structure of the EU interbank network

	Our simulations	Alves et al. (2013)
Density	0.2988	0.34
Number of links	732	988
Assortativity	-0.3098	-0.27
Average path length	1.7959	1.73

Note that we do not replicate the specified topological figures exactly as we seek to preserve the observed scale-free property scale-free property of interbank networks. As shown in the right panel of Figure 3.11 below, this is the case. The node fitness distribution is also clearly scale-free, though this is by construction (as the values are sampled from a truncated power law distribution.

[10]Note that in order to prevent isolated nodes (which occurs for smaller nodes whose probability of forming an edge is small) resulting in a *disconnected* network, we develop a contingency by which a disconnected node will form a link to a randomly-selected node in the top quintile (according to bank size) of nodes.

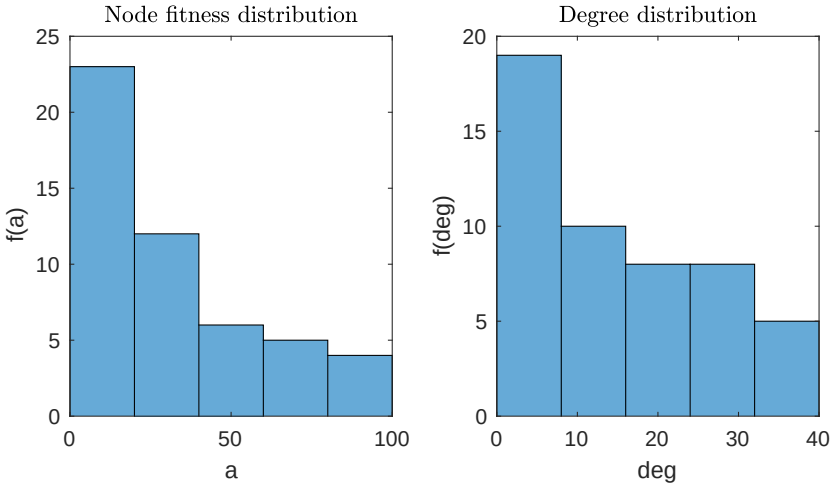

Figure 3.11: Initial bank size and degree distribution

Finally, the initial network structure of the direct exposure layer is provided in Figure 3.12. From the left panel, the tiered/core-periphery topology is immediately apparent. We also provide the network in *circular* format as this will simplify comparison between structures after the network structure becomes dynamic due to the the ABM.

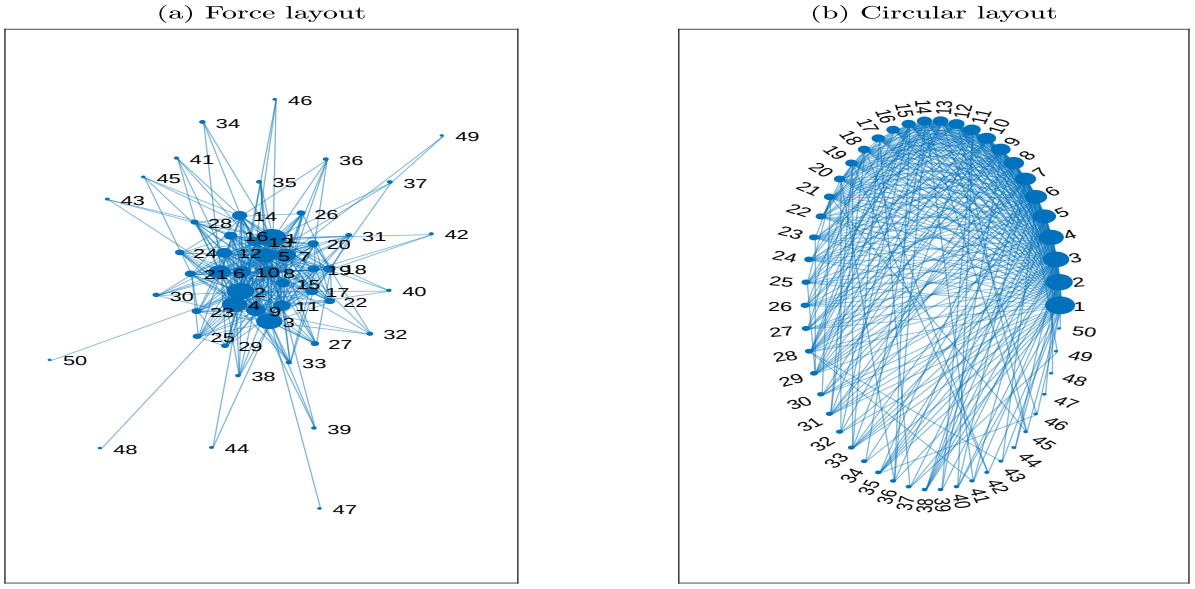

Figure 3.12: Initial core-periphery network of interbank relationships

The bipartite graph of overlapping portfolios is a random network with Poisson degree distribution for both banks and assets. The probability, p of bank-asset pair forming a link is given by μ_b/M. In order to reconcile the parametrisation given by Caccioli et al. (2014) and Montagna and Kok (2016), we select the value of μ_b such that $p = 0.2$. Fixing $M = 50$, this yields $\mu_b = 10$. The initial overlapping portfolio (along with its evolution over the course of the simulation is provided in Appendix 3.B.

3.4.2 Agent-based model

The Agent-Based Model combines calibrated parameters for the heterogenous initial balance sheets of the banks and the stochastic shock regimes with the output from the network generation stage above. Specifically, the node fitness values a_i define banks' total assets which is then used to create the balance sheet parameters via the α and β calibrations given in Table 3.3.

Table 3.3: ABM parameters

Parameter	*Value*	*Definition*	*Notes*
		Initial balance sheet weights	
α	0.9	Securities to assets ratio	Source: (Lux, 2015)
β	0.92	Deposits to liabilities ratio	–
		Interest rates	
r^d	0.02	Deposit rate	Source: (Georg, 2013)
r^e	0.03	Portfolio return	Own calibration
r^z	0.05	Investment return	Own calibration
r^b	0.04	Central bank refinancing rate	Source: (Georg, 2013)
		Shocks	
θ	0.5	Mean reversion factor	Source: (Lux, 2015)
ϕ	0.025	Shock proportionality factor	–
f_{min}	$\{0.9, 0.75\}$	Asset price shock: lower bound $\{s, c\}$	Own calibration
f_{max}	$\{1.1, 1\}$	Asset price shock: upper bound $\{s, c\}$	Own calibration
ω_k	$\{0.2, 0.8\}$	Market depth $\{s, c\}$	Source: (Montagna and Kok, 2016)
M^S	$\{M/10, M/2\}$	Number of shocked assets $\{s, c\}$	Own calibration
		Policy	
ψ	0.02	Minimum reserve requirement	Source: ECB
t^Ω	5	Refinancing frequency	–

Notes: $\{s, c\}$ contains the calibrated value in the stable (first entry) and crisis states (second entry).

3.5 Policy experiment results

Our results are presented in the form of a counterfactual *policy experiment* in which we run the Agent-Based Model developed in Section 3.3 using the calibrations in Table 3.3. We run the simulation for $T = 250$ periods. In order to simulate the onset of the crisis, we switch from the *stable* to the *crisis* financial state in period $T/2 = 125$. Recall that this entails sharp declines in asset prices, $f \in [0.75, 1]$, as well as a reduction in the market liquidity of external assets, $w_k = 0.2$ (thereby mitigating borrowers' ability to meet interbank obligations through firesales). We allow the crisis state to persist for 50 periods, after which the external shock parameters revert to their stable values.

Coinciding with the crisis simulation, the policy experiment compares two alternative scenarios. In the benchmark case, the crisis is allowed to develop unchecked with central bank intervention limited to normal refinancing of lenders and borrowers in the face of liquidity shortages on the interbank market. In the second experiment, the central bank introduces a policy of *fixed rate full allotment* in which additional liquidity is injected into the banking sector in order to counteract mounting insolvencies due to a combination of asset price spirals putting downward pressure on external asset portfolio values and a growing inability to obtain funding on the interbank market. A key feature of this policy measure is its *timing*: In order to keep our simulations grounded in reality, we activate the FRFA policy 25 periods after the onset of the crisis. In this way, we capture the delay between the Lehman trigger on 15$^{\text{th}}$ September 2008 and the introduction of FRFA one month later with the aim of showing that this allowed counterparty and funding liquidity risks to develop and feed back on one another, thereby mitigating the ability of the central bank to restore normal interbank market functioning. As discussed in the general introduction of the thesis, this was largely the case

Lastly, we discuss some technical features of the computational model. First, given that the system is driven by stochastic shocks, the model is run `100` times for each policy experiment after which we average over the number of runs for each variable and each point in simulation time. In order to report the results, we take another average, this time over all banks at each point in simulation time[11]

[11] We also conducted a parallel analysis in which the maximum and minimum values are plotted as upper and lower bounds of the average. However, this did not yield any further insights and complicated visual analysis of the results.

3.5.1 Balance sheet dynamics

We begin our analysis by studying how bank balance sheets have evolved from their initial calibration due to the agent-based model. Starting with average total assets across all 50 banks over 250 time periods, Figure 3.13 shows that prior to the onset of the crisis (whose duration, 50 periods starting at $t = 125$ is indicated by the shaded area), bank balance sheets experience a steady increase. This trend is reversed once the crisis hits, with bank assets dropping precipitously. The red line indicates the baseline scenario in which the central bank continues with its pre-crisis policy of bank refinancing on the basis of correcting liquidity imbalances on the interbank market. As is apparent, such policies are unable to halt the downward trend in bank balance sheets (though a slight tapering is observed once the economy emerges from the crisis).

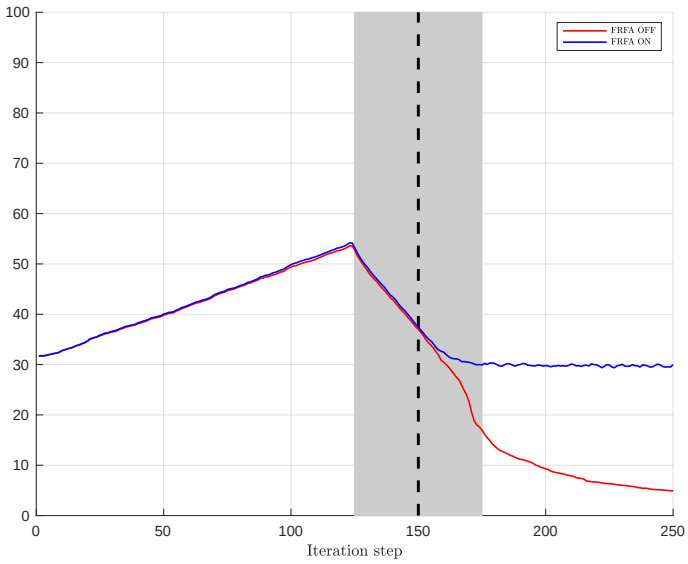

Figure 3.13: Average total assets

The blue line indicates the policy experiment in which the central bank activates its Fixed Rate Full Allotment policy 25 periods after the onset of the crisis. For all figures, the FRFA policy introduction is given by the vertical, dashed line. As expected, the two lines largely overlap from period 0-125 (as the FRFA policy is inactive under both experiments during this period). However, once the central bank activates FRFA, the decline in total assets is halted and remains stable but subdued relative to its pre-crisis level.

The same exercise is performed in Figure 3.14 for the individual components of bank balance sheets: cash and external assets on the asset-side, and deposits and capital on the liabilities-side.

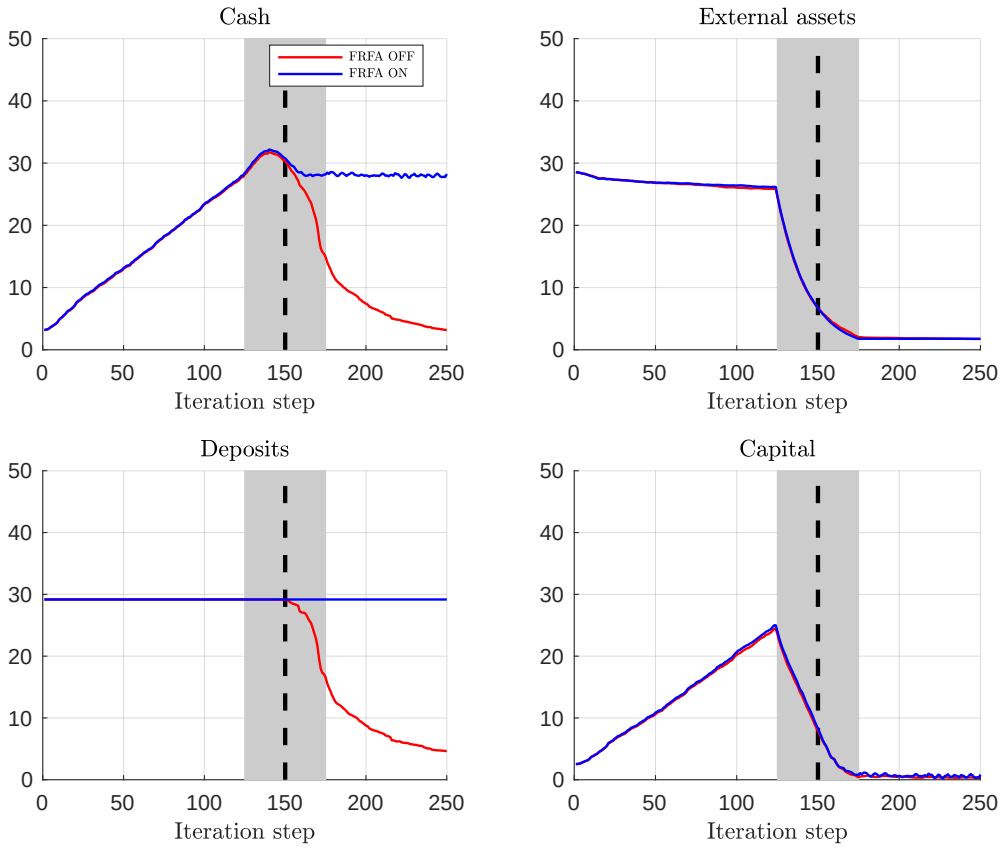

Figure 3.14: Evolution of balance sheet components

Again, the impact of the crisis as well as the mitigating effects played by the FRFA policy are apparent.

Recall that our framework includes an un-modelled private sector dependant on banks for credit. The provision of credit is the first priority for banks hit by a positive (interbank lenders) and a negative (interbank borrowers) shock, both seeking to maintain a constant level of investment: Lenders via reallocation of excess reserves and/or surplus funds from positive deposit shocks and borrowers through interbank credit. As the left panel of Figure 3.15 shows, credit provision to the private sector is severely affected by the crisis, dropping to near-zero levels.

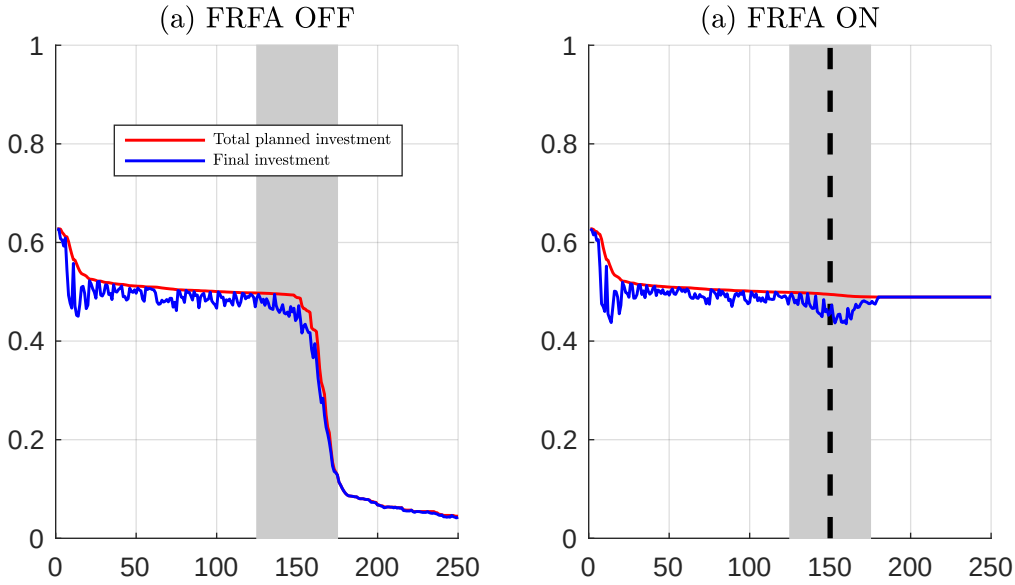

Figure 3.15: Desired vs. final investment

Turning now the right panel, in which the central bank full allotment policy is activated in period 150 (25 periods into the crisis), we observe that while investment does drop over the first ten periods (similar to the baseline scenario), the aggressive intervention by the central bank is successful in stabilising bank credit provision, albeit at a lower level than prior to the crisis[12].

3.5.2 Interbank market dynamics

Where the previous section on balance sheet dynamics served to outline how the model, we now turn to the crux of our argument: to determine the link between bank behaviour on the interbank market (loan and repayment volumes, hoarding and interbank rates) and central bank policy during the crisis period. In the first step banks hit by a negative liquidity shock go to the interbank market as borrowers and make loan requests to their connected counterparties. Loan provision then occurs in two steps: First, lenders compare total incoming requests to available reserves. This constitutes a form of hoarding as it introduces a gap between requests and provisional loans. Hereafter, this is referred to as

[12]However, note the large gap between desired and final investment occurring around the introduction of the FRFA policy. This occurs due to our modelling specification that banks seek to maintain a stable long-term level of investment. As tensions hit the interbank market, banks are forced to adjust their balance sheets to accomodate these shocks, resulting in an investment gap as borrower banks become liquidity constrained.

the *liquidity motive* of bank hoarding behaviour. Subsequently, *precautionary hoarding* by lenders occurs *after* lenders have allocated the appropriate amount of funds towards interbank lending. In this step, lenders assess their current *funding liquidity risk* through backward-looking heuristics examining their ability to attract wholesale funding in the past. Equation 3.15 maps past interbank market outcomes to current hoarding.

Phase 1

Figure 3.16 below summarises interbank market dynamics in *phase 1*. Again, we differentiate between the policy experiment in which the crisis proceeds absent additional central bank intervention (left panel) and one were the central bank injects additional liquidity into the system through its FRFA policy (right panel). Given the complexity and heterogeneity of the system, a certain amount of hoarding is expected in normal times as large banks make liquidity requests to smaller banks who have insufficient reserves to match them in full. Moreover, as with the investment figure above, the system requires a few periods to burn in, as indicated by the higher volumes at the beginning of the simulation after which requests and loans appear to fluctuate around a long-run mean.

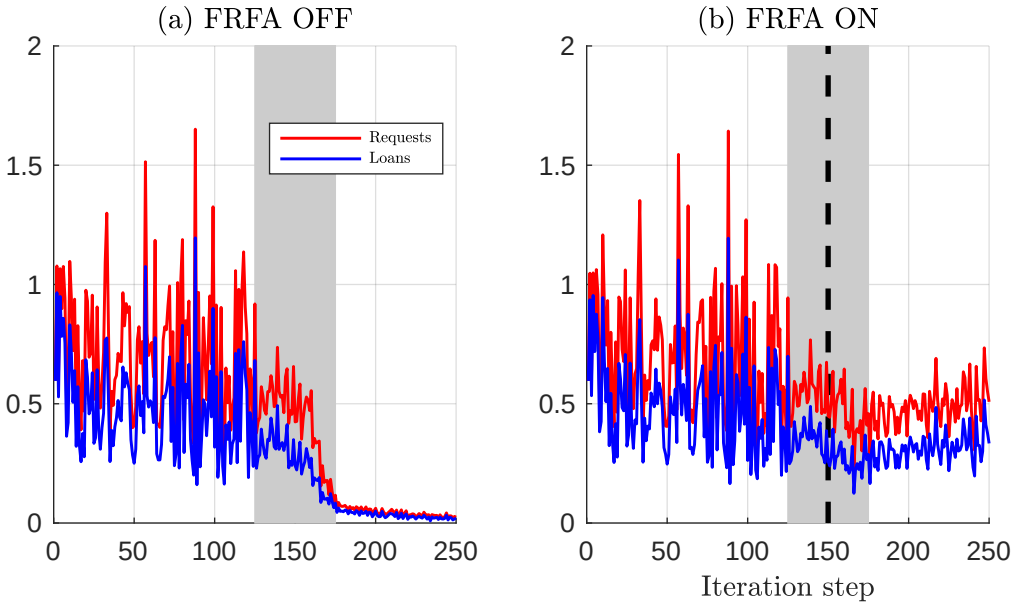

Figure 3.16: Phase 1 dynamics

Following the onset of the crisis, the gap between requests and loans widens as borrowers request additional liquidity on the interbank market. However, lenders, faced with their own liquidity concerns, find themselves unable to meet these requests. As a result, interbank trading declines gradually, culminating in a complete freeze even after the crisis has subsided. However as mentioned, this is a counterfactual exercise. In reality, the FRFA policy of the central bank succeeded in preventing the dry-up of liquidity as mentioned in the general introduction. However, liquidity hoarding becomes the status quo as the gap in the right panel shows. Turning again to the data, this is corroborated by the increasing recourse to the deposit facility. Figure 3.17 plots the difference between requests and loans again, serving as further evidence of the divergence in outcomes under the baseline and when allowing for central bank intervention.

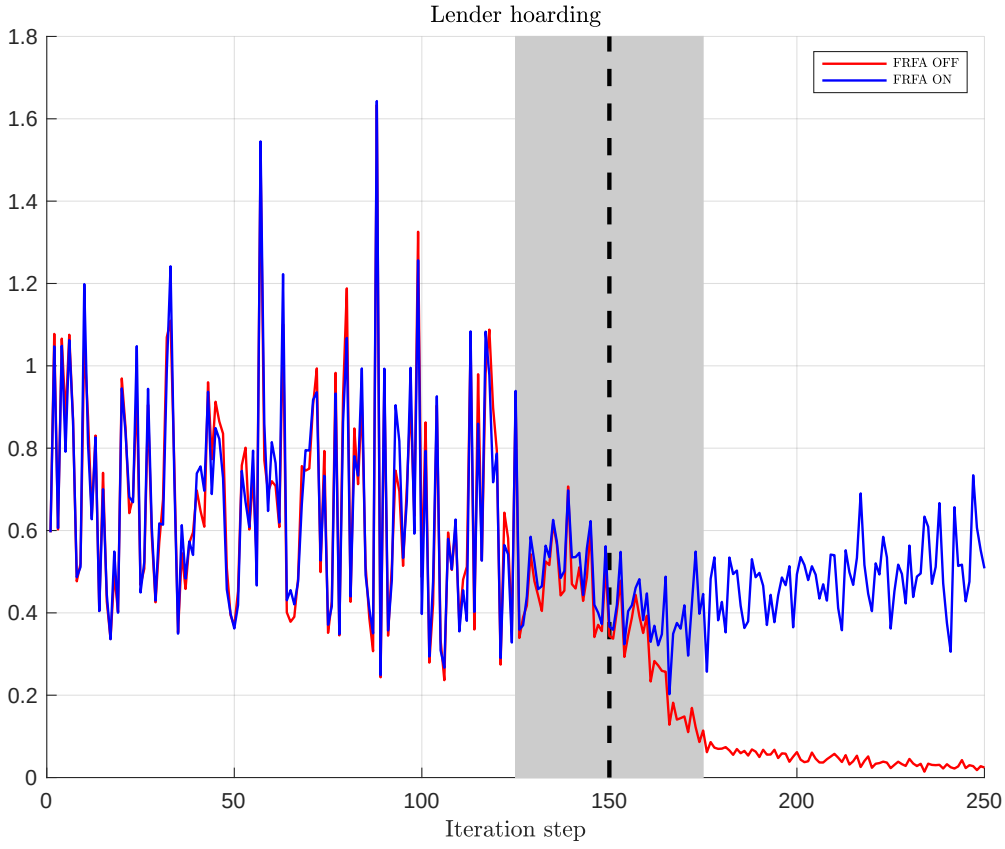

Figure 3.17: Lender hoarding

We end our discussion on phase 1 volumes by recalling that hoarding behaviour is driven by a liquidity as well as a precautionary motive. These are plotted in stacked form in Figure 3.18 below. Firstly, note that the precautionary motive is prevalent throughout the simulation. Again, this is due to the large degree of heterogeneity between banks implying that not all requests are met implying a stable level of funding liquidity risk. Regarding the liquidity motive of hoarding, the same burn-in phenomenon is observed early in the simulation, after which lenders liquidity situation stabilises.

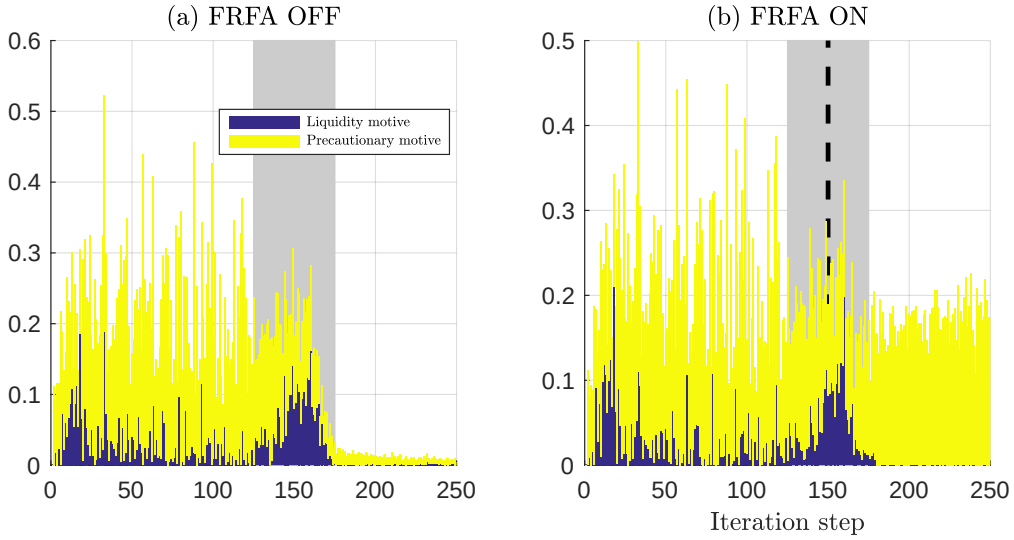

Figure 3.18: Loan decomposition

Regarding the impact of the crisis on hoarding behaviour, we see that lenders' liquidity situation becomes steadily more precarious as the crisis evolves. The freezing of the interbank market in the left panel follows the analysis of Figure 3.16. Note that when the FRFA policy, hoarding due to liquidity concerns is nonexistent (due to the system now being flush with liquidity). Moreover, the precautionary motive is significantly lower than prior to the crisis.

As mentioned in the general introduction, the spike in banks' concerns regarding the creditworthiness of borrowers was one of the distinguishing features of the crisis's manifestation on the interbank market. In our model, interbank risk premiums are assumed to be driven *directly* by lenders' concern over the creditworthiness of borrowers, the so-called *counterparty risk* channel. Using a heuristic based on adaptive expectations (see Equation 3.17), lenders map past loan defaults to set risk premiums in the current period.

As shown in Figure 3.19 below, there was a small buildup of counterparty risk due to past loan defaults prior to the crisis. In the benchmark case where the interbank market dries up, no trades occur hence the interest rate is driven back to its initial value. By contrast, despite the FRFA policy, counterparty risk has already manifested itself, resulting in lenders' continued reticence in providing easy funding.

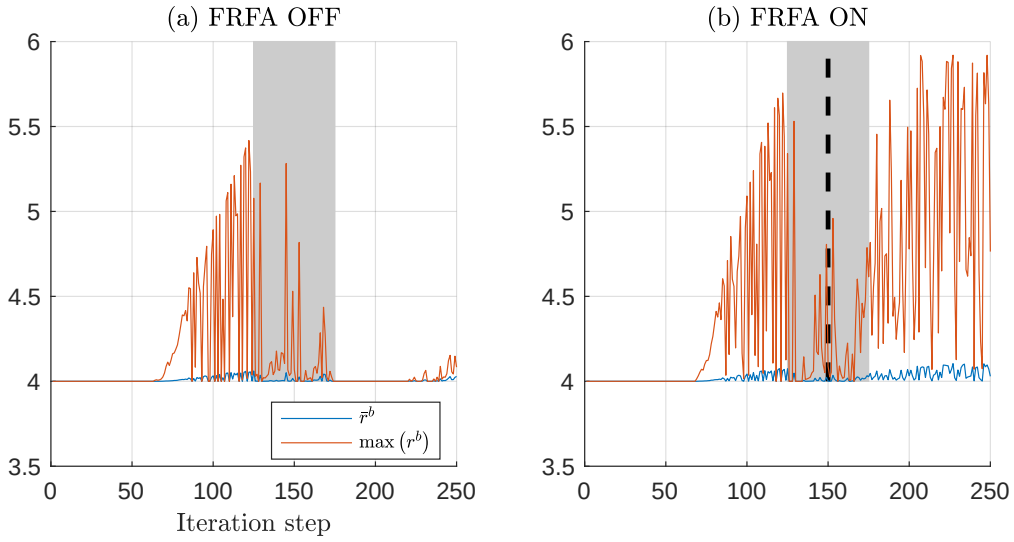

Figure 3.19: Average interbank rate

The results under FRFA support our claim that by the time the ECB intervened to stabilise interbank markets and ensure continued credit provision to the real economy, the buildup of liquidity and counterparty risk (and the associated feedback mechanisms between them) within the banking sector had resulted in banks withdrawing from interbank market lending and borrowing. However, the policy also prevented a much more severe outcome in which a full scale interbank market freeze occurs which spills over to the real economy in the form of a credit crunch.

Phase 2

The last step in banks' interactions on the overnight interbank market involves borrowers repaying the loans made in phase 1. This includes the principal loan amount as well as the interbank rate set by lenders. Note that in our model, interbank loans are redirected towards an illiquid investment. As a result, borrowers tap into their reserves to repay interbank loans. It is in this stage that the interaction between the bilateral exposure and the overlapping portfolio layers of the network are incorporated. Specifically, borrowers with insufficient reserves to pay back loans in full sell off a portion of their external asset portfolios at the prevailing market price. The impact of asset firesales is amplified during the crisis period during which asset prices fall and market liquidity decreases. As a result of falling asset prices, liquidity short banks have to sell off a larger fraction of their portfolio to make the same requirement. This in turn engenders further endogenous asset price spirals via the market impact function given by Equation 3.25.

Figure 3.20 below compares the average amount that borrowers are expected to repay in each period with final repayment volumes. Again, interbank market tensions manifest themselves quite clearly in a similar manner to loan requests and provision in phase 1. Due to falling loans from cash-strapped lenders, required repayment decreases accordingly. Note that the observed increase in interbank rates due to counterparty risk concerns is not sufficient to impact borrowers' loan repayment behaviour.

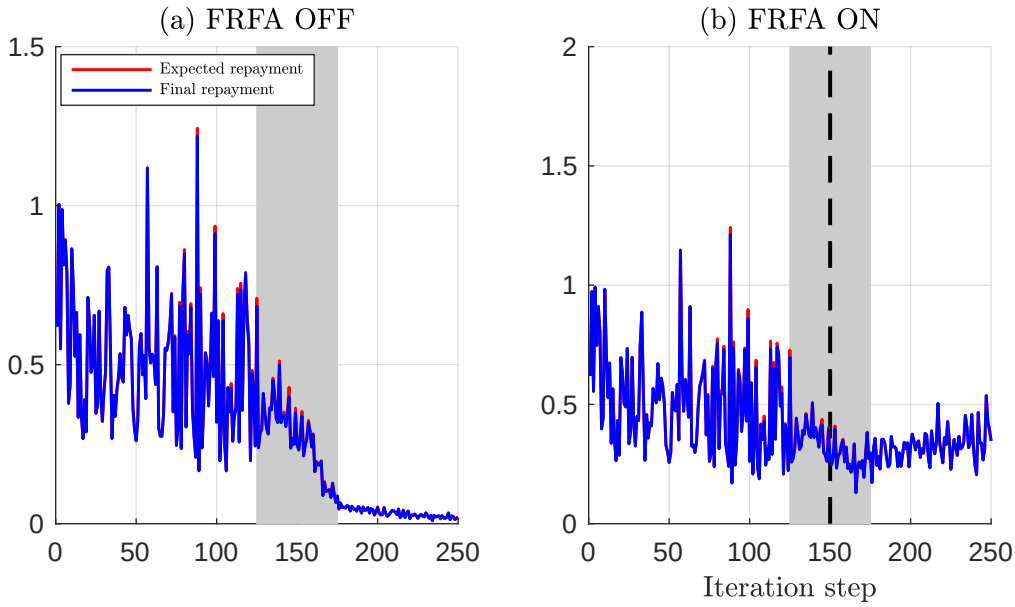

Figure 3.20: Phase 2 dynamics

Based on the above results reporting interbank market dynamics, we conclude that funding liquidity risk plays the dominant role in driving banks' retrenchment from the interbank market. Lenders continue to hoard liquidity which is reinforced given the dynamic nature of the model (i.e. a borrower unable to obtain the requested funds due to hoarding in one period will in turn hoard liquidity in the future). As shown, this would have resulted in a complete freeze of the interbank market. The FRFA policy was shown to alleviate liquidity concerns and ensure the continued but subdued functioning of the interbank market.

Phase 3

After interbank positions are closed at the end of phase 2, the central bank, under its price stability mandate, provides refinancing to banks in the form of cash injections. These are calibrated to compensate for liquidity imbalances on the interbank market. Under normal refinancing operations, this comprises both *borrower* and *lender* refinancing operations. The former involves targeting the liquidity shortfall between borrowers' total interbank requests and loan provision by lenders (which, in addition to the precautionary hoarding motive, is also drive by lenders' available reserves). Similarly, lender refinancing is carried out by calculating the difference between borrowers' expected loan repayment (equal to the principal + interest) and their final repayment.

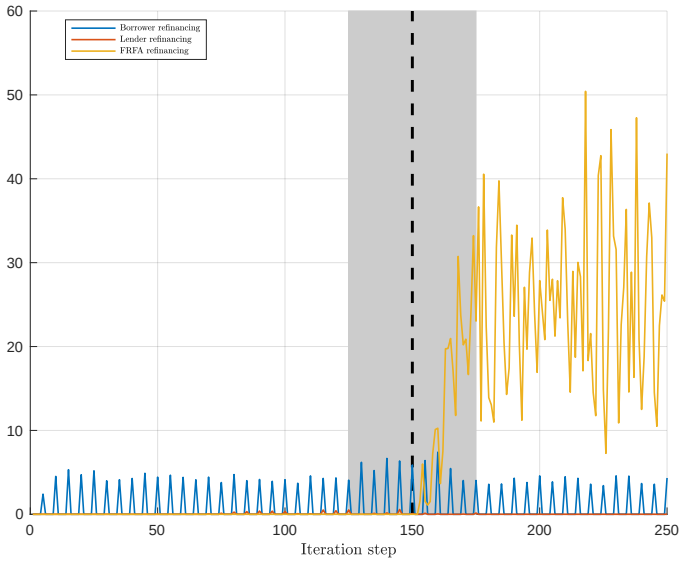

Figure 3.21: Central bank liquidity provision

While normal refinancing continues throughout the entire simulation, the Fixed Rate Full Allotment is introduced in period 125 and maintained for the remaining simulation periods. In this setup, additional liquidity is provided to banks in danger of becoming insolvent in the current period.

Observing the phase 1 and phase 2 dynamics allows us to conclude that funding liquidity risk plays a more significant role in dampening interbank market activity than counterparty risk. This is reflected in central bank activities wherein lender refinancing is insignificant relative to borrower refinancing. As regards the latter, we observe a small increase in liquidity provision to borrowers shortly after the onset of the crisis. However, once the FRFA policy is introduced, this decreases to the pre-crisis level as borrowers' liquidity needs are met under the new policy.

3.5.3 Securities market

In our model, asset prices are driven by exogenous shocks as well as by banks' activities on the interbank market via borrowers' selling off assets to repay their loans. Moreover, the extent of firesales is strongly dependant on interbank market dynamics. For example, rising counterparty risk results in higher interbank rates which implies a larger loan repayment requirement for borrowers. If reserves are insufficient, this increases the likelihood that a bank will have to sell off assets to meet its interbank obligations and put further downward pressure on asset prices. This further exemplifies the complex dynamics that emerge from the simple heuristics of the model. Recall that asset prices are updated twice over the course of phase 2 (see Figure 3.9): First exogenously via a shock to a subset of total system assets[13] then endogenously as market illiquidity and external asset firesales, combined with an inelastic demand function for these assets increases market risk.

To shed light on asset price movements, Figure 3.22 disentangles the percent change in average asset prices due to the exogenous shock and due to firesales. The former is computed by taking the percentage difference between asset prices following the shock, $\tilde{p}^t$ and the initial price p^t equal to the post-MIF price from the previous period. Similarly, the change in asset price due to the market impact function is computed using p^t and the post-APS price in the current period, $\tilde{p}^t$.

[13] Although the shock calibration is the same for all banks, the bipartite graph imbues it with a certain degree of idiosyncrasy as certain banks may hold more shocked assets than others.

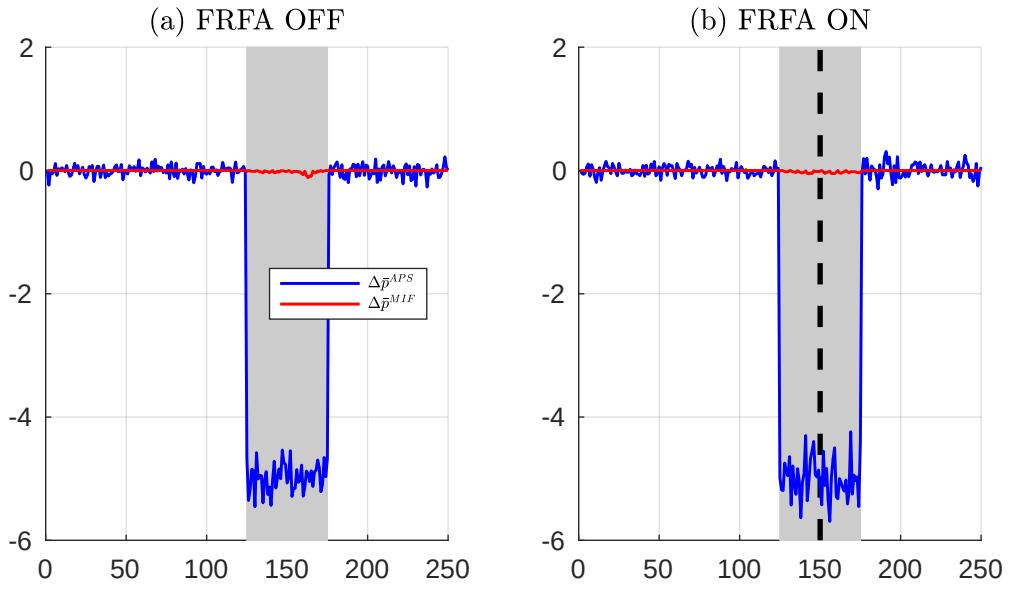

Figure 3.22: Asset price dynamics

Though a small endogenous decrease in asset prices due the market impact function is observed, it is clear that endogenous price spirals do not occur. Again, this stems from the decrease in interbank activity due to funding liquidity observed in phase 1 and 2. Consequently, loan volumes are not high enough to require significant firesales on the part of borrowers.

Despite this, we report banks' firesale behaviour below. Though total firesales can be considered in conjunction with Figure 3.20 given that they determine the extent to which borrowers are successfully able to repay their loans, we include it here as the difference between desired and final firesales is directly related to the liquidity of the securities market. To be precise, a liquidity-short borrower will be unable to fulfil its interbank obligations if it does not possess sufficient external assets in its portfolio to sell for cash. While this could arise simply due to inadequate asset holdings, it is exacerbated by rising market illiquidity as interbank markets become strained. In this scenario of falling valuations, borrowers will need to sell off more assets for the same amount of cash thereby increasing the likelihood that their holdings are insufficient.

Following the same method of analysis as before, we consider asset firesales under normal central bank refinancing and with the addition of FRFA. As Figure 3.23 shows, borrowers with insufficient liquidity to meet their interbank obligations are mostly able to sell off the required volume of assets at the current market price without having a noticeable impact on future prices.

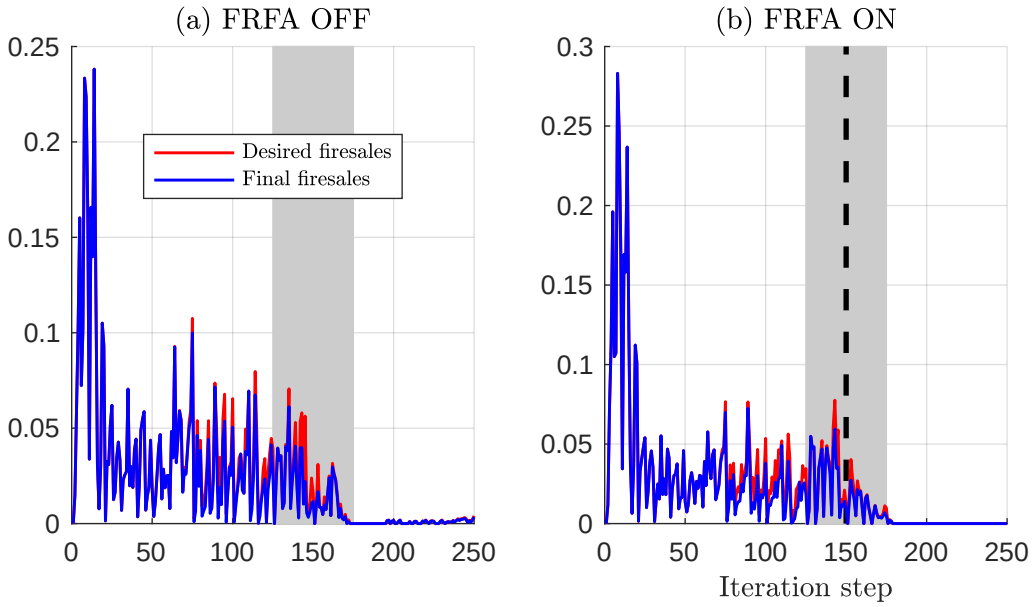

Figure 3.23: External asset firesales

However, analysis of the left panel reveals a prolonged period during which borrowers were unable to sell off enough assets to repay their loans. Moreover, this shortfall is not observed when the FRFA policy is active.

3.5.4 Failures

The final step in the analysis of our computational model takes a more structural perspective. Specifically, we begin by studying the evolution of bank failures during the simulation as well as the resulting *capital loss* when a bank is driven into insolvency. This is defined as the sum of the absolute value of failed banks' capital at the moment of insolvency. This is a negative value by construction and captures the of capital required to bring the system back to full solvency.

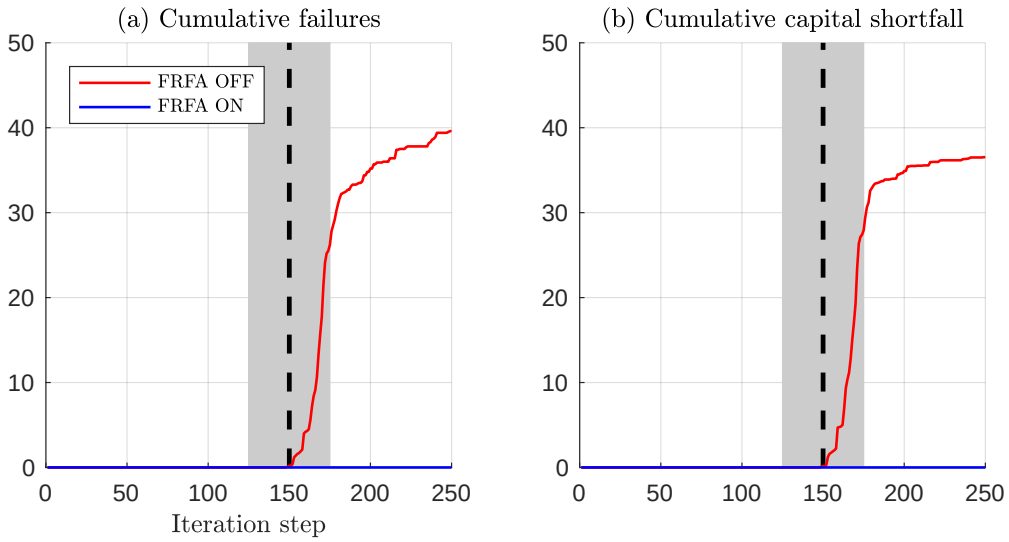

Figure 3.24: Cumulative insolvency dynamics

Given that a key feature of our model has been the interaction between banks as well as between banks and their external assets, we compare the total number of active banks and assets over the simulation period. Where active banks refers to banks that remain solvent, a security is considered active if it is held by at least one bank. Consequently, this variable is driven both by asset firesales and bank insolvencies. While the former is intuitive (repeated firesales such that aggregate holdings of that asset are driven to zero), recall that the latter effect is defined in Phase 3 wherein insolvent banks sell off their remaining external assets which are then redistributed across their counterparties.

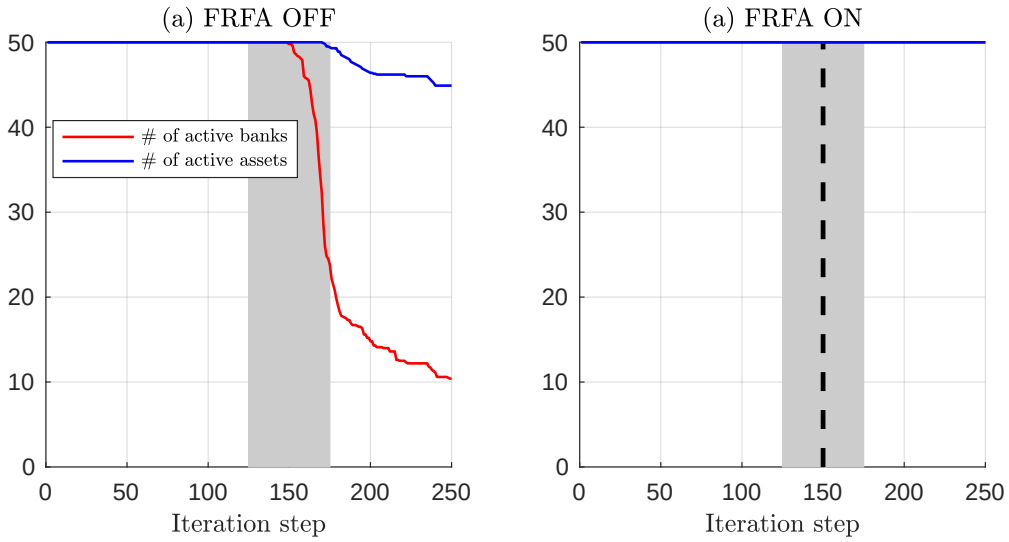

Figure 3.25: Number of active banks and assets

Again, our model reproduces realistic dynamics. Absent any additional policy intervention by the central bank, the banking sector is subject to a growing number of failures as the crisis unfolds. Moreover, we observe a delay of approximately ten periods before the first failures occur after which bank insolvencies compound, resulting in a diminished banking sector relative to the start of the simulation. This delay can be interpreted as a justification that model dynamics are not wholly driven by the exogenous shock. Indeed, banks continue to interact on the interbank market several periods into the crisis, though this eventually decreases at a steady rate, as the prior analysis on interbank market dynamics has also shown.

Comparison of the left and right panels in Figure 3.25 leads to a stronger conclusion than for the balance sheet and interbank market where central bank intervention was unable to restore full functioning (though it did prevent a much worse outcome). Excessive liquidity in the system due to FRFA (as shown in Figure 3.21 implies a high level of solvency amongst banks combined with reduced interbank activity.

3.5.5 Network structure dynamics

Where previous models of cascading defaults in financial networks use an ad hoc approach replicate the spread of localised shocks across the baking sector, typically via a capital buffer that absorbs or propagates incoming shocks, network dynamics in our model are completely driven by bank behaviour within and across the multilayer structure. Thus, we end the results section with a discussion on the evolving network structure of the interbank exposure and the overlapping portfolio layers.

Starting with the interbank exposure layer, we represent the complex network structure through three *network measures*: total number of edges, network density and average degree. As is apparent from Figure 3.26, if the crisis would have been allowed to proceed without the introduction of additional liquidity measures, the number of interbank linkages would have fallen dramatically as indicated by the leftmost and rightmost panels which measure connectivity at the aggregate and average levels, respectively.

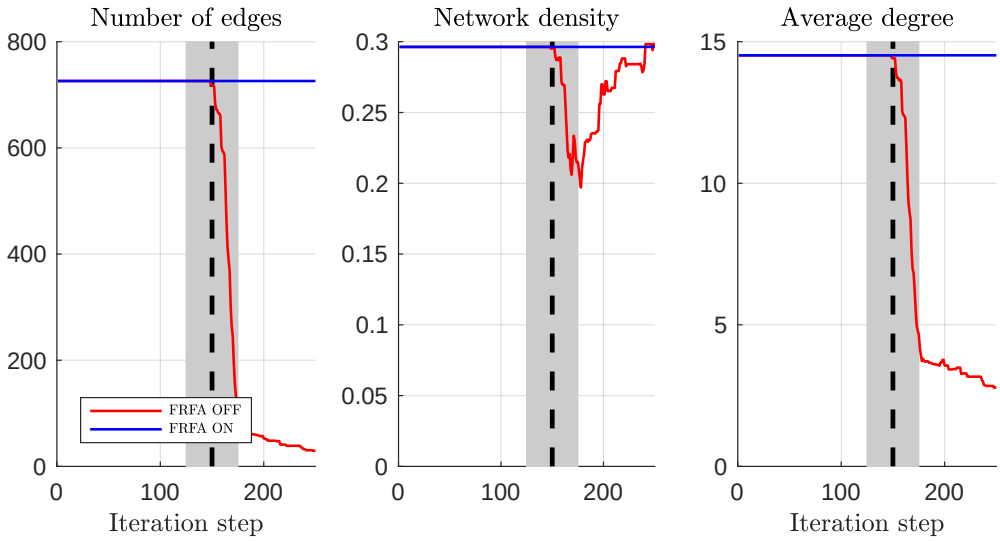

Figure 3.26: Interbank exposure network evolution

As shown in section 3.2.2, the overlapping portfolio network takes the form of a bipartite graph parametrised by μ_A and μ_B respectively denoting the average degree of assets (i.e. the average number or banks holding each asset) and the average degree of banks which can also be interpreted as banks' *average diversification*. Lastly, the crowding parameter, obtained by dividing the total number of banks by the total number of assets provides an indication of the speed at which banks fail relative to assets becoming inactive.

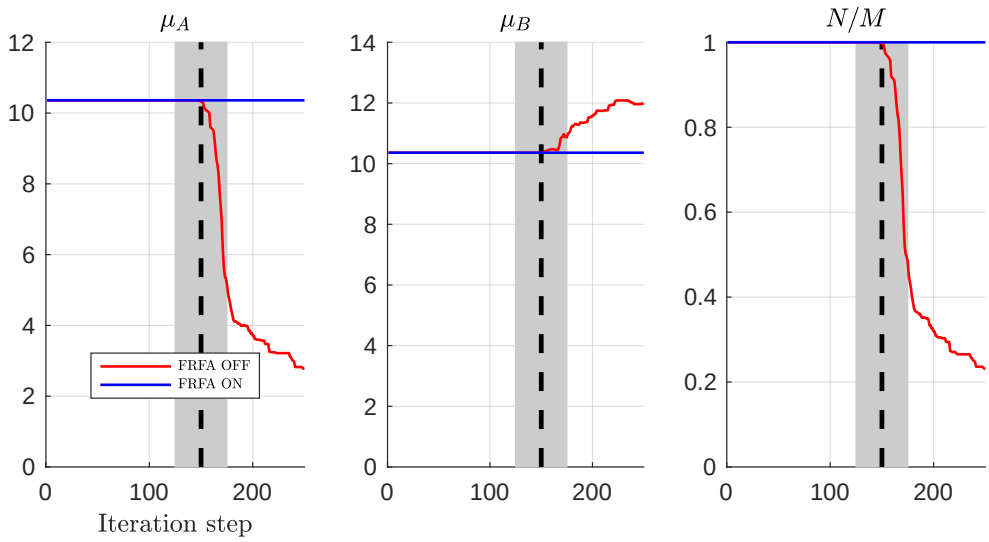

Figure 3.27: Overlapping portfolio network evolution

Comparison of μ_A to μ_B dynamics reveals much larger movements in the former than the latter. Thus, banks fail faster than assets become inactive resulting in an increase in diversification as a small number of banks hold the same number of assets.

As we have shown, the structure of the network is also strongly affected by the crisis and interbank market behaviour. However, while the delay between the onset of the crisis and the introduction of FRFA had a marked impact on interbank market dynamics, the *structure* of the network is more resilient to changes in the economic situation. This is shown in the elapsed time between the onset of the crisis and the first failures.

3.6 Concluding remarks

This paper provides a first attempt at combining the literature on the network topology of interbank markets with an Agent-Based Model tailored specifically to incorporate the bank behavioural dynamics observed during the crisis. Specifically, this revolves around our representation of funding liquidity and counterparty risk through a set of heuristics in which banks use *adaptive expectations* to map past observations to current behaviour. We argue that modelling bank behaviour in such a manner, set within the interactive limits of a realistic interbank network structure represents a new paradigm for the study of financial stability and systemic risk.

Prior to running the ABM, we apply two state-of-the art methodologies to simulate a *multilayer* network comprising two layers: (i) an undirected, disassortative and scale-free network and (ii) a random bipartite network. The parameters associated to each layer respectively represent a different type of bank interdependency namely: (i) direct exposures consisting of interbank lending and borrowing and (ii) indirect exposures arising due to banks' holding certain assets in common i.e. overlapping portfolios. It is now widely accepted that considering multiple transmission channels is imperative to properly understand financial contagion and systemic risk. Our paper is firmly grounded in and further develops this narrative by developing the behavioural specification linking the two layers in a dynamic model featuring heterogenous agents and an evolving network structure.

Embedded within the simulated network, the ABM proceeds in a sequential manner. The system is initiated by a liquidity shock that drives banks to the interbank market as borrowers or lenders. This transforms the initial simulated undirected network into a directed one whose structure changes in each period. Loan repayment by borrowers provides the mechanism through which the two layers interact. Specifically, borrowers with inadequate liquidity to fulfil their interbank obligations sell off external assets at the prevailing market price. The price of *each* asset is updated endogenously as a function of total sales volumes during the period. Since the bipartite graph formulation implies that banks hold assets in common, firesales by one bank decreases the price of its assets which in turn, forces other banks to revalue their portfolios downwards. Thus, despite our use of relatively simple heuristics driving various aspects of bank behaviour, the model features a number of complex feedback loops that occur within and between layers and across time periods.

Given that the model is run as a computer simulation in which agents interact autonomously according to a predefined set of behavioural rules, a large amount of data is generated covering bank balance sheet evolution, interbank market dynamics (volumes and rates) and the changing structure of the bilayer network as banks fail and sell of their asset positions. In order to construct a relevant narrative, we have restricted our attention to the events occurring in the early days of the crisis during which the rapid buildup and unwinding of systemic risks led to a freeze in the interbank market. Against this background, we seek to understand the role played by the central bank in stabilising interbank market tensions and the reason why interbank market activity remained subdued despite aggressive central bank policy interventions. In the paper, we argue that following the onset of the crisis (modelled as a sharp drop in asset prices coupled with a decrease in market liquidity), banks' concerns about their own ability to attract funding results in precautionary hoarding behaviour while an increasing number of loan defaults by stressed counterparties drives up risk premiums on interbank loans.

Our results thus take the form of two *policy experiments*, presented simultaneously for ease of comparison. The first experiment i.e. our baseline is business as usual: The central bank provides refinancing to the banking sector on a regular basis in order to correct liquidity imbalances. In order to keep our model close to reality, these interventions occur at regular intervals. This replicates the main refinancing operations instrument used by all major central banks. In the second, we introduce a policy of Fixed Rate Full Allotment in which additional liquidity is injected into the banking sector in order to prevent cascading bank insolvencies. As was the case in September-October 2008, this policy was introduced with a delay of one month by the ECB following the Lehman Brothers insolvency on September 15^{th}. The crux of our simulation study revolves around the notion that while these emergency measures succeeded in preventing a widespread collapse of the banking system, the buildup in funding liquidity and counterparty risk that occurred after the onset of the crisis and prior to the introduction of the FRFA policy resulted in a widespread withdrawal from the interbank market.

Though the results provide new insights into bank behavioural dynamics and the role of central bank policy interventions, they represent a fraction of the possible research avenues that can be undertaken within the framework of our model. In our view, further work derived from the methodology developed in the paper could revolve around two main elements: (*i*) Use of real balance sheet and interbank network data to set up the model prior to launching the ABM and (*ii*) Introducing different macro- and micro-prudential measures in order to study the resilience of the financial system. Regarding the use of

data, recall that we use a highly stylised balance sheet representation combined with a probabilistic network generation model calibrated to replicate key topological features of real interbank networks. Our framework is flexible enough to allow practitioners to replace Section 3.2 entirely. By doing so, our model could be redirected towards use as a stress-testing device. Lastly, given the growing importance of interconnectedness in the development of financial regulation, a number of policy tools including capital requirements[14], additional capital buffers for G-SIBS etc. could be incorporated. Lastly, we have eschewed a comparative statics analysis of the parameters used to set up the model. While this was done for the sake of brevity and to restrict our attention to understanding bank behaviour and the impact of fixed-rate full allotment, further exploration of the parameter space would yield additional insights on the inner workings of the model.

[14]In this context, heterogeneity in bank capital and the impact on systemic risk would constitute a relevant addition to the literature. The increasing importance of bank capital in times of crisis and the impact on bank performance has been recognised by Demirguc-Kunt et al. (2013).

Chapter 3 Appendices

3.A Computations

Derivation of interbank risk-premium setting equations (Eqs. 3.17 and3.18): Starting from Figure 3.8, we define the corresponding linear function:

$$\rho_{ij}^{t} = \rho_{ij}^{t,m} - \frac{\bar{l}_{i}^{\hat{t}_{ij}^{L}}}{\bar{x}_{j}^{\hat{t}_{ij}^{L}}} x_{ji}^{\hat{t}_{ij}^{L}}, \quad \forall j \in \mathcal{N}_{i,-}^{t} \tag{C.27}$$

where the y-intercept $\rho_{ij}^{t,m}$ corresponds to the maximum possible risk premium arising due to total default in period $\hat{t}_{ij}^{L}$. This is computed from (i) the average interbank behaviour in that period and (ii) the past expected return on loans from i to j.

Beginning with the assumption that full repayment yields a scaling factor of 1 provide us with the coordinate $(l_{ij}^{\hat{t}_{ij}^{L}}, 1)$ which, when substituted into Equation C.27, results in the following value, after re-arranging, for $\rho_{ij}^{t,m}$:

$$\rho_{ij}^{t,m} = 1 + \frac{\bar{l}_{i}^{\hat{t}^{L}}}{\bar{x}_{j}^{\hat{t}^{L}}} l_{ij}^{\hat{t}^{L}} \tag{C.28}$$

Finally, substitution of Eq. C.28 into Eq. C.27 provides the final form of the risk premium equation (Eq. 3.17).

3.B Network visualisation

3.B.1 Interbank relationship dynamics

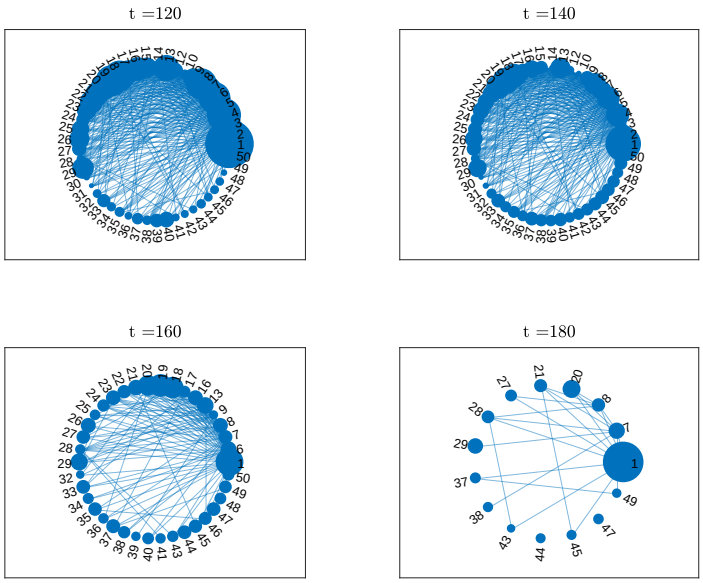

Figure 3.B.1: Evolution of bank relationships during the crisis (undirected, unweighted network)

3.B.2 Interbank loan dynamics

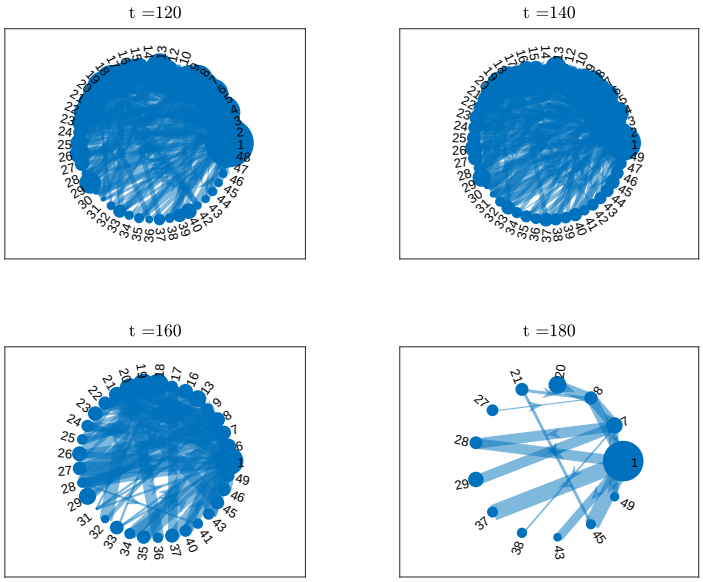

Figure 3.B.2: Evolution of interbank loans during the crisis (weighted, directed network)

3.B.3 Overlapping portfolio dynamics

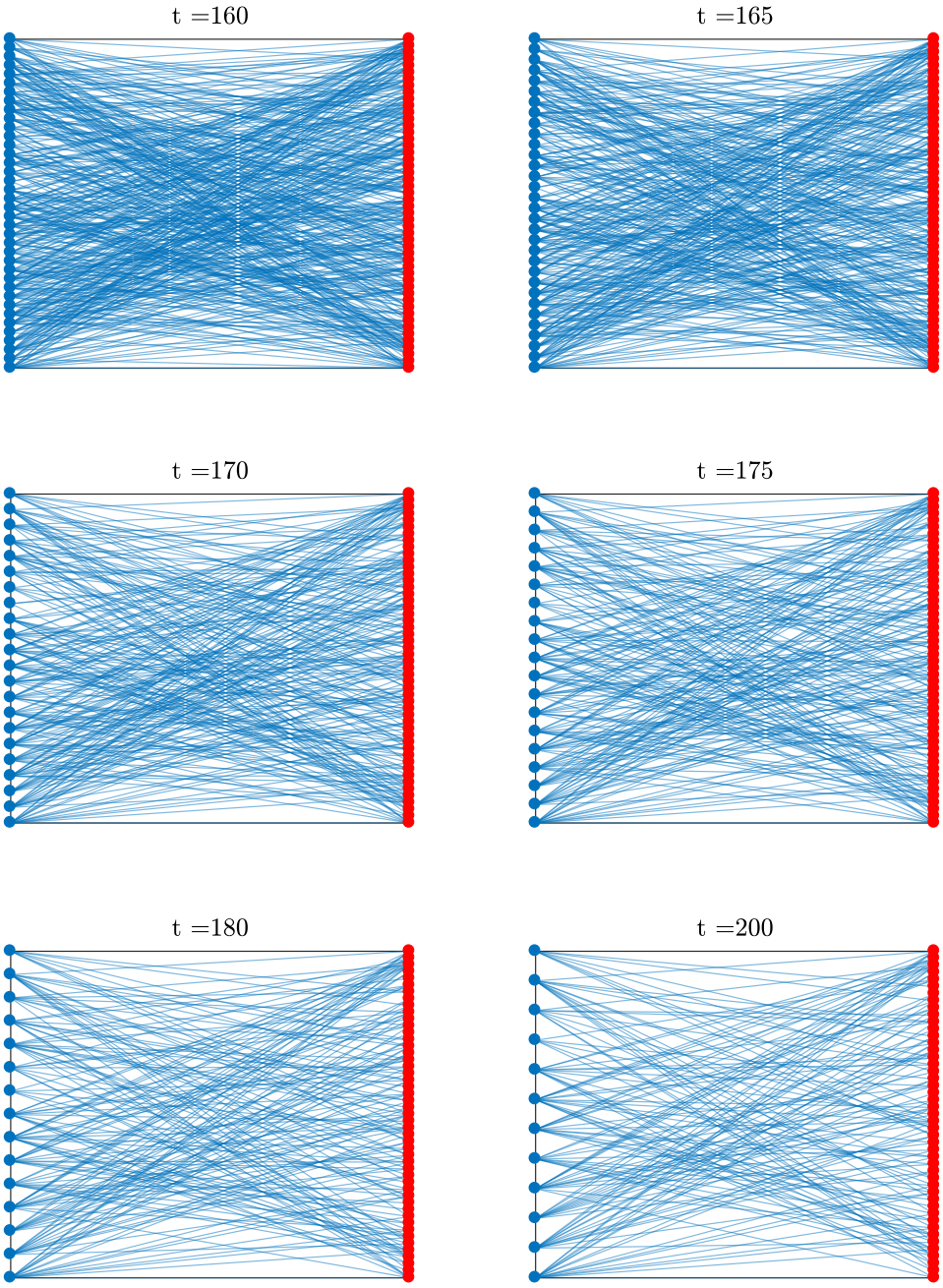

Figure 3.B.3: Evolution of bank portfolios during the crisis (bipartite network)

Closing discussion

As I have demonstrated in the thesis, networks constitute a powerful tool for representing the pattern of interlinkages between banks and understanding the systemic vulnerabilities to the financial system as a whole. Moreover, their ability to represent the underlying dynamic *structure* of financial markets renders them highly useful as a backdrop to studying the complex dynamics between banks during a financial crisis. The narrative developed over the three chapters comprising the thesis can be broadly categorised along two dimensions: (*i*) Understanding the impact of network topology on systemic risk and financial contagion and (*ii*) Developing behavioural models in which agents/banks act within the interactive limits given by the network structure and *network externalities* are transmitted according to the pattern of interlinkages. Below, I briefly restate the current state-of-the-art in order to later establish where each chapter is situated within the literature:

Network topology: Recent advances in using granular financial data to map real interbank networks have gained traction amongst central banks and policymakers. As such data increases in availability and quality, researchers are rapidly converging on a set of common topological properties across a variety of national and international interbank networks: small-world effects, a scale-free degree distribution, disassortative mixing and a core-periphery structure. Against this background, increasingly sophisticated simulation methods stemming from statistical mechanics are being perfected to simulate realistic interbank networks for counterfactual simulations, stress-testing and macroprudential policy analysis. In my opinion, the newest frontier in financial network and systemic risk analysis lies in the use of *multilayer* networks analysis to represent the various types of interdependencies between financial institutions.

Agent behaviour on networks: Extending from mechanical models of *cascading defaults* wherein bank behaviour is *passive* and shock propagation is a binary variable determined by the ability of a banks' capital buffer to absorb the incoming shock from connected counterparties, the current state-of-the-art allows banks to *actively* respond to their environment via a predefined behavioural specification using tools from Agent-Based Modelling. Within this framework, state-of-the-art models introduce *heterogeneity* into the network while incorporating heuristics lifted directly from bank behaviour during the crisis. As I have argued, the network defines the interactive limits of the system in which individual behaviour is driven the ABM. As a result, key ingredients such as information asymmetry and myopic agents arise as intrinsic features of the model.

Each chapter, though different in the theoretical model and research question, is a variation of the above two themes. **Chapter 1** introduces a stylised four-node network à-la Allen and Gale (2000) into a modified version of the DSGE specification developed by De Walque et al. (2010) in order to study how interbank market tensions can spill over into credit markets and impair the ability of the central bank to steer short-term interest rates. Against this background, we take into account that real interbank networks are best represented by the core-periphery topology while providing two extreme cases (cyclical and complete networks) for comparison. Evidently, agent behaviour is provided by the DSGE specification which includes such features as endogenous loan defaults (in both the retail and wholesale markets), dynamic risk-weighted capital requirements and liquidity injections by the central bank, all of which played a key role in the crisis.

With assessing the impact of network topology on financial stability being the main objective, we find that complete networks play a stabilising role by dissipating localised banking shocks across the network. By contrast, when a core-periphery topology is applied, the core bank exhibits large fluctuations while the network as a whole requires larger central bank intervention. This lends support to the "*too interconnected to fail* paradigm wherein certain banks, by virtue of their position in the network pose a higher threat to financial stability.

Chapter 2 shares one common feature with chapter 1 namely, the primary aim is to assess the role of network structure on system dynamics. However, where the first chapter proposed a highly-stylised network structure in order to incorporate behavioural dynamics via a DSGE model, chapter 2 shifts the focus to network topology while abstracting from complex bank behaviour. Against this background, I simulate a wide array of realistic interbank networks using a *latin hypercube design* after which a standard cascading defaults model is run on each one. This creates a dataset in which each network constitutes an

observation. I then develop an empirical model in which the independent variables comprise various topological features of the network (computed ex-ante) while the dependent variables are based on the shock's propagation through the network.

Recall that the main difference between chapters 1 and 2 was the lack of a behavioural specification in the latter due to the higher complexity of the imposed network structure. The model behind **chapter 3** was developed with the aim of combining the state-of-the-art in network modelling with a realistic framework for bank behaviour that takes into account the specificities of the financial crisis. To this end, a thorough review of the literature identified the rapid buildup of counterparty and funding liquidity risk as financial market conditions deteriorated as one of the key features of the crisis and one of the reasons why the large-scale liquidity interventions by central banks failed to restart the interbank market. In order to include both dynamics in a tractable and intuitive framework, I apply tools from the *agent-based modelling* literature by developing a set of heuristics based on adaptive expectations in which banks condition current interbank behaviour on past difficulties in obtaining funding or borrowers' past inability to pay back loans in full. The key strength of this approach is that it allows complex system-wide dynamics (in this case, a retrenchment from wholesale funding) to emerge in a 'bottom up' fashion from simple agent behaviour. Moreover, it can be easily embedded in a network by restricting banks' interbank behaviour to their local counterparties (i.e. their first neighbours in the network). Several studies on the relationship lending and the efficiency repeated interactions between banks corroborate this approach. Though I use the same network simulation approach to generate the initial interbank exposure network as in chapter 2, there are two key differences: (*i*) The simulated network is undirected and unweighted since the direction of lending and borrowing is dictated by idiosyncratic liquidity shocks and the volume of loans is endogenous and driven by the heuristics and (*ii*) I introduce a second set of interdependencies between banks namely, *indirect* links via common exposures to external assets which, when combined with *direct* interbank exposures, results in a *multilayer network*. Against this background, this chapter is firmly situated in the state-of-the-art in interbank network and financial stability modelling due to the combination of multilayer network analysis (allowing for various channels of contagion) and complex bank behaviour.

However, given the nascency of the field, there is no common framework for presenting results in a comprehensive way. Moreover, the model is largely computational in nature and generates a large amount of data on banks' balance sheet evolution, investment behaviour as well as bilateral information on interbank rates, loan requests, loan provision and loan repayment. In order to fit with the policy-oriented narrative of the thesis, I conducted a counterfactual simulation comparing outcomes with and without the emergency liquidity provision by the central bank. The results are largely in line with actual observations on the manifestation of the crisis on the interbank market: while the central bank was able to avert widespread insolvencies and maintain credit provision to the private sector, it was unable to jumpstart the interbank market due to the buildup and feedback of counterparty and liquidity risks.

To summarise, the present thesis not only provides new ways to understand systemic risk through network analysis, but also outlines a foundation on which future work can be built. This can be undertaken either through a sensitivity analysis using alternative calibrations or via the use of real interbank exposure and balance sheet data as an alternative to the simulated networks for the cascading defaults model and ABM in chapters 2 and 3 respectively, thereby introducing additional realism into the models.

Bibliography

Abbassi, P. and Linzert, T. (2012). The effectiveness of monetary policy in steering money market rates during the financial crisis. Journal of Macroeconomics, 34(4):945–954.

Acemoglu, D., Carvalho, V. M., Ozdaglar, A., and Tahbaz-Salehi, A. (2012). The network origins of aggregate fluctuations. Econometrica, 80(5):1977–2016.

Acemoglu, D., Ozdaglar, A., and Tahbaz-Salehi, A. (2015). Systemic risk and stability in financial networks. American Economic Review, 105(2):564–608.

Acharya, V. and Bisin, A. (2014). Counterparty risk externality: Centralized versus over-the-counter markets. Journal of Economic Theory, 149:153–182.

Acharya, V. V. and Merrouche, O. (2012). Precautionary hoarding of liquidity and inter-bank markets: Evidence from the subprime crisis. Review of Finance, page rfs022.

Acharya, V. V. and Skeie, D. (2011). A model of liquidity hoarding and term premia in inter-bank markets. Journal of Monetary Economics, 58(5):436–447.

Adrian, T., Colla, P., and Song Shin, H. (2013). Which financial frictions? parsing the evidence from the financial crisis of 2007 to 2009. NBER Macroeconomics Annual, 27(1):159–214.

Adrian, T. and Shin, H. S. (2010). The changing nature of financial intermediation and the financial crisis of 2007–2009.

Adrian, T. and Shin, H. S. (2011). Financial intermediary balance sheet management. Annual Review of Financial Economics, 3(1):289–307.

Affinito, M. (2012). Do interbank customer relationships exist? and how did they function in the crisis? learning from italy. Journal of Banking & Finance, 36(12):3163–3184.

Afonso, G., Kovner, A., and Schoar, A. (2011). Stressed, not frozen: The federal funds market in the financial crisis. The Journal of Finance, 66(4):1109–1139.

Afonso, G., Kovner, A., and Schoar, A. (2013). Trading partners in the interbank lending market. FRB of New York Staff Report, (620).

Aldasoro, I. and Alves, I. (2016). Multiplex interbank networks and systemic importance: an application to european data. Journal of Financial Stability.

Allen, F. and Babus, A. (2009). Networks in finance. In Kleindorfer, P. R. and Wind, Y., editors, The network challenge: strategy, profit, and risk in an interlinked world, pages 367–382. Pearson Prentice Hall.

Allen, F. and Gale, D. (1994). Limited market participation and volatility of asset prices. The American Economic Review, pages 933–955.

Allen, F. and Gale, D. (2000). Financial contagion. Journal of political economy, 108(1):1–33.

Allen, F. and Gale, D. (2004). Financial intermediaries and markets. Econometrica, 72(4):1023–1061.

Alves, I., Ferrari, S., Franchini, P., Heam, J.-C., Jurca, P., et al. (2013). The structure and resilience of the european interbank market. Technical Report 3, European Systemic Risk Board.

Anand, K., Gai, P., Kapadia, S., Brennan, S., and Willison, M. (2013). A network model of financial system resilience. Journal of Economic Behavior & Organization, 85:219–235.

Arinaminpathy, N., Kapadia, S., and May, R. M. (2012). Size and complexity in model financial systems. Proceedings of the National Academy of Sciences, 109(45):18338–18343.

Ashraf, Q., Gershman, B., and Howitt, P. (2016). How inflation affects macroeconomic performance: an agent-based computational investigation. Macroeconomic dynamics, 20(2):558–581.

Babus, A. (2011). Strategic relationships in over-the-counter markets. Mimeo.

Barabási, A.-L. and Albert, R. (1999). Emergence of scaling in random networks. science, 286(5439):509–512.

Bargigli, L., di Iasio, G., Infante, L., Lillo, F., and Pierobon, F. (2015). The multiplex structure of interbank networks. Quantitative Finance, 15(4):673–691.

Bargigli, L., Riccetti, L., Russo, A., and Gallegati, M. (2018). Network calibration and metamodeling of a financial accelerator agent based model. Journal of Economic Interaction and Coordination, pages 1–28.

Barrat, A. and Weigt, M. (2000). On the properties of small-world network models. The European Physical Journal B-Condensed Matter and Complex Systems, 13(3):547–560.

Basel Committee on Banking Supervision (2010). The basel committee's response to the financial crisis: report to the g20.

Battiston, S., Farmer, J. D., Flache, A., Garlaschelli, D., Haldane, A. G., Heesterbeek, H., Hommes, C., Jaeger, C., May, R., and Scheffer, M. (2016). Complexity theory and financial regulation. Science, 351(6275):818–819.

Battiston, S. and Martinez-Jaramillo, S. (2018). Financial networks and stress testing: Challenges and new research avenues for systemic risk analysis and financial stability implications.

BCBS (2010). Basel iii: A global regulatory framework for more resilient banks and banking systems. Basel Committee on Banking Supervision.

BCBS (2011). Global systemically important banks: assessment methodology and the additional loss absorbency requirement. Bank for international settlements.

Bech, M. L. and Atalay, E. (2010). The topology of the federal funds market. Physica A: Statistical Mechanics and its Applications, 389(22):5223–5246.

Bernanke, B. S. and Blinder, A. S. (1992). The federal funds rate and the channels of monetary transmission. The American Economic Review, pages 901–921.

Bernanke, B. S., Gertler, M., and Gilchrist, S. (1999). The financial accelerator in a quantitative business cycle framework. Handbook of macroeconomics, 1:1341–1393.

Berrospide, J. M. (2013). Bank liquidity hoarding and the financial crisis: an empirical evaluation. Technical report, Board of Governors of the Federal Reserve System (US).

BIS (2014). Basel iii leverage ratio framework and disclosure requirements. Technical report, Basel Committee on Banking Supervision.

Blanchard, O. (2014). Where danger lurks. Finance & Development, 51(3):28–31.

Blanchard, O. et al. (2016). Do dsge models have a future? Technical Report PB 16-11, Peterson Institute for International Economics.

Blenck, D., Hasko, H., Hilton, S., and Masaki, K. (2001). The main features of the monetary policy frameworks of the bank of japan, the federal reserve and the eurosystem. BIS papers, 9:23–56.

Bluhm, M., Georg, C.-P., and Krahnen, J. P. (2016). Interbank intermediation.

Bokan, N., Gerali, A., Gomes, S., Jacquinot, P., and Pisani, M. (2016). Eagle-fli a model for the macroeconomic analysis of banking sector and financial frictions in the euro area. Technical Report 1923.

Bonacich, P. (1987). Power and centrality: A family of measures. American journal of sociology, 92(5):1170–1182.

Bookstaber, R. and Kenett, D. Y. (2016). Looking deeper, seeing more: a multilayer map of the financial system. OFR Brief, 16(06).

Bookstaber, R., Paddrik, M., and Tivnan, B. (2017). An agent-based model for financial vulnerability. Journal of Economic Interaction and Coordination, pages 1–34.

Borgatti, S. P. (2005). Centrality and network flow. Social networks, 27(1):55–71.

Boss, M., Elsinger, H., Summer, M., and Thurner 4, S. (2004). Network topology of the interbank market. Quantitative Finance, 4(6):677–684.

Bramoullé, Y., Galeotti, A., and Rogers, B. W. (2016). The Oxford Handbook of the Economics of Networks. Oxford University Press.

Bräuning, F. and Fecht, F. (2016). Relationship lending in the interbank market and the price of liquidity. Review of Finance, 21(1):33–75.

Brin, S. and Page, L. (1998). The anatomy of a large-scale hypertextual web search engine. Computer Networks and ISDN Systems, 30(1–7):107–117.

Broido, A. D. and Clauset, A. (2018). Scale-free networks are rare. arXiv preprint arXiv:1801.03400.

Brunetti, C., Di Filippo, M., and Harris, J. H. (2010). Effects of central bank intervention on the interbank market during the subprime crisis. The review of financial studies, 24(6):2053–2083.

Brunnermeier, M., Clerc, L., El Omari, Y., Gabrieli, S., Kern, S., et al. (2013). Assessing contagion risks from the cds market. Technical report, European Systemic Risk Board.

Brunnermeier, M. K. (2009). Deciphering the liquidity and credit crunch 2007-2008. Journal of Economic Perspectives, 23(1):77–100.

Brusco, S. and Castiglionesi, F. (2007). Liquidity coinsurance, moral hazard, and financial contagion. The Journal of Finance, 62(5):2275–2302.

Brzoza-Brzezina, M., Kolasa, M., and Makarski, K. (2015). Macroprudential policy and imbalances in the euro area. Journal of International Money and Finance, 51:137–154.

Caballero, R. J. and Simsek, A. (2013). Fire sales in a model of complexity. The Journal of Finance, 68(6):2549–2587.

Caccioli, F., Barucca, P., and Kobayashi, T. (2018). Network models of financial systemic risk: A review. Journal of Computational Social Science, 1(1):81–114.

Caccioli, F., Shrestha, M., Moore, C., and Doyne Farmer, J. (2014). Stability analysis of financial contagion due to overlapping portfolios. Journal of Banking & Finance, 46:233–246.

Caldarelli, G. (2007). Scale-free networks: complex webs in nature and technology. Oxford University Press.

Caldarelli, G., Capocci, A., De Los Rios, P., and Muñoz, M. A. (2002). Scale-free networks from varying vertex intrinsic fitness. Physical review letters, 89(25):258702.

Canabarro, E. and Duffie, D. (2003). Measuring and marking counterparty risk. Asset/Liability Management for Financial Institutions, Institutional Investor Books.

Chan-Lau, J. A. (2018). Systemic centrality and systemic communities in financial networks. Quantitative Finance and Economics, 2(2):468–496.

Chan-Lau, M. J. A. (2017). ABBA: An Agent-Based Model of the Banking System. International Monetary Fund.

Christiano, L. J., Eichenbaum, M. S., and Trabandt, M. (2018). On dsge models. Journal of Economic Perspectives, 32(3):113 – 140.

Christiano, L. J., Motto, R., and Rostagno, M. (2010). Financial factors in economic fluctuations. Technical Report 1192, European Central Bank.

Christiano, L. J., Motto, R., and Rostagno, M. (2014). Risk shocks. American Economic Review, 104(1):27–65.

Ciccarelli, M., Maddaloni, A., and Peydró, J.-L. (2015). Trusting the bankers: A new look at the credit channel of monetary policy. Review of Economic Dynamics, 18(4):979–1002.

Cifuentes, R., Ferrucci, G., and Shin, H. S. (2005). Liquidity risk and contagion. Journal of the European Economic Association, 3(2-3):556–566.

Clauset, A., Shalizi, C. R., and Newman, M. E. (2009). Power-law distributions in empirical data. SIAM review, 51(4):661–703.

Clerc, L., Giovannini, A., Langfield, S., Peltonen, T., Portes, R., and Scheicher, M. (2016). Indirect contagion: the policy problem. ESRB Occasional Paper Series, (9).

Cocco, J. F., Gomes, F. J., and Martins, N. C. (2009). Lending relationships in the interbank market. Journal of Financial Intermediation, 18(1):24–48.

Colander, D., Howitt, P., Kirman, A., Leijonhufvud, A., and Mehrling, P. (2008). Beyond dsge models: toward an empirically based macroeconomics. The American Economic Review, pages 236–240.

Cont, R. and Schaanning, E. (2017). Fire sales, indirect contagion and systemic stress testing. Technical report, Norges Bank Research 2/2017.

Craig, B. and Von Peter, G. (2014). Interbank tiering and money center banks. Journal of Financial Intermediation, 23(3):322–347.

De Bandt, O., Hartmann, P., and Peydró, J. L. (2009). Systemic risk in banking. In The Oxford handbook of banking.

De Haan, L. and van den End, J. W. (2013). Banks' responses to funding liquidity shocks: Lending adjustment, liquidity hoarding and fire sales. Journal of International Financial Markets, Institutions and Money, 26:152–174.

de Haan, L., van den End, J. W., and Vermeulen, P. (2017). Lenders on the storm of wholesale funding shocks: saved by the central bank? Applied Economics, 49(46):4679–4703.

De Masi, G., Iori, G., and Caldarelli, G. (2006). Fitness model for the italian interbank money market. Physical Review E, 74(6):066112.

De Walque, G., Pierrard, O., and Rouabah, A. (2010). Financial (in) stability, supervision and liquidity injections: A dynamic general equilibrium approach*. The Economic Journal, 120(549):1234–1261.

Demirguc-Kunt, A., Detragiache, E., Merrouche, O., et al. (2013). Bank capital: Lessons from the financial crisis. Journal of Money, Credit and Banking, 45(6):1147–1164.

Diamond, D. W. and Dybvig, P. H. (1983). Bank runs, deposit insurance, and liquidity. Journal of political economy, 91(3):401–419.

Diamond, D. W. and Rajan, R. G. (2011). Fear of fire sales, illiquidity seeking, and credit freezes. The Quarterly Journal of Economics, 126(2):557–591.

Dib, A. (2010). Banks, credit market frictions, and business cycles. Technical Report 2010-24, Bank of Canada Working Paper.

Drehmann, M. and Nikolaou, K. (2013). Funding liquidity risk: definition and measurement. Journal of Banking & Finance, 37(7):2173–2182.

Duarte, F. and Eisenbach, T. (2015). Fire-sale spillovers and systemic risk. Technical Report 645, Federal Reserve Bank of New York.

Dubecq, S., Monfort, A., Renne, J.-P., and Roussellet, G. (2016). Credit and liquidity in interbank rates: a quadratic approach. Journal of Banking & Finance, 68:29–46.

ECB (2009). Recent advances in modeling systemic risk using network analysis. Workshop on "Recent advances in modelling systemic risk using network analysis".

Eisenberg, L. and Noe, T. H. (2001). Systemic risk in financial systems. Management Science, 47(2):236–249.

Eisenschmidt, J. and Tapking, J. (2009). Liquidity risk premia in unsecured interbank money markets. Technical report, European Central Bank.

Elliott, M., Golub, B., and Jackson, M. O. (2014). Financial networks and contagion. The American economic review, 104(10):3115–3153.

Epstein, J. M. and Axtell, R. (1996). Growing artificial societies: social science from the bottom up. Brookings Institution Press.

Espinosa-Vega, M. and Sole, J. (2014). Introduction to the network analysis approach to stress testing. A Guide to IMF Stress Testing: Methods and Models, pages 205–208.

Fagiolo, G. (2007). Clustering in complex directed networks. Physical Review E, 76(2):026107.

Farmer, J. D. and Foley, D. (2009). The economy needs agent-based modelling. Nature, 460(7256):685–686.

Filipović, D. and Trolle, A. B. (2013). The term structure of interbank risk. Journal of Financial Economics, 109(3):707–733.

Foster, J. G., Foster, D. V., Grassberger, P., and Paczuski, M. (2010). Edge direction and the structure of networks. Proceedings of the National Academy of Sciences, 107(24):10815–10820.

Freeman, L. C. (1978). Centrality in social networks conceptual clarification. Social networks, 1(3):215–239.

Freixas, X., Parigi, B. M., and Rochet, J.-C. (2000). Systemic risk, interbank relations, and liquidity provision by the central bank. Journal of money, credit and banking, pages 611–638.

Fricke, D., Finger, K., and Lux, T. (2013). On assortative and disassortative mixing in scale-free networks: The case of interbank credit networks. Technical report, Kiel Working Paper.

Fricke, D. and Lux, T. (2015). On the distribution of links in the interbank network: evidence from the e-mid overnight money market. Empirical Economics, 49(4):1463–1495.

Fricke, D. and Roukny, T. (2018). Generalists and specialists in the credit market. Journal of Banking & Finance.

Furfine, C. H. (1999). The microstructure of the federal funds market. Financial Markets, Institutions & Instruments, 8(5):24–44.

Gabrieli, S. and Georg, C.-P. (2014). A network view on interbank market freezes.

Gabrieli, S. and Georg, C.-P. (2015). A network view on interbank liquidity. Technical Report 44/2014, Deutsche Bundesbank Working Paper.

Gai, P., Haldane, A., and Kapadia, S. (2011). Complexity, concentration and contagion. Journal of Monetary Economics, 58(5):453–470.

Gai, P. and Kapadia, S. (2010). Contagion in financial networks. Proceedings of the Royal Society A: Mathematical, Physical and Engineering Science, 466(2120):2401–2423.

Garcia-de Andoain, C., Heider, F., Hoerova, M., and Manganelli, S. (2016). Lending-of-last-resort is as lending-of-last-resort does: Central bank liquidity provision and interbank market functioning in the euro area. Journal of Financial Intermediation, 28:32–47.

Garlaschelli, D. and Loffredo, M. I. (2004). Patterns of link reciprocity in directed networks. Physical review letters, 93(26):268701.

Geanakoplos, J., Axtell, R., Farmer, J. D., Howitt, P., Conlee, B., Goldstein, J., Hendrey, M., Palmer, N. M., and Yang, C.-Y. (2012). Getting at systemic risk via an agent-based model of the housing market. American Economic Review, 102(3):53–58.

Georg, C.-P. (2013). The effect of the interbank network structure on contagion and common shocks. Journal of Banking & Finance, 37(7):2216–2228.

Gerali, A., Neri, S., Sessa, L., and Signoretti, F. M. (2010). Credit and banking in a dsge model of the euro area. Journal of Money, Credit and Banking, 42(s1):107–141.

Gertler, M. and Kiyotaki, N. (2010). Financial intermediation and credit policy in business cycle analysis. Handbook of monetary economics, 3(3):547–599.

Giannone, D., Lenza, M., Pill, H., and Reichlin, L. (2012). The ecb and the interbank market. The Economic Journal, 122(564):F467–F486.

Glasserman, P. and Young, H. P. (2015). How likely is contagion in financial networks? Journal of Banking & Finance.

Gode, D. K. and Sunder, S. (1993). Allocative efficiency of markets with zero-intelligence traders: Market as a partial substitute for individual rationality. Journal of political economy, 101(1):119–137.

Goodhart, C. A., Sunirand, P., and Tsomocos, D. P. (2006). A model to analyse financial fragility. Economic Theory, 27(1):107–142.

Gorton, G. and Metrick, A. (2012). Securitized banking and the run on repo. Journal of Financial economics, 104(3):425–451.

Greenwood, R., Landier, A., and Thesmar, D. (2015). Vulnerable banks. Journal of Financial Economics, 115(3):471–485.

Hałaj, G. (2018). Agent-based model of system-wide implications of funding risk. Technical report, European Central Bank.

Halaj, G. and Kok, C. (2015). Modelling the emergence of the interbank networks. Quantitative Finance, 15(4):653–671.

Haldane, A. (2009). Rethinking the financial network. Speech delivered at the Financial Student Association, Amsterdam, April, 28.

Haldane, A. (2016). The dappled world. GLS shackle biennial memorial lecture. Bank of England.

Haldane, A. G. and May, R. M. (2011). Systemic risk in banking ecosystems. Nature, 469(7330):351–355.

Heider, F., Hoerova, M., and Holthausen, C. (2015). Liquidity hoarding and interbank market spreads: The role of counterparty risk. Journal of Financial Economics, 118:336–354.

Huang, X., Vodenska, I., Havlin, S., and Stanley, H. E. (2013). Cascading failures in bi-partite graphs: model for systemic risk propagation. Scientific reports, 3.

Hüser, A.-C. (2015). Too interconnected to fail: A survey of the interbank networks literature. Journal of Network Theory in Finance, 1(3).

Hüser, A.-C., Hałaj, G., Kok, C., Perales, C., and van der Kraaij, A. (2017). The systemic implications of bail-in: a multi-layered network approach. Journal of Financial Stability.

Iman, R. L. and Conover, W. J. (1979). The use of the rank transform in regression. Technometrics, 21(4):499–509.

International Monetary Fund (2010). Understanding financial interconnectedness. IMF Policy Paper.

Iori, G., De Masi, G., Precup, O. V., Gabbi, G., and Caldarelli, G. (2008). A network analysis of the italian overnight money market. Journal of Economic Dynamics and Control, 32(1):259–278.

Iori, G., Mantegna, R. N., Marotta, L., Miccichè, S., Porter, J., and Tumminello, M. (2015). Networked relationships in the e-mid interbank market: A trading model with memory. Journal of Economic Dynamics and Control, 50:98–116.

Iyer, R., Peydró, J.-L., da Rocha-Lopes, S., and Schoar, A. (2013). Interbank liquidity crunch and the firm credit crunch: Evidence from the 2007–2009 crisis. The Review of Financial Studies, 27(1):347–372.

Katz, L. (1953). A new status index derived from sociometric analysis. Psychometrika, 18(1):39–43.

Kiyotaki, N. and Moore, J. (1997). Credit cycles. The Journal of Political Economy, 105(2):211–248.

Klemm, K. and Eguiluz, V. M. (2002). Growing scale-free networks with small-world behavior. Physical Review E, 65(5):057102.

Langfield, S., Liu, Z., and Ota, T. (2014). Mapping the uk interbank system. Journal of Banking & Finance, 45:288–303.

Langfield, S. and Soramäki, K. (2016). Interbank exposure networks. Computational Economics, 47(1):3–17.

LeBaron, B. (2001). Empirical regularities from interacting long-and short-memory investors in an agent-based stock market. Ieee transactions on evolutionary computation, 5(5):442–455.

Lee, S. H. (2013). Systemic liquidity shortages and interbank network structures. Journal of Financial Stability, 9(1):1–12.

León, C. and Berndsen, R. J. (2014). Rethinking financial stability: challenges arising from financial networks' modular scale-free architecture. Journal of Financial Stability, 15:241–256.

Lindé, J. (2018). Dsge models: still useful in policy analysis? Oxford Review of Economic Policy, 34(1-2):269–286.

Linzert, T. and Schmidt, S. (2011). What explains the spread between the euro overnight rate and the ecb's policy rate? International Journal of Finance & Economics, 16(3):275–289.

Lux, T. (2015). Emergence of a core-periphery structure in a simple dynamic model of the interbank market. Journal of Economic Dynamics and Control, 52:A11 – A23.

Marin, A. and Wellman, B. (2011). Social network analysis: An introduction. The SAGE handbook of social network analysis, 11.

May, R. M. and Arinaminpathy, N. (2010). Systemic risk: the dynamics of model banking systems. Journal of the Royal Society Interface, 7(46):823–838.

McKay, M. D., Beckman, R. J., and Conover, W. J. (1979). Comparison of three methods for selecting values of input variables in the analysis of output from a computer code. Technometrics, 21(2):239–245.

Michaud, F.-L. and Upper, C. (2008). What drives interbank rates? evidence from the libor panel. BIS Quarterly Review, March.

Milgram, S. (1967). The small-world problem. Psychology Today, 1(1).

Modigliani, F. and Miller, M. H. (1958). The cost of capital, corporation finance and the theory of investment. The American economic review, pages 261–297.

Montagna, M. and Kok, C. (2016). Multi-layered interbank model for assessing systemic risk. Technical Report 1944, ECB Working Paper.

Montagna, M. and Lux, T. (2016). Contagion risk in the interbank market: a probabilistic approach to cope with incomplete structural information. Quantitative Finance, 0(0):1–20.

Newman, M. (2010). Networks: an introduction. Oxford university press.

Newman, M. E., Strogatz, S. H., and Watts, D. J. (2001). Random graphs with arbitrary degree distributions and their applications. Physical review E, 64(2):026118.

Nier, E., Yang, J., Yorulmazer, T., and Alentorn, A. (2007). Network models and financial stability. Journal of Economic Dynamics and Control, 31(6):2033–2060.

Olivier Blanchard (2015). Blanchard: Looking forward, looking back. IMF Survey Magazine.

Owen, A. B. (2013). Monte carlo theory, methods and examples. Monte Carlo Theory, Methods and Examples. Art Owen.

Pariès, M. D., Sørensen, C. K., Rodriguez-Palenzuela, D., et al. (2011). Macroeconomic propagation under different regulatory regimes: Evidence from an estimated dsge model for the euro area. International Journal of Central Banking, 7(4):49–113.

Peltonen, T. A., Scheicher, M., and Vuillemey, G. (2014). The network structure of the cds market and its determinants. Journal of Financial Stability, 13:118–133.

Poledna, S., Bochmann, O., and Thurner, S. (2017). Basel iii capital surcharges for g-sibs are far less effective in managing systemic risk in comparison to network-based, systemic risk-dependent financial transaction taxes. Journal of Economic Dynamics and Control, 77:230–246.

Poledna, S., Molina-Borboa, J. L., Martínez-Jaramillo, S., Van Der Leij, M., and Thurner, S. (2015). The multi-layer network nature of systemic risk and its implications for the costs of financial crises. Journal of Financial Stability, 20:70–81.

Rochet, J.-C. and Tirole, J. (1996). Interbank lending and systemic risk. Journal of Money, credit and Banking, 28(4):733–762.

Roukny, T., Battiston, S., and Stiglitz, J. E. (2016). Interconnectedness as a source of uncertainty in systemic risk. Journal of Financial Stability.

Rubinov, M. and Sporns, O. (2010). Complex network measures of brain connectivity: uses and interpretations. Neuroimage, 52(3):1059–1069.

Salle, I. and Yıldızoğlu, M. (2014). Efficient sampling and meta-modeling for computational economic models. Computational Economics, 44(4):507–536.

Santner, T. J., Williams, B. J., and Notz, W. I. (2013). The design and analysis of computer experiments. Springer Science & Business Media.

Sarkar, A. (2009). Liquidity risk, credit risk, and the federal reserve's responses to the crisis. Financial Markets and Portfolio Management, 23(4):335–348.

Schinasi, G. J. (2004). Defining Financial Stability. Number 4-187. International Monetary Fund.

Schwarz, K. (2015). Mind the gap: Disentangling credit and liquidity in risk spreads.

Schweitzer, F., Fagiolo, G., Sornette, D., Vega-Redondo, F., Vespignani, A., and White, D. R. (2009). Economic networks: The new challenges. Science, 325(5939):422–425.

Sheldon, G. and Maurer, M. (1998). Interbank lending and systemic risk: An empirical analysis for switzerland. Swiss Journal of Economics and Statistics, 134(IV):685–704.

Shleifer, A. and Vishny, R. (2011). Fire sales in finance and macroeconomics. The Journal of Economic Perspectives, 25(1):29–48.

Smets, F. and Wouters, R. (2003). An estimated dynamic stochastic general equilibrium model of the euro area. Journal of the European economic association, 1(5):1123–1175.

Smithson, M. and Verkuilen, J. (2006). A better lemon squeezer? maximum-likelihood regression with beta-distributed dependent variables. Psychological methods, 11(1):54.

Soramäki, K., Bech, M. L., Arnold, J., Glass, R. J., and Beyeler, W. E. (2007). The topology of interbank payment flows. Physica A: Statistical Mechanics and its Applications, 379(1):317–333.

Squartini, T., Van Lelyveld, I., and Garlaschelli, D. (2013). Early-warning signals of topological collapse in interbank networks. Scientific reports, 3.

Stiglitz, J. E. (2018). Where modern macroeconomics went wrong. Oxford Review of Economic Policy, 34(1-2):70–106.

Stulz, R. M. (2010). Credit default swaps and the credit crisis. Journal of Economic Perspectives, 24(1):73–92.

Summer, M. (2013). Financial contagion and network analysis. Annu. Rev. Financ. Econ., 5(1):277–297.

Taylor, J. B. and Williams, J. C. (2009). A black swan in the money market. American Economic Journal: Macroeconomics, 1(1):58–83.

Temizsoy, A., Iori, G., and Montes-Rojas, G. (2017). Network centrality and funding rates in the e-mid interbank market. Journal of Financial Stability, 33:346–365.

Tesfatsion, L. and Judd, K. L. (2006). Handbook of computational economics volume 2: Agent-based computational economics, volume 2. Elsevier.

The Group of Ten (2001). Report on consolidation in the financial sector.

Trichet, J.-C. (2010). State of the union: The financial crisis and the ecb's response between 2007 and 2009. JCMS: Journal of Common Market Studies, 48(s1):7–19.

Upper, C. (2011). Simulation methods to assess the danger of contagion in interbank markets. Journal of Financial Stability, 7(3):111–125.

van der Leij, M., Hommes, C., et al. (2014). The formation of a core periphery structure in heterogeneous financial networks. Technical report, Tinbergen Institute Discussion Paper.

van Lelyveld, I. et al. (2014). Finding the core: Network structure in interbank markets. Journal of Banking & Finance, 49:27–40.

Vlcek, M. J. and Roger, M. S. (2012). Macrofinancial modeling at central banks: Recent developments and future directions. Number 12-21. International Monetary Fund.

Watts, D. J. and Strogatz, S. H. (1998). Collective dynamics of small-world networks. nature, 393(6684):440.

Yellen, J. (2013). Interconnectedness and systemic risk: Lessons from the financial crisis and policy implications. Board of Governors of the Federal Reserve System, Washington, DC.